

4

GL-TR-90-0032(I)  
ENVIRONMENTAL RESEARCH PAPERS, NO. 1052

Proceedings of the Second Symposium on  
GPS Applications in Space

EDITOR:  
CHRISTOPHER JEKELI

AD-A219 978



13 February 1990



Approved for public release; distribution unlimited.

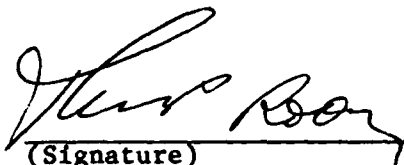


DTIC  
ELECTE  
APR 3 1990  
S B D


EARTH SCIENCES DIVISION PROJECT 2309  
**GEOPHYSICS LABORATORY**  
HANSCOM AFB, MA 01731-5000

90 04 03 072

"This technical report has been reviewed and is approved for publication"

  
(Signature)

THOMAS P. ROONEY, Chief  
Geodesy and Gravity Branch

  
(Signature)

DONALD H. ECKHARDT, Director  
Earth Sciences Division

This report has been reviewed by the ESD Public Affairs Office (PA) and is releasable to the National Technical Information Service (NTIS).

Qualified requestors may obtain additional copies from the Defense Technical Information Center. All others should apply to the National Technical Information Service.

If your address has changed, or if you wish to be removed from the mailing list, or if the addressee is no longer employed by your organization, please notify GL/IMA, Hanscom AFB, MA 01731. This will assist us in maintaining a current mailing list.

UNCLASSIFIED

SECURITY CLASSIFICATION OF THIS PAGE

REPORT DOCUMENTATION PAGE				Form Approved OMB No. 0704-0188		
1a. REPORT SECURITY CLASSIFICATION <b>UNCLASSIFIED</b>			1b. RESTRICTIVE MARKINGS			
2a. SECURITY CLASSIFICATION AUTHORITY			3. DISTRIBUTION/AVAILABILITY OF REPORT <b>APPROVED FOR PUBLIC RELEASE: DISTRIBUTION UNLIMITED</b>			
2b. DECLASSIFICATION/DOWNGRADING SCHEDULE						
4. PERFORMING ORGANIZATION REPORT NUMBER(S) GL-TR-90-0032 (I) ERP, No. 1052			5. MONITORING ORGANIZATION REPORT NUMBER(S)			
6a. NAME OF PERFORMING ORGANIZATION <b>GEOPHYSICS LABORATORY (AFSC)</b>		6b. OFFICE SYMBOL (If applicable) <b>LWG</b>	7a. NAME OF MONITORING ORGANIZATION			
6c. ADDRESS (City, State, and ZIP Code) <b>Hanscom Air Force Base Bedford, MA 01731-5000</b>			7b. ADDRESS (City, State, and ZIP Code)			
8a. NAME OF FUNDING/SPONSORING ORGANIZATION		8b. OFFICE SYMBOL (If applicable)	9. PROCUREMENT INSTRUMENT IDENTIFICATION NUMBER			
8c. ADDRESS (City, State, and ZIP Code)			10. SOURCE OF FUNDING NUMBERS			
			PROGRAM ELEMENT NO	PROJECT NO	TASK NO	WORK UNIT ACCESSION NO
			61102F	2309	2309G1	2309G112
11. TITLE (Include Security Classification) <b>Proceedings of the Second Symposium on GPS Applications in Space, Volume I (pp.1-244) and Volume II (pp.245-458)</b>						
12. PERSONAL AUTHOR(S) <b>Christopher Jekeli (editor)</b>						
13a. TYPE OF REPORT <b>Scientific</b>		13b. TIME COVERED FROM _____ TO _____		14. DATE OF REPORT (Year, Month, Day) <b>1990 February 13</b>		
15. PAGE COUNT <b>254</b>						
16. SUPPLEMENTARY NOTATION						
17. COSATI CODES			18. SUBJECT TERMS (Continue on reverse if necessary and identify by block number)			
FIELD	GROUP	SUB-GROUP	<b>Global Positionin System, Orbit Determination, Space Navigation, Attitude Determination. (E)</b>			
19. ABSTRACT (Continue on reverse if necessary and identify by block number)						
<p>-This collection of abstracts, papers, and presentation material constitutes the Proceedings of the Second Symposium on GPS Applications in Space, which was held at the Geophysics Laboratory (Air Force Systems Command), Hanscom Air Force Base, Massachusetts, on 10-11 October, 1989. The Symposium was divided into four sessions covering "Space Missions with GPS", "Orbit Determination with GPS", "Attitude Determination with GPS", and "Other Applications and Topics." Both the application of GPS to a variety of NASA and DOD space missions, as well as corresponding GPS receiver development were discussed at this symposium. Specific applications included orbit determination of the GPS satellites and low Earth orbiters, space navigation, and, in particular, attitude determination of space vehicles.</p>						
20. DISTRIBUTION/AVAILABILITY OF ABSTRACT <input checked="" type="checkbox"/> UNCLASSIFIED/UNLIMITED <input type="checkbox"/> SAME AS RPT. <input type="checkbox"/> DTIC USERS			21. ABSTRACT SECURITY CLASSIFICATION <b>Unclassified</b>			
22a. NAME OF RESPONSIBLE INDIVIDUAL <b>Christopher Jekeli</b>			22b. TELEPHONE (Include Area Code) <b>617-377-5255</b>		22c. OFFICE SYMBOL <b>GL (AFSC)/LWG</b>	

# FORWARD

The contents of these Proceedings are primarily the viewgraphs shown at The Second Symposium on GPS Applications in Space, held at the Geophysics Laboratory (Air Force Systems Command), Hanscom Air Force Base, Massachusetts, on 10-11 October, 1989. In order to enhance the informational content of these volumes, each set of viewgraphs is preceded by a synopsis that was extracted from a recording of the audible portion of the author's presentation. In some cases, the author provided his/her own abstract or a complete paper and, naturally, these were used instead. Also included are the post-presentation discussions between author and audience. However, the transcriptions of these are unfortunately not always complete as some questions from the audience were not recorded clearly. Each author was given the opportunity to review the synopsis, albeit with short response time; therefore, responsibility for any misrepresentations or errors in the synopses rests with the editor. Following the formal presentations, Thomas Yunck (Jet Propulsion Laboratory) led an open discussion on Selective Availability and Anti-Spoofing and how these affect a variety of GPS applications in space. There is no synopsis of this discussion (it was not recorded), but a set of viewgraphs is included.

I wish to extend my sincerest thanks and appreciation to all participants of the symposium and especially to the speakers for making this a successful and productive symposium. In particular, I thank the co-convenors, Dr. Triveni N. Upadhyay (Mayflower Communications Company, Inc.) and Thomas Yunck (Jet Propulsion Laboratory) who were the driving forces behind the agenda of the symposium and ensured that all relevant private industries and government agencies were well represented.

Christopher Jekeli



<b>Accession For</b>	
NTIS GRA&I	<input checked="" type="checkbox"/>
DTIC TAB	<input type="checkbox"/>
Unannounced	<input type="checkbox"/>
Justification	
By _____	
Distribution/	
<b>Availability Codes</b>	
Dist	Avail and/or Special
A-1	

# TABLE OF CONTENTS - VOLUME I

Foreword . . . . .	iii
Conference Agenda . . . . .	vi
Geoscience From GPS Tracking By Earth Satellites, William G. Melbourne . . . . .	1
The GPS Precise Orbit Demonstration (POD) Experiment, E.S. (Ab) Davis . . . . .	25
NRL Activities On Spaceborne GPS Receivers, Ronald L. Beard . . . . .	43
GL's Proposed Satellite-to-Satellite Tracking Mission Using GPS: STAGE (STS-GPS Tracking for Anomalous Gravitation Estimation), Christopher Jekeli . . . . .	57
GPS Attitude Determination Activities At The Naval Surface Warefare Center, Alan G. Evans . . . . .	65
GPS Application To NASA Upper Stages, A. Wayne Deaton . . . . .	79
Space Station Freedom GPS Implementation Plans - An Overview, Penny E. Saunders . . . . .	95
Recent Results In High-Precision GPS Orbit Determination, Stephen Lichten, Susan Kornreich Wolf, Willy I. Bertiger, Ulf J. Lindqwister, and Geoff Blewitt . . . . .	107
Closed Loop Orbit Trim Using GPS, Penina Axelrad and Bradford W. Parkinson . . . . .	135
Global Gravity Field Mapping With GPS Tracking Of The Space Shuttle, George J. Priovolos, Triveni N. Upadhyay, and Christopher Jekeli . . . . .	161
Techniques Of GPS-Based Precision Orbit Determination For Low Earth Satellites, Sien C. Wu . . . . .	179
Ambiguity Bootstrapping To Determine GPS Orbits And Baselines, Charles C. Counselman . . . . .	193
Status Of DARPA Guidance And Control Program, Larry Stotts and Joseph M. Aein . . . . .	205
"The Multipath Simulator", A Tool Toward Controlling Multipath, George A. Hajj . . . . .	229

## TABLE OF CONTENTS - VOLUME II

Autonomous Integrated GPS/INS Navigation Filter For Advanced Spacecraft Applications, Triveni N. Upadhyay, George J. Priovolos, Harley Rhodehamel . . . . .	245
An Experiment In Attitude, Position And Velocity Determination With Rogue GPS Receivers, Tom K. Meehan . . . . .	271
Preliminary GPS Pointing Data Results, Phil Ward . . . . .	281
Algorithms For Spacecraft Attitude Determination With GPS, Duncan B. Cox, Haywood S. Satz, Ronald L. Beard, and G. Paul Landis . . . . .	303
Preliminary Experimental Performance Of The TOPEX Global Positioning System Demonstration Receiver (GPSDR), Lance Carson . . . . .	323
Design and Performance For The GPS Receiver Unit (GPSRU) For The NASA Orbital Maneuvering Vehicle, Roger M. Weninger and Richard Sfeir . . . . .	333
Applications Of GPS To Space-Based Tethered Array Radar, Horst Salzwedel, Ken Kessler, and Fred Karkalik . . . . .	343
Special Purpose Inexpensive Satellite (SPINSAT) GPS Receiver, Roger M. Weninger, Richard Sfeir, and Ronald L. Beard . . . . .	363
The Defense Mapping Agency's Operational GPS Orbit Processing System, James A. Slater . . . . .	371
A Shuttle Experiment To Demonstrate 6-Degree-Of-Freedom Navigation With GPS, Duncan B. Cox, Steven Gardner, and Neal Carlson . . . . .	415
Large Space Structure Displacement Sensing Using Advanced GPS Technology, Gaylord K. Huth . . . . .	437
Alternatives to Becoming an "Authorized User", Thomas Yunck . . . . .	445
List of Attendees and Addresses . . . . .	453

SECOND SYMPOSIUM  
ON  
GPS APPLICATIONS IN SPACE

Agenda

10 October 1989

- 9:00 Registration
- 9:45 Welcome Air Force
- 10:00 - 12:00 Session I: SPACE MISSIONS WITH GPS  
Chairman: Dr. Christopher Jekeli  
Geophysics Laboratory (AFSC)
1. W.G. Melbourne (Jet Propulsion Laboratory): "The GPS Geoscience Instrument on EOS and Space Station"
  2. Ab Davis (Jet Propulsion Laboratory): "The GPS Precise Orbit Demonstration on TOPEX/POSEIDON"
  3. Ron Beard (Naval Research Laboratory): "NRL Activities on Spaceborne GPS Receivers"
  4. Chris Jekeli (Geophysics Laboratory, AFSC): "GL's Proposed Satellite-to-Satellite Tracking Mission Using GPS"
  5. Alan G. Evans (Naval Surface Warfare Center): "GPS Attitude Determination Activities at the Naval Surface Warfare Center"
  6. A. Wayne Deaton (NASA Marshall Space Flight Center): "GPS Application to NASA Upperstages"
  7. Penny Saunders (NASA Johnson Space Center): "Space Station GPS Implementation Plans and Overview"
- 12:00 - 13:30 LUNCH NCO Club

13:30 - 17:00      Session II: ORBIT DETERMINATION WITH GPS  
Chairman: Dr. Thomas Yunck  
Jet Propulsion Laboratory

1. S.M. Lichten, Susan Kornreich Wolf, Willy I. Bertiger, Ulf J. Lindqwister, and Geoff Blewitt (Jet Propulsion Laboratory): "Recent Results in High Precision GPS Orbit Determination"
2. Penina Axelrad and B.W. Parkinson (Stanford University): "Closed-Loop Orbit Trim Using GPS"
3. George J. Pirovolos\*, Triveni Upadhyay\*, and Christopher Jekeli\*\* (\*Mayflower Communications, \*\*Geophysics Laboratory (AFSC)): "Global Gravity Field Mapping with GPS Tracking of the Space Shuttle"
4. S.C. Wu (Jet Propulsion Laboratory): "Techniques of GPS-Based Precision Orbit Determination for Low Earth Satellites"

BREAK

5. C.C. Counselman (MIT): "Ambiguity Bootstrapping to Determine GPS Orbits and Baselines"
6. Larry Stotts\* and Joe Aein\*\* (\*DARPA, \*\*Rand Corporation): "Status of DARPA GPS Guidance and Control Program"
7. George Hajj (Jet Propulsion Laboratory): "The Multipath Simulator, A Tool Toward Controlling Multipath"

11 October 1989

9:00 - 12:00      Session III: ATTITUDE DETERMINATION WITH GPS  
Chairman: Dr. Triveni Upadhyay  
Mayflower Communications Company, Inc.

1. Triveni Upadhyay\*, George Pirovolos\*, Harley Rhodehamel\*, A. Wayne Deaton\*\* (\*Mayflower Communications, \*\*NASA Marshall SFC): "Autonomous Integrated GPS/INS Navigation Filter for Advanced Spacecraft Application"
2. Tom Meehan (Jet Propulsion Laboratory): "An Experiment in Attitude, Position, and Velocity Determination with Rogue GPS Receivers"
3. Phil Ward (Texas Instruments): "Preliminary GPS Pointing Data Results"
4. Duncan Cox, Jr.\*, Haywood W. Satz\*, G. Paul Landis\*\*, and Ronald Beard\*\* (\*Mayflower Communications, \*\*Naval Research Laboratory): "Algorithms for Spacecraft Attitude Determination with GPS"

BREAK



5. Lance Carson (Motorola Government Electronics Group): "Preliminary Performance of the TOPEX Global Positioning System Demonstration Receiver (GPSDR)"
6. Roger M. Weninger and Richard Sfeir (Rockwell): "Design and Performance of the GPS Receiver for NASA Orbital Maneuvering Vehicle"
7. Horst Salzwedel, Ken Kessler and Fred Karkalik (System Control Technology): "Application of GPS to Space-based Tethered Array Radar"

12:00 - 14:00 LUNCH

14:00 - 16:00 Session IV: OTHER APPLICATIONS AND TOPICS  
Chairman: Dr. Christopher Jekeli  
Geophysics Laboratory (AFSC)

1. Roger Weninger\*, Richard Sfeir\*, and Ronald Beard\*\* (\*Rockwell International, \*\*Naval Research Laboratory): "SPINSAT GPS Receivers"
2. James Slater (Defense Mapping Agency): "The Defense Mapping Agency's Operational GPS Orbit Processing System"
3. Duncan Cox, Jr.\*, Steven Gardner\*, and Neal Carlson\*\* (\*Mayflower Communications, \*\*Integrity Systems): "A Shuttle Experiment to Demonstrate Six-Degree-of-Freedom Navigation with GPS"
4. Gaylord K. Huth (Axiomatix): "Large Space Structure Displacement Sensing Using Advanced GPS Technology"

BREAK

5. PANEL DISCUSSION (Triveni Upadhyay and Thomas Yunck)
6. CLOSING REMARKS (Christopher Jekeli)

## GEOSCIENCE FROM GPS TRACKING BY EARTH SATELLITES

William G. Melbourne  
JET PROPULSION LABORATORY

This paper reviews some of the potential geoscience applications available to NASA satellite missions of the 1990's whose manifests include a GPS flight receiver. The applications exploit the greater GPS viewing angle given to an observing platform at altitude as well as its unique atmospheric environment. They include improvements in Earth-surface baseline determinations, satellite ephemeris prediction, satellite attitude determination, and gravity modeling, temperature profiling of the atmosphere, and ionospheric tomography. Some of the missions that offer opportunities for these types of GPS geoscience applications include TOPEX/POSEIDON (primarily a satellite altimetry mission for oceanography), ARISTOTELES (a mission to map the Earth's gravity field using a gravity gradiometer), GRAVITY PROBE-B (general relativity experiment), EOS-A and EOS-B (NASA's Earth Observing platforms), EPOP (European version of EOS), and SPACE STATION. The geoscience to be derived from GPS-based platforms in space relies on all the major system elements, including the full constellation of GPS satellites, a global standardized ground tracking network, the type of flight receiver, and the computing abilities. Much of these are already being honed for the upcoming TOPEX/POSEIDON mission where orbital position (radial) in the decimeter range is desired to complement the altimeter precision of a few cm.

The TOPEX/POSEIDON satellite, whose mission is to provide accurate sea surface heights for the study of ocean currents and tides, will, during its projected life, provide hundreds of repeat orbits at ten-day intervals and ground separation of about 300 km (at the equator). Precise orbit determination at the estimated 13 cm level or better using the GPS will begin to penetrate the barrier to mapping the larger-scale boundary currents (several thousands to ten thousand km).

The EOS platform will have three GPS antennas (fore, aft, and center) to enable maximum viewing of satellites including those that rise and set on the horizon, to allow attitude determination of the platform, and to perform the standard navigation function. The full system of EOS platforms and data reduction centers will provide more rapidly (improved resolution in time) precise geodetic quantities and geophysical signatures, such as precise baselines and Earth rate and orientation. Other applications enabled by monitoring radio occultations of the GPS satellites (by the Earth) include atmospheric temperature profiling, three-dimensional ionospheric tomography, and acoustic gravity wave detection. A major challenge presented here is the enormous data processing required to acquire, sense, and decipher the signals of thousands of rising and setting GPS satellites each day.

The occultation observation lasts only about one minute during which time the GPS phase residual due to the presence of an atmosphere increases by up to  $10^4$  cycles, a fairly large signal. This is related by Snell's law to the atmospheric index of refraction as a function of radial distance. The mass density of the atmosphere is proportional to the molecular number density which in turn is proportional to the refractivity. Integrating the hydrostatic equation yields the pressure which then by thermodynamic principles leads to the vertical temperature profile. The predicted accuracy of this technique is on the order of a few tenths of Kelvin degrees for altitudes between 10 and 30 km. These will be valuable data for comparison with other techniques and for calibration purposes.

# **JPL** GEOSCIENCE FROM GPS TRACKING BY EARTH SATELLITES

## **OVERVIEW**

- NASA MISSIONS OF THE 1990'S THAT MAY CARRY A GPS FLIGHT RECEIVER
- SCIENTIFIC APPLICATIONS OF GPS-BASED SATELLITE TRACKING SYSTEM
  - Geodesy
  - Gravity
  - Atmospheric Temperature Profiling
  - Ionospheric Structure by Tomography
  - Platform Position and Attitude Determination
  - Enhanced Accuracies of GPS Ephemerides
- ARCHITECTURE OF A GPS-BASED SATELLITE TRACKING SYSTEM
- TOPEX/POSEIDON MISSION
  - Science Objectives & Precision Orbit Determination Requirements
  - GPS Flight Experiment for Precision Orbit Determination
- EOS GEOSCIENCE FROM HIGH PRECISION GPS TRACKING SYSTEM
  - Science Objectives
  - GPS Flight Experiment

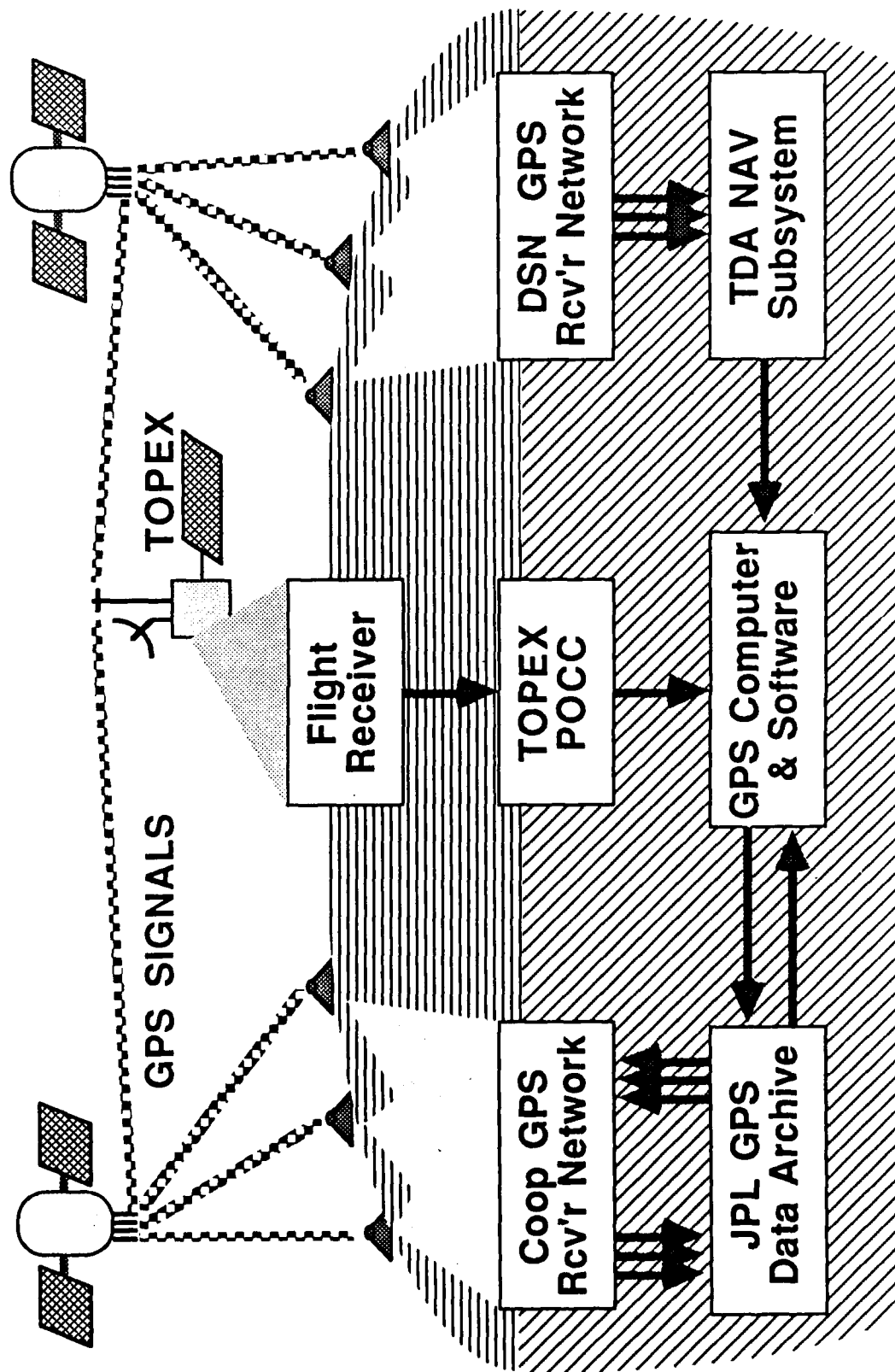
## **FUTURE MISSION OPPORTUNITIES**

- **TOPEX/POSEIDON (1992 launch, NASA/CNES)**
  - subdecimeter positioning for POD
  - limited gravity recovery,  $n < \sim 25$
- **ARISTOTELES (planned for 1995, ESA/NASA?)**
  - positioning
  - gravity recovery in conjunction with gravity gradiometer
- **GRAVITY PROBE - B ( proposed for  $>\sim 1995$ , NASA)**
  - positioning for general relativity experiment
  - gravity recovery (drag-free),  $n < \sim 65$
- **EOS-A & EOS-B ( planned for 1997 & 1999, NASA)**
  - positioning and attitude
  - high temporal resolution geodesy
  - atmospheric sounding for temperature
  - ionospheric tomography
- **EPOP (planned for 1997, ESA)**
  - same as EOS plus pratee
- **SPACE STATION**

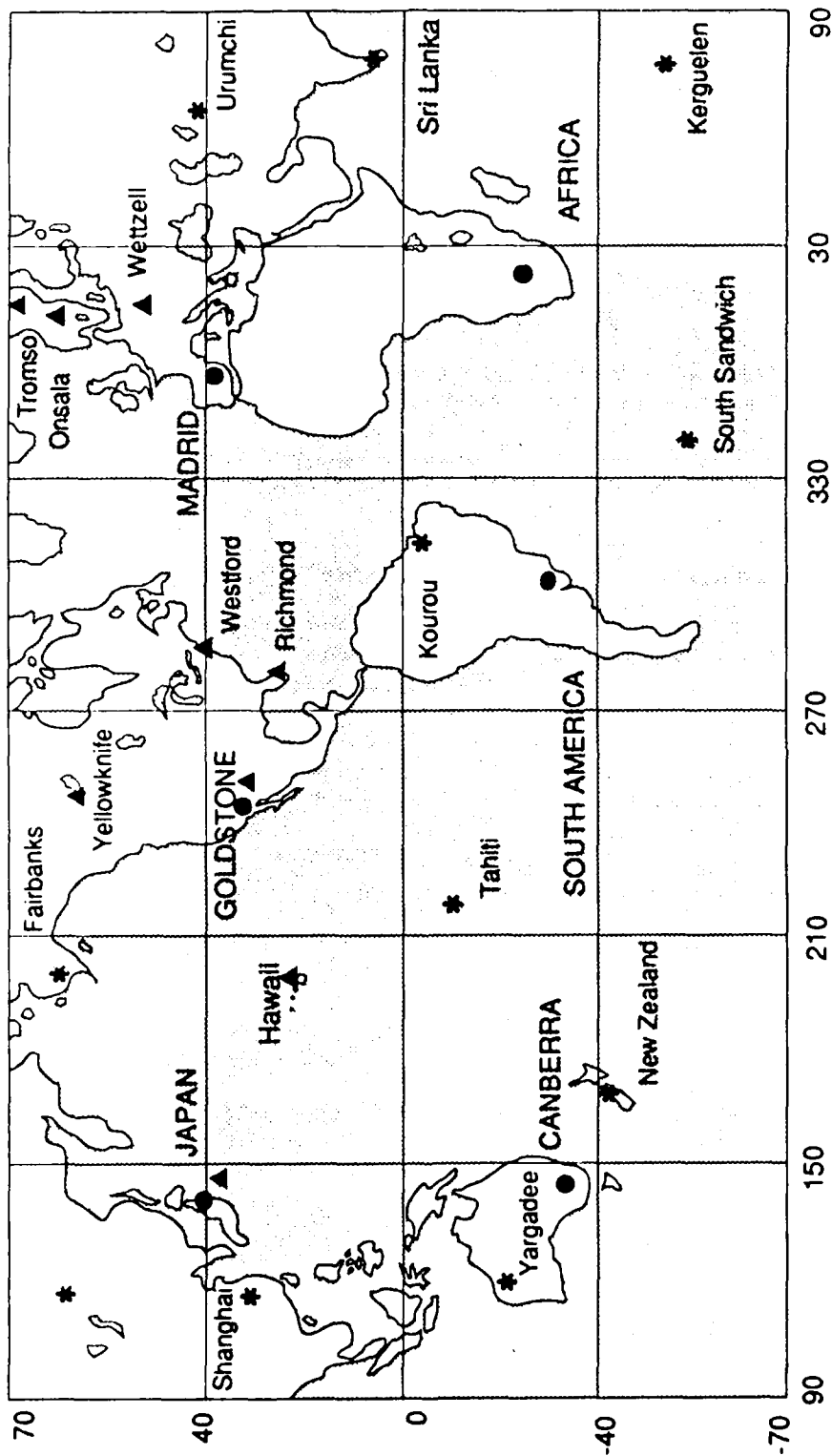
**TOPEX**

# GPS POD SYSTEM ELEMENTS

## 21--SATELLITE GPS CONSTELLATION

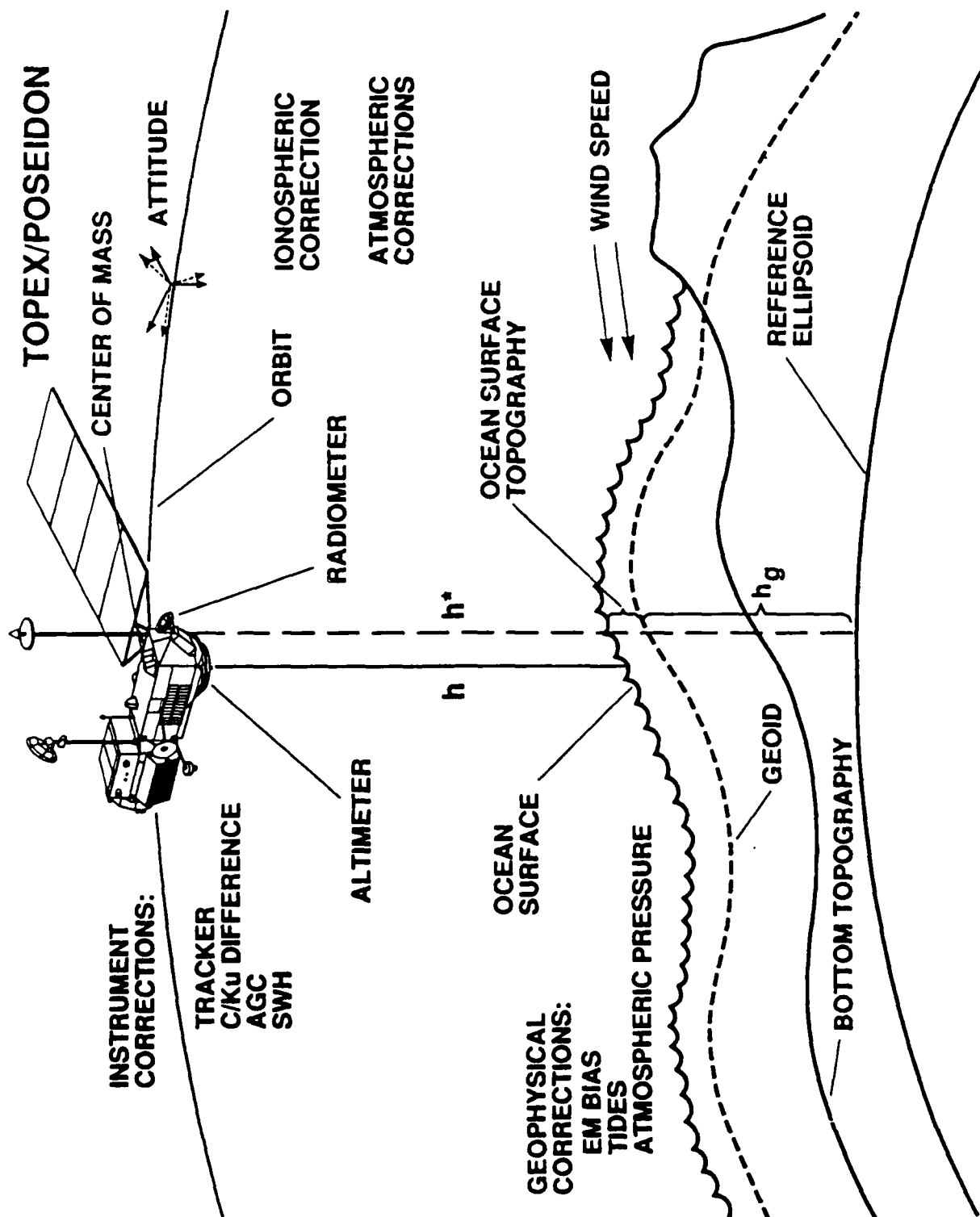


# AN INTERNATIONALLY SPONSORED GPS GLOBAL TRACKING NETWORK

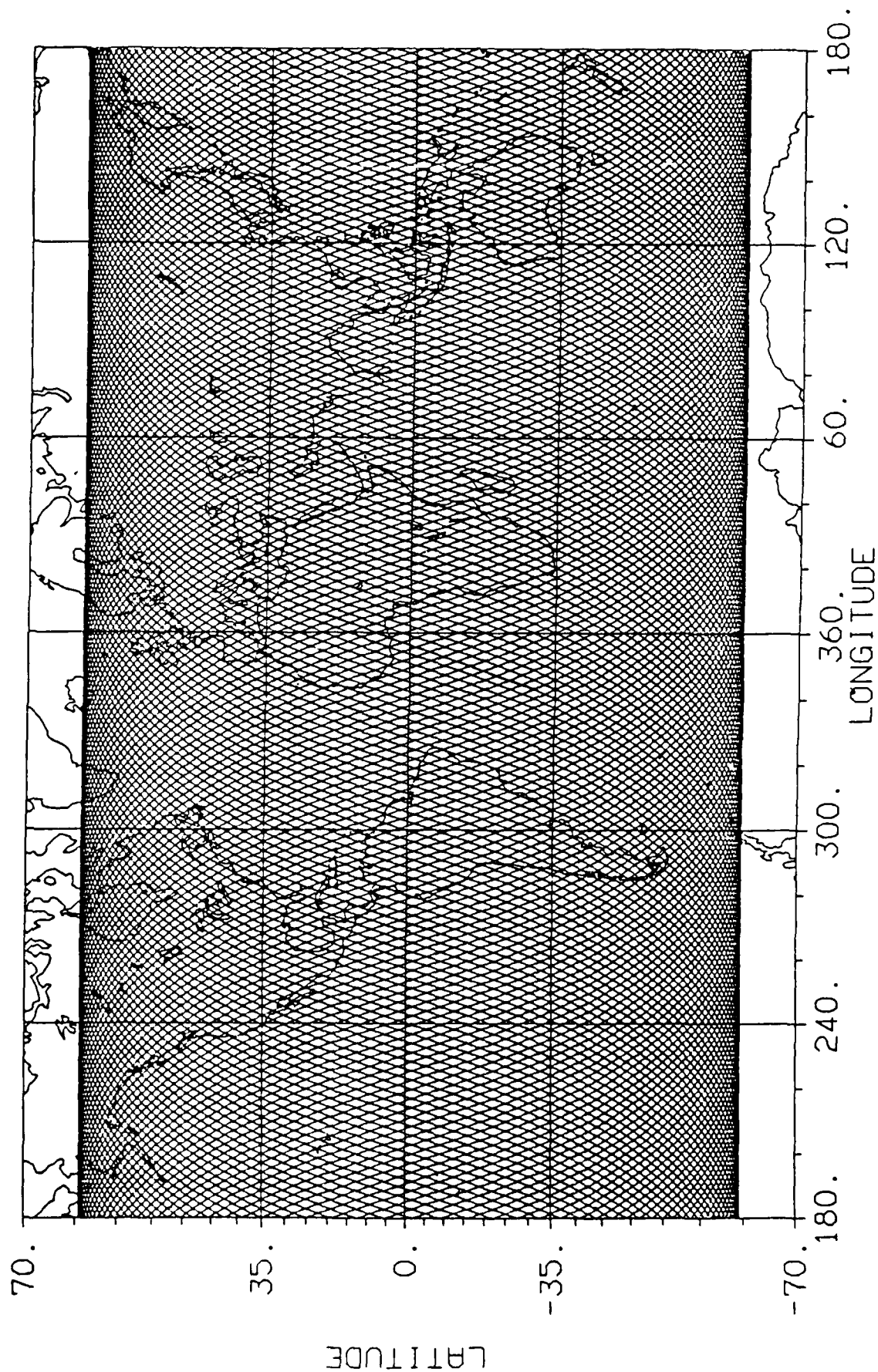


- ▲ CIGNET STATIONS
- PRIMARY SIX-STATION GLOBAL CONFIGURATION FOR TOPEX/POSEIDON
- \* POTENTIAL TRACKING STATION LOCATIONS

# OCEAN ALTIMETRY WITH TOPEX/POSEIDON



TOPEX GROUND TRACKS







*GPS-Based POD Experiment*

## **TOPEX MISSION GOALS**

### **STUDY OF OCEAN DYNAMICS**

**Mean and Variable Surface Currents**

**Tides of the World's Oceans**

### **SCIENCE REQUIREMENTS**

#### **MEASURE THE OCEAN SURFACE TOPOGRAPHY**

**Precision : 2.4 cm (1-sigma)**

**Accuracy : 14.0 cm (1-sigma)**

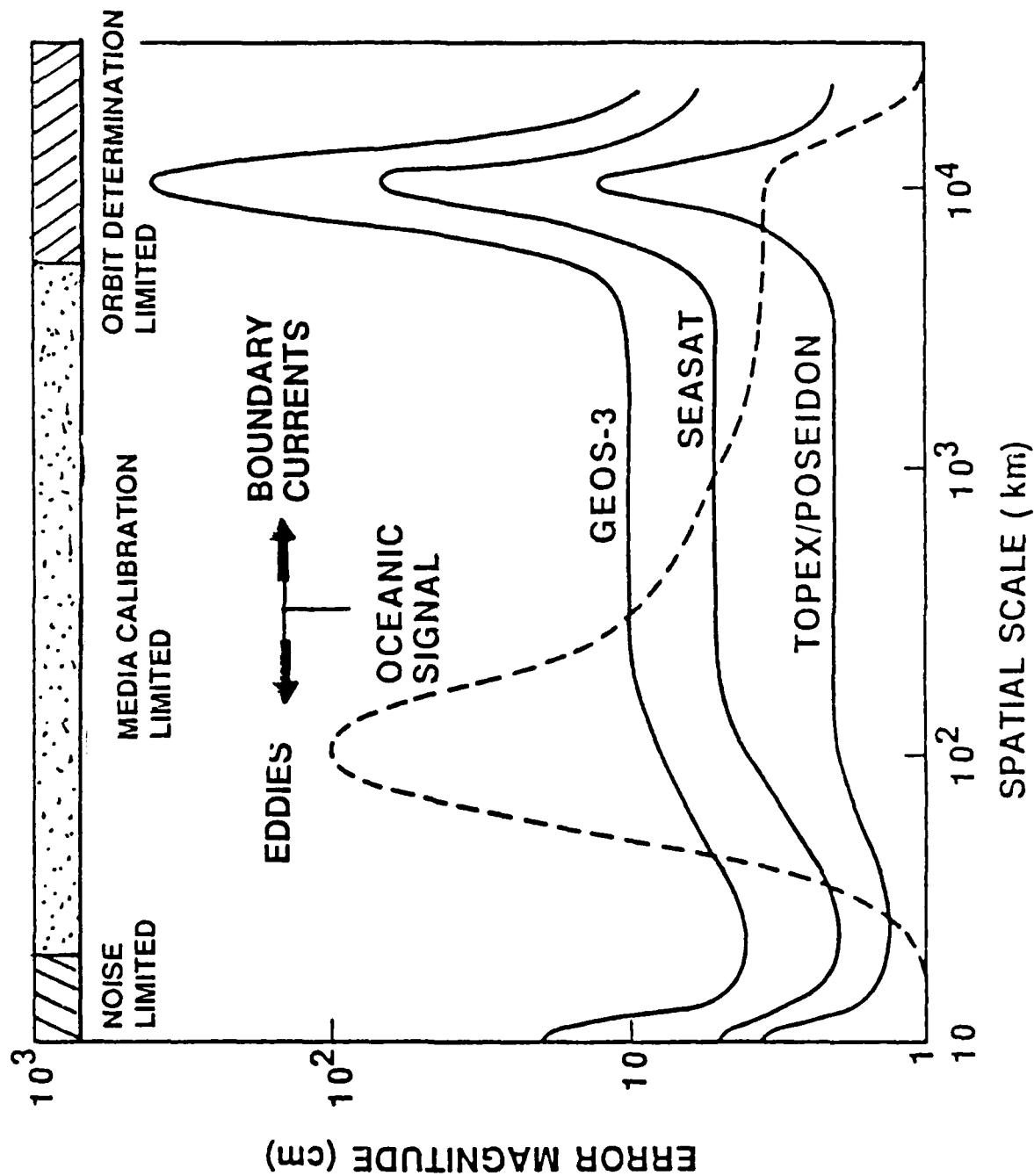
**TOPEX**

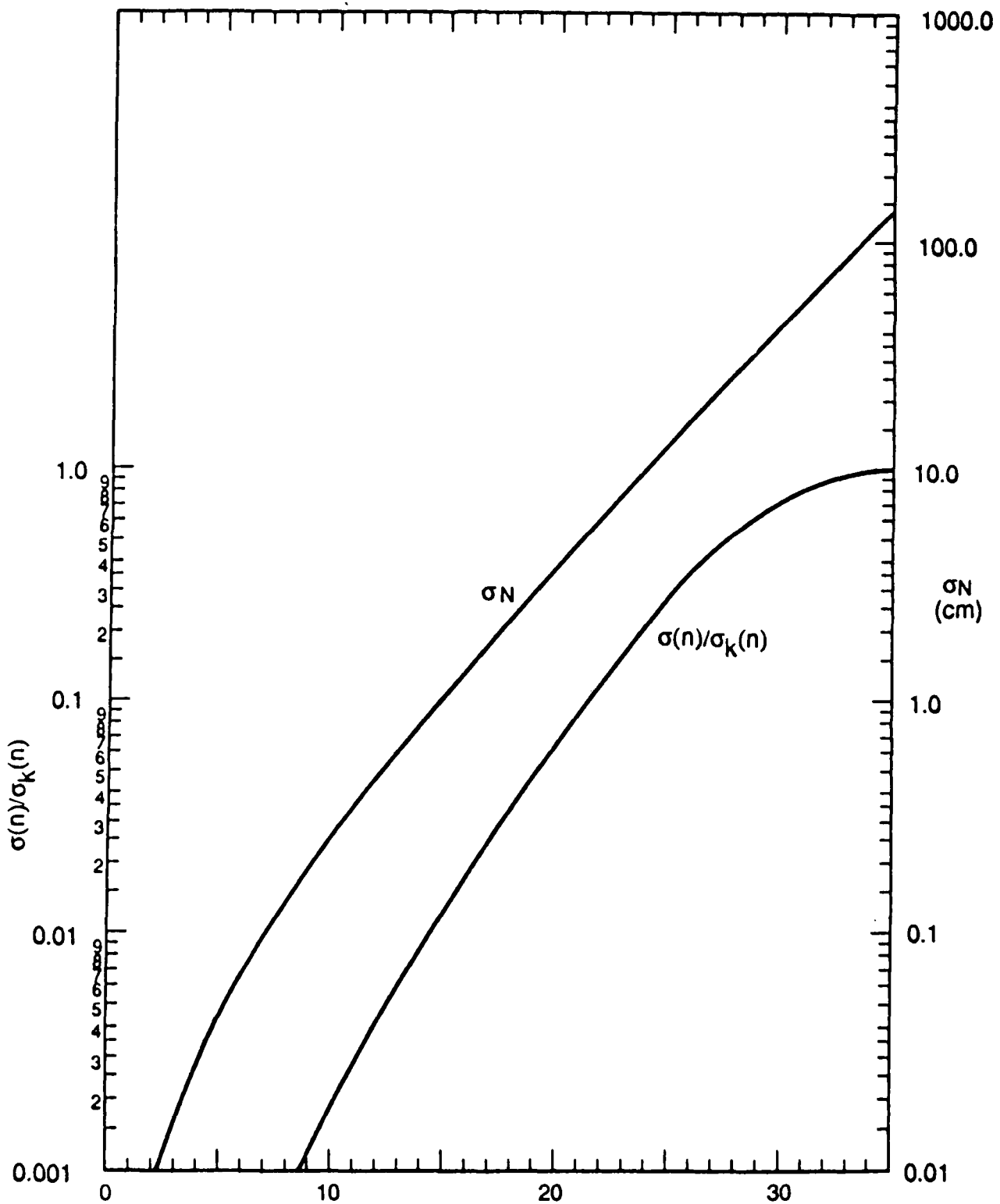
*GPS-Based POD Experiment*

## **MEASUREMENT UNCERTAINTY**

<b>ALTIMETER</b>	<b>2 cm</b>
<b>MEDIA</b>	<b>3 cm</b>
<b>TOPEX EPHEMERIS</b>	<b>13 cm</b>
<hr/>	
<b>TOTAL</b>	<b>13.5 cm</b>

# SPATIAL SCALE OF SEA LEVEL ERRORS (SCHEMATIC)





GEOSCIENCE FROM GPS TRACKING BY EARTH SATELLITES

**Predicted gravity and geoid recovery with  
GPS on TOPEX/Poseidon, 3-year mission**

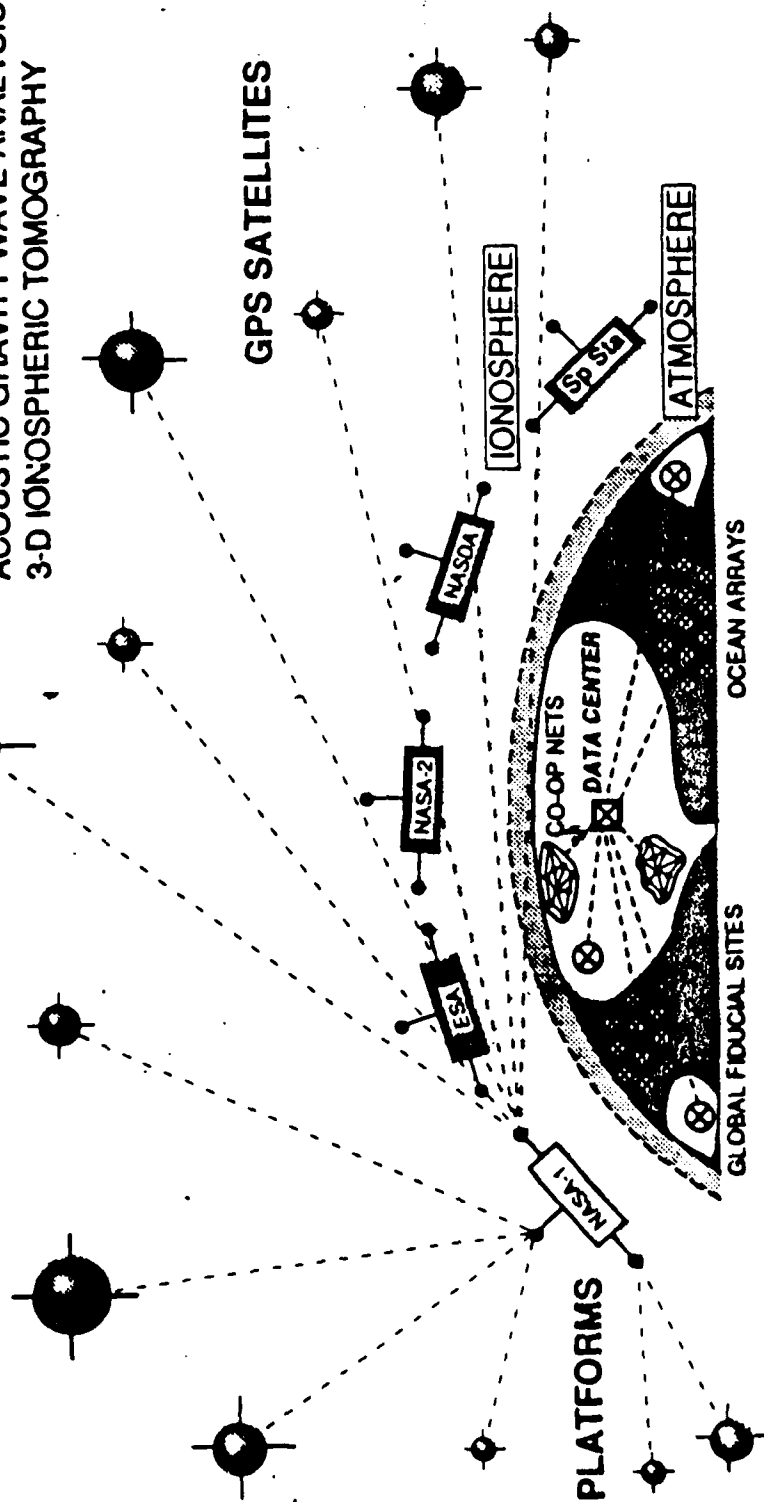
# THE GPS EARTH OBSERVATORY

## SYSTEM

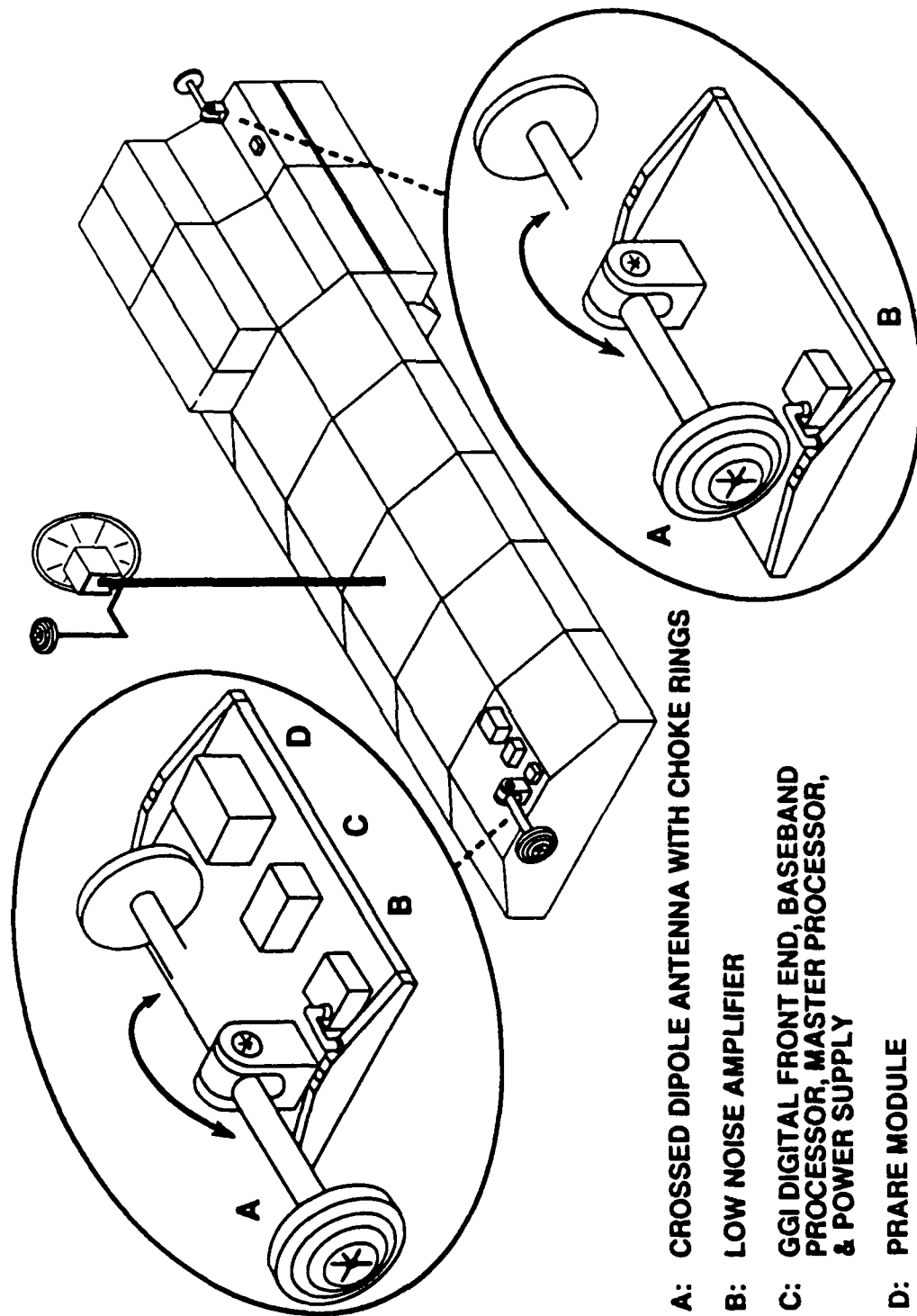
FIVE OR MORE ORBITING PLATFORMS  
 MULTI-CHANNEL GPS FLIGHT RECEIVERS  
 3 OR MORE DISTRIBUTED ANTENNAS  
 ~10 GROUND REFERENCE RECEIVERS  
 DATA REDUCTION & ARCHIVE CENTER  
 REGIONAL SCIENCE CENTERS

## SCIENCE ROLES

RAPID & PRECISE GLOBAL GEODESY  
 LAND & OCEAN BASELINES  
 EARTH ORIENTATION & UT1 RATE  
 EARTH GRAVITY MODEL REFINEMENT  
 PRECISE ORBIT & ATTITUDE DETERM.  
 RADIO OCCULTATION ANALYSIS  
 DAILY ATMOSPHERIC TEMP PROFILES  
 ACOUSTIC GRAVITY WAVE ANALYSIS  
 3-D IONOSPHERIC TOMOGRAPHY



# NOMINAL GGI LAYOUT ON EOS PLATFORMS



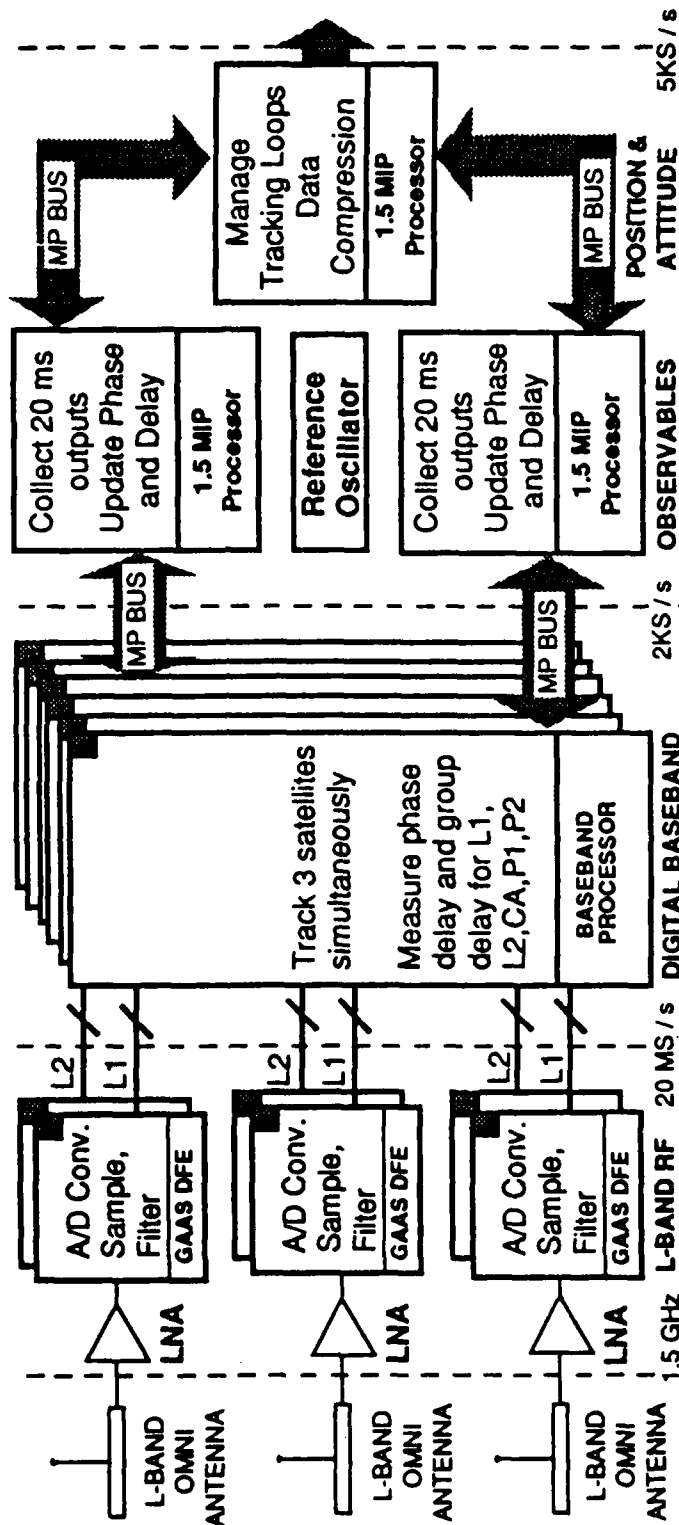
A: CROSSED DIPOLE ANTENNA WITH CHOKE RINGS

B: LOW NOISE AMPLIFIER

C: GGI DIGITAL FRONT END, BASEBAND PROCESSOR, MASTER PROCESSOR, & POWER SUPPLY

D: PRARE MODULE

# GGI FUNCTIONAL BLOCK DIAGRAM



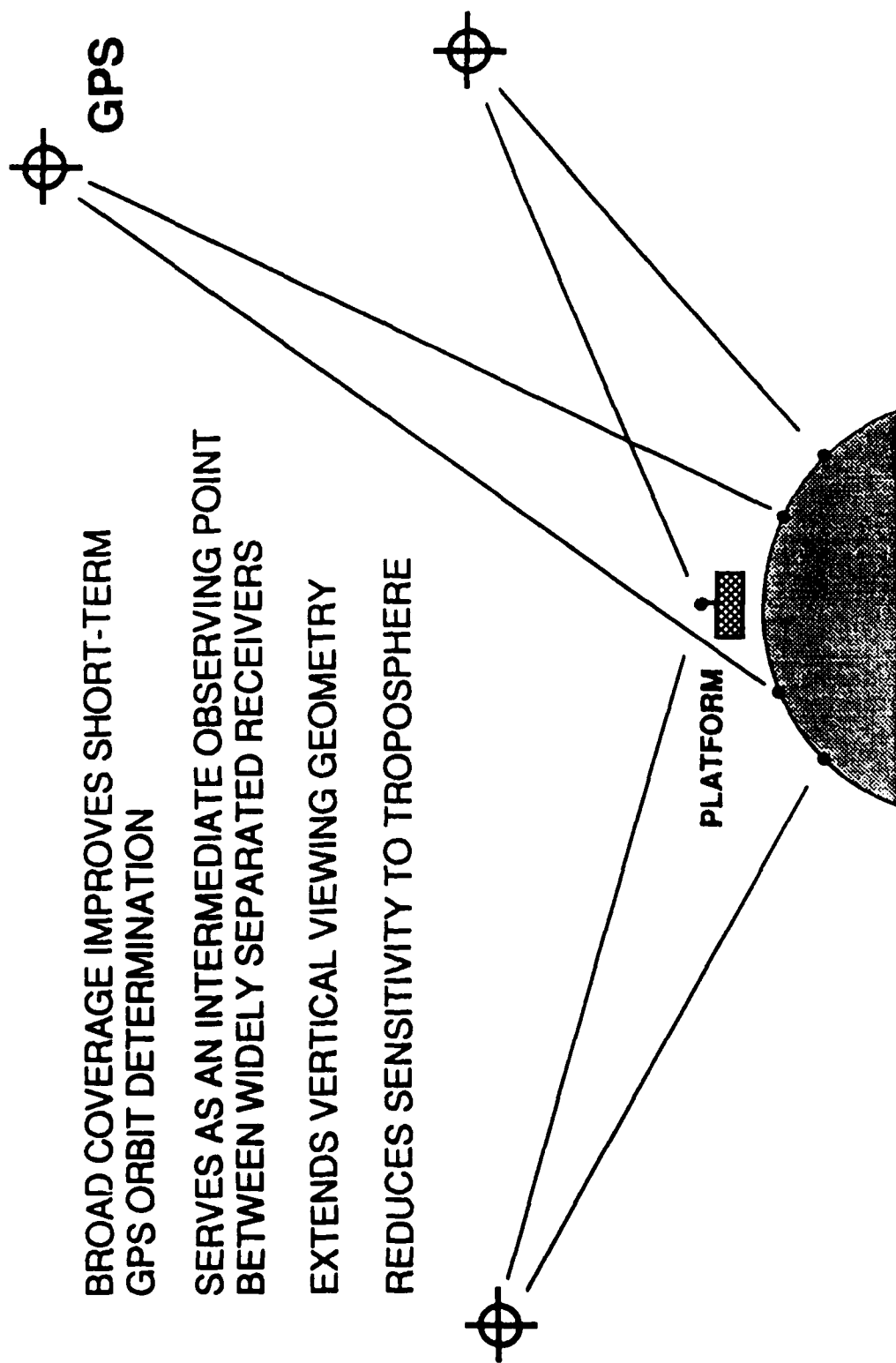
## CONTRIBUTION OF LOW ORBITING GPS RECEIVERS TO EARTH-BASED GPS GEODESY

BROAD COVERAGE IMPROVES SHORT-TERM  
GPS ORBIT DETERMINATION

SERVES AS AN INTERMEDIATE OBSERVING POINT  
BETWEEN WIDELY SEPARATED RECEIVERS

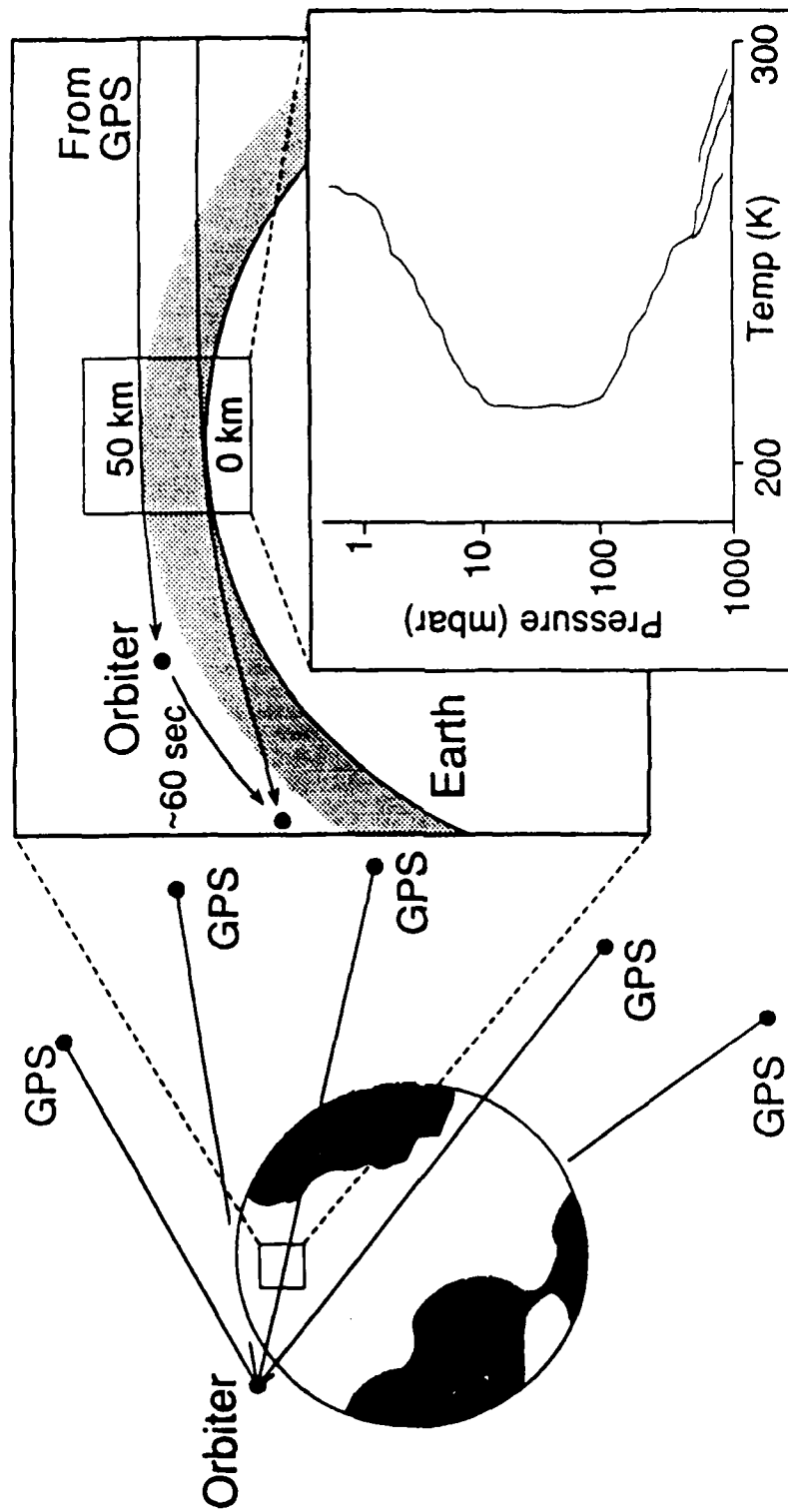
EXTENDS VERTICAL VIEWING GEOMETRY

REDUCES SENSITIVITY TO TROPOSPHERE

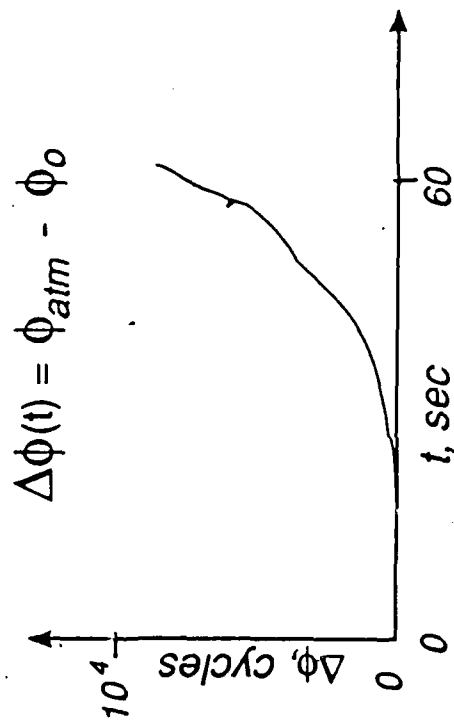
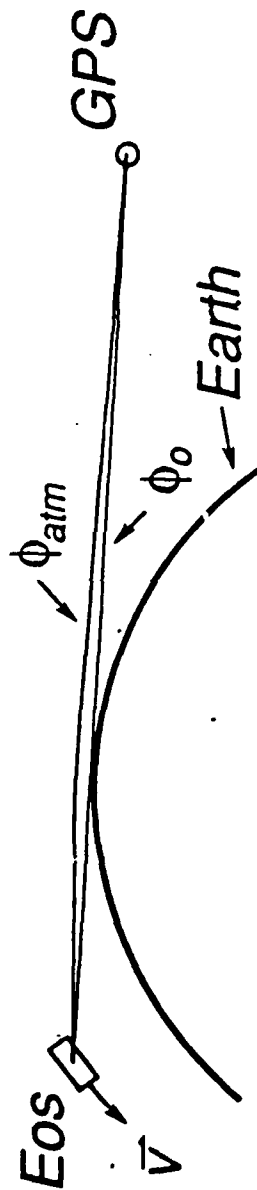




# GPS-BASED ATMOSPHERIC TEMPERATURE PROFILING



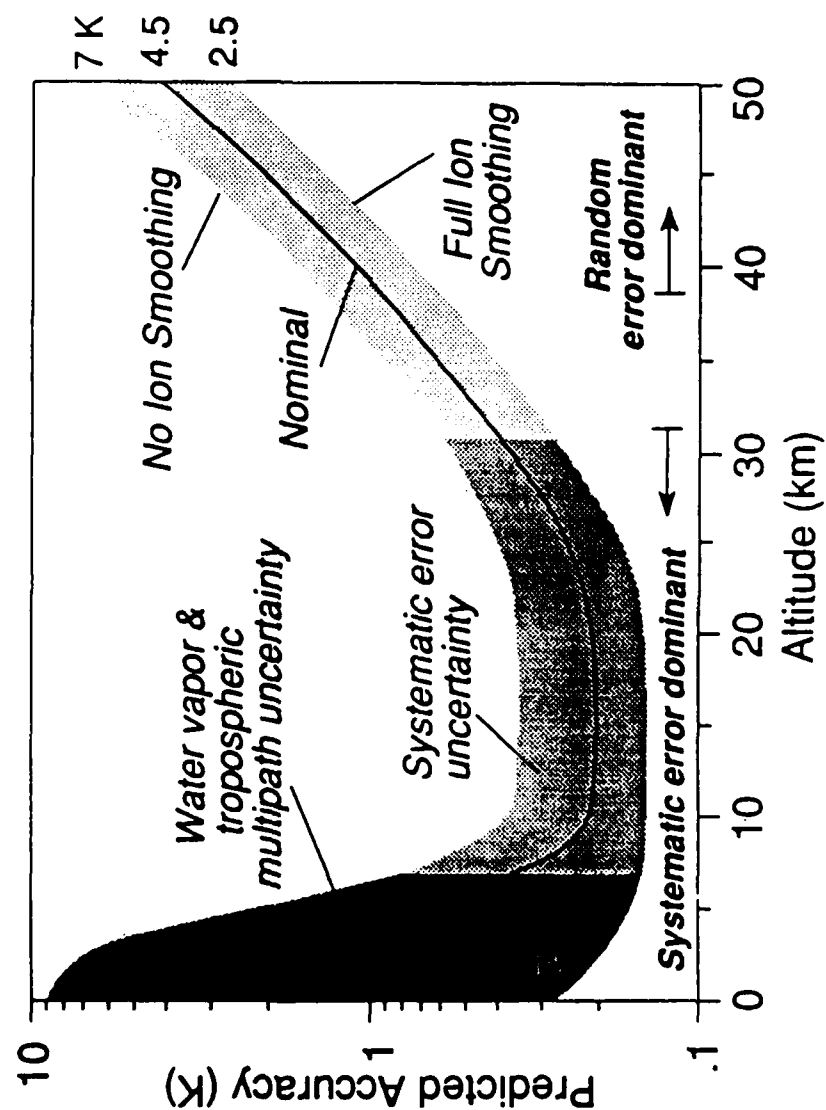
# ATMOSPHERIC PHASE PERTURBATIONS



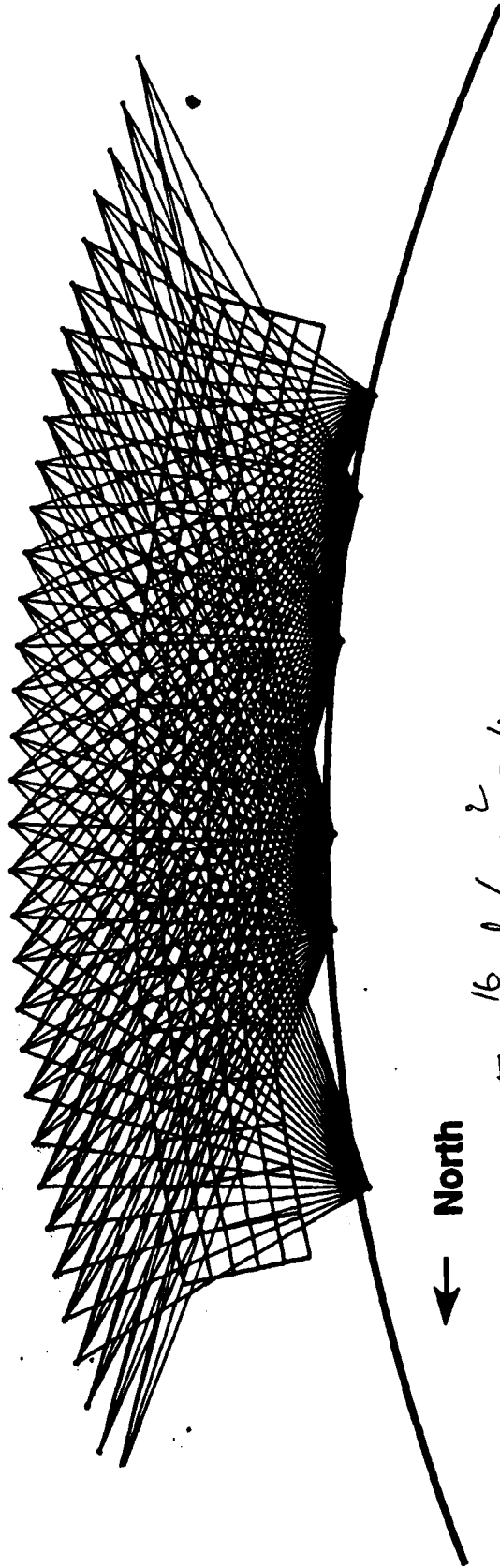
## On Recovering Atmospheric Temperature Profiles From GPS Occultations

1. Data:  $\lambda[\varphi_{\text{atm}}(t_i) - \varphi_o(t_i)] = \min_{r_i} \{ \int n(r_i) ds \} - \lambda \hat{\phi}_o(t_i), \quad i = 1, \dots, N$
2. Invert Above System (via Abel Transformation or equivalent) to Obtain Profile of Index of Refraction:  $n(r)$
3. Molecular Number Density:  $n(r) = \alpha(n(r) - 1)$
4. Mass Density:  $\rho(r) = \mu n(r), \quad \mu = \text{Mean Molecular Weight}$
5. Pressure:  $p(h) = \int_h^\infty g \rho(h) dh \quad (\text{Hydrostatic Equilibrium})$
6. Gas Law:  $T(h) = T(p(h), \rho(h))$

# PREDICTED GPS ATMOSPHERIC TEMPERATURE ACCURACY



# PLATFORM-TO-GROUND IONOSPHERIC TOMOGRAPHY



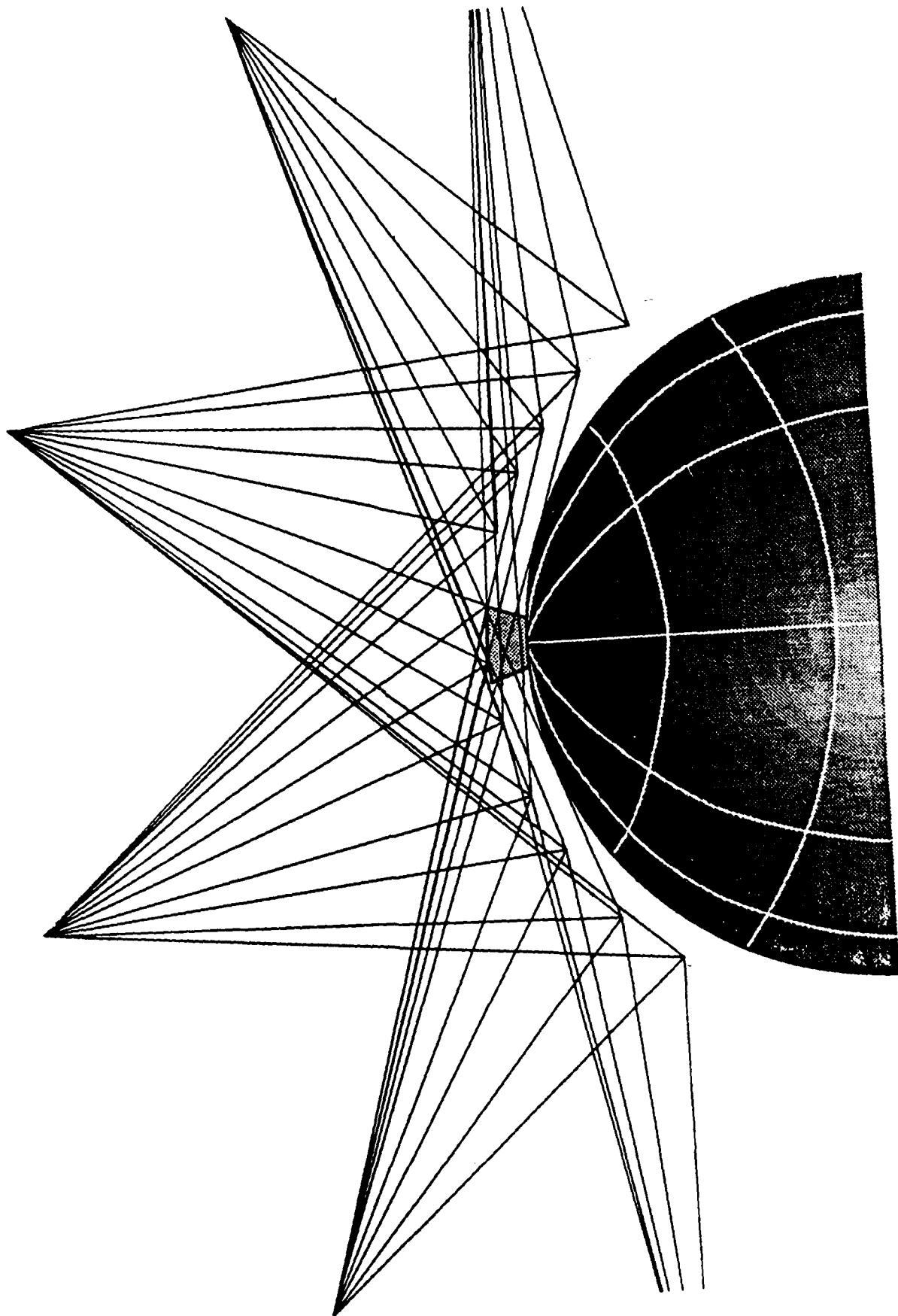
$$\pm 10^{16} \text{ el/m}^2 = 16 \text{ cm}$$

$$\pm 10^{15} \text{ " } \approx 2 \text{ cm}$$

$$\pm 10^{14} \text{ el/m}^2 \text{ for } \Delta \varphi \approx 2 \text{ mm}$$

with smoothing peak against carrier  $\approx 0.9$  of  $\frac{dV}{V}$   
 $\approx 0.5\%$  of  $\frac{dV}{V}$

# ADDED COVERAGE WITH ONE ORBITING RECEIVER



# ACOUSTIC GRAVITY WAVE DETECTION IN THE IONOSPHERE

AGWs CAN BE CAUSED BY:

EARTHQUAKES

VOLCANIC ERUPTIONS

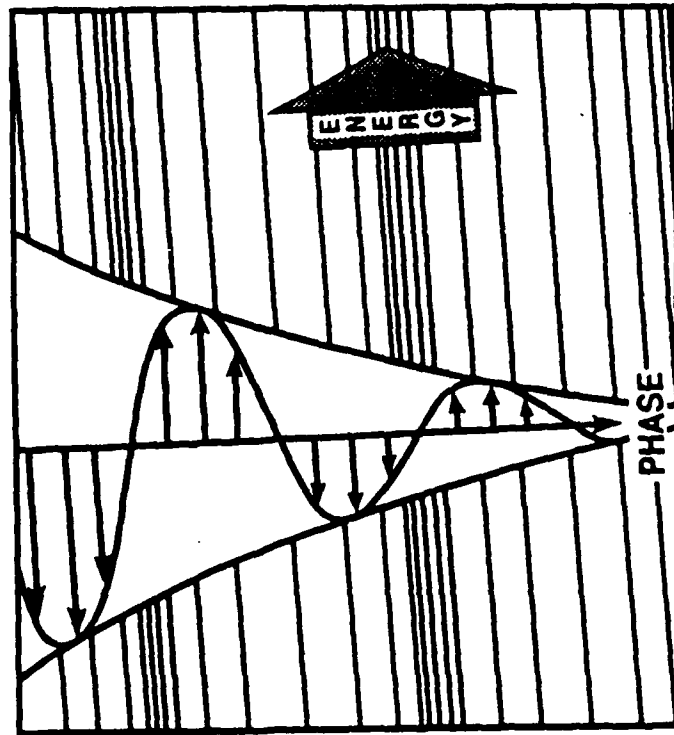
TSUNAMIS

STRONG WIND SHEAR

DISTORTION IN JET STREAMS

CONVECTIVE STORMS & FRONTS

AURORAL RELATED EVENTS



# **JPL** OFFICE OF SPACE SCIENCE AND INSTRUMENTS

<b>DIRECTOR'S REPORT AND DISCUSSION</b>	<b>GPS GEOSCIENCE INSTRUMENT FOR EOS AND SPACE STATION</b>	<b>PRESENTATION DATE: February 27, 1989</b>
---	--	---

## **PRINCIPAL SCIENCE OBJECTIVES**

PROVIDE 1 m REAL TIME POSITION & 20 arcsec REAL TIME ATTITUDE TO SUPPORT POINTING OF OTHER SCIENCE INSTRUMENTS

PROVIDE 1-3 cm POST PROCESSING ORBIT ACCURACY TO SUPPORT OCEAN ALTIMETRY AND OTHER PRECISE EOS INSTRUMENTS

IMPROVE PRECISION AND TIME RESOLUTION OF GROUND BASELINE MEASUREMENTS TO ENABLE MONITORING OF POST-SEISMIC STRAIN REDISTRIBUTION

PROVIDE 2000 DAILY PROFILES OF ATMOSPHERIC DENSITY, PRESSURE & TEMPERATURE FOR STUDYING REGIONAL AND GLOBAL CLIMATIC CHANGE

DETECT AND ANALYZE ACOUSTIC GRAVITY WAVES IN THE IONOSPHERE, CAUSED BY SEISMIC, VOLCANIC, TSUNAMI, AND A VARIETY OF ATMOSPHERIC PHENOMENA, TO LEARN MORE ABOUT THESE EVENTS AND STUDY THE FLOW OF ENERGY THROUGHOUT THE EARTH SYSTEM

PERFORM 3-D IONOSPHERIC TOMOGRAPHY TO STUDY THE STRUCTURE AND VARIATION OF BOTH LONG-LIVED AND TRANSIENT IONOSPHERIC FEATURES





## THE GPS PRECISE ORBIT DEMONSTRATION (POD) EXPERIMENT

E.S. (Ab) Davis  
JET PROPULSION LABORATORY

An experiment will be conducted by JPL to evaluate the performance and operational potential of using GPS to determine very precise orbits of Earth-orbiting satellites. The satellite mission TOPEX/POSEIDON will serve as catalyst - its primary operational orbit determination will be accomplished by a laser tracking system. The goal is to demonstrate sub-decimeter accuracy with GPS.

TOPEX/POSEIDON is to be launched aboard an ARIANE rocket some time in 1992 and achieve a circular orbit at 1334 km altitude and 63° inclination. The experiment requires observation of L1 and L2 pseudorange and carrier phase using a 180° field-of-view antenna tracking up to six satellites from rise to set with an accuracy of better than 1 cm in the phase and 10 cm in the range. The data will be processed in the double-difference mode from three to six ground stations of the DSN network (whose positions must be known to better than 5 cm; this is achievable using VLBI).

The data set will consist of 90 days' worth of GPS tracking data which will be used to simultaneously solve for the orbits of the 21 GPS satellites and TOPEX/POSEIDON, as well as the ground stations. All software modeling will be done at the subcentimeter level. It is estimated that with 3 ground stations, the orbital uncertainty is comparable to the accuracy obtainable with the laser tracking system (15 to 25 cm), but will improve to 5 to 10 cm using all six ground stations.

The important data collected for post processing are the L1 and L2 phase and pseudorange time-tagged to within a microsecond. The estimated performance of the flight receiver with respect to random and uncalibrated systematic errors is expected to exceed all requirements for Doppler and pseudorange, as well as TOPEX clock calibration, by a wide margin, except in the case of the systematic error for Doppler which is just outside the margin of our requirement. This will require corrective measures during post processing but we do not foresee any problem in doing this.

The GPS antenna design on the TOPEX satellite is driven by the field-of-view requirements. Originally, directly on top of the satellite, where it was subjected to severe multipath signals from the TDRSS antenna and solar panel, the GPS antenna now is located on a boom to suppress the multipath 20 db below the direct signal.

The strategies for processing the data to produce the POD results include the dynamic solution, the kinematic solution (geometric), and a combination of these. Using two-hour and six-hour arcs and considering the sensitivity (of the dynamic solution methods) to uncertainty in the gravity model, all methods will achieve subdecimeter accuracy. The longer arcs will yield better accuracy.

The POD experiment relies on the efforts of many groups including DOD (responsible for deploying GPS) and the international organizations responsible for filling out the six-station DSN network. The flight receiver is currently in the hardware integration phase and at JPL the POD software is in the coding phase.

Discussion:

Question: On the multipath viewgraph, where is the direct signal and where is the multipath signal?

Answer: The dots correspond to the direct signal. For a particular zenith angle, if there is a direct signal from a satellite then the multipath associated with that signal is plotted directly below the dot even though the zenith angle of the multipath is different.

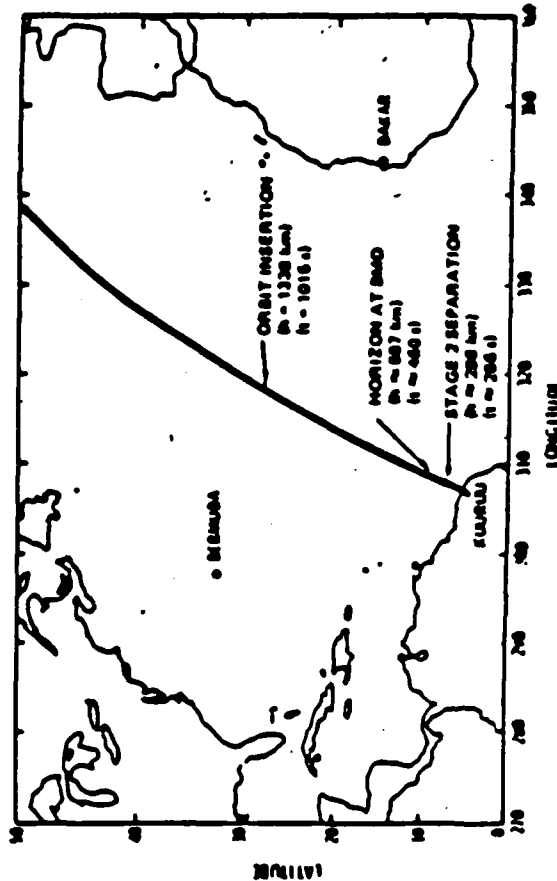
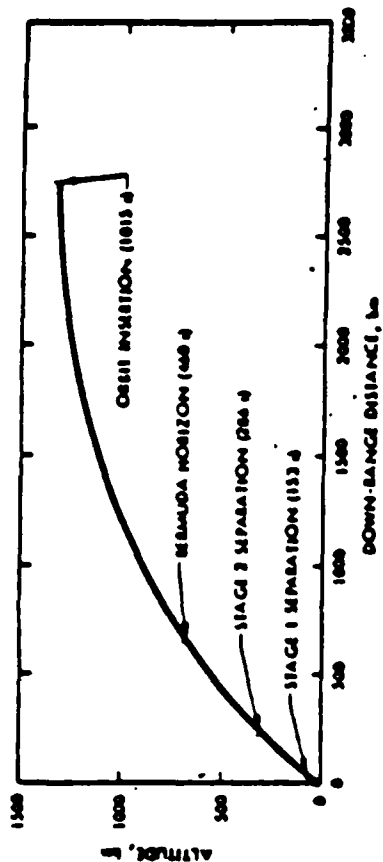
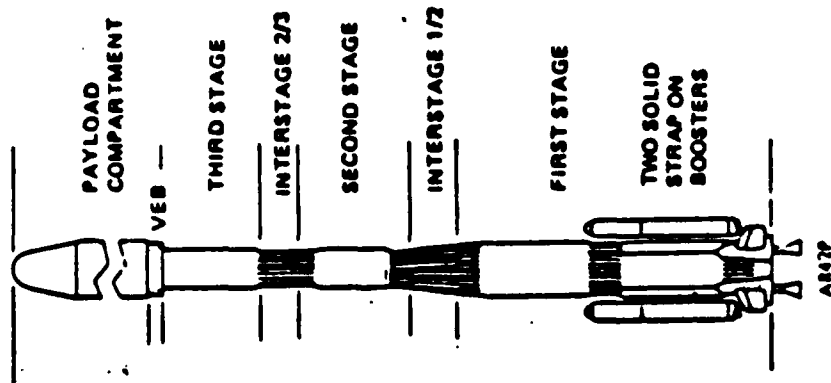
Question: Can you predict the multipath reasonably well knowing the geometry of the satellite and make corrections?

Answer: We're not sure of the accuracy of this multipath model. We first need real data to calibrate the model geometrically; then we could do what you suggest.

**TOPEX**

*Gps-Based Pod Experiment*

# TOPEX/POSEIDON MISSION



## **GOALS AND OBJECTIVES**

### **PRIMARY GOAL :**

- Evaluate performance of a new system for tracking earth satellites based on the Global Positioning System (GPS)
  - Accuracy
  - Operational potential

### **OBJECTIVES:**

- Demonstrate sub-decimeter topex orbit accuracy with 9 10-day arcs of GPS tracking data
  - < 15 cm accuracy with 3 GPS ground stations  
( 15 to 25 cm accuracy expected)
  - < 10 cm accuracy with 6 GPS ground stations  
( 5 to 10 cm accuracy expected)

## **TOP-LEVEL SYSTEM REQUIREMENTS**

### **OBSERVATIONS: FLIGHT & GROUND**

- Pseudorange & phase measurements on L1& L2
- Omni antennas: ~ 180 degree FOV
- Continuous GPS SV tracking from rise to set
- Carrier measurements are phase-connected
- Accuracy: phase < 1cm ; range <10 cm (with multipath)
- Multiple SV's tracked: Gnd Rcvr's -8; Flight Rcvr- 6

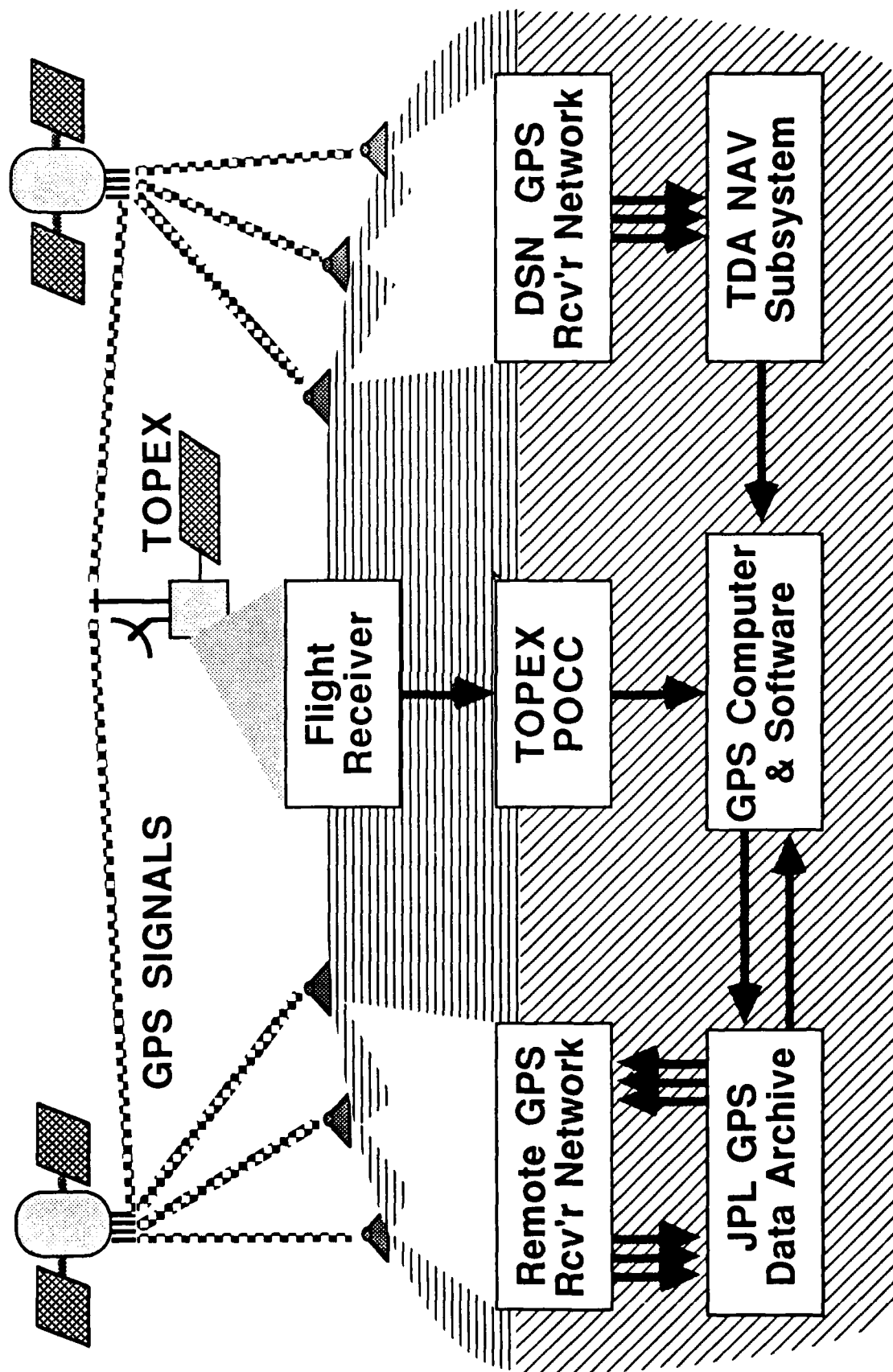
### **GPS DATA PROCESSING FACILITY**

- 3-station DSN network
- 6-station DSN-managed international network
- Positions of GPS receivers in DSN must be known to <5cm
- Data processing to run at a real-time rate: ~15 VAX 11/780's

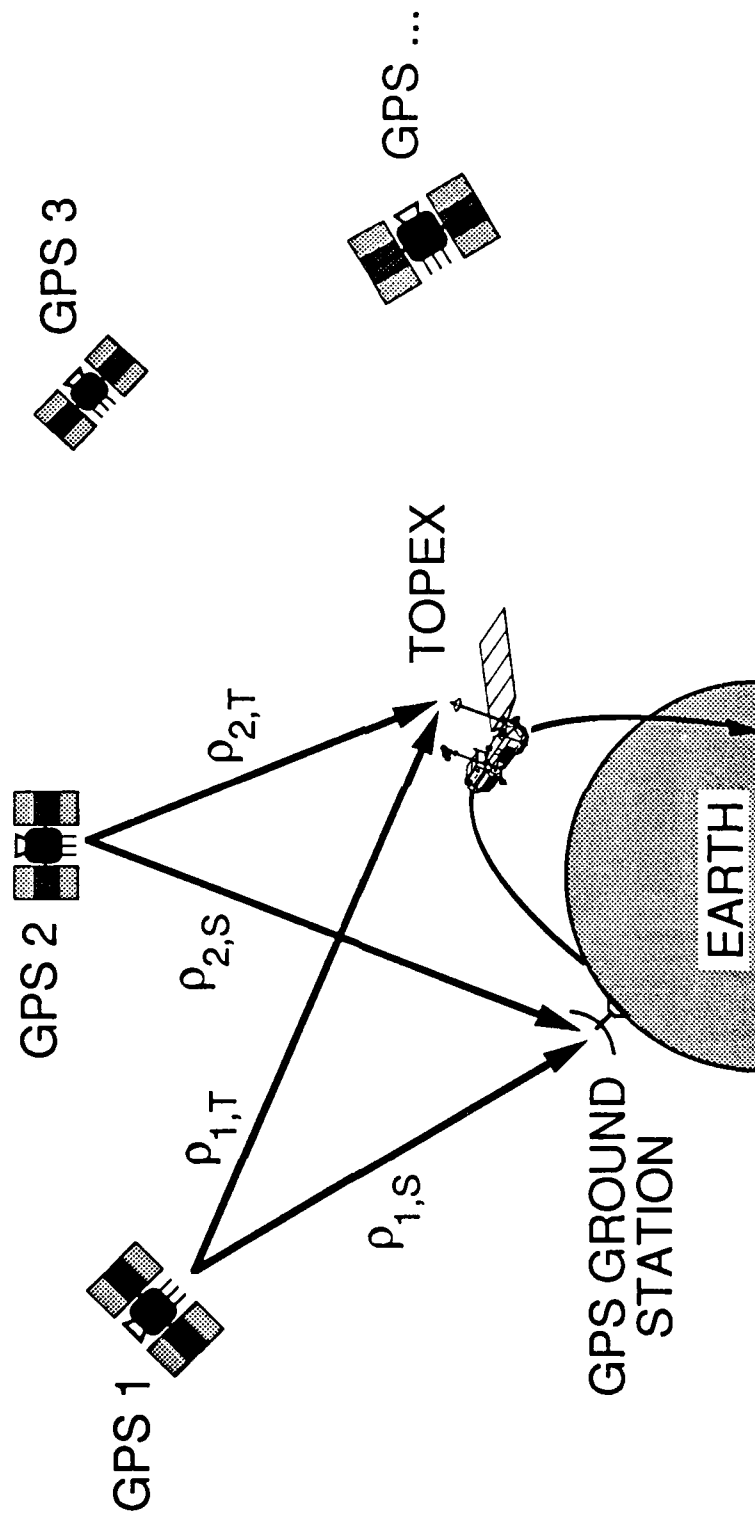
### **PRECISION ORBIT DETERMINATION**

- Subcentimeter modeling in S/W
- Simultaneous solution for 21 GPS SVs ,TOPEX, & ground sites
- Preliminary assessment due @ launch +9 months

# SYSTEM ELEMENTS



## GPS METRIC OBSERVABLE



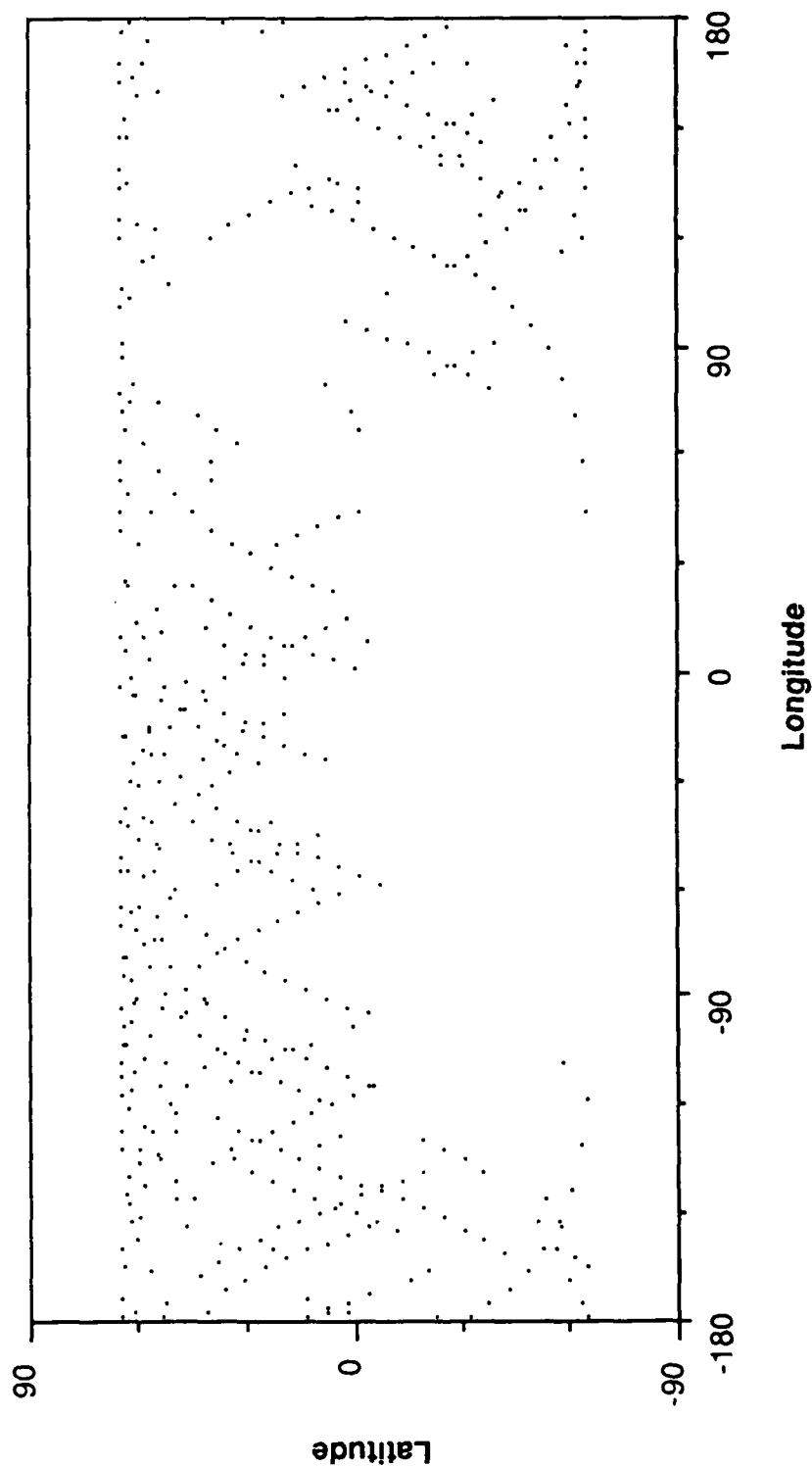


# GEOGRAPHIC COVERAGE OF A 3-STATION NETWORK

48hrs

160° View Window

Double-differenced data available from at least 4 or more GPS SVs

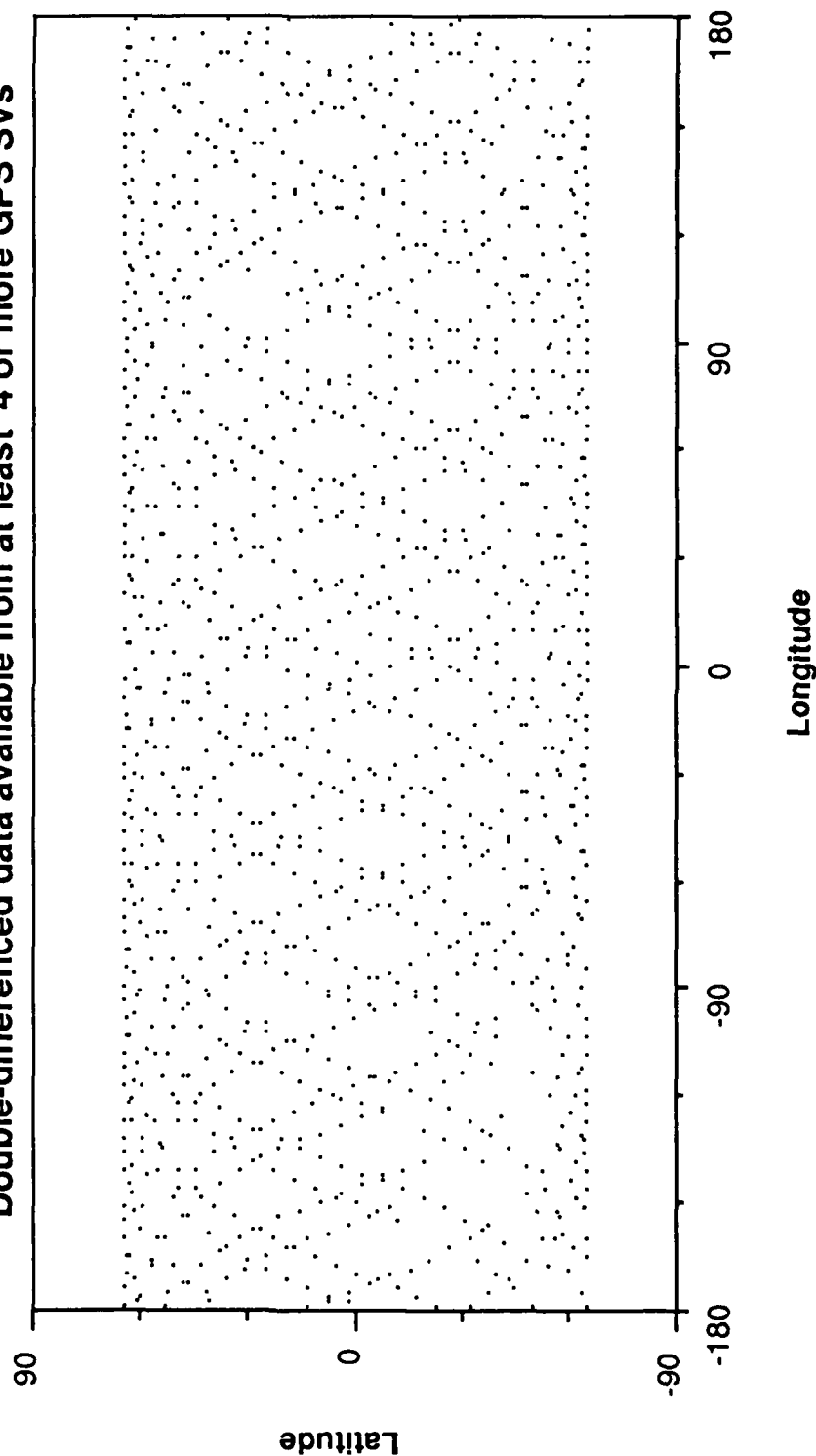


# GEOGRAPHIC COVERAGE OF A 6-STATION NETWORK

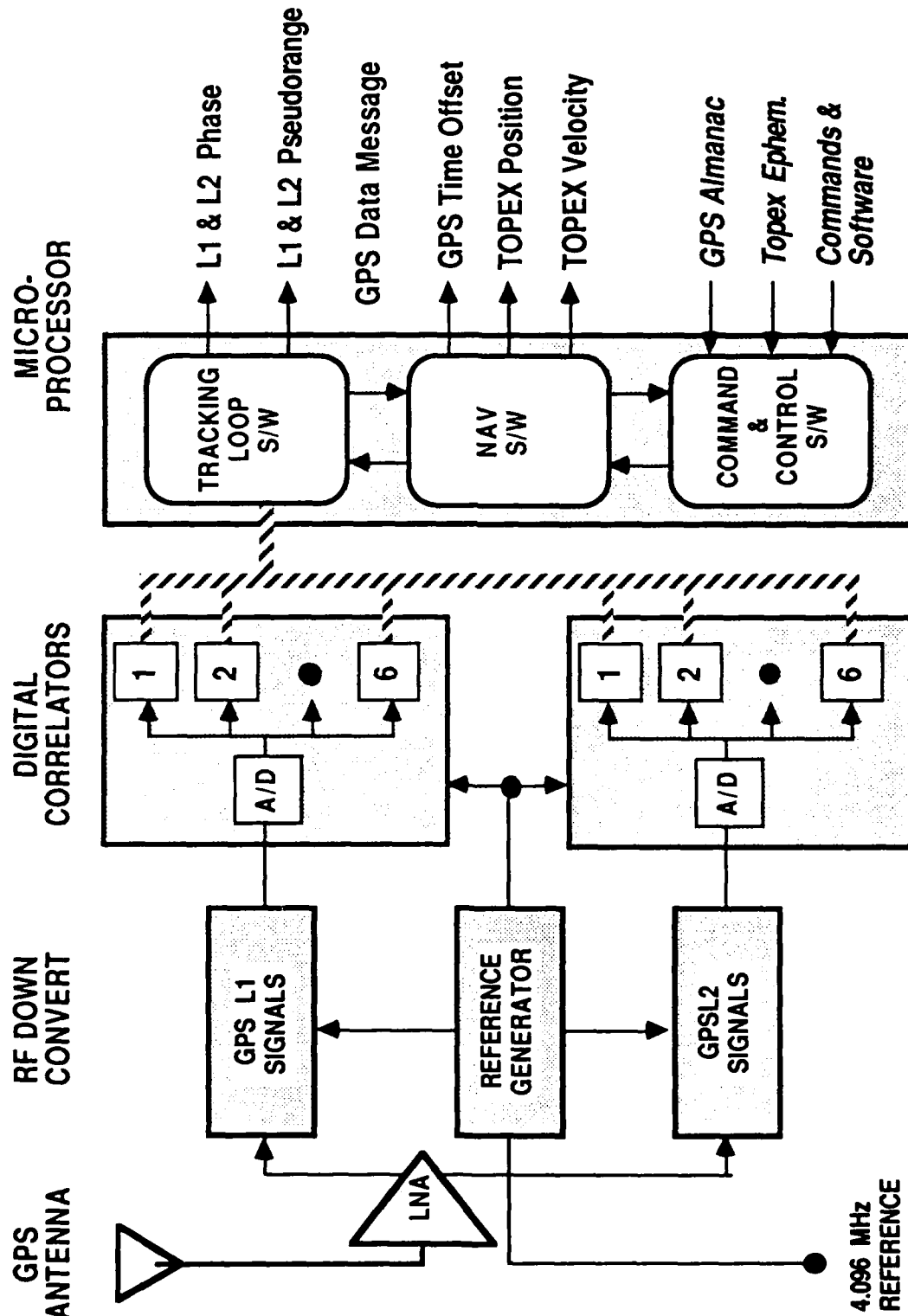
48hrs

160° View Window

Double-differenced data available from at least 4 or more GPS SVs



# GPSDR ARCHITECTURE



# GPSDR PERFORMANCE

## EXPERIMENT REQUIREMENTS ESTIMATED GPSDR PERFORMANCE

### TIME OFFSET MEASUREMENT

TOPEX Calibration	<10 microsec	.5 (SA on)
GPSDR Time Tag	<.5 microsec	.015 (SA off)

### CONTINUOUS CARRIER PHASE

Random Error	- <1 cm	.15	.16	.11
Uncalibrated Systematic	- <0.5 cm	-	-	-
<i>Maximum Systematic</i>		.71	.5	.7

### PSEUDORANGE

Random Error	<60cm	<300cm	13	13	130
Uncalibrated Systematic	- <10 cm	-	<1	<1	<1

## **GPSDR CHARACTERISTICS**

### **FIELD-OF-VIEW REQUIREMENTS:**

**4 GPS SVs are needed to update on-board ephemeris**

**$\pm 80$  degree cone needed to operate 99% of the time**

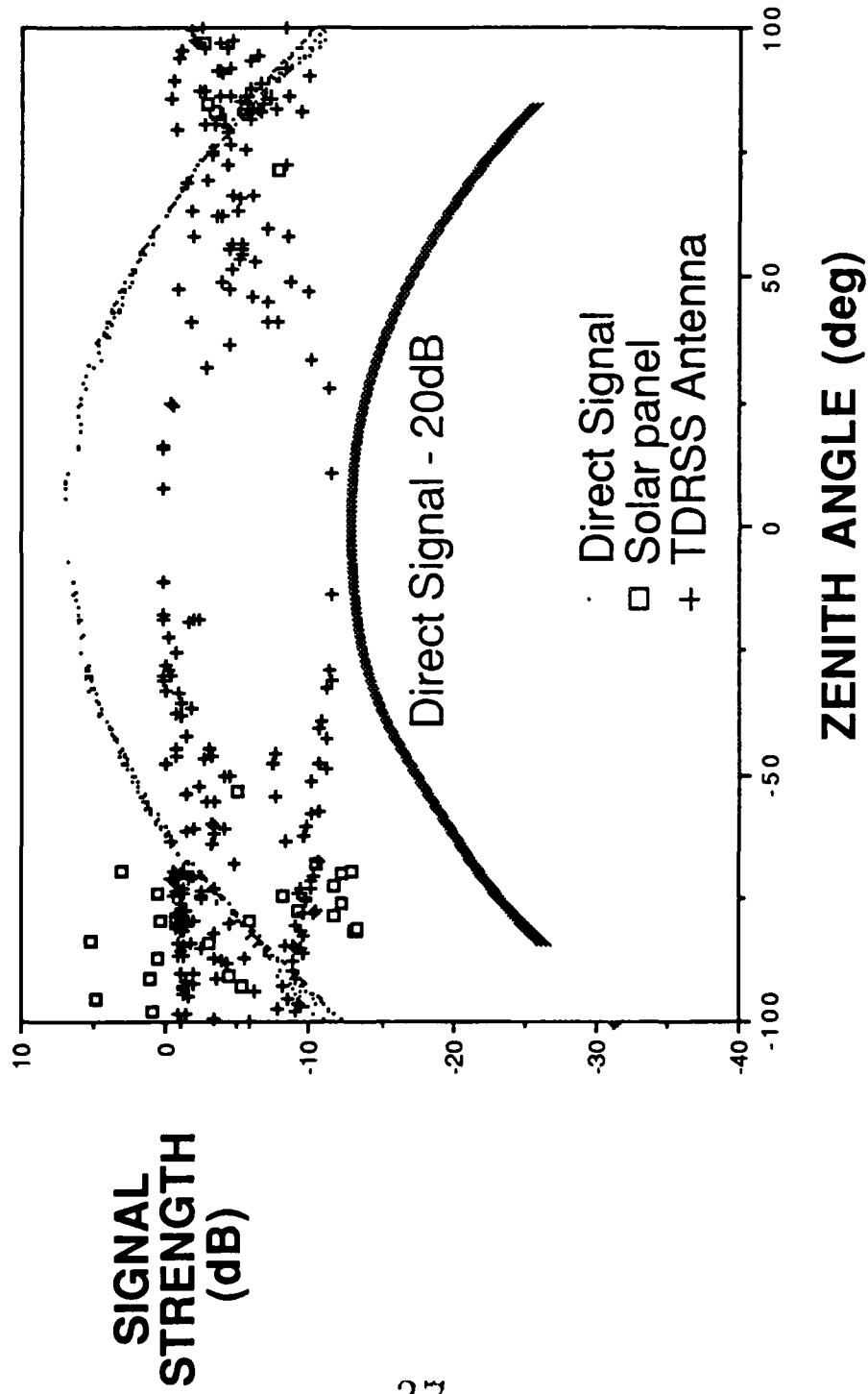
### **OPERATING REQUIREMENTS:**

**Software is uploaded from the ground -- uplink time=30 minutes**

**Needs initial TOPEX ephemeris -- accurate to 50 km**

**Initiated by transmitting GPS time -- accurate to 1 second**

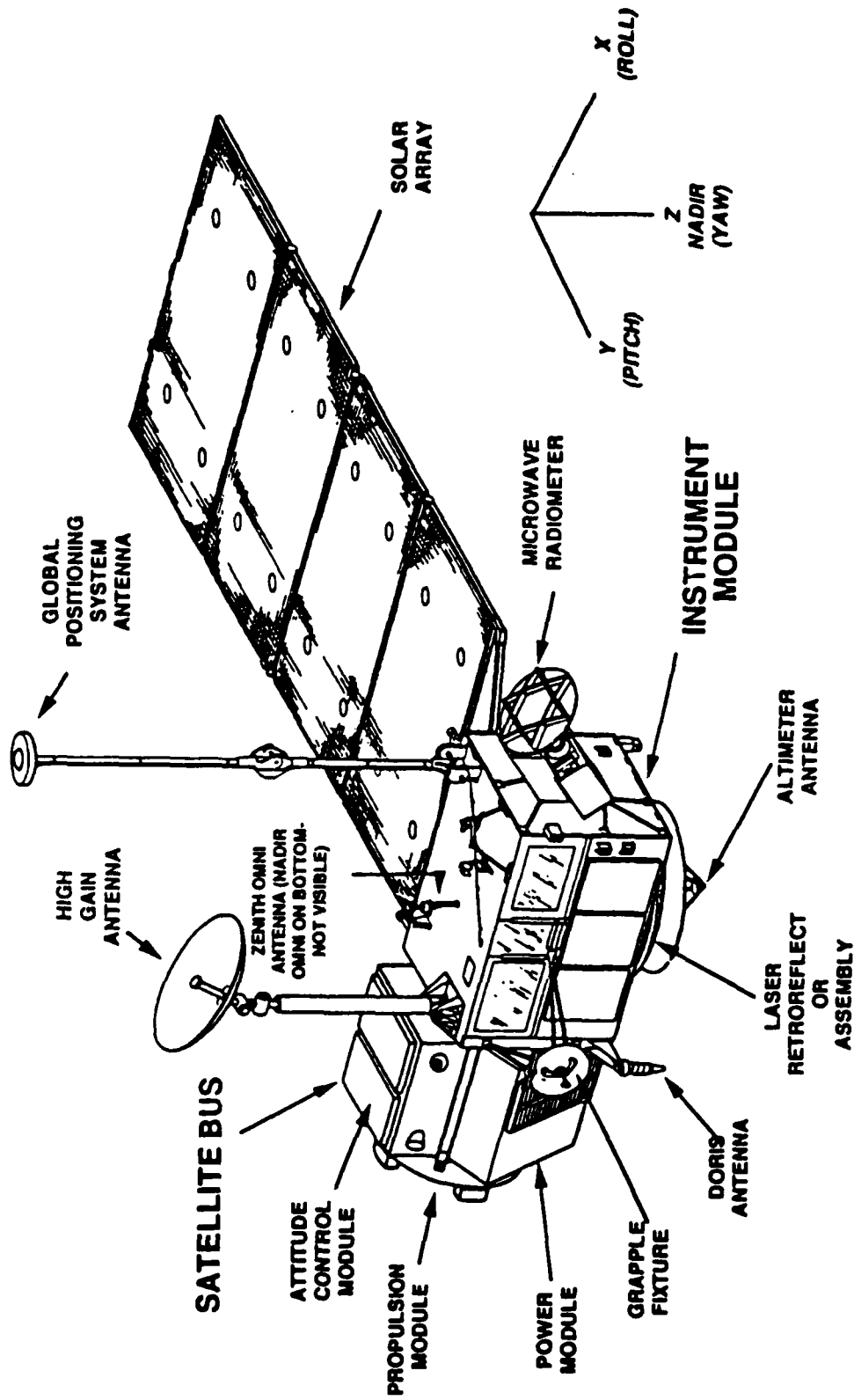
# GPS MULTIPATH - 0.0-m BOOM



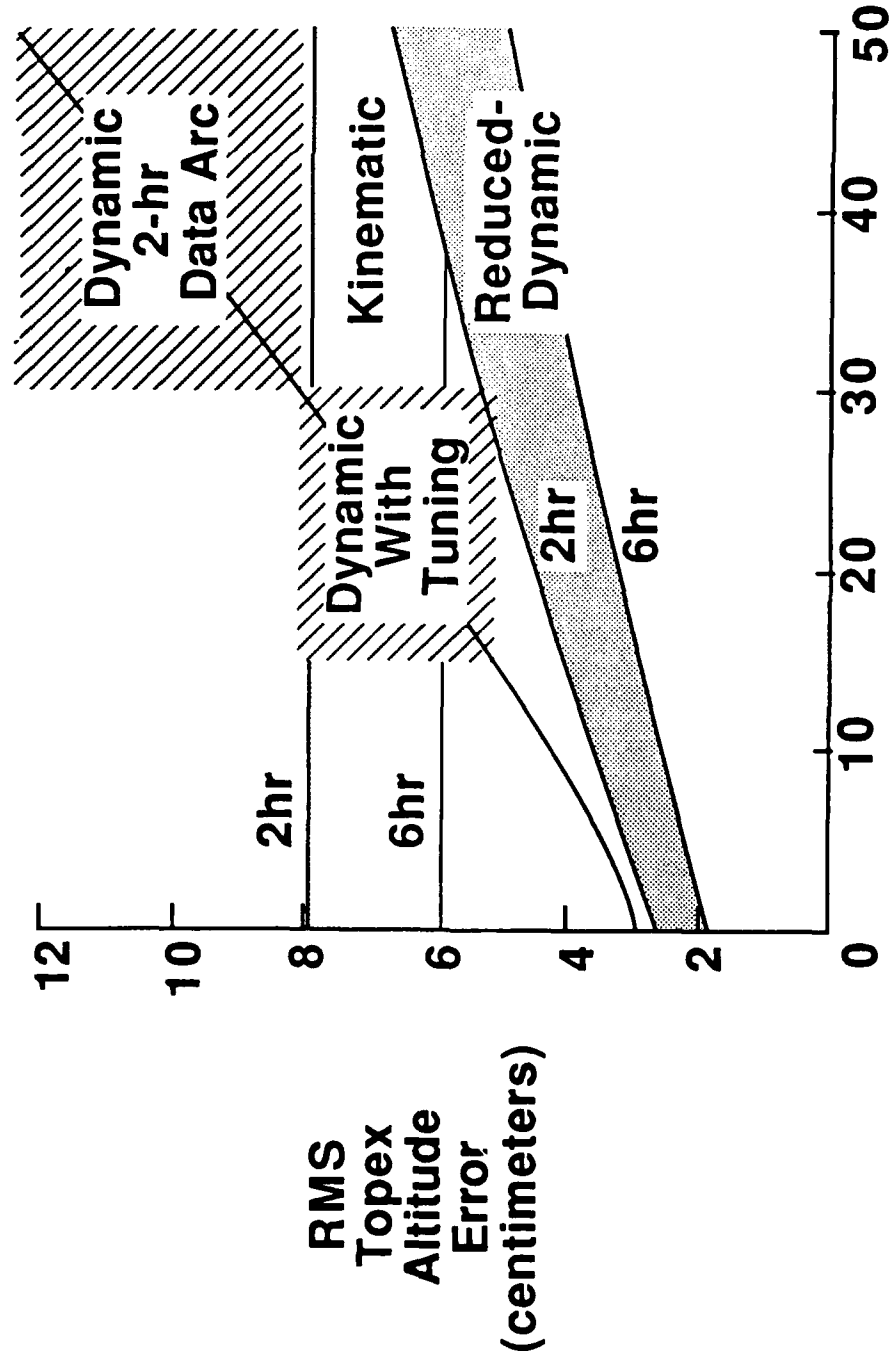
**TOPEX**

*Gps-Based Pod Experiment*

# TOPEX/POSEIDON SATELLITE



# GPS POD PERFORMANCE



**Gravity Model Uncertainty (% of GEM10-GEML2)**



# GPS-Based POD Experiment

## TOP-LEVEL SCHEDULE

Block II Schedule, March 1989

	87	88	89	90	91	92	93	94	95	96
DEPLOY GPS BLOCK II (DoD)										
GPS RECEIVERS FOR THE DSN (T)	START PROTO-TYPE IONOSPHERE CALIBRATION OPERATIONAL PROCUREMENT									
GPS REMOTE NETWORK										
GPS GROUND DATA PROCESSING FACILITY (T)	COMPUTERS CONNECT TO TERMINALS OF COOPERATING AGENCIES									
DSN MULTIMISSION NAVIGATION SOFTWARE DEV.(T)	DSGN / CODE / TEST									
GPS FLIGHT RECEIVER AND ANTENNA (E)	DELIVERY LAUNCH CONTRACT									
GPS POD SOFTWARE (E)	RQTS / DSGN / CODE / TEST									
GPS POD DATA ANALYSIS (T/E)	INITIAL ASSESSMENT FINAL REPORT									
TOPEX POSEIDON MISSION (E)	LAUNCH 3-YR MISSION EXTEN									

09-26-89

**GPS-BASED POD: A TOPEX FLIGHT EXPERIMENT  
GROUND RECEIVER REQUIREMENTS**

- PRECISION TIMING SIGNALS
  - NASA's DSN SITES HAVE HYDROGEN MASERS
  - DMA GROUND TERMINALS HAVE CESIUM FREQUENCY STANDARDS
- RANDOM COMPONENT OF ERROR ..... 1.2 CM
  - ZENITH TROPOSPHERE DELAY ..... 1.0 CM
  - WATER-VAPOR RADIOMETERS (WVR)
- PSEUDO-RANGE ACCURACY FOR THE DSN GROUND RECEIVERS
  - RANDOM COMPONENT (1 SECOND, 1 SIGMA) ..... 22 CM
  - SYSTEMATIC COMPONENT (2 HOUR, 1 SIGMA) ..... 4 CM
  - MULTIPATH (PEAK)
    - FOR PERIODS < 5 MINUTES ..... 30 CM
    - FOR PERIODS > 30 MINUTES ..... 5 CM



## NRL ACTIVITIES ON SPACEBORNE GPS RECEIVERS

Ronald L. Beard  
NAVAL RESEARCH LABORATORY

For the last couple of years, under an Air Force project, we have been looking at the development of a generic GPS receiver for military space applications capable of very precise attitude determination. The original accuracy requirement was at the microradian level using GPS alone without inertial aiding.

One of the major challenges was to use the Virginia Slims concept which calls for a very small, unobtrusive receiver which would be easily integrated into a generic system. One of the problems with this is the broad range of user satellite configurations. Other problems include the stringent requirements for radiation hardening. A significant aspect was our desire to integrate this with a rubidium standard in order to get a very low noise coherent signal source.

The current status of the development is in the first out of three phases concerning definition and design. In this phase we plan to do a ground demonstration to determine experimentally what sort of attitude accuracy we can get from this receiver. The results of these tests will go toward developing a flight model which will eventually be flown and tested.

The candidate, generic user that we have identified is a satellite in a 700 km polar orbit with good antenna field of view assuming the full GPS constellation is up. We assume that 3 to 6 antennas will be available with a maximum baseline of 5 m. We have allowed for a variety of geometries for the antenna locations but assume the satellite to be very rigid (one cannot tolerate bending of booms etc. for this type of accuracy).

The basic design is assumed to be a two frequency system with low multipath, completely digital (digitize as soon as possible to eliminate receiver biases). We assume a set of 15 - 20 continuous channels so that we would be looking at every channel simultaneously. The antennas, we believe, will offer the greatest technical problem, specifically with respect to eliminating the multipath.

The design concept allows continuous attitude determination without inertial aiding, however we are expanding our investigation to include inertial system interfaces. We have also evaluated some of the different commercial and spaceborne rubidium standards. We originally thought to use small militarized units, but due to their instability, turned to EG&G to have them redo the rubidium units they developed for GPS with some improvement to meet our specifications.

We have done some experiments with our (NRL) receivers, as well as the Motorola Golden Eagle receivers (on loan). Some of the results using the Motorola receivers are shown in the figure, where with double differencing to eliminate as many errors as possible, we got residuals in baseline determination of about 10 to 20 mm. In order to do attitude determination in the microradian regime, one would have to do at least an order of magnitude better.

I want to mention some related efforts at NRL. NRL is also the Naval Center for Space Technology (NCST). There is a project called Sea Launch and Recoverable Booster System where rockets are launched out of the water to put satellites in orbit and the stages are recovered. The concept is only in the beginning phases and includes using GPS for inertial alignment before the launch and for trajectory inertial guidance on the way up. We also provide the Office of Naval Research with engineering and technical support on some of their contracts, specifically one with Rockwell which is designing a receiver using DARPA's Chipset for the ONR's SPINSAT.

Discussion:

Question: What was your motivation to use GPS alone rather than with an inertial system?

Answer: The sponsor, the GPS Joint Program Office, wanted to see how much one could get out of GPS.

Question: What is the requirement in terms of accuracy on carrier phase. How does this translate into attitude accuracy? I think there are better results on baseline accuracy than what you showed - are those 1 second samples?

Answer: The Motorola data were 6 second samples. If you work through the calculations, you'll find that a 5 m baseline needs to be known to 6 microns for microradian attitude accuracy. This is a rather difficult goal to meet. These were just examples, there may be better results.

Question: Do you have each of the 3 - 6 antennas feeding to more than one channel or each of the 15-20 channels receiving signals from more than one antenna?

Answer: All antennas feed into one receiver, so you might have four different channels for one antenna.

## **Performance Requirements**

- \* Positioning - < 10 m - 3 D Absolute, < 1 m - 3D Relative
- \* Velocity - < 0.1 m/s 3 D
- \* Attitude - 1 mrad to 1 microrad
- \* Timing - < 100 ns UTC (USNO)
- \* Data Interface - GPS standard

## **GPS SPACEBORNE RECEIVER**

### **Hardware Requirements - Generic Design for Military Satellites**

- \* Size - Virginia Slims concept**
- \* Weight - < 15 lbs**
- \* Power - < 25 watts**
- \* Host Vehicle Interface - SGLS**
- \* Integral Rb Standard**
- \* Radiation hardened - Milstar Levels**
- \* Selective Availability/Anti-Spoofing**
- \* Lifetime - 5 to 10 Years (Host Requirements)**

## **PROGRAM PHASES**

### **Phase 1: Definition and Design**

Define Requirements and Characteristics  
Survey Industry and Receiver Manufacturers  
Procure Evaluation Equipment (e.g. Small Rubidium)  
Initial Definition of Flight Testing Methodology  
Ground Demonstration Experiment

### **Phase 2: Develop Flight Model**

Contract

Ground Testing

### **Phase 3. Flight Testing**

Integrate Receiver into Host Vehicle  
Refine Methodology of Testing  
Perform tests



## USER PARAMETER DEFINITION

- \* Baseline Altitude 400 n. mi., Polar orbit
- \* Good GPS Satellite antenna coverage and number in view
- \* Spacecraft antenna designs
  - Maximum Baseline 5 meters
  - Spacecraft Geometry
  - Number of antennas (3-6)
  - Spacecraft structural considerations (rigidity, attitude control )
  - Other Limiting Factors

## TECHNICAL APPROACH

### General Design Specifications

- \* **Antenna subsystem**
  - L1 and L2
  - Low profile with low multipath ground plane
  - Pre-amp, A/D at or close to antenna
- \* **Receiving subsystem**
  - Multi-channel (15 - 20, 2 freq channels) coherent carrier tracking
  - C/A and P codes, SA/AS
  - All digital design
- \* **Computer**
  - Optional host interfaces
  - Redundant

## TECHNICAL APPROACH

### Major Technical Problems

- \* Antennas

- Geometry (dependent on host vehicle)

- Multipath

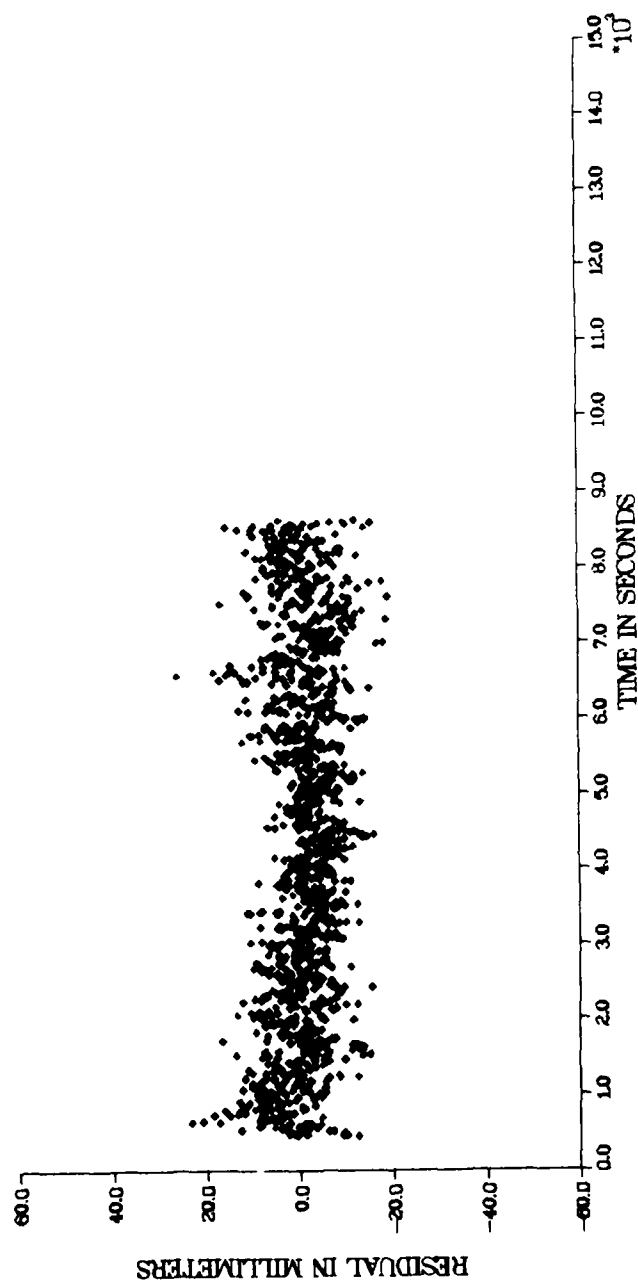
- Stable phase center

- Interference (Jamming)

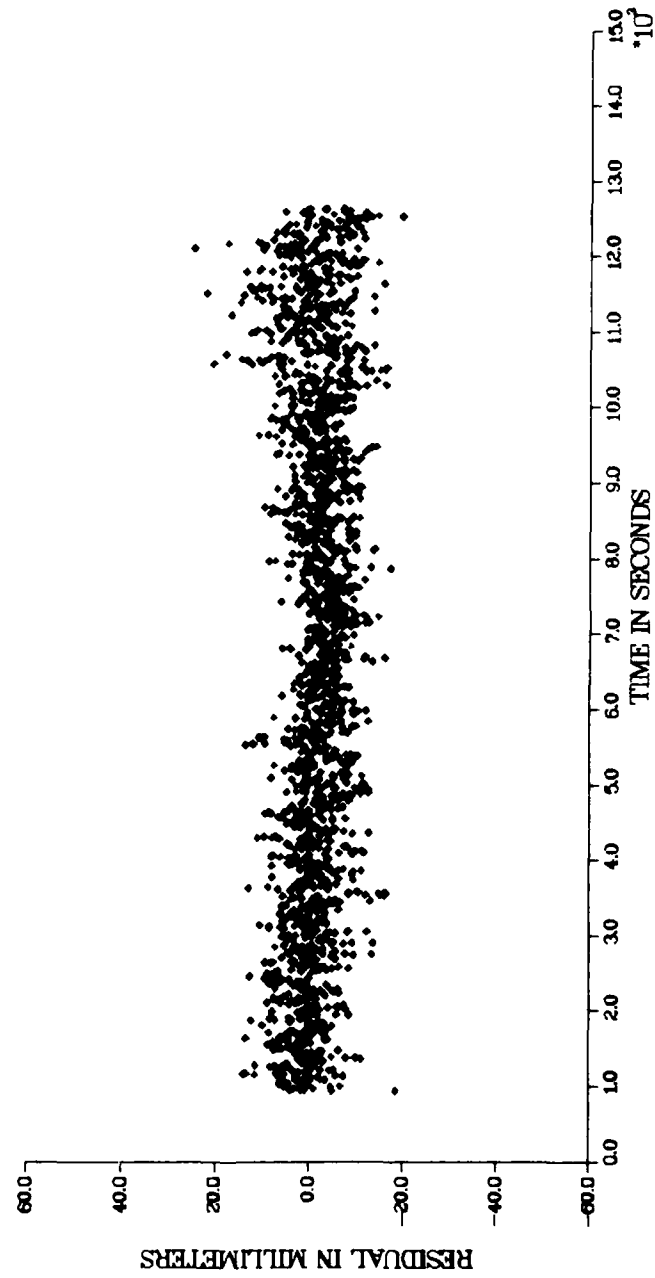
## CONCEPT DEFINITION

- \* Preliminary design concept developed
  - 15 - 20 channels with 3 - 6 antennas
  - Error sources for interferometric receiver
  - Preliminary specifications
  - Ionospheric evaluation
  - 1750 A microcomputer chosen
- \* Receiver Survey
- \* Rubidium Evaluation
  - Small militarized units
- \* Experimental receiver data
  - NRL Time transfer receiver
  - Motorola receiver
  - NOAA data collection

SATELLITES 03/11, ON JUNE 14/15, 20 METER BASELINE



SATELLITES 11/13, ON JUNE 14/15, 20 METER BASELINE



## **GPS SPACEBORNE RECEIVER**

### **Contracts**

- \* Mayflower Communication Inc.**  
Examine conceptual work for software development  
Major thrust to be interface definitions
- \* Rubidium Hardware**  
EG&G selected  
To deliver qual and two experimental flight units  
First delivery in 12 months, final at 24 months

## **GPS SPACEBORNE RECEIVER**

### **Related Efforts**

- \* **NSTC Initiative in sea launched booster system**
  - Use GPS and Inertial for guidance
  - GPS attitude for inertial alignment before launch
- \* **SPINSAT Receiver - Small Satellite Altimeter (SALT)**
  - Rockwell to build Receiver with DARPA Chipset
  - Launch in Spring 1990





GL'S PROPOSED SATELLITE-TO-SATELLITE TRACKING MISSION USING GPS:  
STAGE (STS-GPS TRACKING FOR ANOMALOUS GRAVITATION ESTIMATION)

Christopher Jekeli  
GEOPHYSICS LABORATORY (AFSC)

This paper builds on a similar presentation given at the first GPS symposium on applications in space; it attempts to better define the mission concept and some results of an error analysis based on a refined error budget are also given.

In concept, the Shuttle is to be tracked by the constellation of GPS satellites thus yielding the total acceleration vector of the Shuttle with respect to the GPS satellites. An IMU on board the Shuttle will sense all non-gravitational forces and these data are subtracted from the GPS-derived accelerations to obtain the gravitational signal. The STAGE mission is primarily a demonstration since the Shuttle presents the least desirable environment for precise gravitation measurements. On the other hand, it offers a low-cost, low-altitude, and hardware-retrievable opportunity to test the integration of GPS and IMU for a variety of applications.

The essential hardware for the mission includes a GPS receiver, an IMU (two TDF gyros and a three-axis accelerometer package), a microprocessor, and a recorder. Although two antennas are available on the Shuttle, only one is required for STAGE (two can be used for other applications). Two options for data retrieval are built into the system to allow flexibility with Shuttle integration (telemetry, probable not permitted on the Shuttle, and onboard recording of data).

The error budget for a single line-of-sight acceleration component at altitude has been refined from previous presentations. The erstwhile dominant error due to satellite clock bias can be eliminated by performing single difference observations; all error sources now contribute approximately equally (hence, optimally) yielding a total error for single differences of about 0.3 micro-g. It is noted that the IMU errors shown here represent performance levels for the relatively noisy Shuttle. Much less IMU error is expected on a free-flyer. It is also noted that the differential tracking technique (either single or double differences) does not require tracking the Shuttle from the ground (see figure); therefore, only a few, say six, globally distributed tracking stations are needed and are, in fact, already in existence for GPS.

A covariance analysis was performed to estimate the accuracy of calculating gravity on the Earth's surface from gravitation data at altitude. Both STAGE and a polar-orbiting, free-flyer at 160 km altitude (GEN-GPS) were considered. Although STAGE would yield quite respectable accuracies and definite improvement in gravity models where today few data exist (such as Asia, Africa, S. America), the full benefit can be realized with a free-flyer at the lower altitude. Further enhancement of the error budget could make this a very attractive alternative to other currently envisaged gravity mapping missions.

Originally designed for gravity field measurement, our proposed IMU/GPS system clearly has a synergism demonstrable for other applications. In particular, its utilization for real-time navigation, tracking and attitude control would benefit missions requiring rendezvous and docking maneuvers, as well as space-based surveillance and radar.

Discussion:

Question: Is the 1 m position accuracy of the Shuttle only for the case when the shuttle is in the non-thrust mode? Can the orbits during which it is quiet be disjoint?

Answer: When the shuttle is in the thrust mode, it will probably be too noisy an environment to make precise gravitational measurements. Any data we can get, even for a number of short disjoint periods of time, will be useful to demonstrate the concept which is the minimum goal of using the shuttle.

Question: Are the quoted gravity anomaly error estimates for anomalies on the earth's surface?

Answer: Yes.

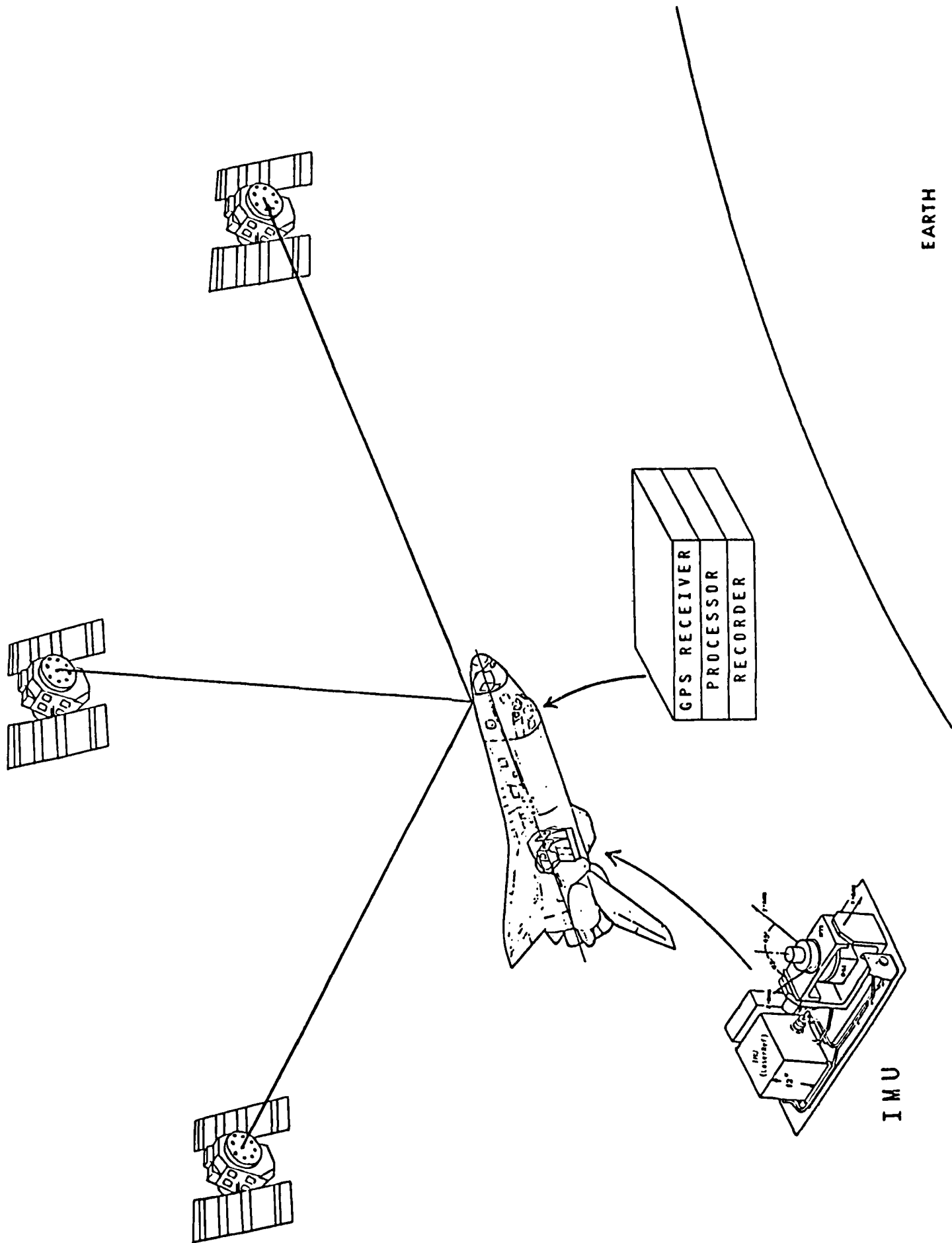
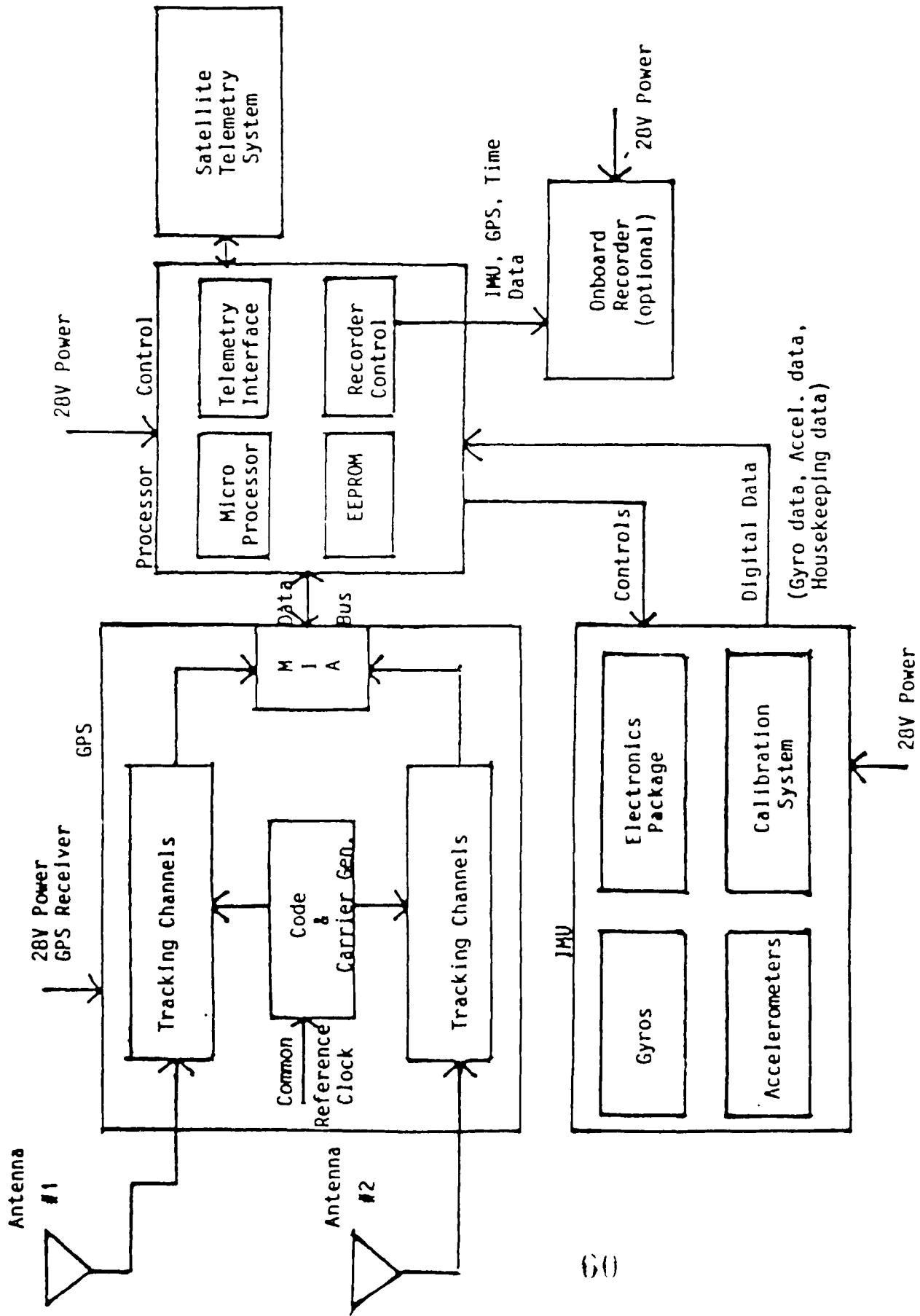


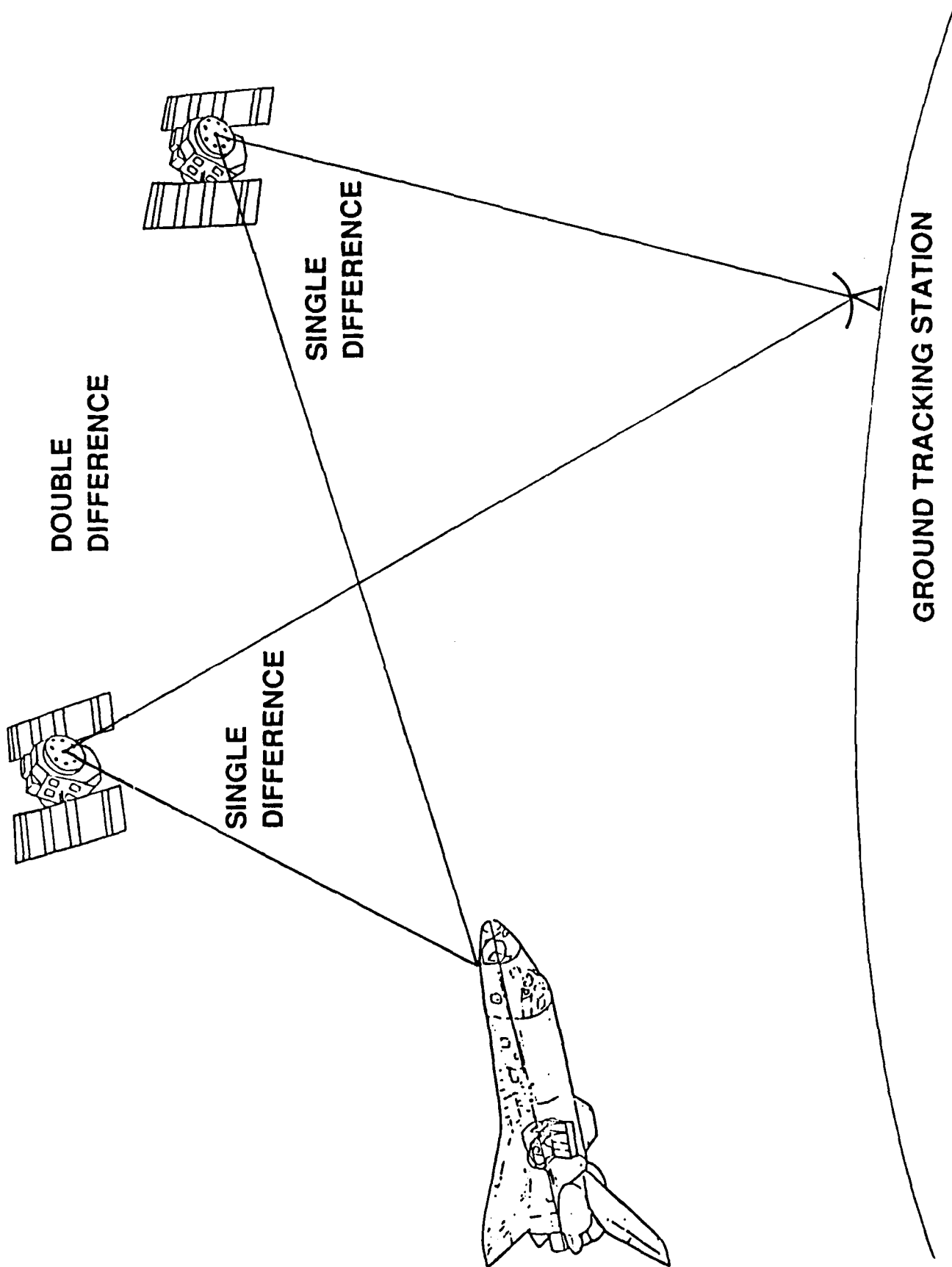
FIGURE 1: STAGE MEASUREMENT SYSTEM



MIA: Multiplex Interface Adapter

Error Source	Error Per Axis	Effect on Acceleration (Per Axis) [mgal]
Shuttle position error	0.58 m	< 0.13
Receiver phase measurement noise (includes excess due to ionos. corr.)	6 mm	0.1 *
Shuttle Receiver clock error	TDOP • (6 mm)	0.12 *^
Satellite clock frequency error (Allan variance)	$1.2 \times 10^{-23} / \sqrt{\tau}$	0.60 *
Wet tropospheric error (s.d.) (20° elevation angle)	$.003 \tau^{5/6}$ cm	0.07 *
Accelerometer scale factor error	500 ppm	0.1
and bias error	0.1 mgal	0.1
Gyro scale factor error	5 ppm	0.05
and bias error	0.002 °/hr	0.09
Alignment error	0.4 mrad	0.08
Other (multipath, shuttle flexure, etc.)		0.1

\*  $\tau$  is the integration interval [s], here  $\tau = 60$  s.  
 ^ TDOP (Time Dilution of Precision)  $\approx 1.2$



# GRAVITY ESTIMATION ACCURACY

[mgal]

		Data Density (No. of pts. per 1° square)					
		1	2	3	4	5	6
2° mean $\Delta g$ *Global RMS Value: 15.6 mgal	STS-GPS	10°x10°	6.7	6.1	5.9	5.7	5.5
		15°x15°	6.5				
		20°x20°	6.4				
GEN-GPS		10°x10°	3.3				2.3
		15°x15°	3.2				
1° mean $\Delta g$ *Global RMS Value: 20.4 mgal	STS-GPS	10°x10°	13.2				12.1
		15°x15°	13.0				
	GEN-GPS	10°x10°	9.5				8.2
		15°x15°	9.5				

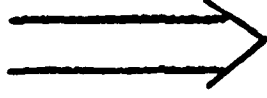
\* With respect to an 8-degree reference field.



## OTHER APPLICATIONS

### EXPLOIT GPS/IMU SYNERGISM

- PRECISE SPACECRAFT ORIENTATION, POINTING, AND ATTITUDE CONTROL
- PRECISE SPACECRAFT NAVIGATION, RENDEZVOUS AND DOCKING MANEUVERS



LOW-COST AUTONOMOUS SPACE-BASED SURVEILLANCE AND REMOTE SENSING SYSTEMS

## GPS ATTITUDE DETERMINATION ACTIVITIES AT THE NAVAL SURFACE WARFARE CENTER

Alan G. Evans  
NAVAL SURFACE WARFARE CENTER

This is a review of work done at NSWC with respect to attitude determination using GPS. In one of the first tests an antenna was rotated in a plane and the Doppler change of phase was measured on a very short baseline. One reason for mentioning this technique is that it has possible application on satellites where by rotating it one can obtain orientation information using just one antenna. Another early experiment involved two TI4100 receivers connected to the same clock with antennas separated by 25 m. This was a static test to determine the attitude between the two antennas by interferometric means.

Earlier this year we performed a test jointly with the National Geodetic Survey and the Defense Mapping Agency to determine astronomic azimuth. This, too, was a static test involving several days of data to get the best results. To convert geodetic azimuth as determined from GPS to astronomic azimuth one requires deflections of the vertical. We used two types of vertical deflections - those obtained by conventional (theodolite) astronomic measurements and those obtained by GPS. The latter are obtained by comparing heights above the reference ellipsoid as determined by GPS with heights above the geoid as determined by first-order leveling. The GPS vertical deflections were computed from four baselines (solid lines) from 1.2 to 4.8 km in length at Dahlgren. Compared to the conventionally obtained values there is hardly any difference. In fact, to better assess the GPS deflections, the U.S. Naval Observatory is determining more accurate values using their Danjon astrolabe. The azimuths were then determined for the baselines of length 1.2 km and 8.3 km (dashed lines) using either conventional or GPS deflections and compared to the astronomically determined azimuth. In both cases, the longer baseline had the higher accuracy in azimuth. Also, the GPS deflections yielded better results for both baselines.

In a dynamic test to determine attitude, a specially designed and built Trimble receiver (developed under an SBIR contract) with three antennas was put on the Yorktown. Our choice of locating the antennas was very restricted - the setup was adequate but not ideal. The antennas formed baselines 60 cm and 40 cm long and we obtained azimuth accuracy of about 1.5°; the other angles (pitch and roll) were worse mainly due to poor geometry. Although not very accurate, I am satisfied with this first result given the constraints of the experiment. The error sources consisted mainly of multipath. Also, there was some antenna crosstalk; they should have been further apart. Front-end noise remained a problem with the receivers which also had a significant dwell time causing an error due to ship motion.

Finally, we have embarked on integrating GPS with an inertial navigation system. Our approach is first to perform a covariance analysis for one to three antennas (incidentally, one can get orientation information from one antenna if the vehicle is moving and the geometry is known). We are now doing a test vehicle validation using a dead reckoning system (not an inertial system, yet) comprising an odometer and an azimuth gyro.

In summary, not much has changed in dynamic GPS attitude determination over the years in terms of goals and instruments; progress is being made but we still have far to go.

Discussion:

Questions: What is antenna crosstalk? Are both antennas connected to the same amplifier?

Answer: If antennas are too close they radiate from one to the other; they should be 4 to 6 wavelengths apart. The antennas are connected to one receiver but different channels; the satellites are tracked continuously, there is no sequencing.

Question: What is the L-band noise from the ship?

Answer: The ship was pretty quiet.

Question: What kind of multipath did you see?

Answer: We did not compute it. The maximum you would see is 2 to 4 cm; it was noticeable in the residuals.

# DISCUSSION

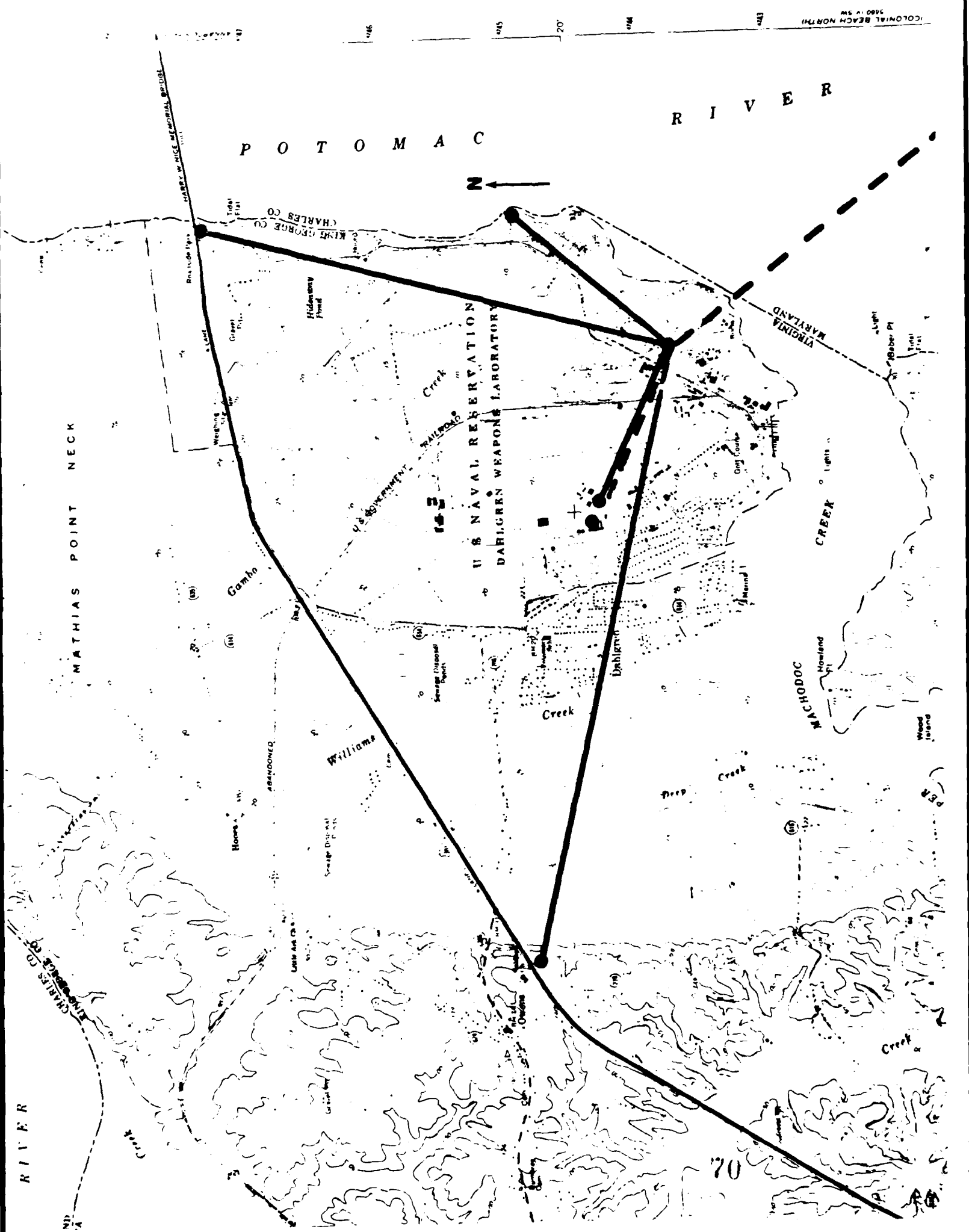
---

- EARLY STATIC TESTS
- ASTRONOMIC AZIMUTH AND DEFLECTIONS OF THE VERTICAL:  
JOINT TEST RESULTS
- SHIP TEST OF TRIMBLE NAVIGATION HEADING AND ATTITUDE  
RECEIVER
- COMBINED GPS AND INERTIAL NAVIGATION FOR ORIENTATION

## EARLY ORIENTATION TESTS

test	baseline m	accuracy deg	year
rotating antenna	2	0.5	1983
static	25	0.01	1985

**DEMONSTRATION OF THE USE OF GPS TO  
DETERMINE ASTRONOMIC AZIMUTH AND  
GRAVITY VERTICAL DEFLECTIONS:  
JOINT TEST DESCRIPTION AND RESULTS**



RIVER

POTOMAC

RIVER

MATHIAS POINT NECK

U.S. NAVAL RESERVATION  
DAHLGREN WEAPONS LABORATORY

VIRGINIA  
MARYLAND

CREEK

Williams

Dahlgren

ANAPOLIS

70

# COMPARISON OF NORTH AND EAST DEFLECTION OF VERTICAL COMPONENTS --ALL BASELINES--

$$\Delta H - \Delta h = \Delta s (\cos \alpha) \xi + \Delta s (\sin \alpha) \eta$$

	$\xi$ (ARCS)	$\eta$ (ARCS)	$\sigma_{\xi}$	$\sigma_{\eta}$
CONVENTIONAL (T4)	-2.58	5.19	0.5	0.5
GPS WITH LEVELING	-2.49	5.40	0.4	0.3
DIFFERENCE	0.09	0.21		



# COMPARISON OF ASTRONOMIC AZIMUTHS

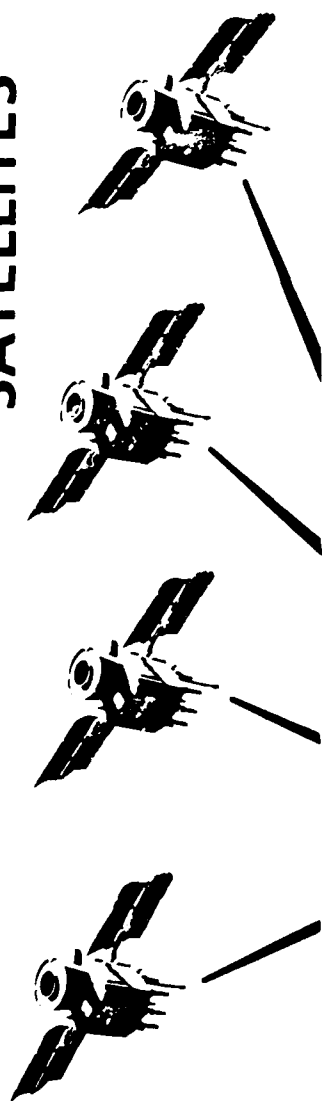
$A_{CONV}$  = CONVENTIONAL

$A_{GPS/CONV}$  = GPS DETERMINED USING CONVENTIONAL VERTICAL DEFLECTIONS

$A_{GPS/GPS}$  = GPS DETERMINED USING GPS VERTICAL DEFLECTIONS

STATIONS FROM TO		$A_{GPS/CONV} - A_{CONV}$ (ARCS)	$A_{GPS/GPS} - A_{CONV}$ (ARCS)
MBRE	RAD 9	-0.27	-0.11
MBRE	HERO	-0.97	-0.81

# GLOBAL POSITIONING SYSTEM SATELLITES



SHIP ATTITUDE TEST  
ROLL, PITCH AND YAW  
USS YORKTOWN JULY 1988

# **USS YORKTOWN TEST ERROR SOURCES**

---

- **SIGNAL MULTIPATH**
- **ANTENNA CROSSTALK**
- **FRONT-END NOISE**
- **TIME SYNCHRONIZATION OF PHASE DIFFERENCE MEASUREMENTS**

• • • • •

# **INCORPORATION OF GPS INFORMATION WITH INERTIAL NAVIGATION**

# APPROACH

---

- COVARIANCE ANALYSIS
  - GPS WITH INERTIAL NAVIGATION
  - ONE TO THREE ANTENNAS
- TEST VEHICLE VALIDATION
  - GPS WITH DEAD RECKONING NAVIGATION
  - ONE AND TWO (HEADING) ANTENNAS

# SUMMARY

---

- DYNAMIC GPS ATTITUDE DETERMINATION:
  - HAS BEGUN
  - IS MOVING
  - HAS FURTHER TO GO



## GPS APPLICATION TO NASA UPPER STAGES

A. Wayne Deaton  
MARSHALL SPACE FLIGHT CENTER

This is a review of baseline concepts and applications of a GPS/INS integrated navigation system for the Orbital Maneuvering Vehicle (OMV) and other NASA upper stages.

The OMV is to be used in low earth orbit to retrieve and boost satellites for servicing and mission launches. It will have two GPS systems with two antennas. The receivers are Rockwell/Collins two-channel receivers (current baseline). The depicted missions are compatible with the design of the OVM (propulsion and power system), but may not be the actual missions flown. An example of an OMV mission is the servicing of a large observatory such as the Hubble telescope. Starting at 250 nm altitude, the OMV would go to 380 nm to retrieve the telescope, bring it down to 250 nm where it is serviced, then boost it back up to 380 nm, and return to 250 nm. The retrieve and boost phases must be done at very low thrust (0.002 g) and this implies long burn arcs which can lead to large errors building up in the inertial navigation system.

The current baseline GPS/INS system comprises an IMU (gyros and accelerometers), attitude sensors (sun and horizon sensors), dynamic models accounting for gravity and atmosphere, and a GPS receiver and navigation processor. The accelerometer-derived inertial velocities will be supplied to the processor which together with pseudoranges and pseudo delta ranges from GPS will derive position/velocity updates and time and which are then used to reset the inertial navigation system. During the coast phase updates are purely derived from GPS. Updates are given once per second during the power phase, less often during the coast phase.

Some research questions related to GPS/INS technology applications on NASA upper stages include: Can GPS be used to calibrate the gyros and accelerometers of the IMU in the OMV (low) acceleration environment? Can GPS be used during the coast phases for attitude updates to eliminate attitude sensors? (We are not yet ready to make this big jump, but with some experience, perhaps this can be implemented.) Can the integrated GPS/INS system be designed? (We have a contract with Mayflower Communications who have more to say about this in another presentation.)

To answer some of these questions, we plan to do an experiment to prove the concept of GPS/INS integration. On the OMV flight, inertial navigation data will be collected and down-linked along with the GPS data. Using post-processing an integrated GPS/INS error filter will be built. Software can then be up-linked on board for implementation.

Other NASA upper stages where the integrated GPS/INS has application include the lunar and mars initiatives. The lunar mission scenario begins with a shuttle launch of the cargo to low earth orbit where the OMV would take it to Space Station Freedom (SSF) for hardware integration. OMV would then deploy the lunar transfer vehicle which would execute its mission and return to SSF. Within the GPS operational sphere precise GPS/INS navigation can be used to reduce to number of course corrections and the mission time required to



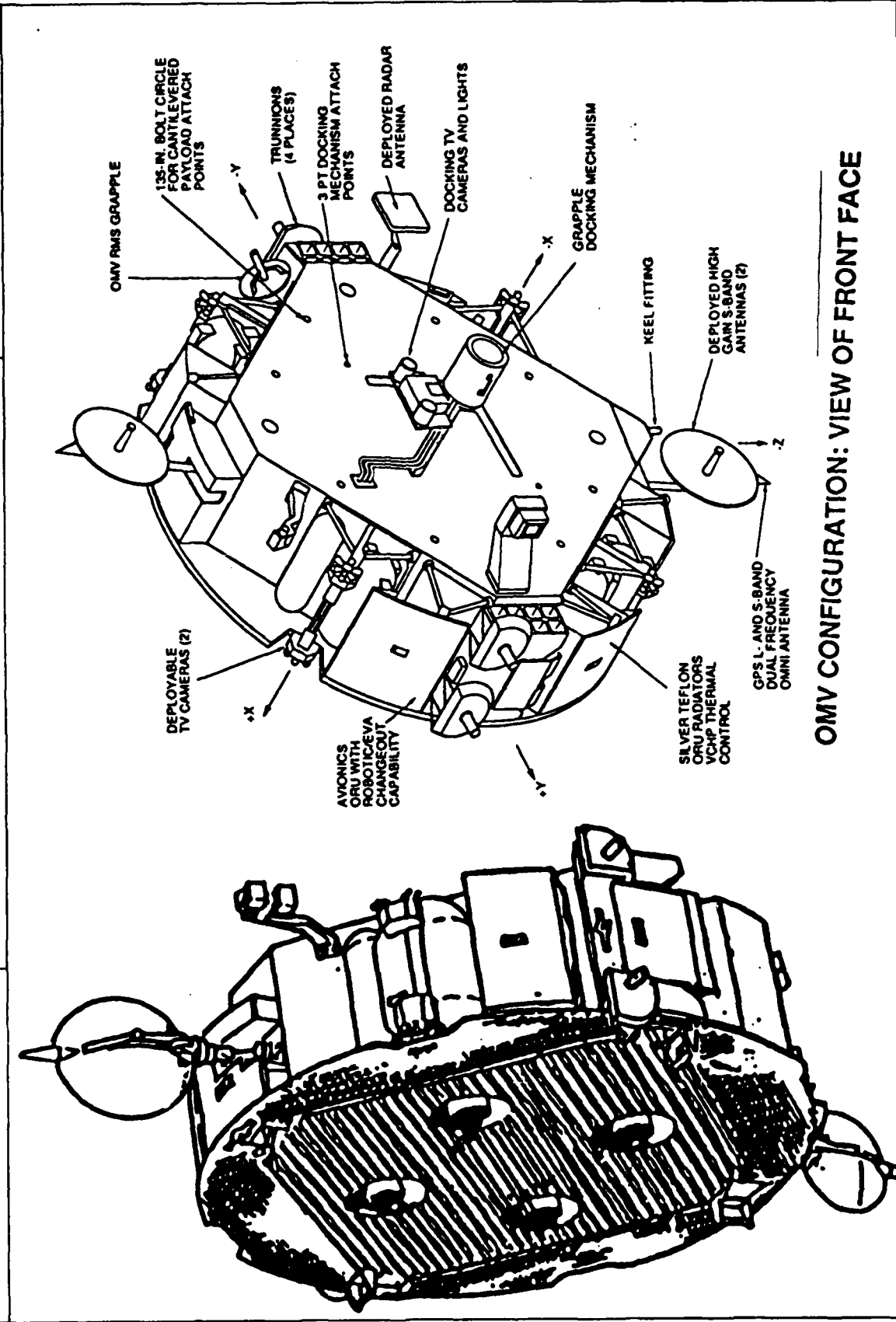
perform the aerobraking on reentry to earth orbit. Navigation at the moon will use similar technology as used for Apollo mission. Later we may place navigation beacons on the moon to aid in navigation - these would be operationally similar to GPS (this is all in the concept phase).

In summary, the integrated GPS/inertial technology will augment current navigation and attitude update capability of NASA Upper Stage missions. Specifically, low earth orbit users, such as OMV, Space Station, and the Shuttle will receive maximum benefit; but also high altitude users, such as geosynchronous orbit platforms and lunar- and mars-return missions could use this technology to obtain critical navigation data to complete their missions. Application of GPS/inertial system technology provides flexibility in contingency planning by providing more precise knowledge of the state vector which in turn offers potentially more maneuver options. We hope eventually to eliminate the attitude update sensors. Finally, the design of an onboard GPS/inertial system will not seriously constrain the existing computing capabilities.

ORGANIZATION: <b>NASA</b> /MSFC/EL23	MARSHALL SPACE FLIGHT CENTER  GPS APPLICATION TO NASA UPPER STAGES ---OUTLINE-----		NAME: A. W. DEATON
CHART NO.:  1		DATE: OCT. 10, 1989	

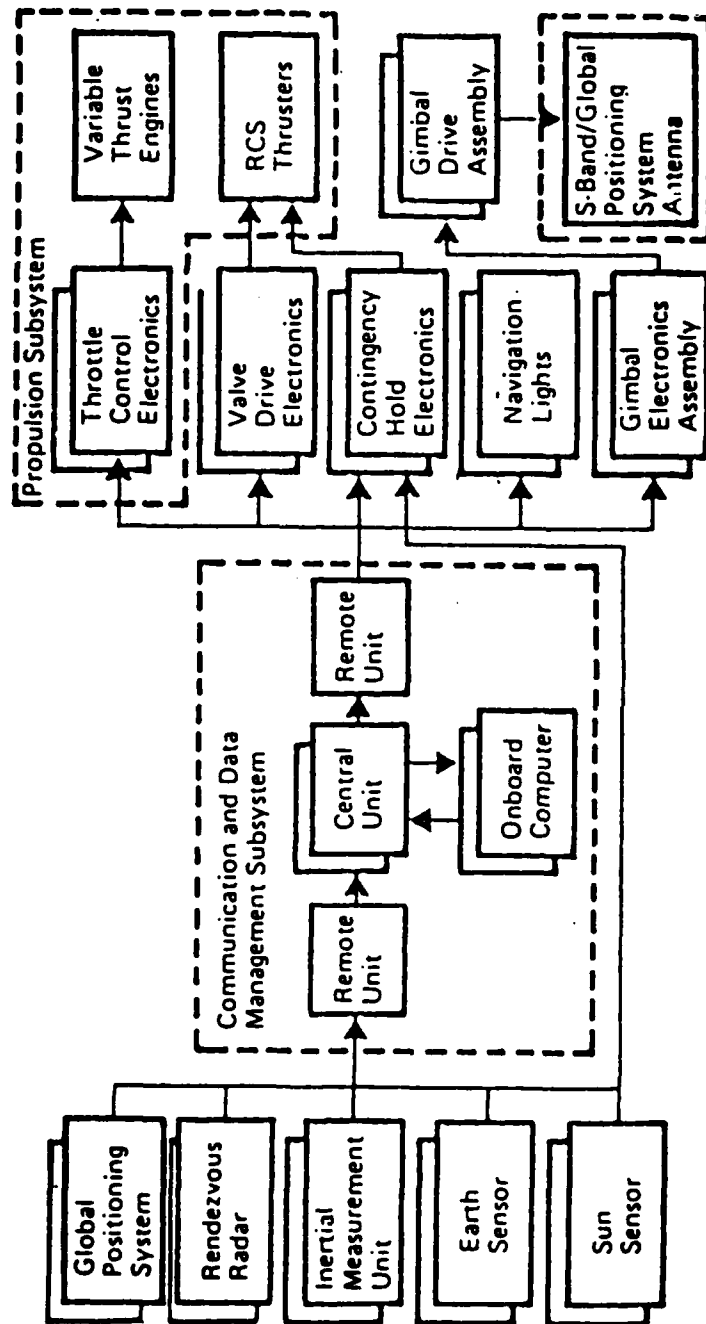
- 1) ORBITAL MANEUVERING VEHICLE (OMV) BASELINE
  - a) CONFIGURATION
  - b) AVIONICS
  - c) MISSIONS
- 2) CURRENT BASELINE -GPS/INS NAVIGATION PROCESSING FOR OMV
- 3) QUESTIONS TO BE ANSWERED BY THE GPS RESEARCH STUDIES
- 4) BASIC CONCEPT OF INTEGRATED GPS/INS NAVIGATION SYSTEM
- 5) OTHER POTENTIAL NASA UPPER STAGE USERS OF INTEGRATED GPS/INS
- 6) SUMMARY

ORGANIZATION: <b>NASA</b> /MSFC/EL23	MARSHALL SPACE FLIGHT CENTER GPS APPLICATION TO NASA UPPER STAGES---OMV CONFIGURATION	NAME: A. W. DEATON
CHART NO.: 2	DATE: OCT. 10, 1989	



OMV CONFIGURATION: VIEW OF FRONT FACE

ORGANIZATION:		MARSHALL SPACE FLIGHT CENTER		NAME:	
NASA /MSFC/EL23		GPS APPLICATION TO NASA UPPER STAGES---OMV AVIONICS		A. W. DEATON	
CHART NO. :		3		DATE:	
				OCT. 10, 1989	

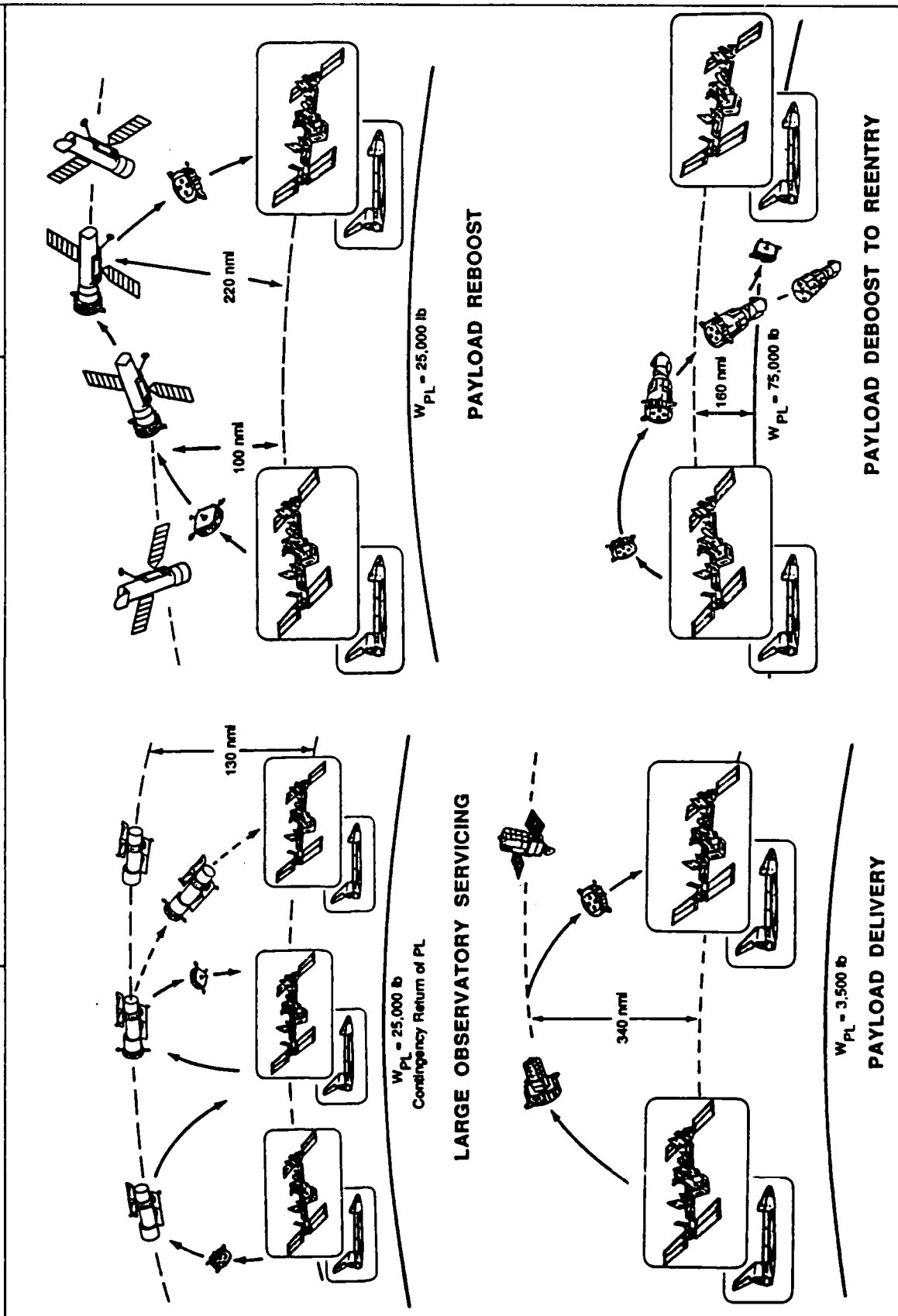


Simplified GN&C Block Diagram

ORGANIZATION:		MARSHALL SPACE FLIGHT CENTER		NAME:
NASA /MSFC/EL23		GPS APPLICATION TO NASA UPPER STAGES---MISSIONS		A. W. DEATON
CHART NO. : 4				DATE: OCT. 10, 1989

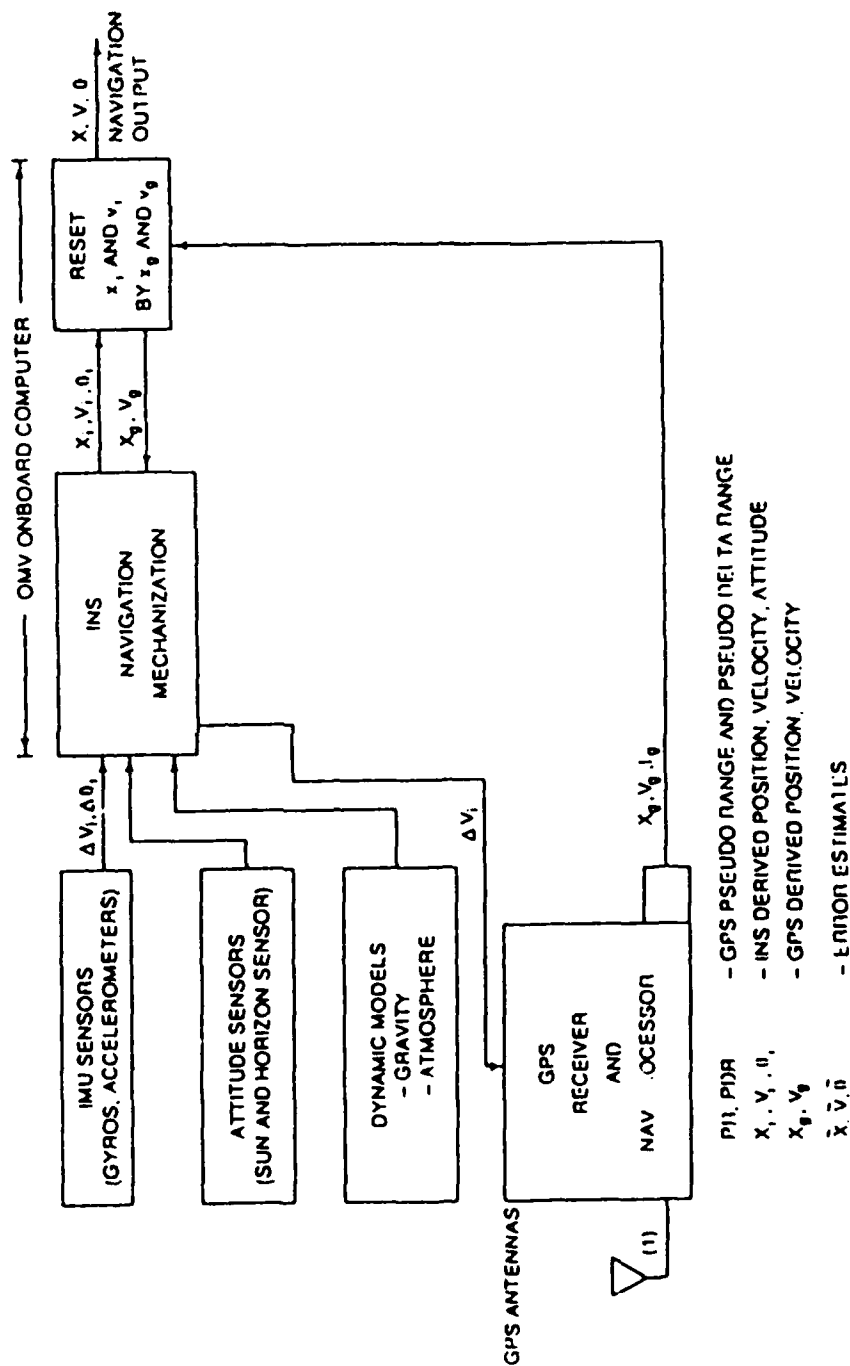
MISSION	ALTITUDES (NMI)	PAYLOAD WEIGHT (LB)
1. LARGE OBSERVATORY SERVICE	250/380/250/380/250	25,000
2. PLACEMENT	250/590/250	3,500
3. RETRIEVAL	250/470/250	11,000
4. REBOOST	250/350/470/250	25,000
5. DEBOOST	250/160/250	75,000
6. VIEWING	250/1090/250	200
7. SUBSATELLITE	250	5,000
8. PLACE AND RETRIEVE	230/335/360/250	5,000/10,000
9. SERVICING	250/650/250	5,000
10. LOGISTICS MODULE TRANSFER	250/360/250	50,000
11. SPACE STATION SUPPORT	250	1,000
12. OTV/PAYLOAD TRANSFER	250	75,000

ORGANIZATION: <b>NASA /MSFC/EL23</b>		MARSHALL SPACE FLIGHT CENTER GPS APPLICATION TO NASA UPPER STAGES---MISSIONS		NAME: A. W. DEATON
CHART NO.: 5				DATE: OCT. 10, 1989



ORGANIZATION:	MARSHALL SPACE FLIGHT CENTER		NAME:
<b>MSFC/EL23</b>	GPS APPLICATION TO NASA UPPER STAGES---GPS/INS PROCESSING		A. W. DEATON
CHART NO.:	6		DATE:
			OCT. 10, 1989

## CURRENT BASELINE GPS/INS NAVIGATION PROCESSING FOR THE OMV



ORGANIZATION:		MARSHALL SPACE FLIGHT CENTER		NAME:	
NASA /MSFC/EL23		GPS APPLICATION TO NASA UPPER STAGES---QUESTIONS		A. W. DEATON	
CHART NO.:		7		DATE:	
				OCT. 10, 1989	

QUESTIONS TO BE ANSWERED BY THE GPS OMV RESEARCH STUDIES

- ☐ HOW CAN THIS NEW TECHNOLOGY BE USED BY NASA?
- ☐ CAN GPS BE USED TO CALIBRATE THE INERTIAL MEASUREMENT UNIT SYSTEM (GYROS AND ACCELEROMETERS) IN THE OMV ACCELERATION ENVIRONMENT?
- ☐ CAN GPS BE USED DURING THE COAST PHASES AS AN INTERFEROMETER FOR ATTITUDE UPDATE AND POSSIBLY ELIMINATE ATTITUDE UPDATE SENSORS?
- ☐ CAN REDUNDANCY REQUIREMENT BE SATISFIED?
- ☐ CAN AN INTEGRATED GPS/INS SYSTEM BE DESIGNED?



ORGANIZATION:

**NSA** /MSFC/EL23

CHART NO.:

8

MARSHALL SPACE FLIGHT CENTER

GPS APPLICATION TO NASA UPPER STAGES---BASIC CONCEPT

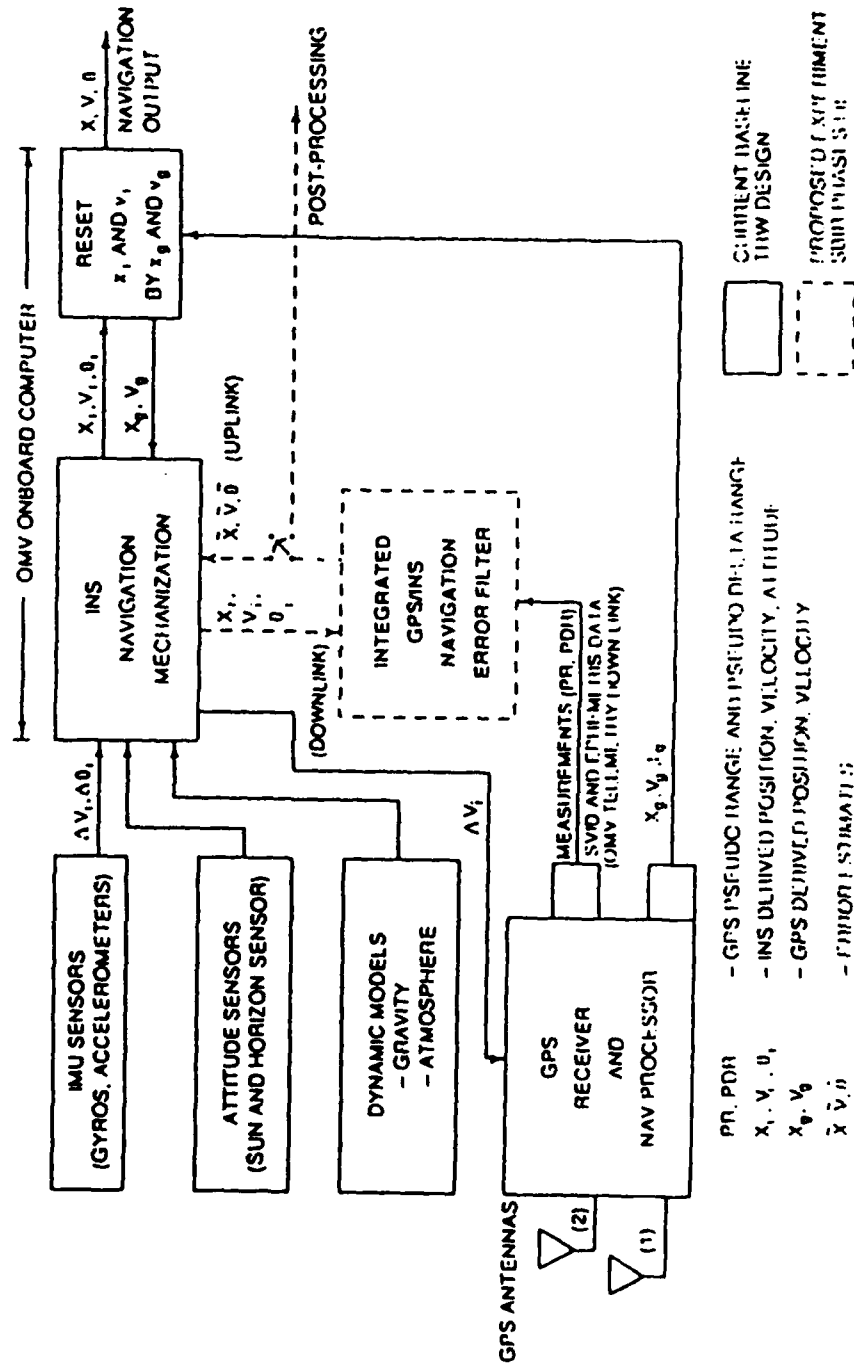
NAME:

A. W. DEATON

DATE:

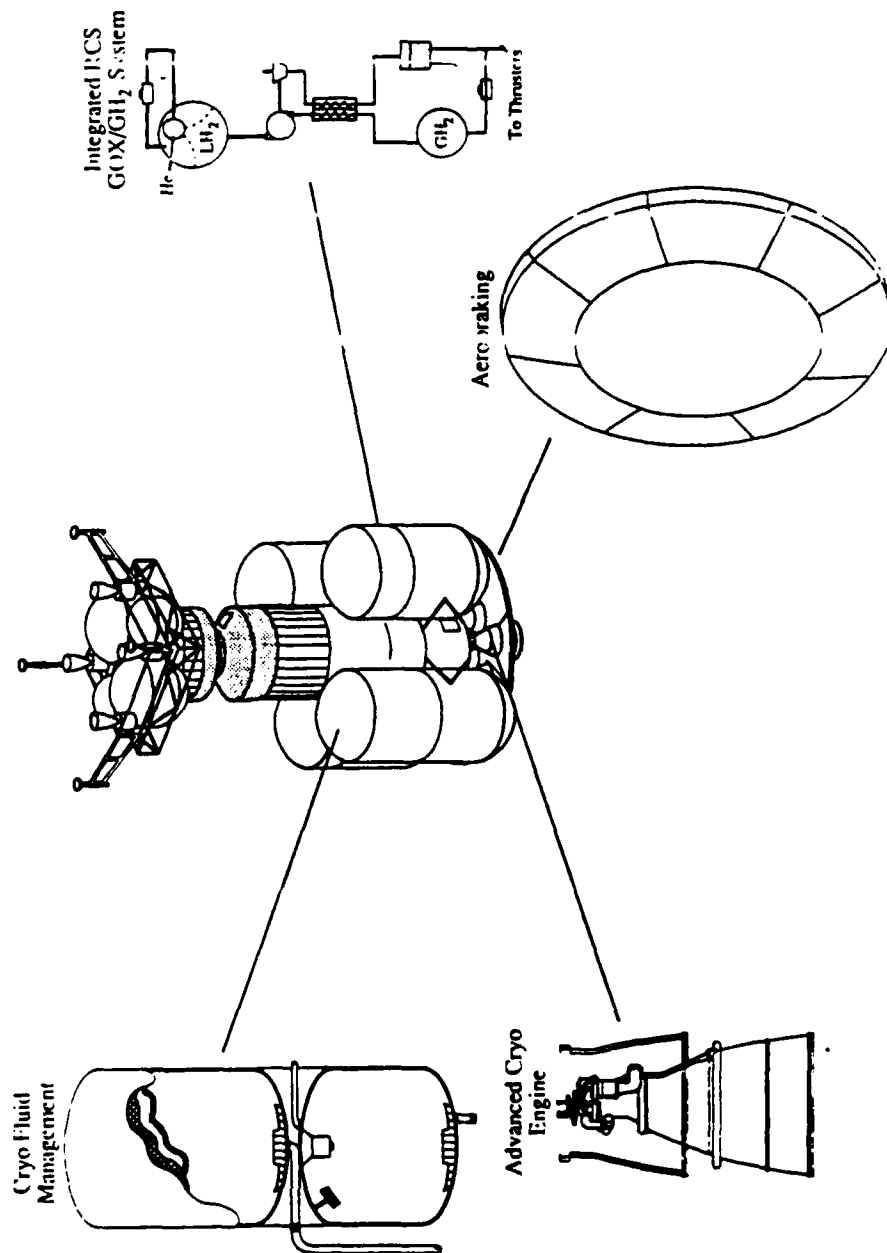
OCT. 10, 1989

# AUTONOMOUS INTEGRATED GPS/INS NAVIGATION PROCESSING FOR THE OMV (Proof-Of-Concept Demonstration)



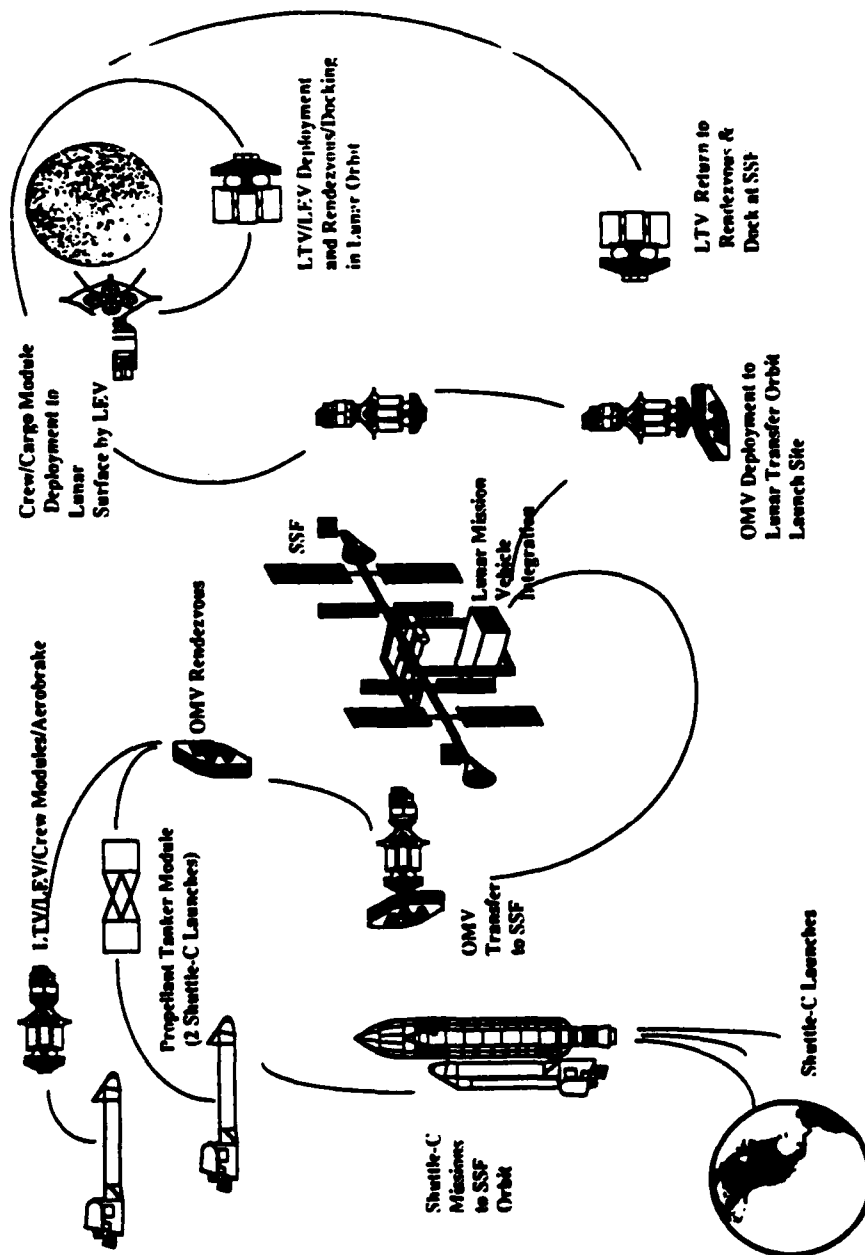
ORGANIZATION:		MARSHALL SPACE FLIGHT CENTER		NAME:	
NASA /MSFC/EL23		GPS APPLICATION TO NASA UPPER STAGES-OTHER POTENTIAL UPPER STAGE USERS OF INTEG. GPS/INS		A. W. DEATON	
CHART NO.:		9		DATE:	
				OCT. 10, 1989	

## LTV/LEV Technology/Advanced Development



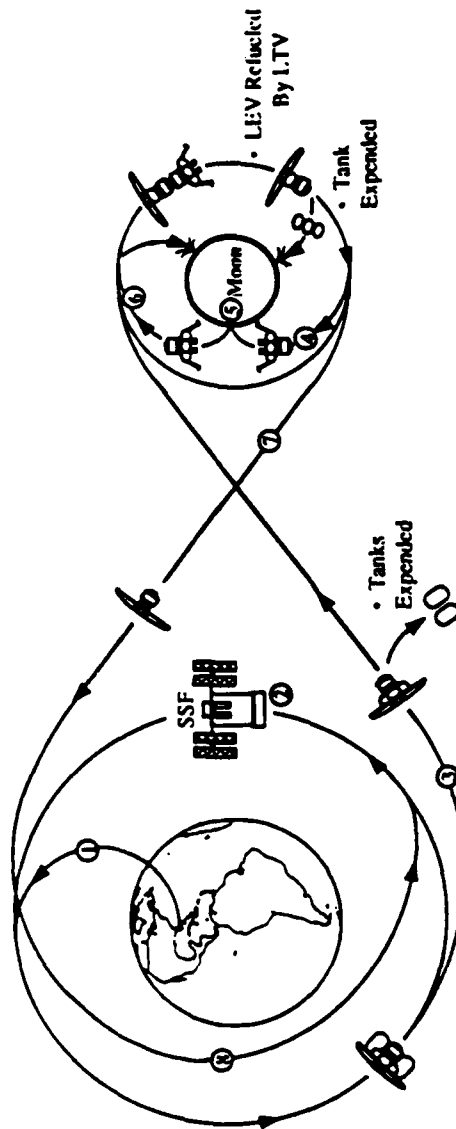
ORGANIZATION:		MARSHALL SPACE FLIGHT CENTER		NAME:
NASA /MSFC/EL23		GPS APPLICATION TO NASA UPPER STAGES-OTHER POTENTIAL UPPER STAGE USERS OF INTEG. GPS/INS		A. W. DEATON
CHART NO.:		10		DATE:
				OCT. 10, 1989

## Lunar Mission Scenario



ORGANIZATION:		MARSHALL SPACE FLIGHT CENTER		NAME:
NASA /MSFC/EL23		GPS APPLICATION TO NASA UPPER STAGES-OTHER POTENTIAL UPPER STAGE USERS OF INTEG. GPS/INS		A. W. DEATON
CHART NO.:		11		DATE:
				OCT. 10, 1989

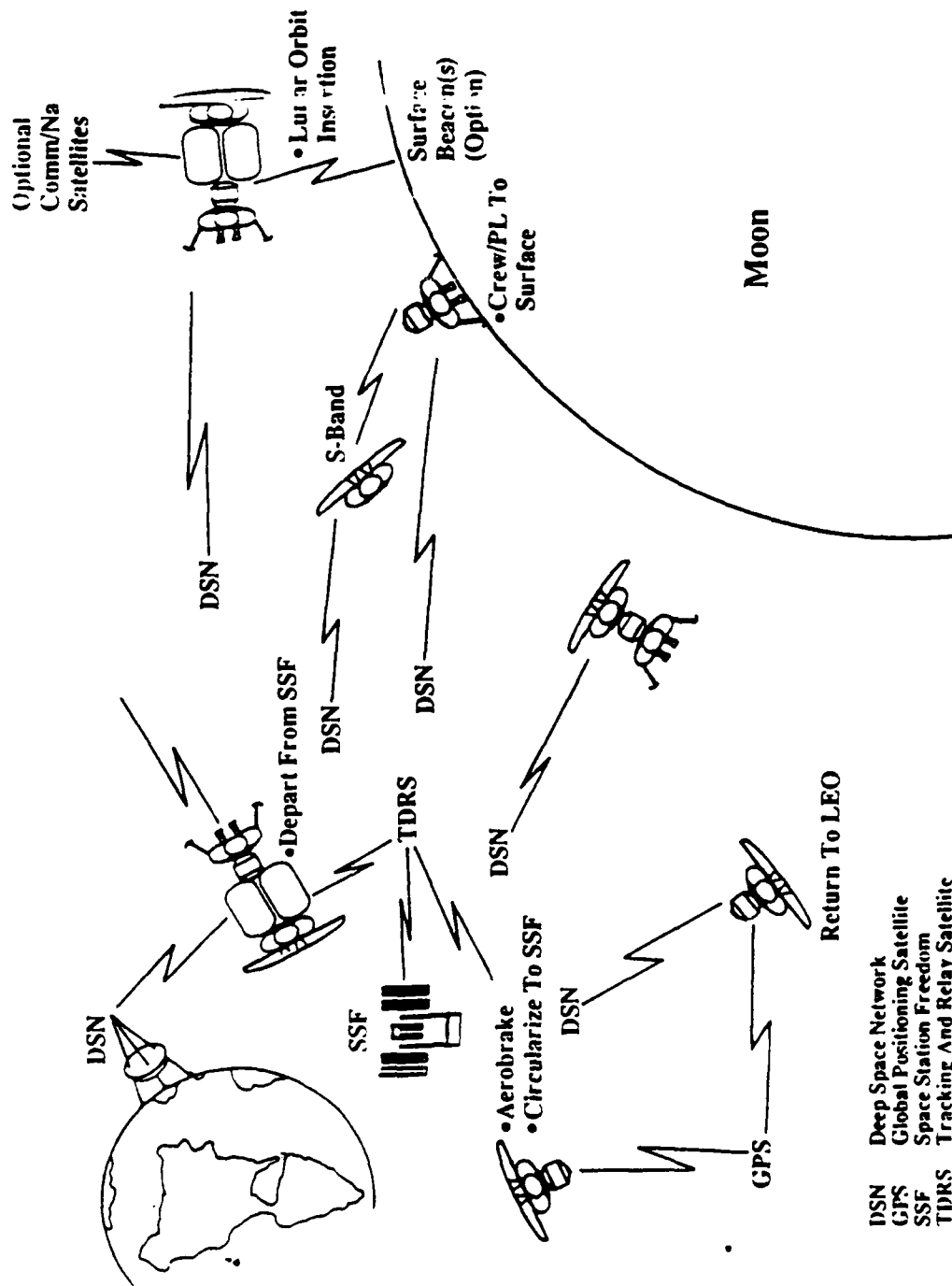
## Lunar Mission Profile



### Lunar Mission Phases

- ① Earth to Orbit (ETO) Transportation System
- ② Earth Orbit Support Facility (EOXF) at ESSF
- ③ Trans Lunar Phase With LTV  
Trans Lunar Injection  $\Delta V = 3100$  M/S  
Midcourse Corrections  $\Delta V = 10$  M/S  
Lunar Orbit Insertion  $\Delta V = 1100$  M/S
- ④ LLO to LS With LEV  
Lunar Landing  $\Delta V = 2000$  M/S  
Lunar Orbit Ops  $\Delta V = 50$  M/S
- ⑤ Lunar Surface Activities
- ⑥ LS to LLO With LEV  
Lunar Takeoff  $\Delta V = 1900$  M/S
- ⑦ Trans-Earth Phase With LTV  
Trans Earth Injection  $\Delta V = 1100$  M/S  
Midcourse Corrections  $\Delta V = 10$  M/S  
Pre-entry Correction  $\Delta V = 6$  M/S
- ⑧ Aerobreak Maneuver  
Post-Aero Circularize  $\Delta V = 310$  M/S

ORGANIZATION:		MARSHALL SPACE FLIGHT CENTER		NAME:	A. W. DEATON
NASA /MSFC/EL23		GPS APPLICATION TO NASA UPPER STAGES-OTHER POTENTIAL UPPER STAGE USERS OF INTEG. GPS/INS		DATE:	OCT. 10, 1989
CHART NO.: 12					



ORGANIZATION: <b>NASA</b> /MSFC/EL23		MARSHALL SPACE FLIGHT CENTER  GPS APPLICATION TO NASA UPPER STAGES---SUMMARY---	NAME: A. W. DEATON
CHART NO.: 13			DATE: OCT. 10, 1989

## GPS APPLICATION TO NASA UPPER STAGES

- Integrated GPS/Inertial system technology augments the current navigation and attitude update capability of NASA Upper stage missions.
  - low earth users (LEO), such as OMV, Space Station, Shuttle-C will receive maximum benefit via improved performance
  - high altitude users, such as GEO Platform, Lunar-return and Mars-return missions can potentially use this technology to obtain critical navigation data to complete their mission
- Application of Integrated GPS/Inertial system technology provides improved total navigation performance and flexibility in contingency mission planning
  - may eliminate attitude update sensors
- An onboard real-time Integrated GPS/Inertial system can be designed without seriously constraining the onboard computing resources (within 10 - 20%).



## SPACE STATION FREEDOM GPS IMPLEMENTATION PLANS - AN OVERVIEW

Penny E. Saunders  
JOHNSON SPACE CENTER

This talk concerns the Space Station application of GPS. The Station is now in the phase of building prototype hardware - within a few years we should be building flight hardware. This overview will assume the baseline configuration of the Station and not consider the "scrub activity" which phases down the Station program.

Application of GPS on the Space Station include orbit determination, time determination, and relative tracking. The organizational structure comprises four different work packages - WP2 and WP3 are involved in this particular development. WP3 is the responsibility of the Goddard Space Flight Center and concerns the polar orbiting platform; WP2 is managed by Johnson Space Center (JSC) which includes responsibility for communications, tracking, guidance, navigation, and control system as far as GPS is concerned.

Accuracy requirements (1 sigma) for the GPS functions are: 10 m in position, 0.01 m/s in velocity, 0.013 sec for orbital period (for payload pointing), 1  $\mu$ sec in time. Tracking accuracy is a function of range from the Station - the requirement is to track any GPS equipped vehicle within a range of about 37 km. The Station will do relative processing of data transmitted by vehicle.

The system architecture includes a tracking subsystem with a GPS receiver/processor that interfaces with the GN&C, time generation system (two frequency standards referenced to GPS), and communications & tracking systems. (There is an interface (not shown) from the time generation system to the data management system core network providing time to users throughout the Station.) The guidance and navigation system provides position to all the users. GPS will provide the primary navigation system for the Station - there are no inertial navigation systems on the Station (there are some gyros and star trackers for attitude determination). There are three GPS antennas, two on the starboard boom and one on the port boom and three receiver/processors.

The mission life of the Station is about 30 years and the key updates for GPS are scheduled at once per year so we need to devise a secure technique to rekey the receivers using TDRSS up-links without interference to the users of the Station which include international partners.

The schedule for engineering and integration of the tracking subsystem includes various developments, procurements, providing specifications, doing design analyses and trade-off studies. Some of these are on hold due to the scrub; one recommendation is to put all GPS activities on hold for four years. Although a final decision has not been made, alternatives to the GPS system is TDRSS for ground based position and velocity determination and time transfer. Since there will be no co-orbiters under the phased down version, there are no relative tracking requirements (the shuttle has its own navigation system). JSC is, however, lobbying hard to keep GPS a part of the Station because it offers such versatility for mission objectives and operational requirements.



Discussion:

Question: Instead of keyed receivers, why not just use codeless receivers?

Answer: We have looked into the issue of codeless receivers, but opted not to utilize this technique. The reason for this decision was based on the requirement for ephemeris updates from the ground. If NASA decides to utilize an unkeyed receiver, it will be a C/A-code receiver with state estimation of the ionospheric delay.



Johnson Space Center - Houston, Texas

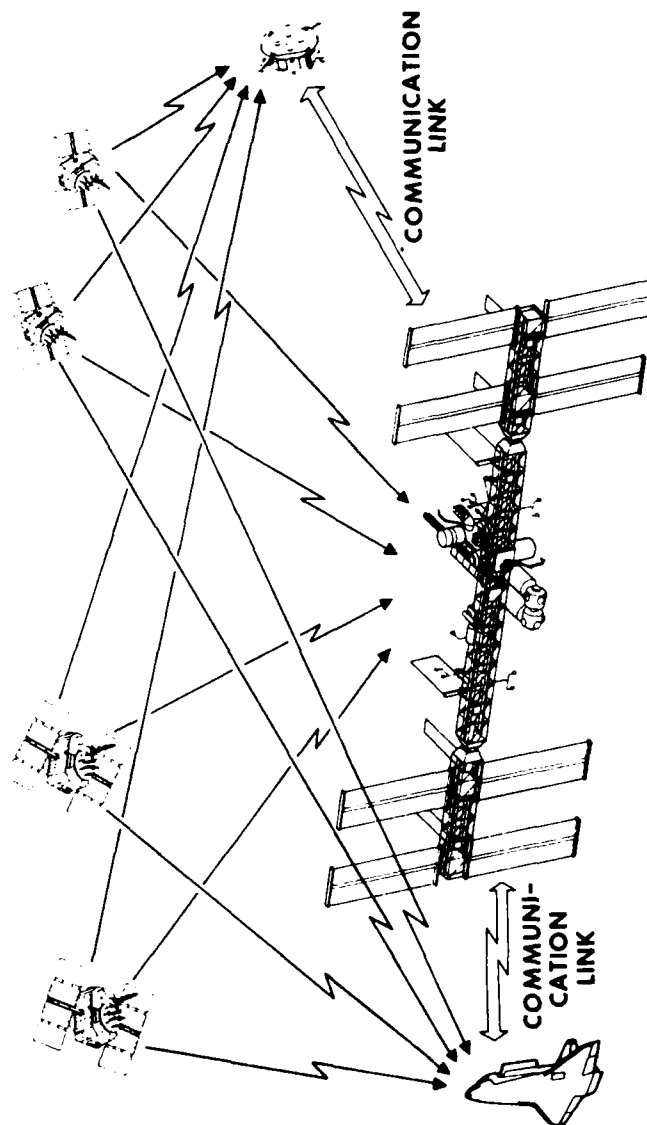
SPACE STATION GPS  
IMPLEMENTATION PLANS:  
AN OVERVIEW

TCD/TRACKING TECHNIQUES BRANCH

EE6/P.E. SAUNDERS

OCTOBER 1989

SPACE STATION FREEDOM PROGRAM  
GPS IMPLEMENTATION PLANS:  
AN OVERVIEW





Johnson Space Center - Houston, Texas

SPACE STATION GPS IMPLEMENTATION PLANS: AN OVERVIEW		TRD/TRACKING TECHNIQUES BRANCH
		EE6/P.E. SAUNDERS
		OCTOBER 1989

## OUTLINE

# SPACE STATION GPS ORGANIZATION IMPLEMENTATION PLANS STATUS



Johnson Space Center - Houston, Texas

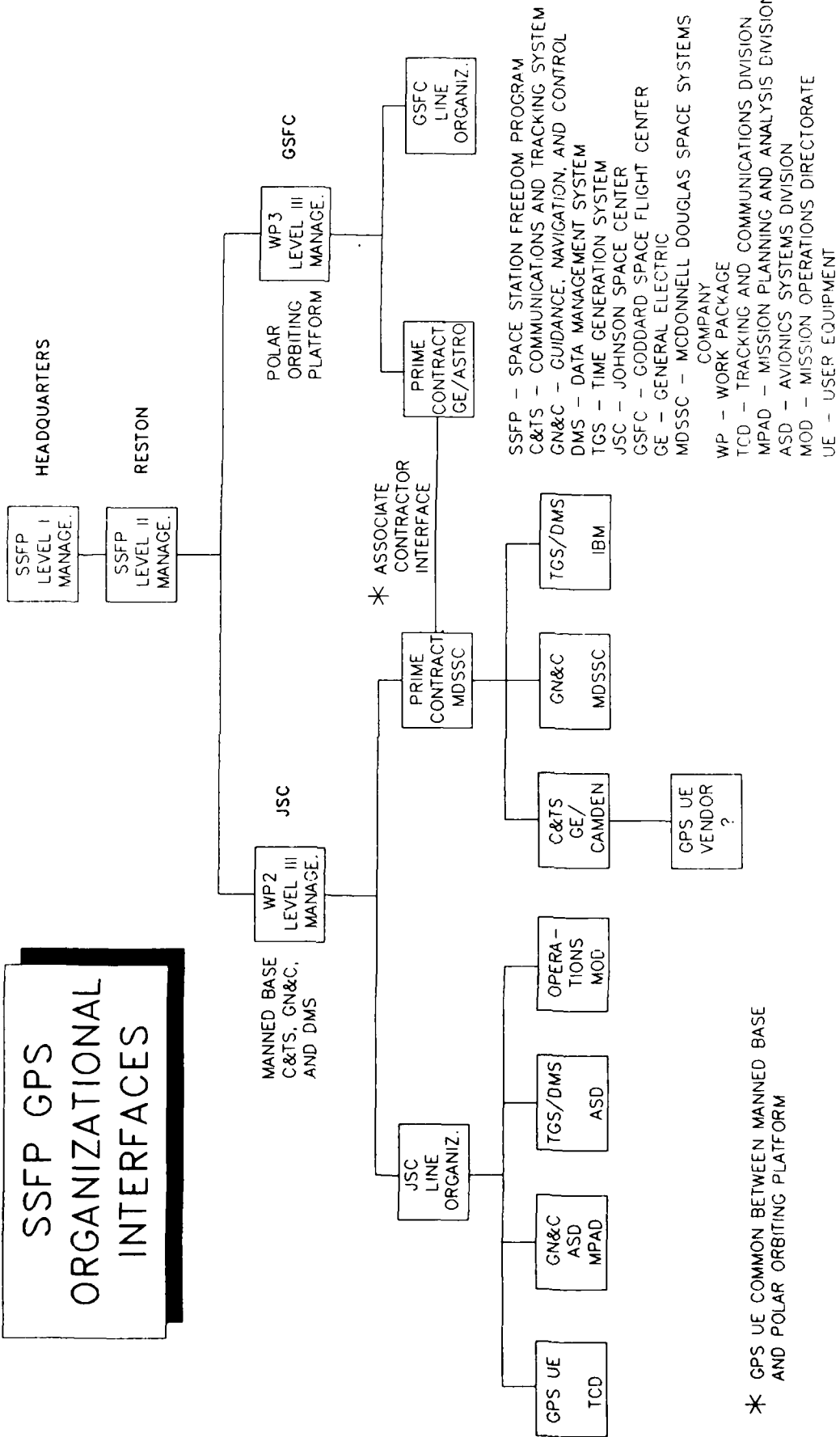
# SPACE STATION GPS IMPLEMENTATION PLANS: AN OVERVIEW

TCD/TRACKING TECHNIQUES BRANCH

EE6/P.E. SAUNDERS

OCTOBER 1989

## SSFP GPS ORGANIZATIONAL INTERFACES





SPACE STATION GPS  
IMPLEMENTATION PLANS:  
AN OVERVIEW

TCD/TRACKING TECHNIQUES BRANCH

EE6/P.E. SAUNDERS

OCTOBER 1989

## SSFP GPS APPLICATIONS

ORBIT DETERMINATION

TIME DETERMINATION

RELATIVE POSITION AND VELOCITY  
(GPS EQUIPPED VEHICLE TRACKING)



SPACE STATION GPS  
IMPLEMENTATION PLANS:  
AN OVERVIEW

TCD/TRACKING TECHNIQUES BRANCH

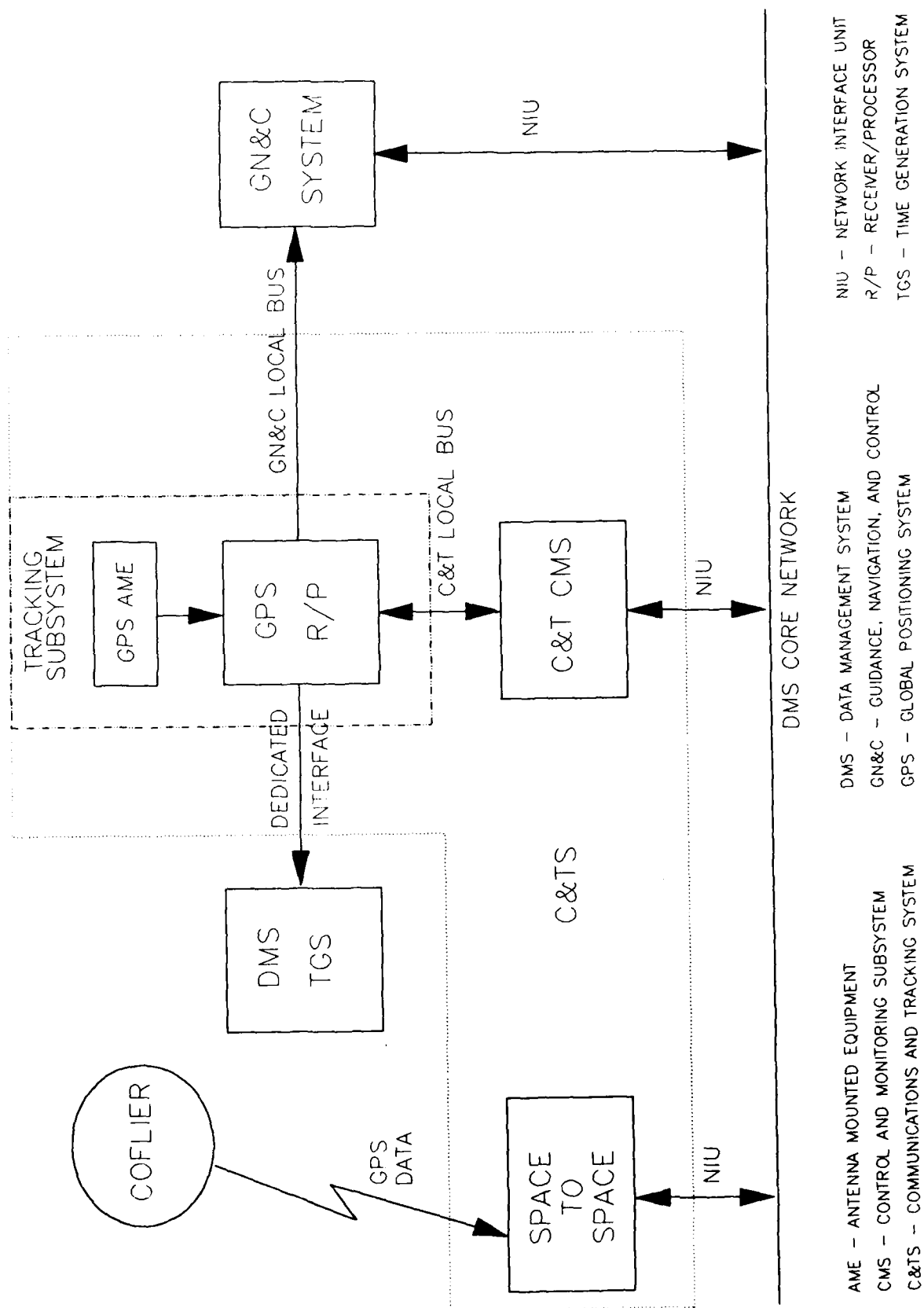
EEG/P.E. SAUNDERS

OCTOBER 1989

## REQUIREMENTS/SPECIFICATIONS

- ORBIT DETERMINATION ACCURACY: (1 SIGMA)
  - POSITION  $\leq +/ - 10.0$  METERS
  - VELOCITY  $\leq +/ - 0.01$  METERS/SECOND
  - PERIOD  $\leq +/ - 0.013$  SECOND
- TIME DETERMINATION ACCURACY:
  - TIME  $\leq 1$  MICROSECOND
- TRACKING ACCURACY ( FOR RANGE  $> 1$  KILOMETER): (1 SIGMA)
  - RELATIVE POSITION  $\leq +/ - 1.83 \times 10^{-3} * \text{!RANGE!}$  METER
  - RELATIVE VELOCITY  $\leq +/ - 1.83 \times 10^{-6} * \text{!RANGE!}$  METER/SECOND
- VOLUME  $\leq 15,572$  CUBIC CENTIMETERS
- WEIGHT  $\leq 10.75$  KILOGRAMS
- POWER  $\leq 56$  WATTS
- PRECISE POSITIONING SERVICE GPS USER EQUIPMENT (C/A & P(Y) CODES)

# GPS USER EQUIPMENT INTERFACES





Johnson Space Center - Houston, Texas

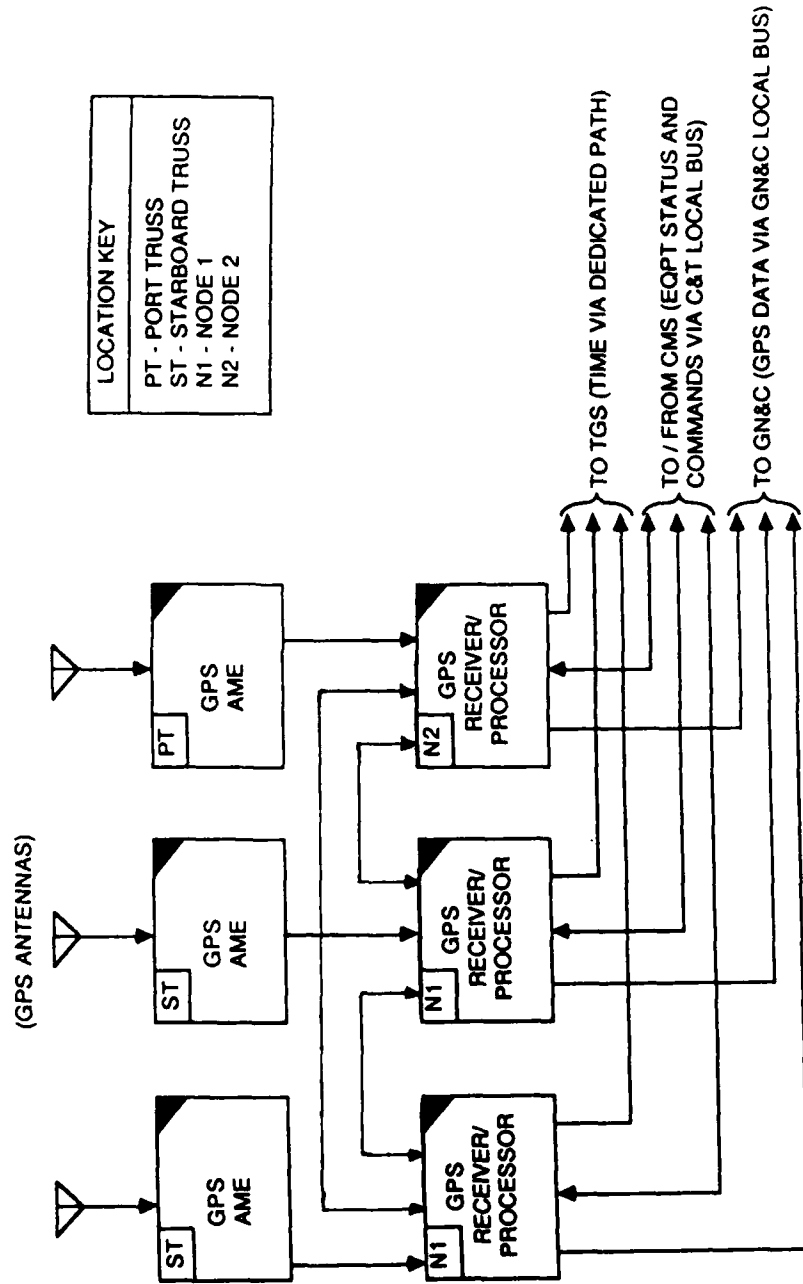
# SPACE STATION GPS IMPLEMENTATION PLANS: AN OVERVIEW

TCD/TRACKING TECHNIQUES BRANCH

EE6/P.E. SAUNDERS

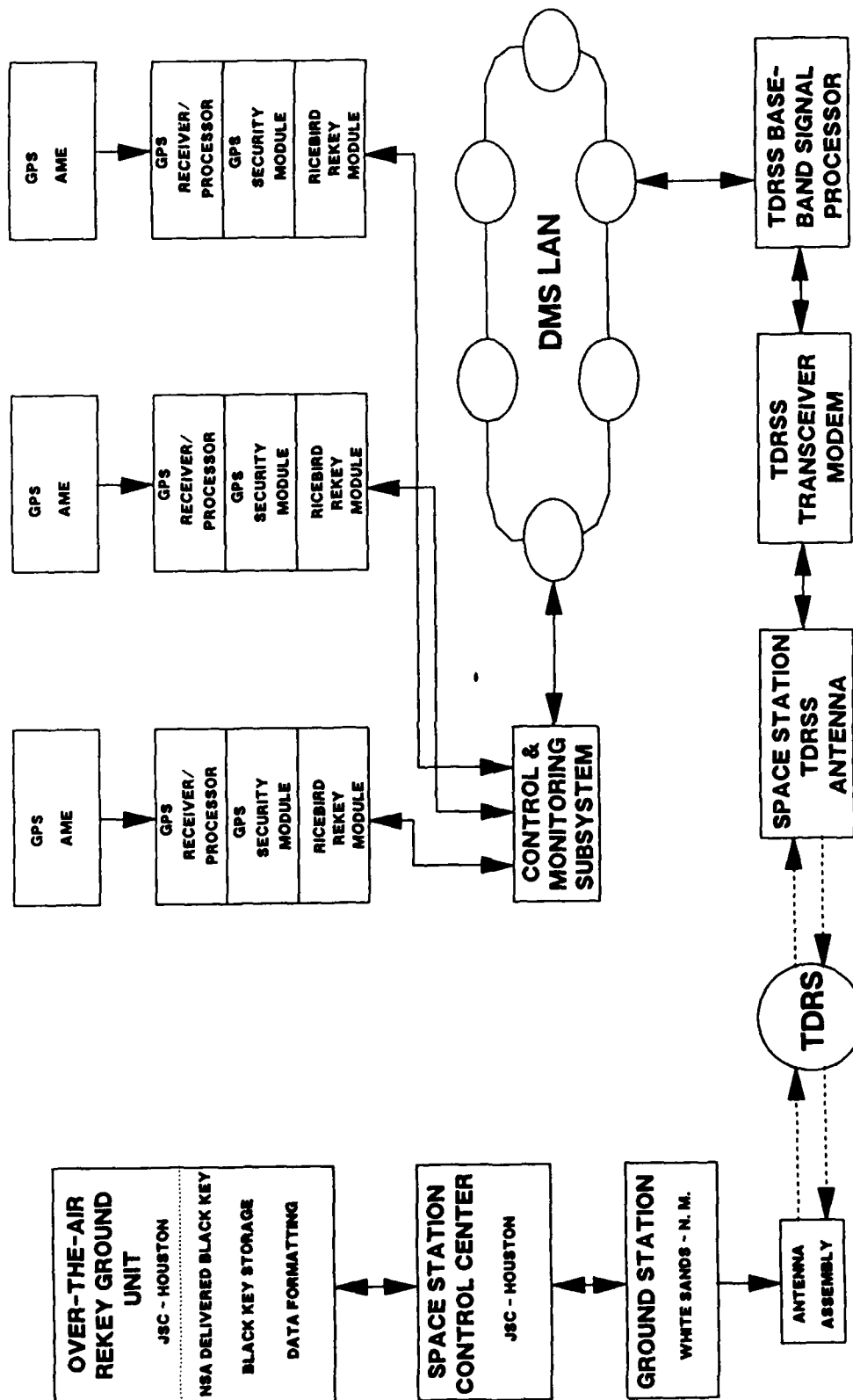
OCTOBER 1989

## GPS USER EQUIPMENT INTERFACES

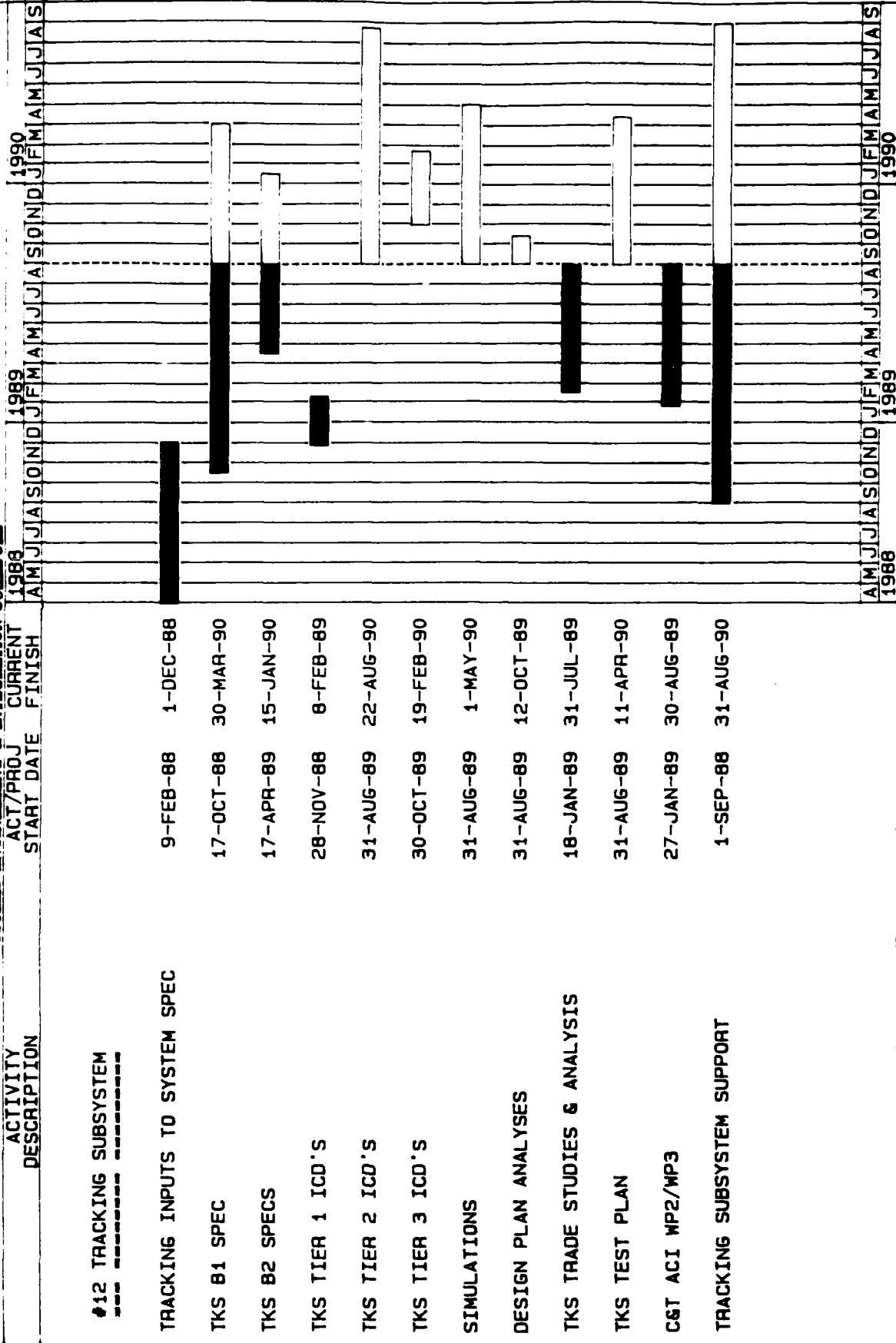




# PROPOSED GPS KEY TRANSFER



# SYSTEMS ENGINEERING & INTEGRATION SCHEDULE



SUMMARY SCHEDULE - TRACKING SUBSYSTEM  
 DATE: 31-AUG-89  
 /SUMTKS1

RESPONSIBILITY: B. TYREE, S. GOLDMAN



## RECENT RESULTS IN HIGH-PRECISION GPS ORBIT DETERMINATION

Stephen Lichten, Susan Kornreich Wolf, Willy I. Bertiger,  
Ulf J. Lindqwister, and Geoff Blewitt  
JET PROPULSION LABORATORY

The motivations for high-precision GPS orbit determination include high precision requirements for low orbiters tracked by GPS and high-precision geodetic and geophysical ground applications (e.g. baselines for seismic monitoring). We did an experiment to demonstrate sub-meter precision in GPS orbit determination. The results of this experiment, the salient reasons for the high precision, and the means to confirm this precision are reviewed here.

The primary data type was the carrier phase which gives the geometric strength; we also used pseudorange (which was quite noisy due to multipath) to constrain clock bias parameters. We used data from a global tracking network and three ground sites whose coordinates were held fixed as determined by VLBI. We used a Kalman filter to estimate various parameters for multi-day arcs and we used special dynamic modeling techniques to be discussed below.

As a result, 4 out of 7 satellites had better than 1 m repeatability (i.e., precision) (about 50 cm in each component). Also, 2 out of 7 showed agreement at the sub-meter level with predicted orbits. Repeatability is derived from a comparison of two orbit determination solutions that overlap by a few hours. Prediction agreement means that there is no overlap (more stringent test of the orbits). The repeatability was consistent with the formal errors obtained by our estimation procedure.

Aside from repeatability and prediction agreements, we looked for ground measurements to further confirm the precision of the orbits. Using VLBI-determined baselines as an independent source for comparison, we computed the length, horizontal, and vertical components of these baselines from the observed orbits. On a 2000 km baseline the GPS determined components scatter around 2 cm (repeatability) while agreement with VLBI is 2 cm, or better, with especially good agreement in baseline length. We did this comparison for a number of different lengths up to about 3000 km and find agreement on the order of 1 part in  $10^8$  of the baseline length. For shorter baselines (a few hundred km) we get a few mm of repeatability from day to day (1 - 2 cm in the vertical). For longer baselines (up to 6000 km) all comparisons were well below the 1 part in  $10^8$  level for baseline length.

The reasons for improvement since the last experiment in 1985 are several in number. For this experiment we used a global tracking network covering four continents rather than just one (there were additional sites in Europe, in the South Pacific, and in South America). Also, software improvements were implemented (better carrier phase ambiguity resolution; uniformity in antennas and receivers; better estimation strategy). Using the global tracking network had the effect of reducing the scatter in baseline solutions dramatically (see figure). Also, instead of solving for three constant parameters per satellite per arc for the solar radiation pressure model, we implemented a process noise force model in which these parameters were allowed to vary within prescribed limits. This adds extra degrees of freedom to the model and made the orbit prediction more difficult because of the stochastic behavior of solar pressure coefficients. However, the RMS scatter of baseline determinations using pro-

cess noise force models was considerably less (dropping from several cm to only a few mm, except in the vertical which had just over 1 cm scatter) than using conventional dynamic modeling. This was particularly important since some of the satellites were in the eclipse season where the earth blocked out the sun for some time in each revolution and the radiation pressure model required special attention. With further global densification of the tracking network and the full GPS constellation, and, in addition, use of an advanced receiver with better pseudorange, we expect 20 cm orbits for GPS.

Summarizing, we believe we have achieved 50 - 60 cm GPS orbital precision using a worldwide tracking network and careful dynamical modeling. Using repeatability, prediction, and comparison with independently determined ground baselines, this precision is confirmed. User positioning (static) is available to the cm level over 1000's of km and few mm (horizontal only) over hundreds of km.

#### Discussion:

Question: On the second to last viewgraph, why are the orbit prediction comparisons sinusoidal?

Answer: The period of the sinusoids is about once per rev of the GPS satellite; any small difference in the orbital elements (such as inclination - making the arcs cross each other twice per rev) will cause this type of effect.

Question: How does your conclusion regarding sub-meter accuracy translate to real-time users of GPS.

Answer: I project precision of about a meter in real time provided differential observations are made to cancel errors associated with selective availability.

Question: What is the repeatability of the 2000 km baseline for shorter than two-week arcs?

Answer: For one-week arcs (we did not use process noise force models and did not have global network) repeatability was about 3 cm and also 50% worse agreement with VLBI baselines. Shorter arcs (1-day) results are three to four times worse.



## RECENT RESULTS IN HIGH-PRECISION GPS ORBIT DETERMINATION

- 1989: DATA FROM A 1988 WORLDWIDE GEODETIC TRACKING NETWORK HAS BEEN PROCESSED
  - GLOBAL TRACKING => MORE REALISTIC ORBIT SOLUTIONS
  - IMPROVED MODELING DEVELOPED FOR STOCHASTIC GPS ACCELERATIONS AND FOR NOISE CHARACTERISTICS OF TROPOSPHERIC DELAY FLUCTUATIONS
  - < 1 m ORBIT PRECISION (~ 55 cm) OBTAINED FOR 4 OF 7 GPS SATELLITES
  - ORBIT ACCURACY CONFIRMED BY COMPARING GROUND COORDINATE ESTIMATES TO INDEPENDENT SOLUTIONS FROM RADIO ASTROMETRIC TECHNIQUES
- DEMONSTRATES AN IMPROVEMENT BY FACTOR OF 2-3 DURING PAST TWO YEARS



## **HIGH-ACCURACY GPS ORBIT DETERMINATION**

- CARRIER PHASE (1 cm) AND PSEUDORANGE (~ 200 cm) PROCESSED TOGETHER
- 3 REFERENCE GROUND SITES HELD FIXED AT VLBI PRE-DETERMINED COORDINATES
  - VLBI — VERY LONG BASELINE INTERFEROMETRY ... USES RADIO ASTRONOMICAL OBSERVATIONS OF QUASARS
- USE GPS DATA TO ESTIMATE PARAMETERS WITH FACTORIZED KALMAN FILTER:
  - GPS ORBITAL EPOCH STATES AND STOCHASTIC ACCELERATION PARAMETERS
  - CORRECTIONS TO THE ROCK4 GPS SOLAR RADIATION PRESSURE COEFFICIENTS
  - PROCESS NOISE TROPOSPHERIC DELAY PARAMETERS
  - BIAS PARAMETERS AND WHITE NOISE CLOCKS
- MULTI-DAY ARCS (3-14 days) USED TO IMPROVE ORBIT ACCURACY



## **GPS DYNAMIC MODELS**

- GRAVITY FIELD 8X8 (GODDARD MODEL GEM-L2)
- ROCK4 SOLAR RADIATION PRESSURE REPRESENTATION IS CRITICAL FOR ORBIT ACCURACY
  - THREE PARAMETERS: GX, GZ AND GY
  - 1985 EXPERIMENT: STOCHASTIC ADJUSTMENT OF GX, GZ FOR ARCS > 1 week  
EQUIVALENT TO ~ 3% VARIATION PER 24 hrs
  - 1988 EXPERIMENT: FOUND THAT MUCH HIGHER LEVELS OF PROCESS NOISE WERE NEEDED  
EQUIVALENT TO ~ 10% VARIATION PER 24 hrs

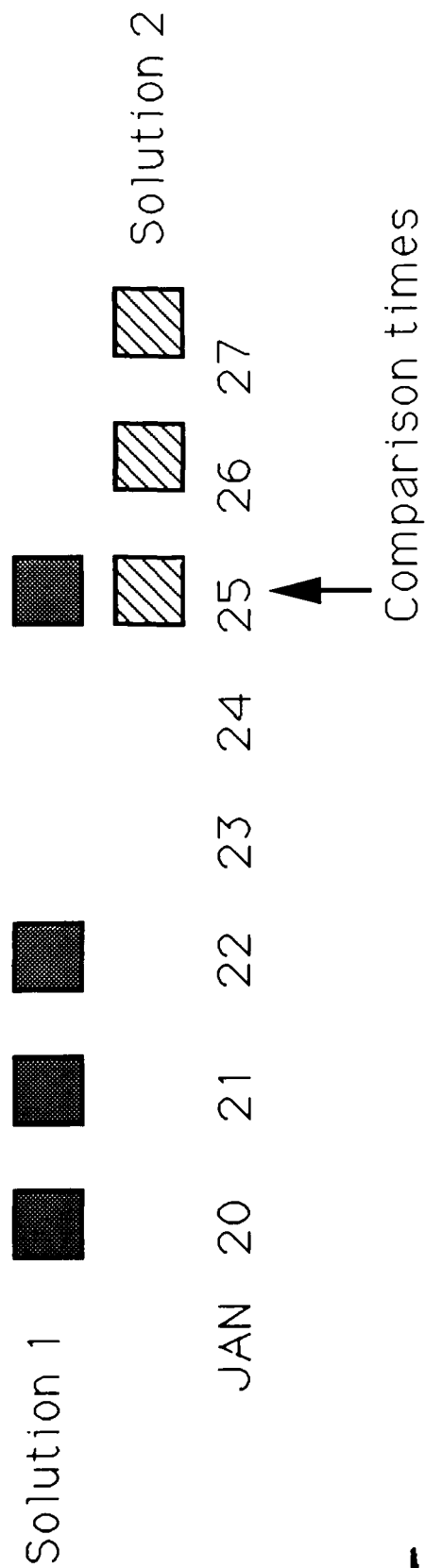




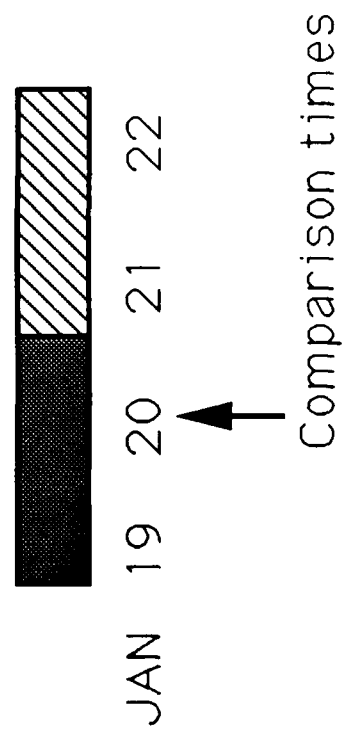
## REPEATABILITY AND ORBIT PREDICTION RESULTS

- JAN 88 EXPERIMENT: 4 GPS (OF 7) SHOW SUB-METER ORBIT REPEATABILITY
  - AVERAGE SINGLE ORBIT COMPONENT DIFFERENCE FOR THESE 4 SATELLITES: 0.54 m  
(FOR NOV 85 EXPERIMENT, 2 GPS SHOWED SUB-METER REPEATABILITY)
- JAN 88 ORBIT PREDICTION INTO ADJOINING DAY: 3 GPS (OF 7) SHOW SUB-METER AGREEMENT
  - AVERAGE SINGLE ORBIT PREDICTION DIFFERENCE 0.80 m  
(FOR NOV 85 EXPERIMENT, 1 GPS PREDICTION WAS BETTER THAN 1 m)

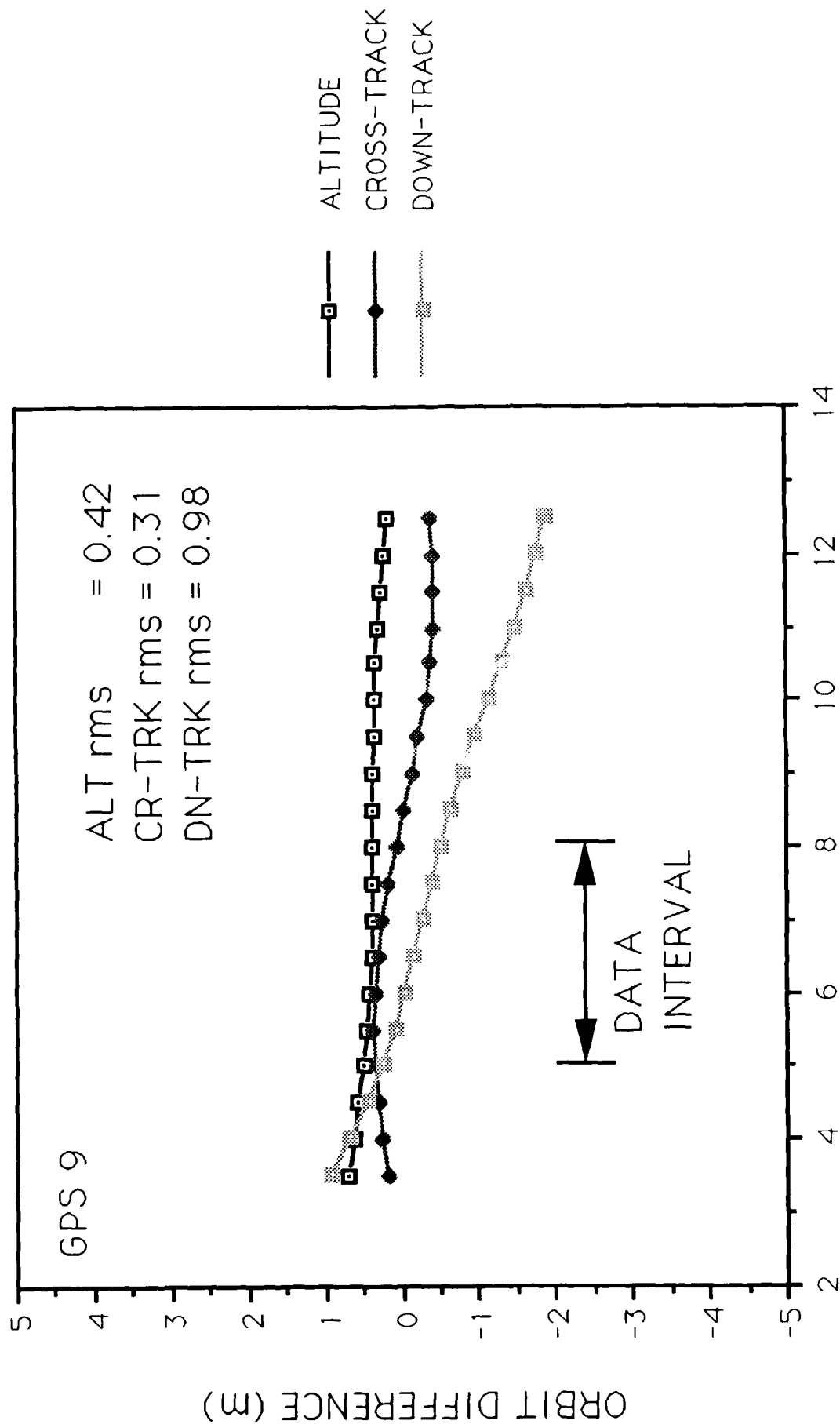
# OBSERVATION INTERVALS FOR ORBIT REPEATABILITY TEST



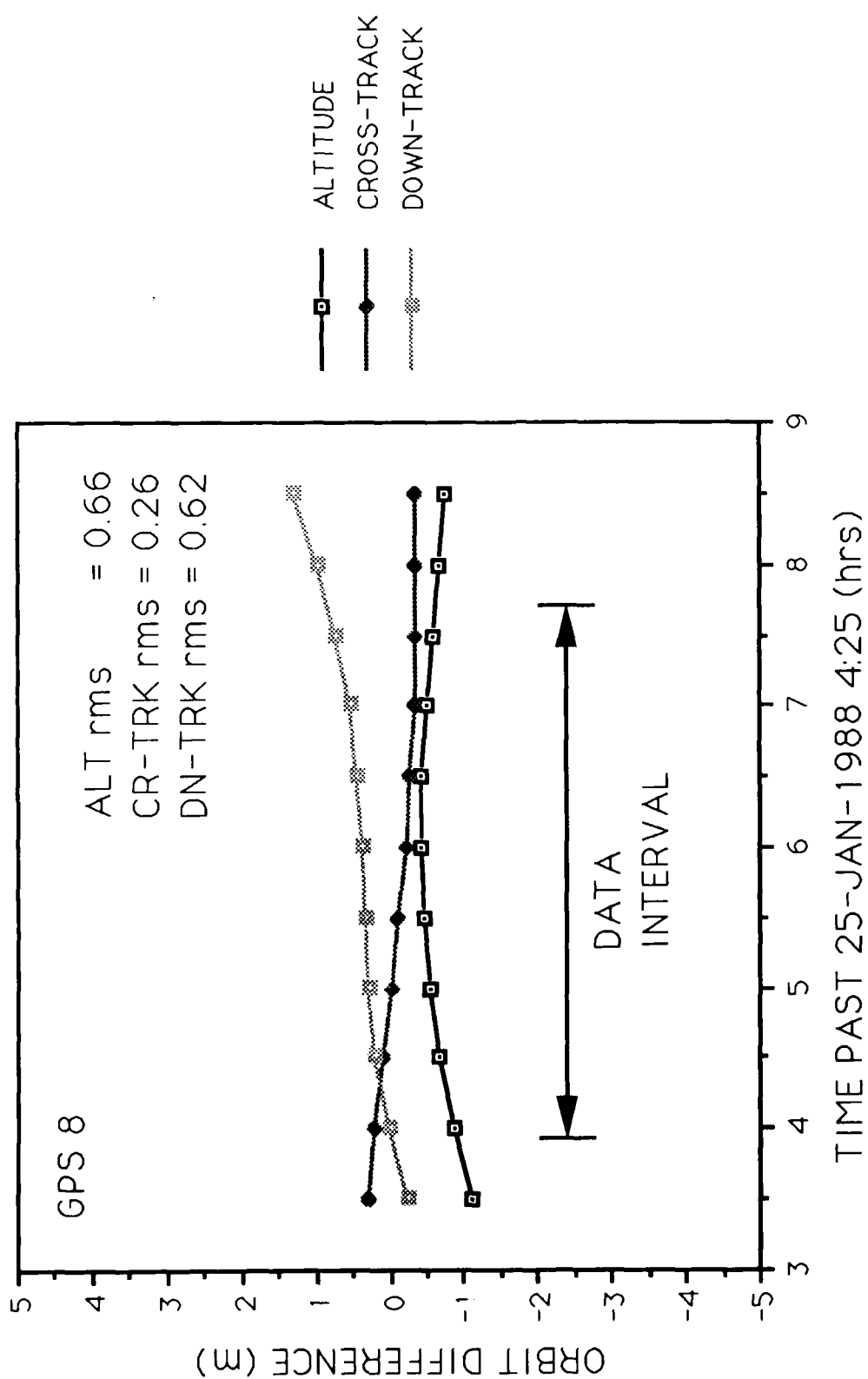
# OBSERVATION INTERVALS FOR ORBIT PREDICTION TEST



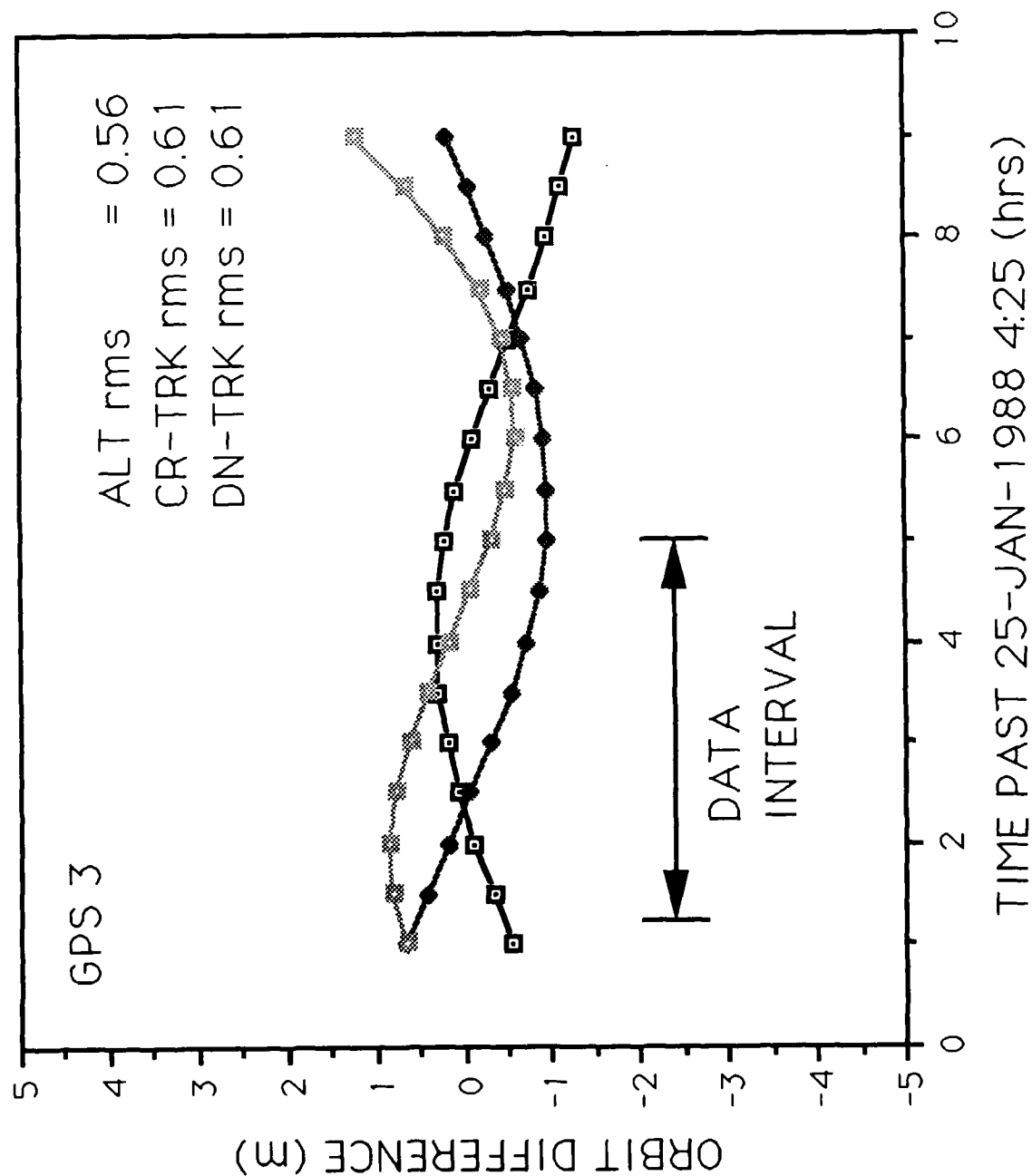
# GPS ORBIT REPEATABILITY



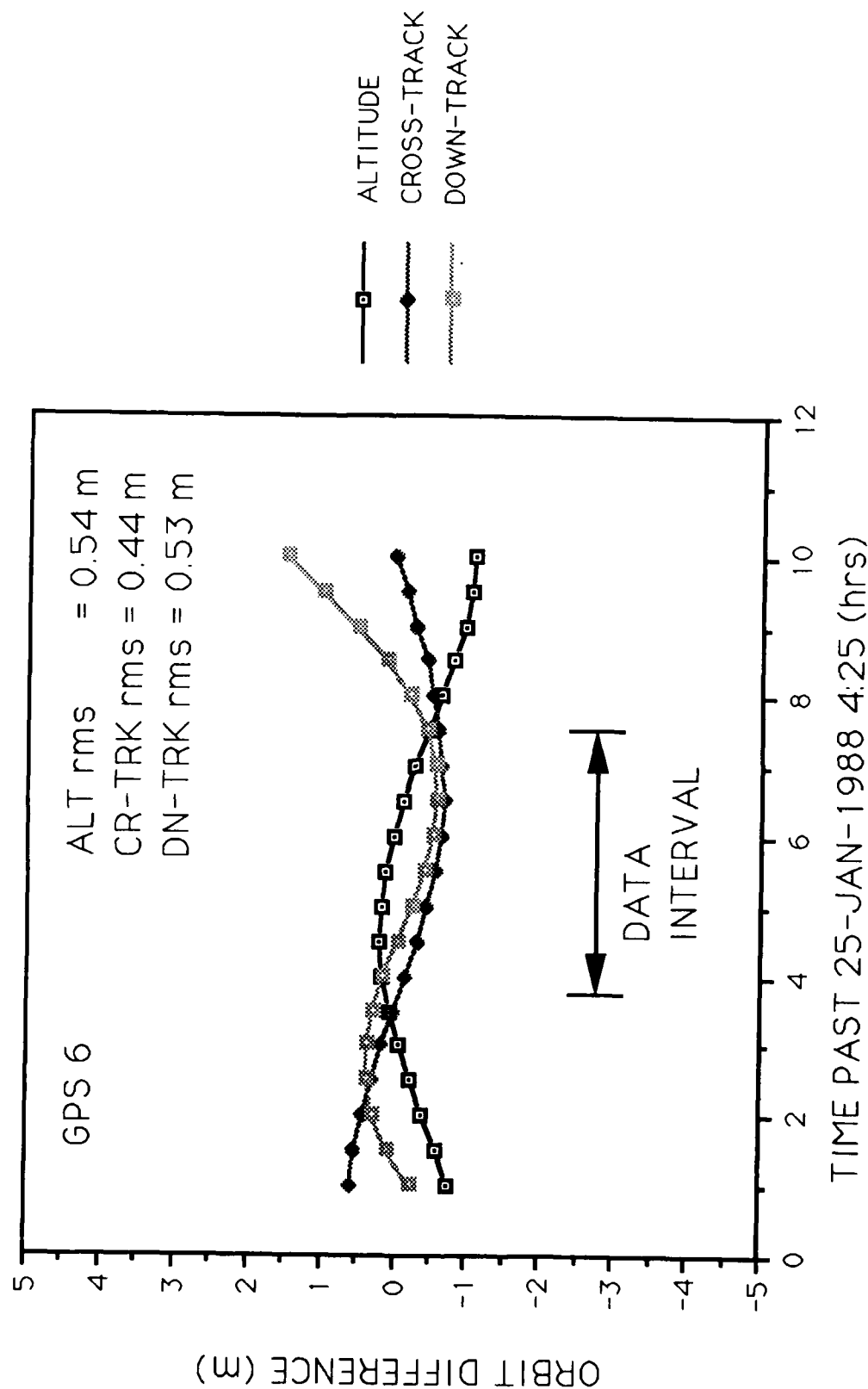
# GPS ORBIT REPEATABILITY



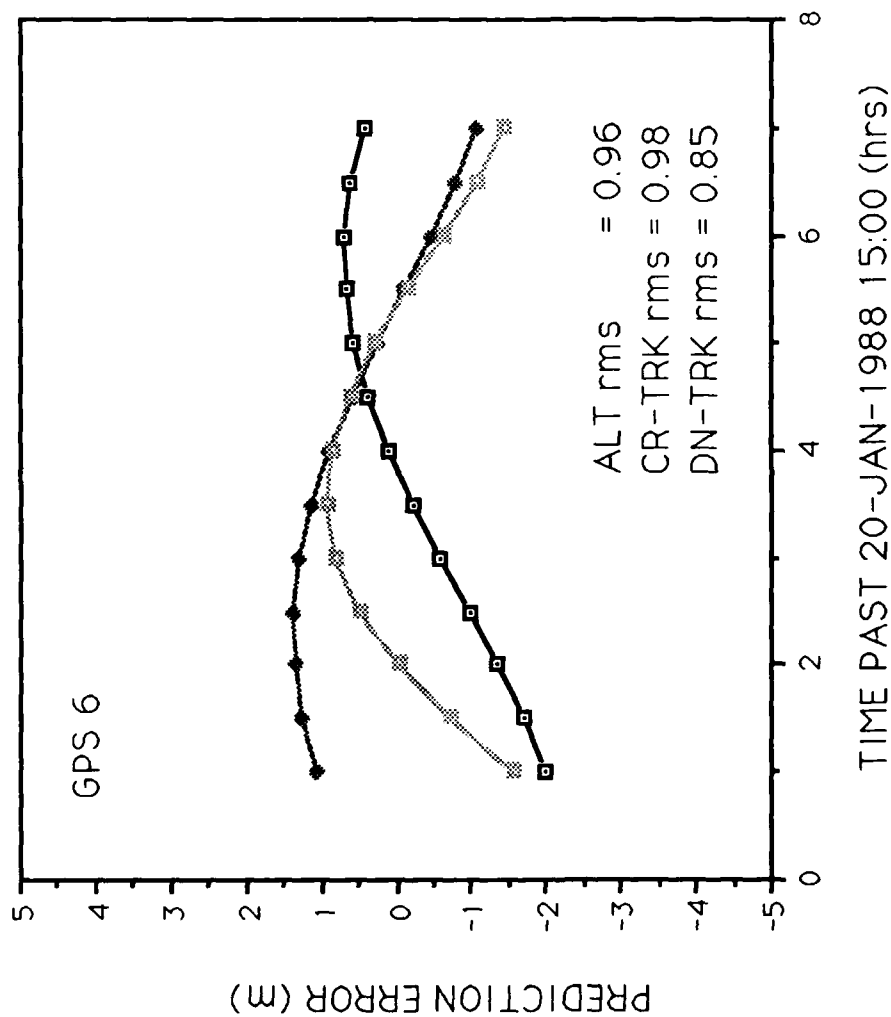
# GPS ORBIT REPEATABILITY



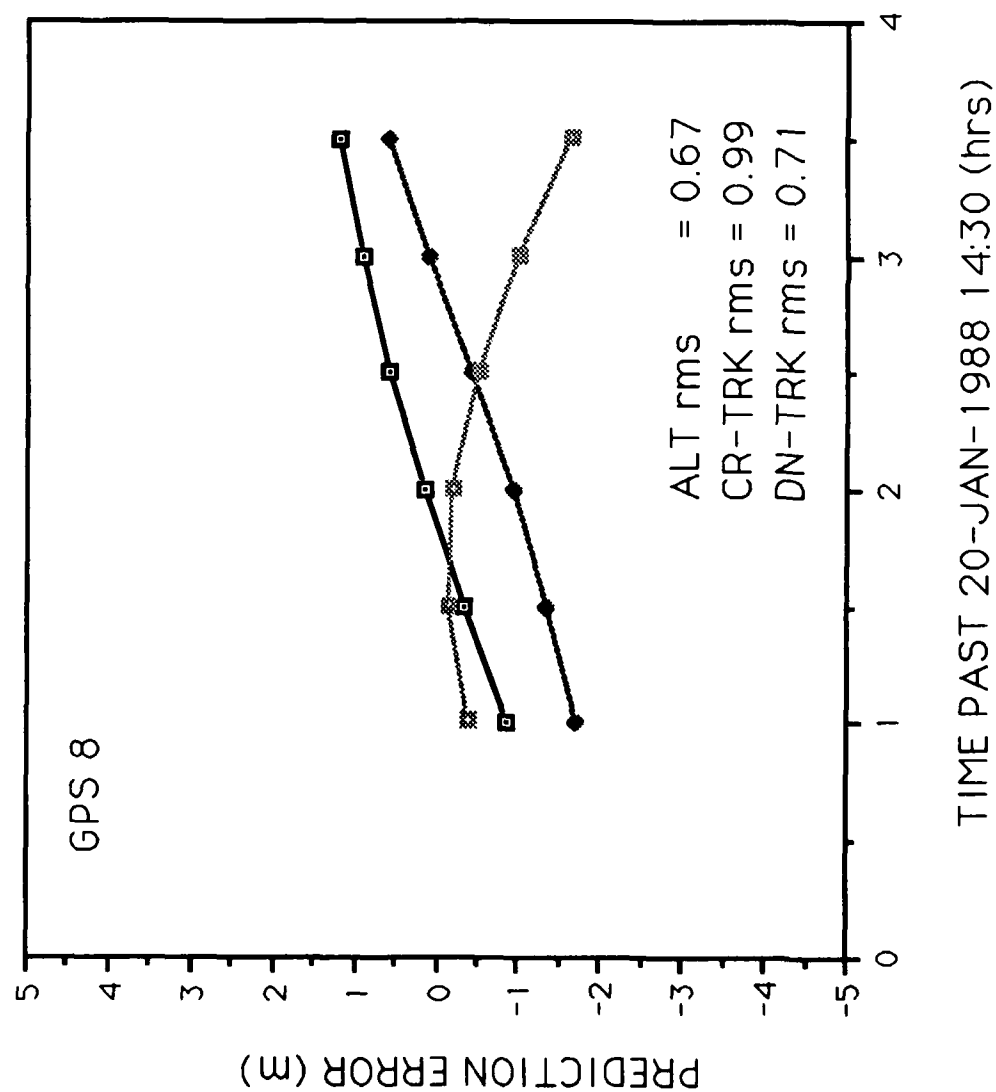
# GPS ORBIT REPEATABILITY



# ORBIT PREDICTION WITH MULTI-DAY ARCS



# ORBIT PREDICTION WITH MULTI-DAY ARCS



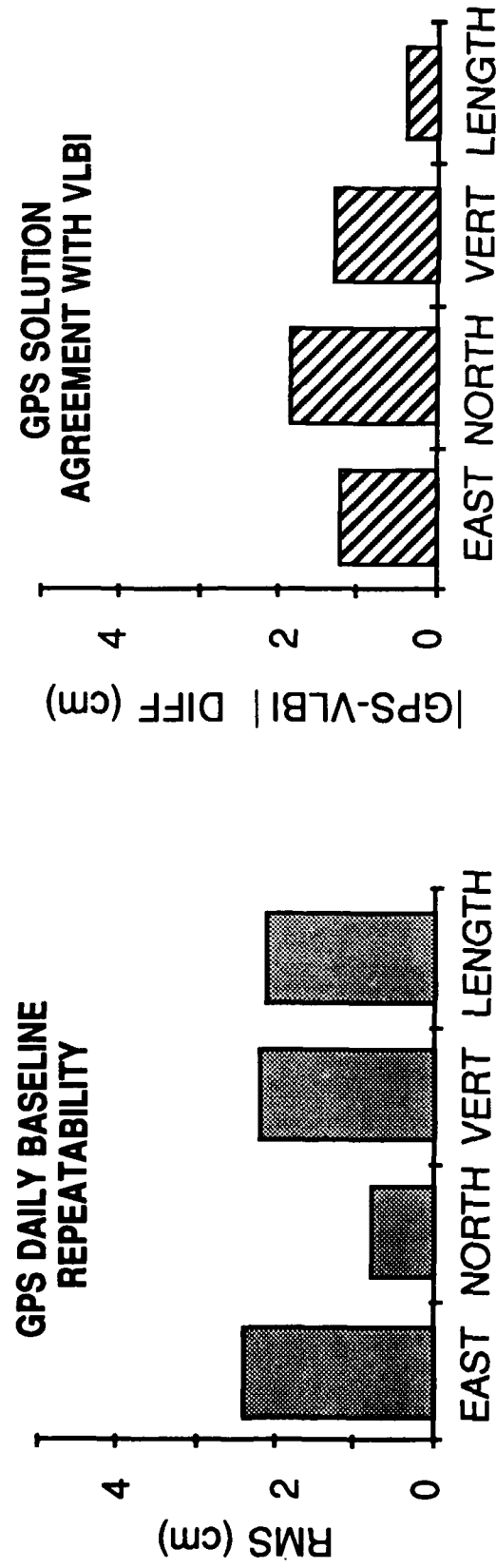




## **PRECISION AND ACCURACY FOR GPS GROUND BASELINE SOLUTIONS**

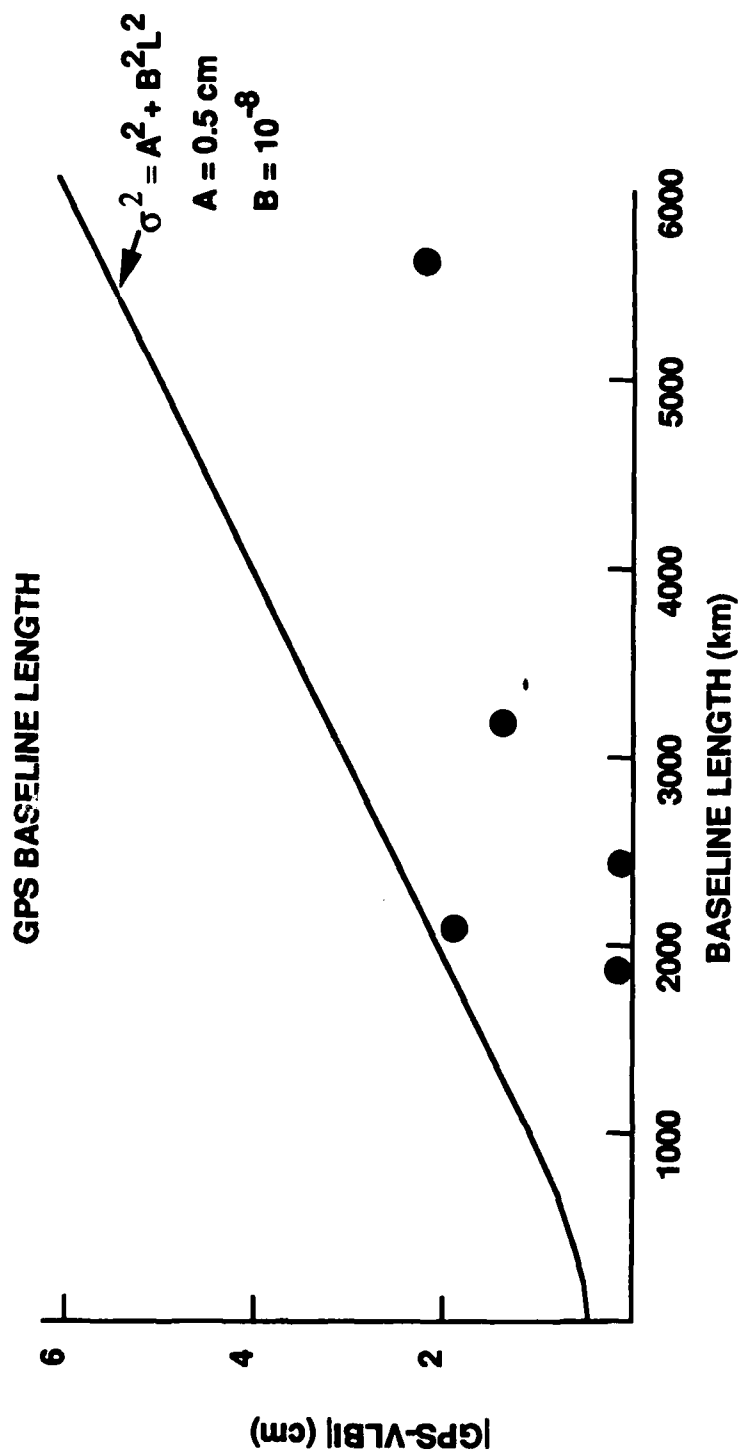
- ACCURACY JUDGED BY GPS-VLBI AGREEMENT
  - VLBI IS AN INDEPENDENT AND EXTREMELY PRECISE RADIO ASTROMETRIC TECHNIQUE
- PRECISION JUDGED BY DAILY BASELINE REPEATABILITY
  - $\sim 1$  PART IN  $10^8$  FOR BASELINES 2000-3000 km
  - $\sim 0.5$  cm (IN HORIZONTAL) FOR SHORTER BASELINES OF SEVERAL HUNDRED km
  - SEVERAL PARTS IN  $10^9$  (several cm) IN LENGTH DETERMINATION FOR BASELINES 2000-6000 km

# HATCREEK - FORT DAVIS 2000 km



121

2-WEEK ORBIT ARC (NOV 1985)  
 STOCHASTIC TROPOSPHERE AND SOLAR PRESSURE ESTIMATION  
 FIDUCIAL SITES: HATCREEK, RICHMOND, HAYSTACK



Data from 1985 North American field test and from 1988 Casa Uno Experiment  
 JPL Multi-day arc orbits

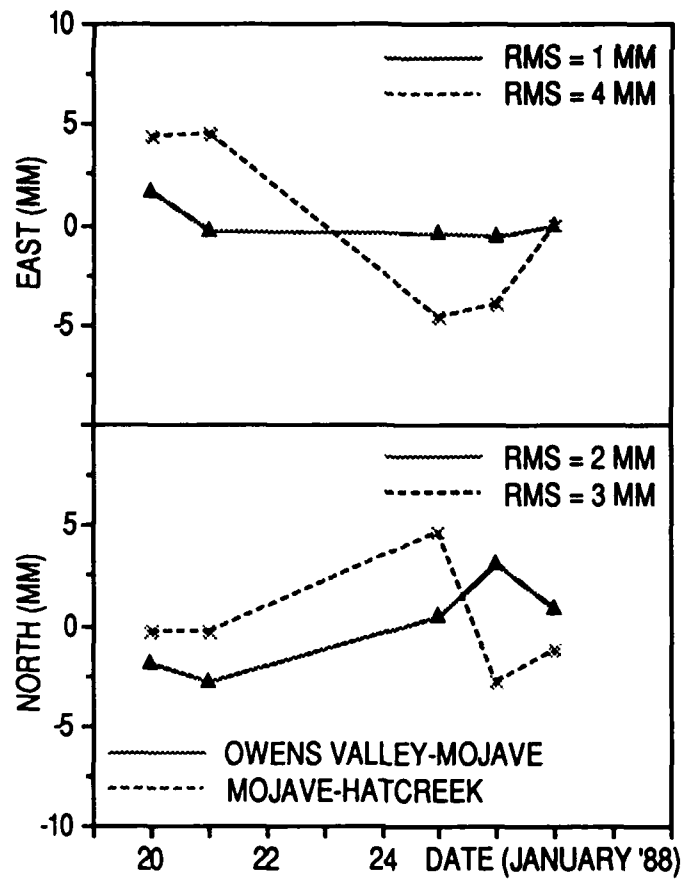


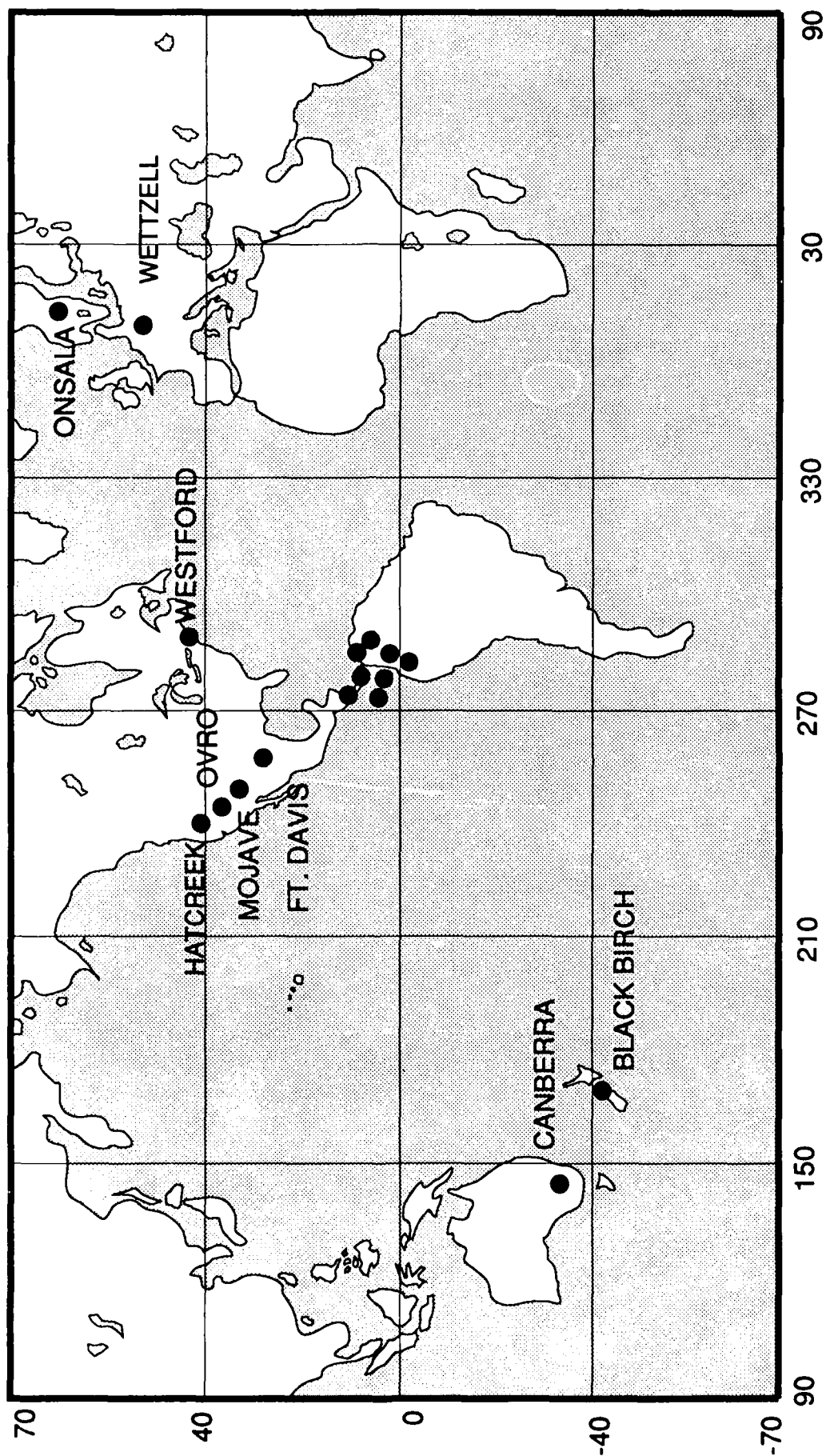
Fig. 2. Millimeter-level precision in horizontal baseline components with GPS for the Mojave-Hatcreek (729 km) and the Owens Valley-Mojave (245 km) baselines. Results based on single-day constrained and bias fixed filter solutions.



## REASONS FOR RECENT IMPROVEMENT IN GPS ORBIT DETERMINATION AND GROUND POSITIONING

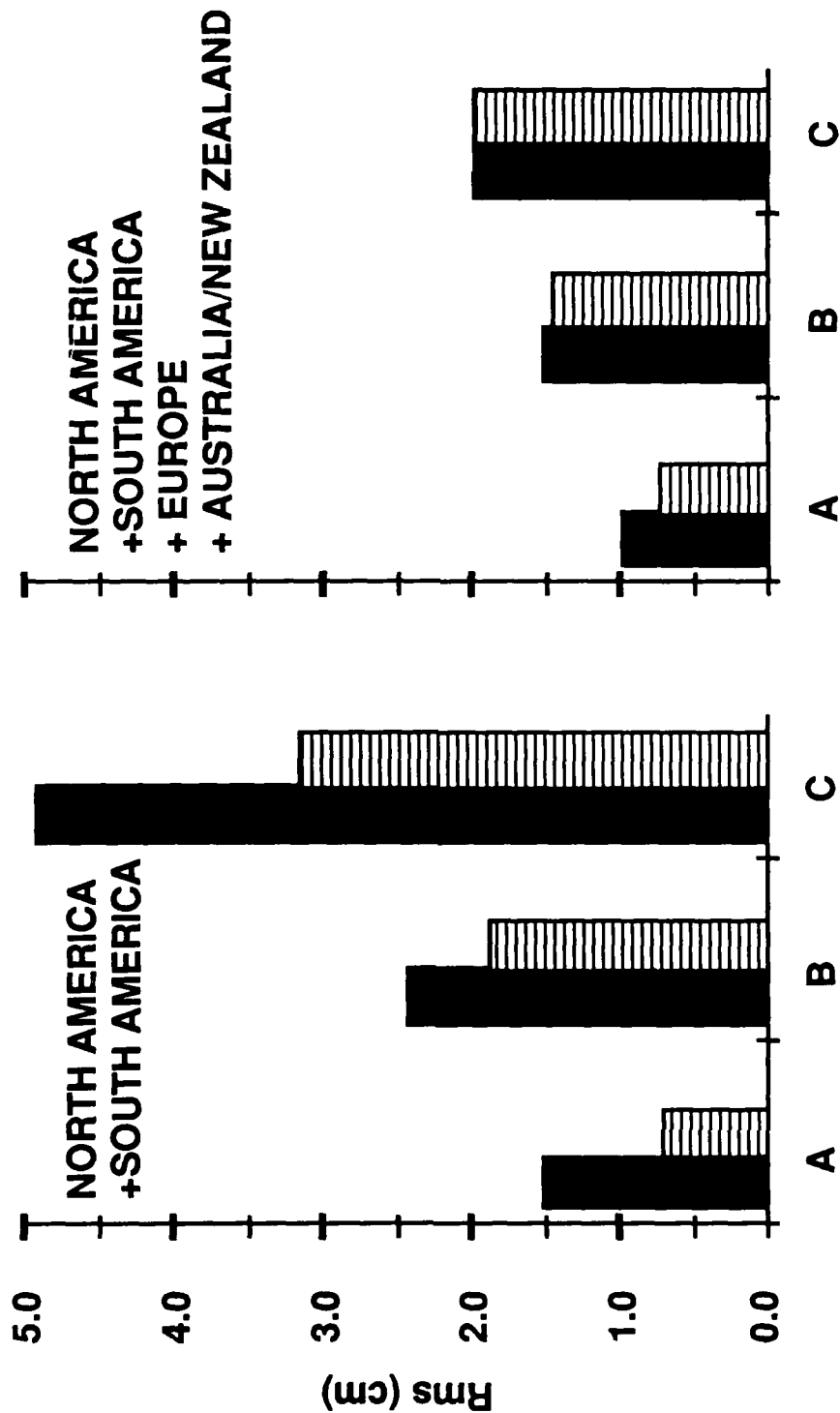
- LARGER, MORE GLOBAL TRACKING NETWORK COVERED 4 CONTINENTS (AS OPPOSED TO 1)
- IMPROVED CARRIER PHASE CONNECTION SOFTWARE AND DATA EDITOR  
IMPROVED CARRIER AMBIGUITY RESOLUTION TECHNIQUES  
OFTEN USED IN SHORTER ARCS TO STRENGTHEN ORBITS AND GROUND BASELINES  
SUCCESSFUL OVER DISTANCES AS LONG AS 3000 km
- UNIFORMITY OF RECEIVER AND ANTENNA TYPES
- REFINEMENTS IN ESTIMATION STRATEGY, PARTICULARLY IN USE OF PROCESS NOISE
- COVARIANCE ANALYSIS: EXPECT ~ 20 cm GPS ORBITS WITH EXPANDED GROUND NETWORK, FULL  
GPS CONSTELLATION (18 SATELLITES), AND ADVANCED RECEIVERS/ANTENNAS IN mid-1990s

# 1988 CASA UNO GLOBAL TRACKING NETWORK



# **SOUTH AMERICA DAILY BASELINE REPEATABILITY 1988 CASA UNO EXPERIMENT**

Rms east  
 Rms north



A: 50-300 km baselines (6)  
 B: 300-600 km baselines (6)  
 C: 600-1000 km baselines (5)

ALL BASELINES ARE IN  
 SOUTH AMERICA AND ARE  
 BIAS FIXED



## DISCUSSION OF GPS ORBIT PREDICTION

- JAN 88 ORBIT *PREDICTION* ERRORS GREW FASTER THAN WITH NOV 85 EXPERIMENT
  - 4 SATELLITES WERE IN ECLIPSE SEASON IN JAN 88
  - REQUIRED EXTRA PROCESS NOISE FORCE MODELING (SOLAR RADIATION PRESSURE)
  - STOCHASTIC SOLAR RADIATION FORCES MADE ORBIT PREDICTION MORE DIFFICULT



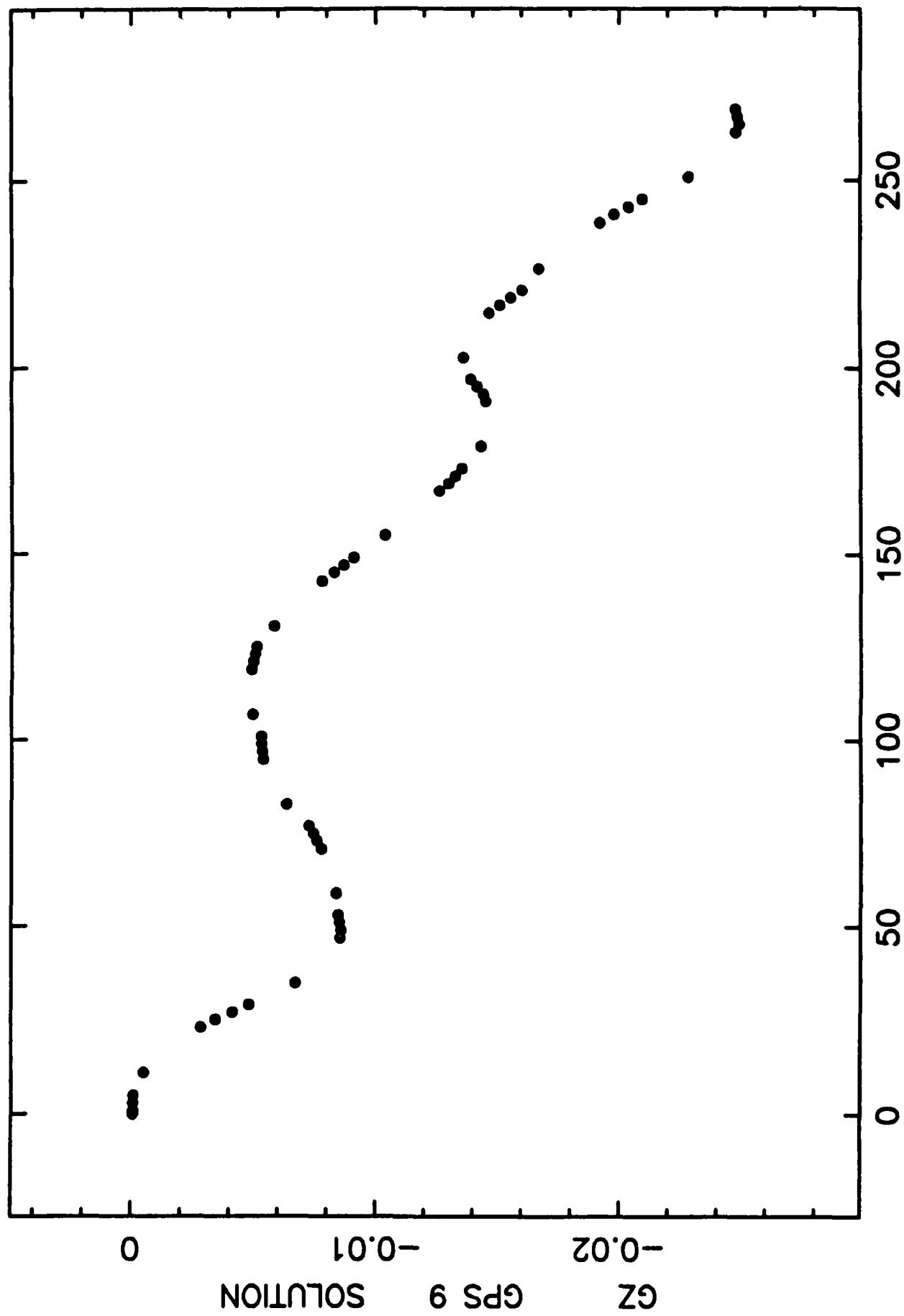
# DAILY BASELINE REPEATABILITY

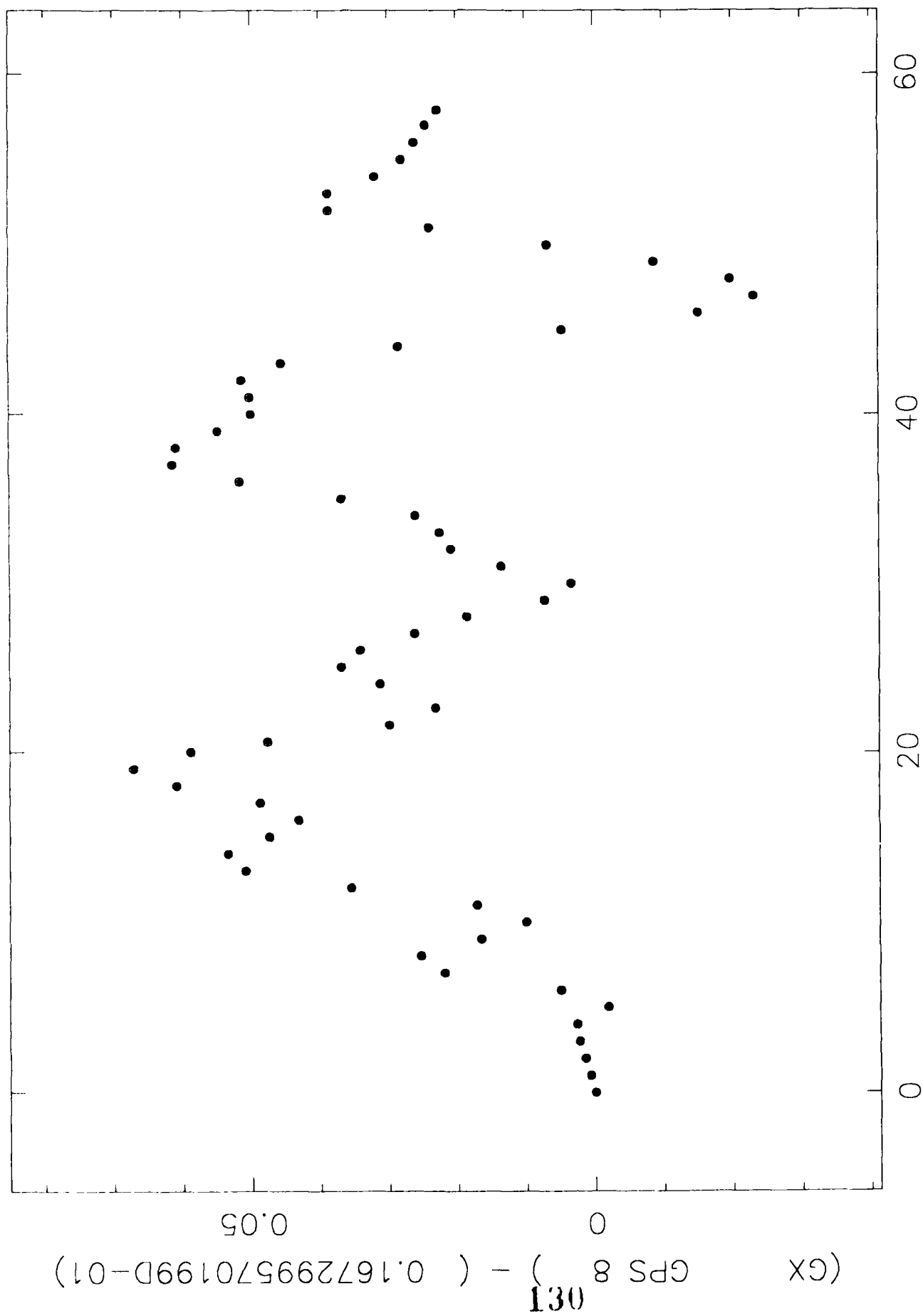


## MOJAVE - HATCREEK (729 km)

CASA UNO JAN 1988

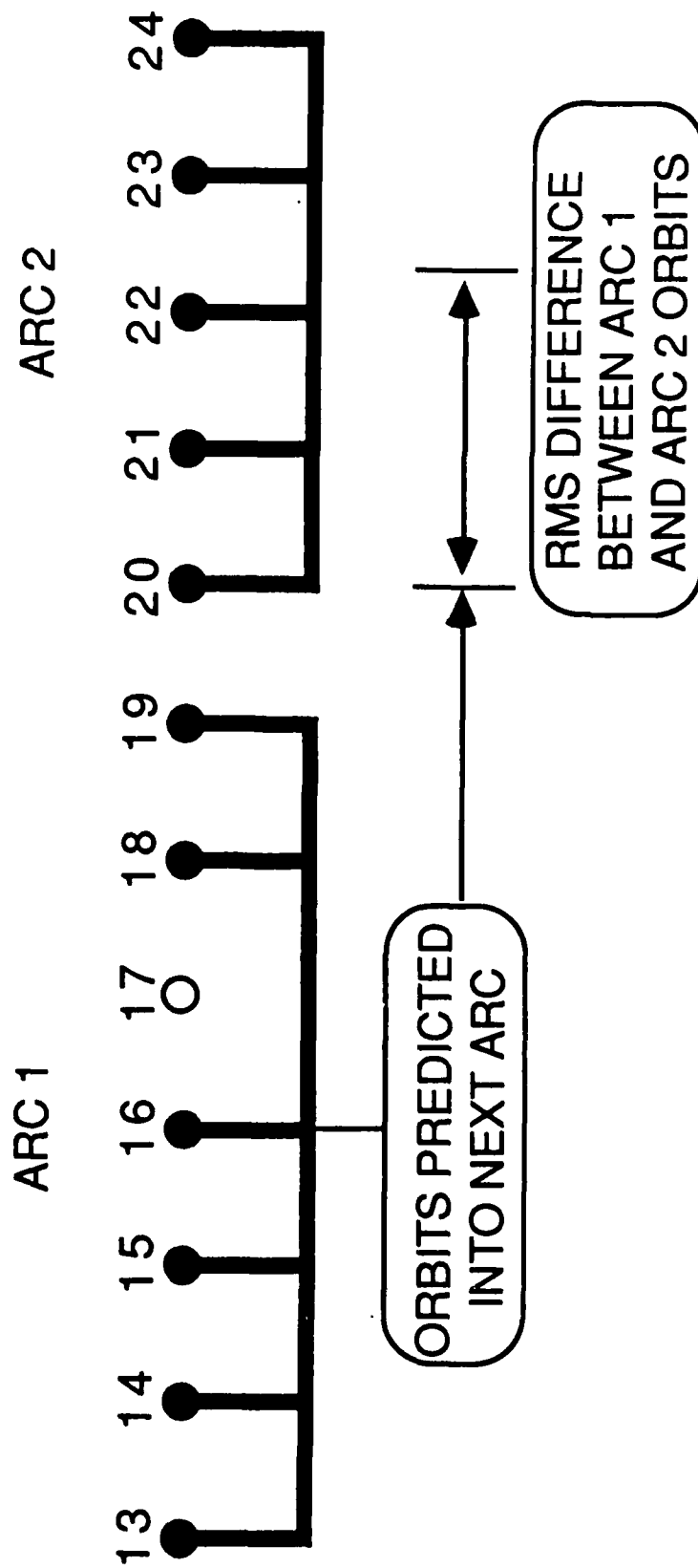
6 North American + 2 European + 4 South American stations  
(3 North American fiducials)

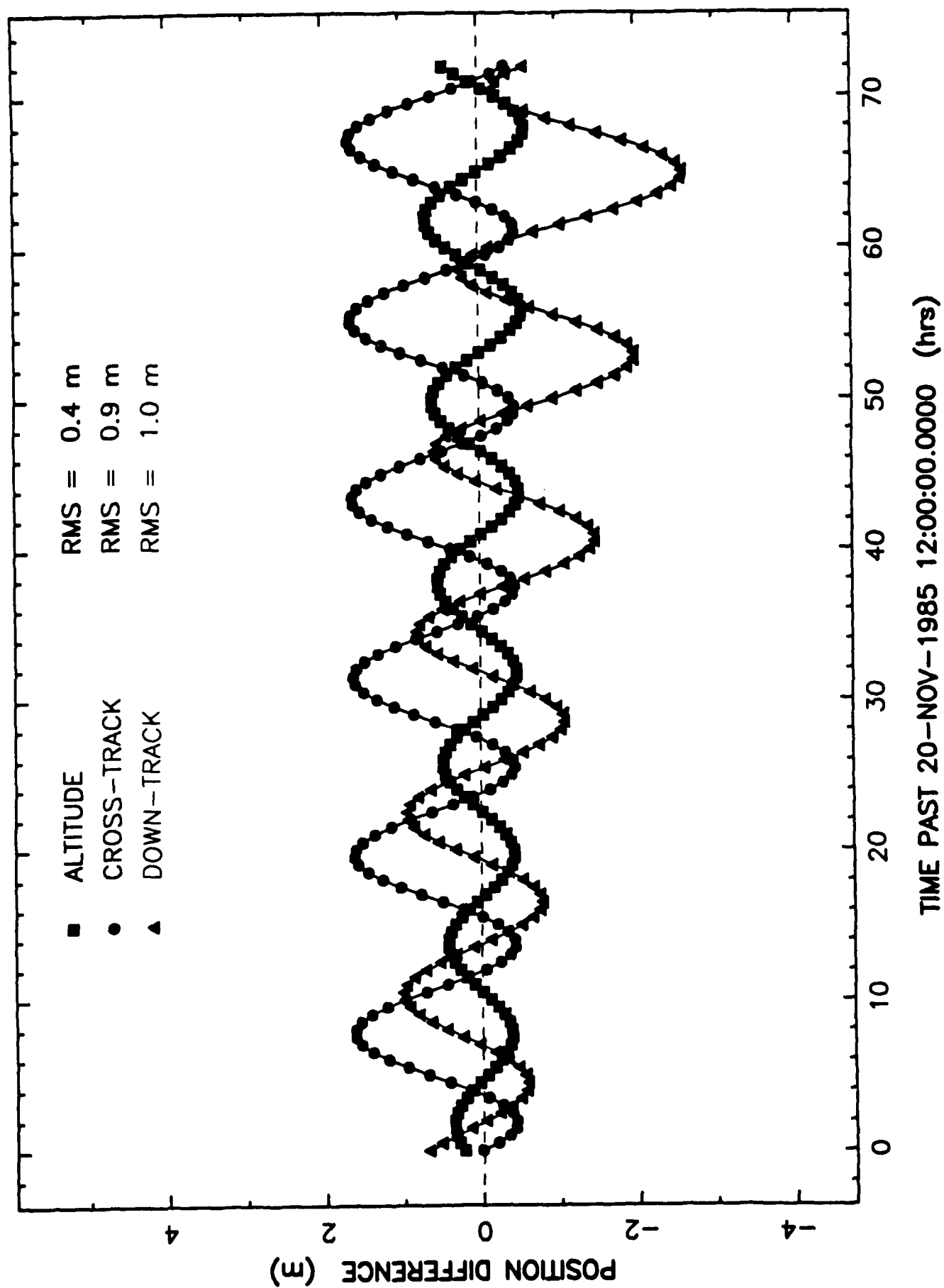




. . TIME PAST 25-JAN-1988 05:22:30.0000 (HRS).

# NOVEMBER 1985 MULTI-DAY ARCS







## SUMMARY

- 50-60 cm GPS ORBIT PRECISION ACHIEVED WITH WORLDWIDE GROUND TRACKING
  - ORBIT FORMAL ERRORS
  - ORBIT REPEATABILITY
  - ORBIT PREDICTION COMPARISONS
  - GROUND STATION COORDINATES COMPARED TO INDEPENDENT VLBI MEASUREMENTS
- USER POSITIONING ACCURACY (STATIC) WITH THESE ORBITS:    ~ cms OVER THOUSANDS OF km ( $1:10^8$ )  
   ~ mms OVER HUNDREDS OF km
- THESE RESULTS WERE OBTAINED WITH DEGRADED PSEUDORANGE, COMPARABLE TO FUTURE CODELESS OPERATION FROM ADVANCED RECEIVERS
- IMPORTANCE SHOWN FOR USING WORLDWIDE GPS TRACKING AND CAREFUL DYNAMICAL MODELING TO REACH HIGHEST ACCURACY
- GPS APPLICATIONS REQUIRING cm-LEVEL USER POSITIONING ARE FEASIBLE: THIS LEVEL OF ACCURACY HAS BEEN DEMONSTRATED WITH GROUND BASELINES (STATIC POSITIONING)



## Closed Loop Orbit Trim Using GPS

Penina Axelrad and Bradford W. Parkinson  
*Stanford University*

The paper presented describes an onboard closed-loop navigation and control system capable of executing extremely precise orbit maneuvers. It uses information from the Global Positioning System (GPS) and an onboard controller to perform orbit adjustments. As a result, the system *circumvents the need for extensive ground support*. The particular application considered is an orbit injection system for NASA's Gravity Probe B (GP-B) spacecraft. Eccentricity adjustments of 0.0004 to 0.005, and inclination and node changes of 0.001 to 0.01 deg. are demonstrated. The same technique can be adapted to other satellite missions.

GP-B is a NASA project primarily designed to test two aspects of Einstein's theory of General Relativity. Based on General Relativity, L.I. Schiff predicted that a gyroscope in orbit around the Earth will undergo two motions not predicted by Newtonian analysis. These are known as the *geodetic* and *frame dragging* precessions. In a precisely polar orbit at an altitude of approximately 650 km, the two effects would be orthogonal, with magnitudes of 6.6 arcsec/yr and 42 milliarcsec/yr respectively. The objective of the GP-B mission is to place a gyroscope in such an orbit and measure its relativistic drift to an accuracy of three tenths of a milliarcsecond.

The orbit of the GP-B satellite is critical to minimize the disturbances on the gyro. Ideally the spacecraft must follow a purely gravitational path (geodesic) through space. It should also be in a precisely polar orbit aligned with the guide star, Rigel. (A telescope pointed at the guide star serves as a directional reference for the gyro.) Such an orbit causes the geodetic and frame dragging effects to be orthogonal. In addition a circular orbit is desired to simplify the data reduction and to improve the geodetic information which can be derived from the GP-B orbit data.

There are two unusual aspects of the GP-B orbit injection system. First is that the orbit control system will only be used at the start of the mission to guide the satellite to its target orbit after separation from the launch vehicle upper stage. After this final orbit trim, the spacecraft will follow a "drag-free" orbit, and no additional translational control may be applied. On a more conventional mission, the closed-loop system would be employed continuously or perhaps periodically. The second feature is the extremely low level of thrust available. Thrust is provided by directing the flow of helium as it is vented from the experimental dewar through the appropriate set of thrusters. The maximum acceleration provided to the spacecraft is approximately 0.5  $\mu\text{g}$ .

The role of the navigation system is to provide orbit information to the control system. A GPS receiver onboard the spacecraft furnishes both range and range rate measurements to the navigation processor. Using state of the art components, GPS range accuracy is expected to be approximately 5 m (1- $\sigma$ ) and range rate accuracy about 0.01 m/s (1- $\sigma$ ). The navigation processor determines the orbit by propagating a target orbit plus the current deviation from the target orbit. The target orbit is modeled accounting for the effects of the Earth oblateness, whereas the deviations are small



enough to warrant the use of a linearized dynamic model. A Kalman filter propagates the estimated deviations using this linearized model and GPS information. The navigation system does not provide the ultimate in accuracy, but rather is adequate to meet the needs of the onboard controller.

The objective of the GP-B orbit trim system is to achieve the target orbit in minimum time. The optimal control in this case calls for full thrust capability at all times or "bang-bang" control. In the linearized dynamic model the out of plane and in plane deviations are decoupled, thus simplifying the control algorithm. Two levels of thrust were considered - the nominal 0.5  $\mu$ g helium thrusters and a higher powered 10  $\mu$ g alternative.

The results of this design and simulation study demonstrated that both the high and low power thrusters can effectively execute small orbit trim maneuvers for GP-B and other similar missions. For the low power helium thrusters it is crucial to account for the dynamics caused by the Earth's nonspherical mass distribution, because the thrust level is the same order of magnitude, and in some cases significantly smaller than the disturbing forces.

GPS provides a whole new basis for satellite orbit maneuvering. By providing accurate position and velocity information directly to the spacecraft, it permits the design of an effective onboard closed-loop orbit correction system. This holds great promise not only for the spacecraft orbit trim system described here, but also for a host of other missions such as automatic missile trajectory control, orbital transfer vehicle guidance, and launch vehicle control. We have demonstrated the feasibility of such a system and outlined the general design approach.

Discussion:

Question: How well do you have to know the spacecraft center of mass?

Answer: An onboard mass trim system is used to balance the spacecraft after launch.

Question: What is the altitude?

Answer: 650 km.

Question: What is length of mission for meaningful results?

Answer: Data will be collected for 18 months starting in 1995.

## CLOSED LOOP NAVIGATION AND CONTROL

**Objective:** Design a *closed loop* system to perform orbit adjustments for a near Earth spacecraft.

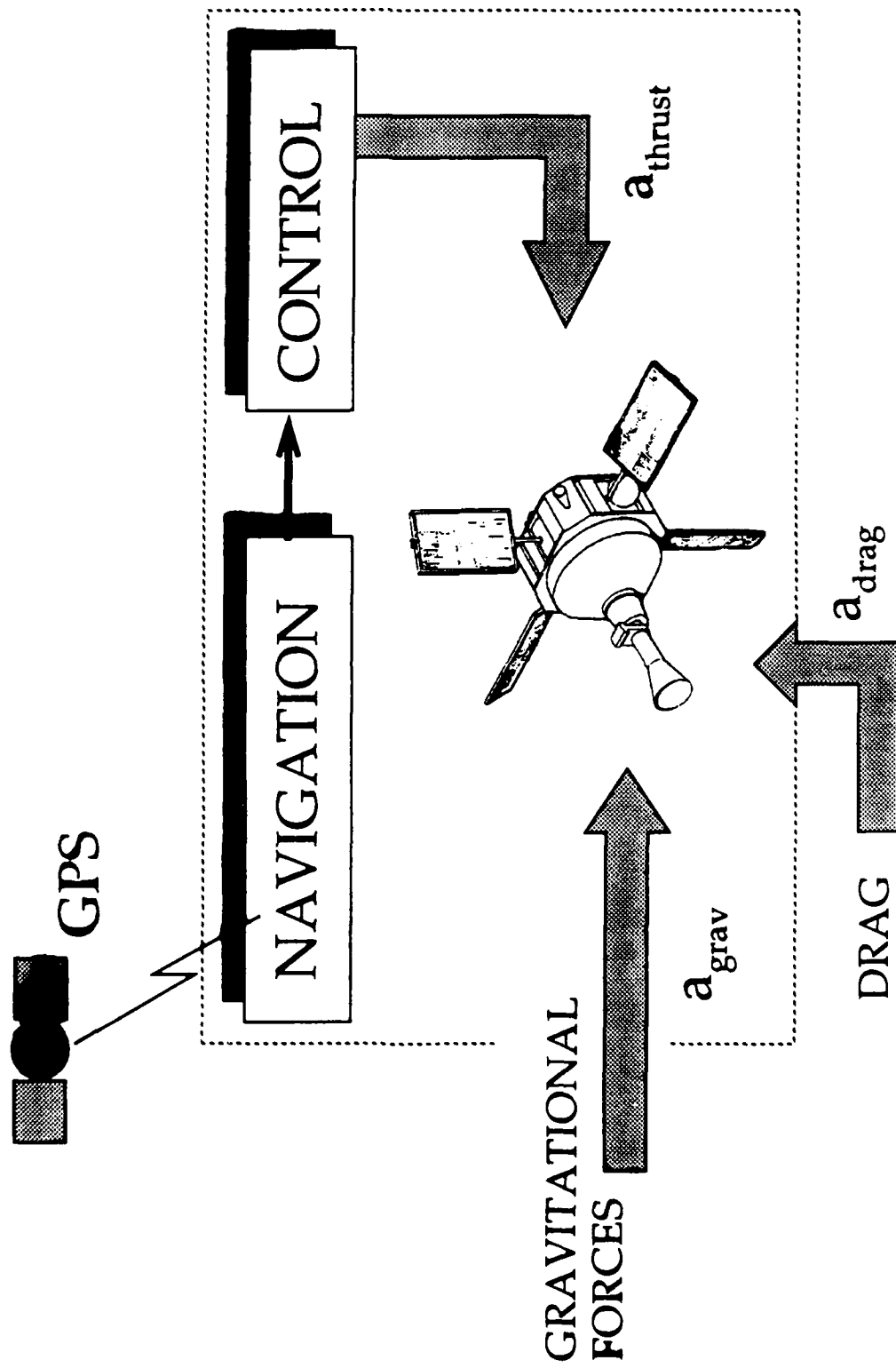
**Application:** NASA's Gravity Probe B (GP-B).

**Technique:**

Use the Global Positioning System (GPS) to provide navigation information *onboard* the satellite. Treat orbit adjustment as a closed loop control problem.

**Benefits:** Highly precise orbit maneuvers without the need for extensive ground support.

## CLOSED LOOP NAVIGATION AND CONTROL



## GPS USE on GRAVITY PROBE - B

- Closed Loop Orbit Trim
  - Navigation data needed onboard the spacecraft.
  - Bandwidth of at least 0.1 Hz.
  - Both position and velocity required.
  - Only one or two ground stations planned with daily data dump and emergency link through TDRSS
- Geodesy Coexperiment
  - Pseudorange, carrier phase, and doppler collected and telemetered to the ground for post-processing.
  - Bandwidth of at least 0.1 Hz.
- GP-B Receiver Requirements
  - All-in-view, carrier phase tracking receiver.
  - Minimum of 4 multipath resistant antennas.
  - C/A code pseudoranges.



**WHAT GP-B  
WILL TEST**

**NASA  
STANFORD  
Lockheed**

PREVIOUSLY UNVERIFIED PREDICTIONS OF  
ALBERT EINSTEIN'S GENERAL THEORY OF RELATIVITY

DRAGGING OF SPACE-TIME BY ROTATING MASSIVE BODIES

EFFECT OF WARPING OF SPACE-TIME ON SPINNING TEST BODY

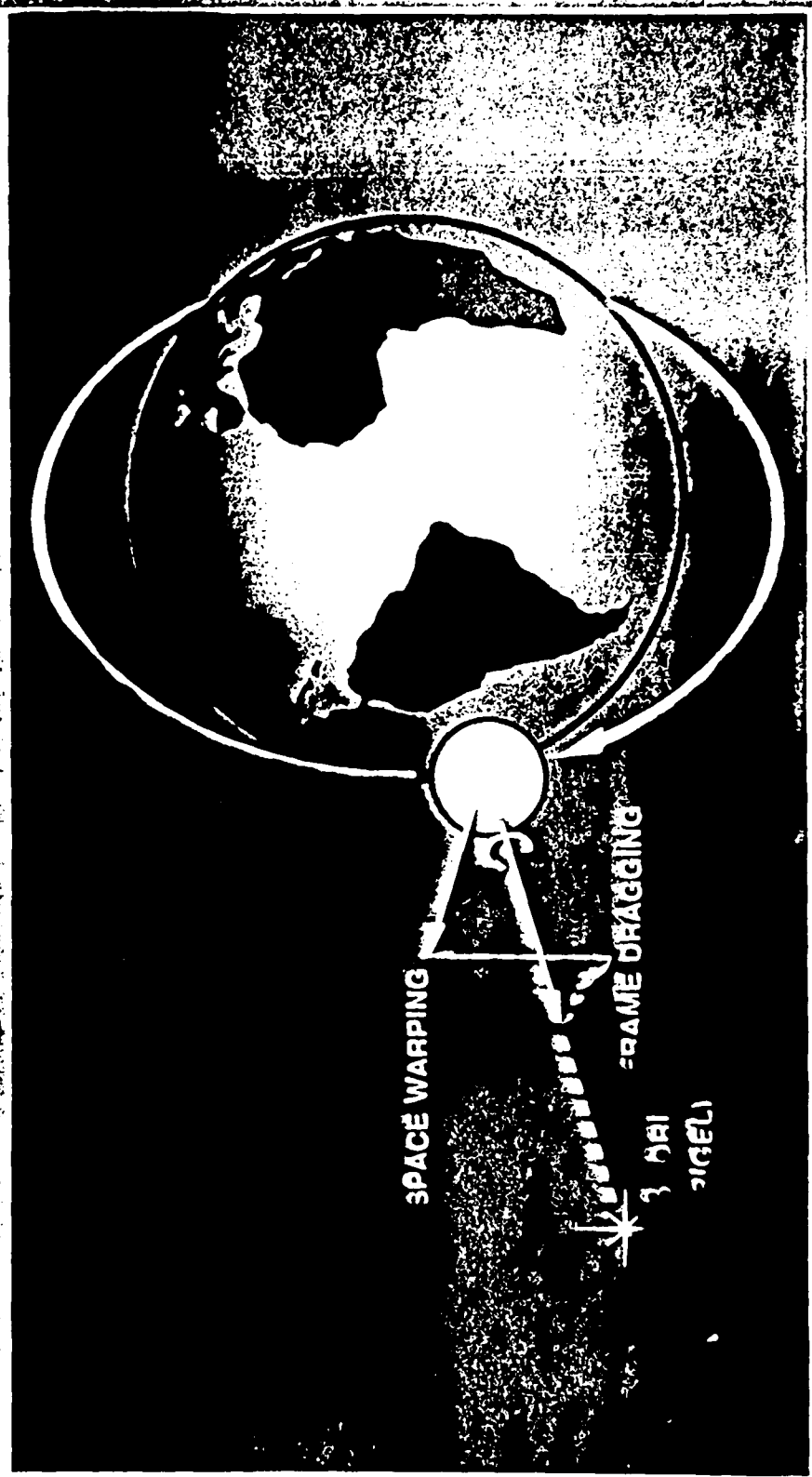
- A PRECISE AND DEFINITIVE TEST OF EINSTEIN'S THEORY

287.004

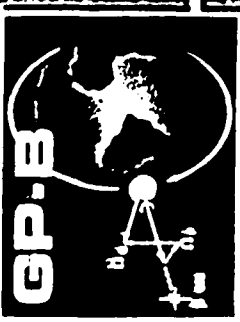


NASA  
STANFORD  
LOCKHEED

# THE EXPERIMENT



287.007



## REQUIREMENTS

NASA  
STANFORD  
Lockheed

- ULTRA LOW DRIFT GYRO
- REFERENCE GYRO TO GUIDE STAR
- REFERENCE GUIDE STAR TO INERTIAL SPACE



- SEPARATE RELATIVISTIC EFFECTS
- DEVISE CREDIBLE CALIBRATION METHOD

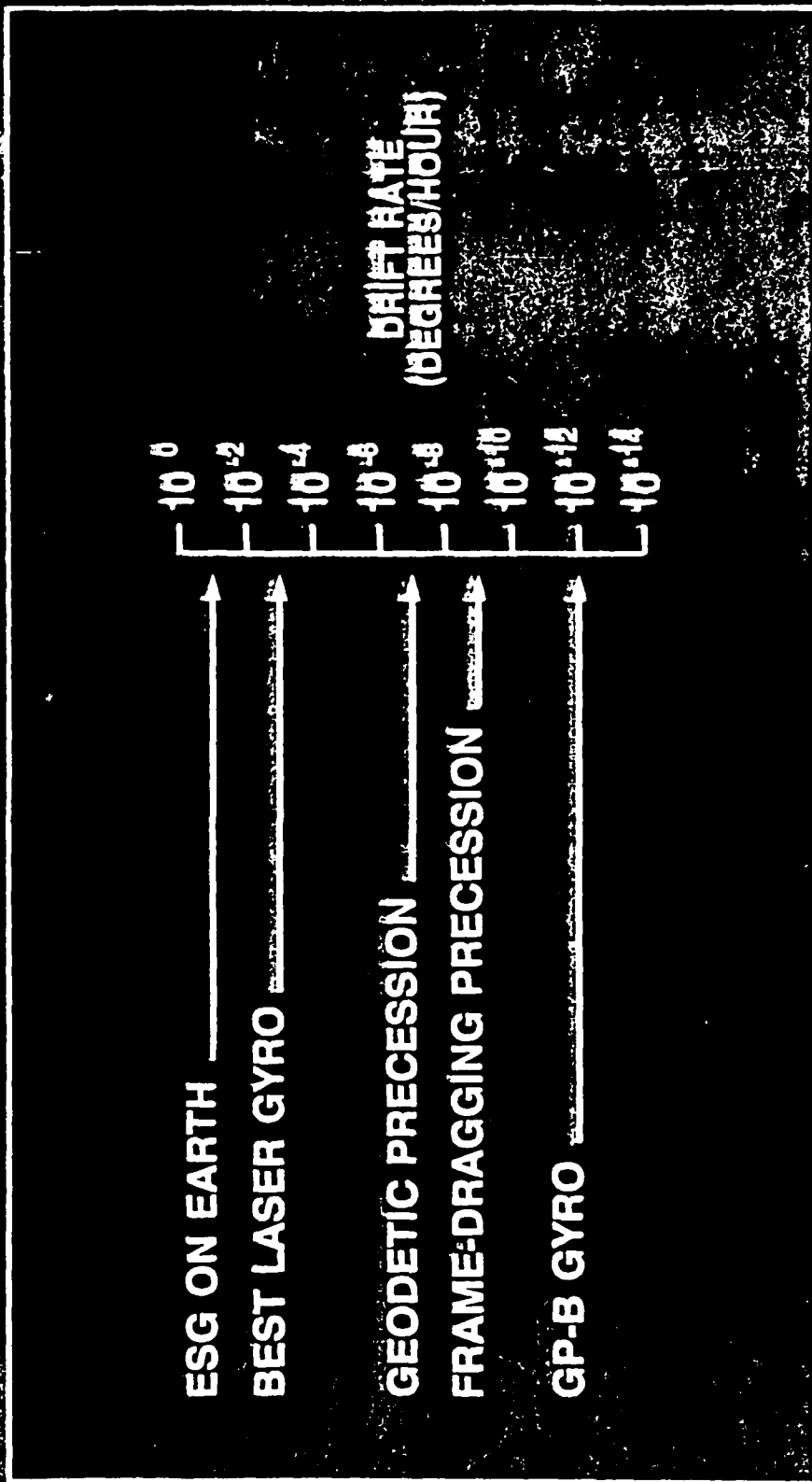
287.013





# GYRO PERFORMANCE COMPARISONS

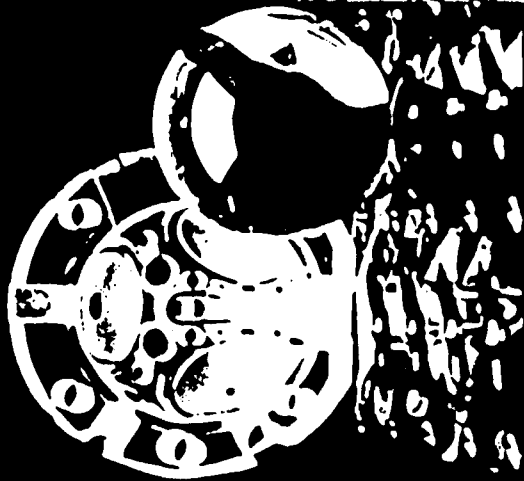
GP-B  
STATIONARY  
LOCKHEED



287.006

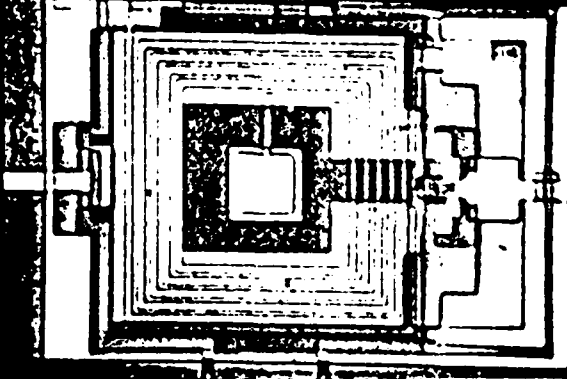


# NAVSTA STANFORD lockhead EXPERIMENT REQUIREMENTS

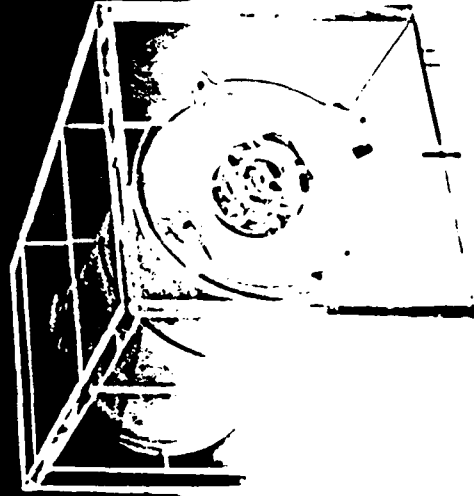


QUARTZ SPHERE GYRO  
(MILIO-INCH TOLERANCES)

DISTURBANCE-FREE  
GYRO HEADOUT  
(SUPERCONDUCTIVE LOGS)



ACCURATE TELESCOPE  
(0.1 ARC SEC HEADOUT)

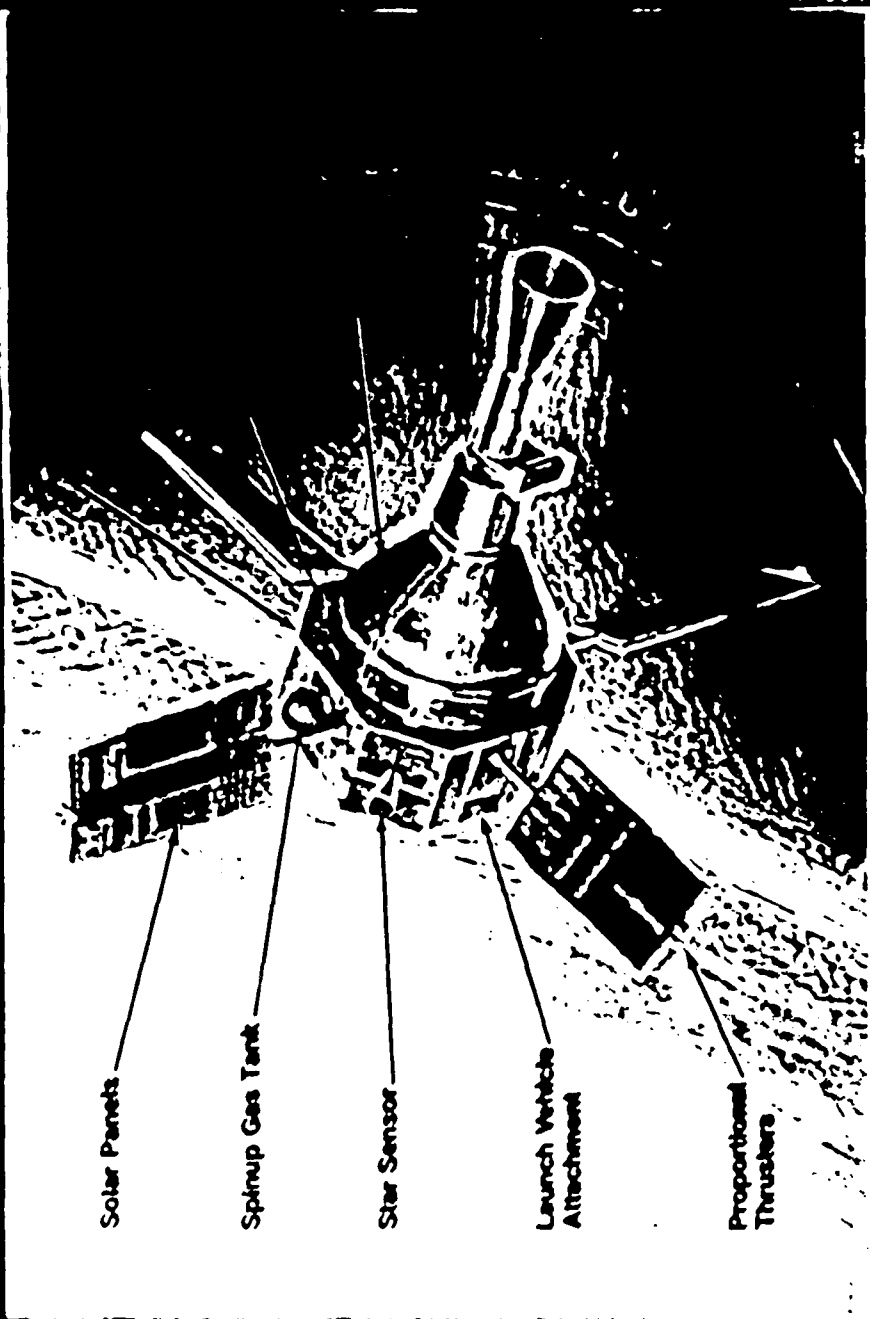


287.016



# SCIENCE MISSION SPACECRAFT

UNIVERSITY  
LOCKHEED



287.019

## DRAG FREE CONTROL

- Translational control system which compensates for all surface forces such as aerodynamic drag and solar pressure.
- A *Proof-mass* floats within an evacuated cavity near the spacecraft's center of mass, and follows an ideal gravitational orbit.
- The spacecraft chases the proof mass, resulting in mean acceleration environment of  $10^{-10}$  g.
- Technique was demonstrated on U.S. Navy's Triad Transit navigation satellite in 1972.
- Control actuators for translational control are proportional Helium Thrusters which also vent Helium from the dewar.  
Maximum thrust is 0.01 N per axis (acceleration of 0.5  $\mu$ g).

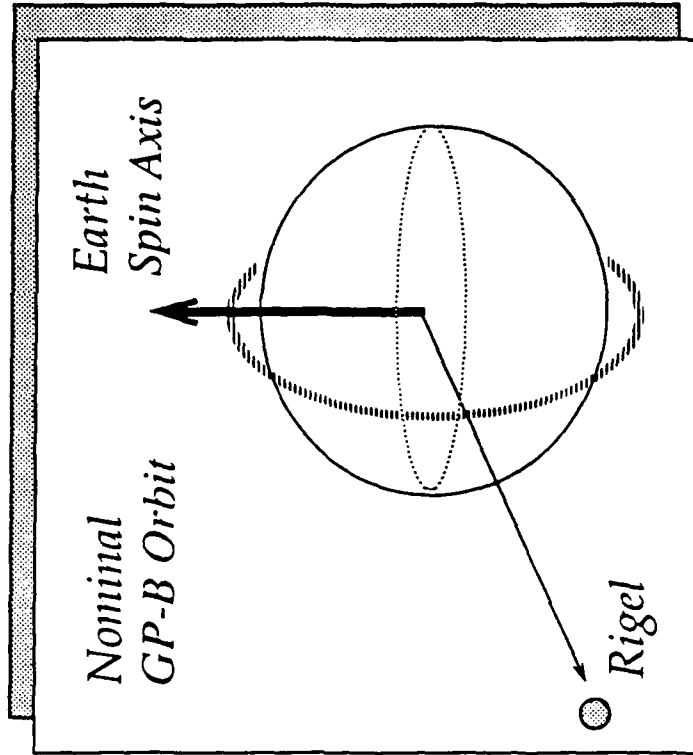
## NOMINAL GP-B ORBIT

- Polar
- Circular
- Orbit Plane Contains the star Rigel.

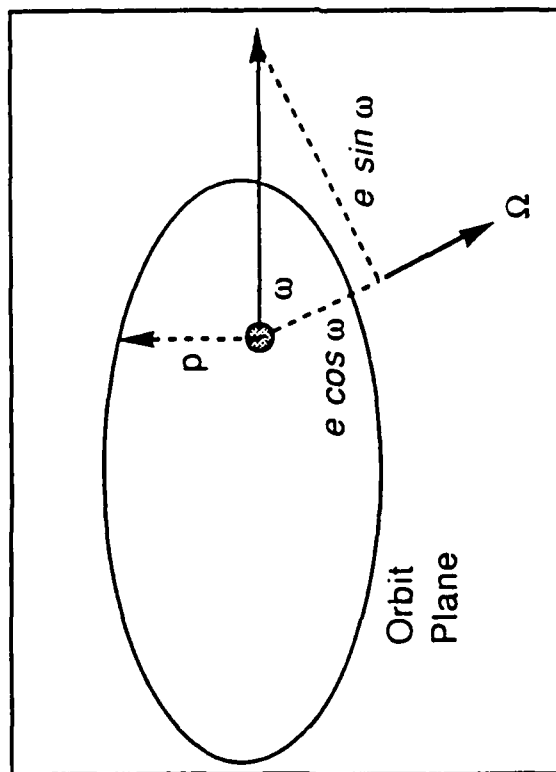
BUT

- Purely Gravitational once the experiment starts.

Control System TARGET is the orbit which is "closest" to the nominal on average.



## ORBIT ELEMENTS



$p$  - parameter

$e \cos \omega$

- component of  $e$  vector in equatorial plane

$e \sin \omega$

- component of  $e$  vector orthogonal to equatorial plane

$i'$

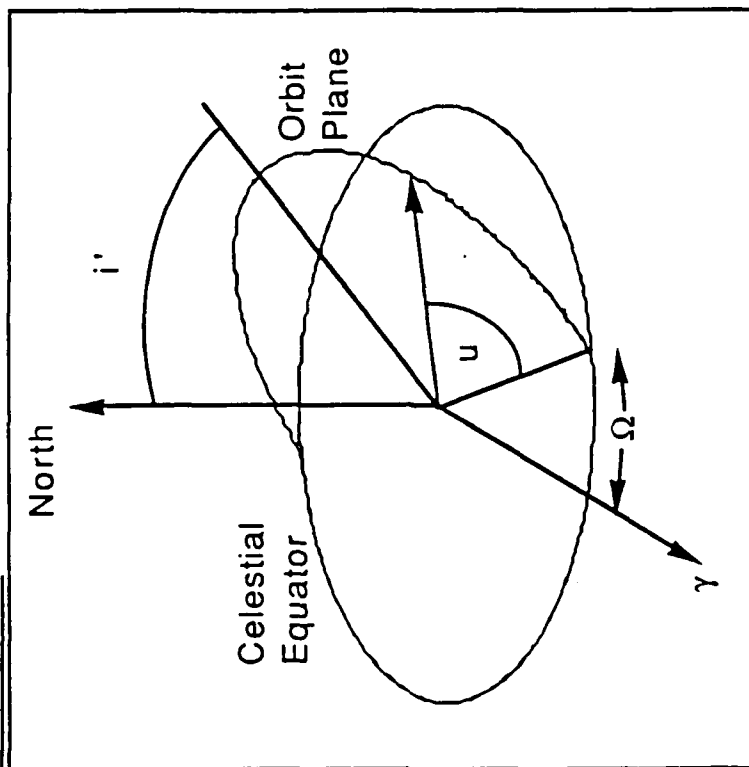
- inclination

$\Omega$

- right ascension of the ascending node

$u$

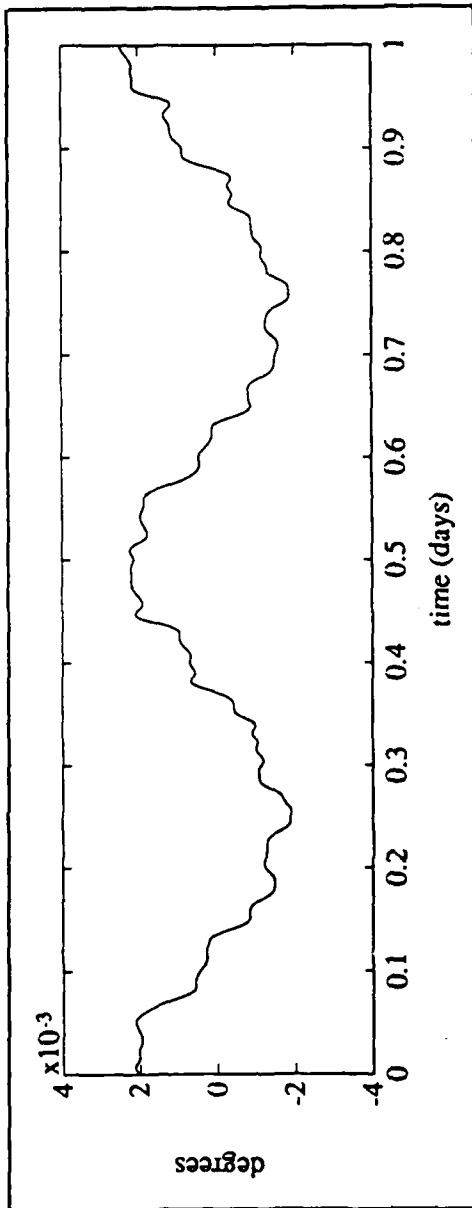
- argument of latitude



# TARGET ORBIT ELEMENTS (OUT-OF-PLANE)

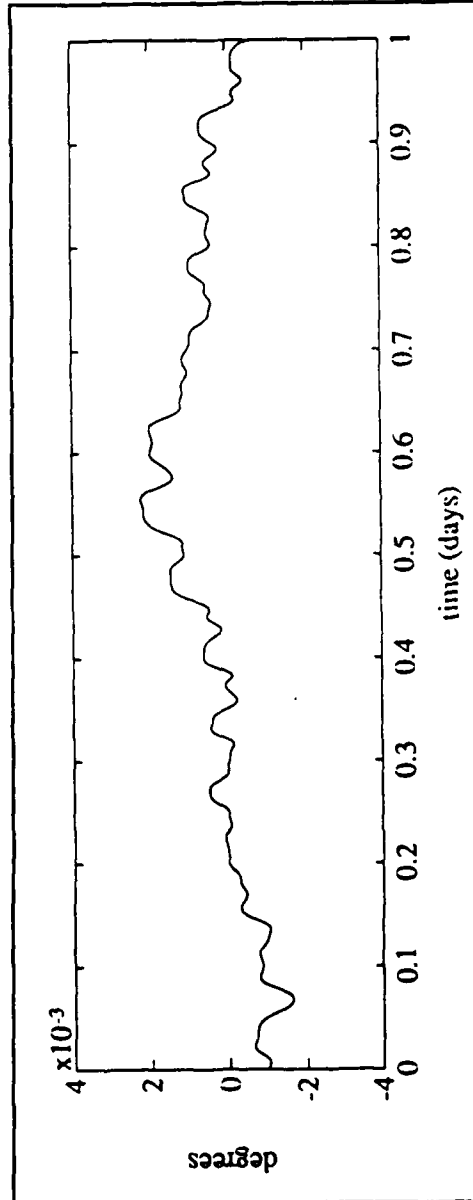
COINCLINATION ( $i''$ )

Main Variation  
caused by  $U_{2,2}$



NODE ( $\Omega$ )

Main Variation  
caused by  $U_{4,1}$

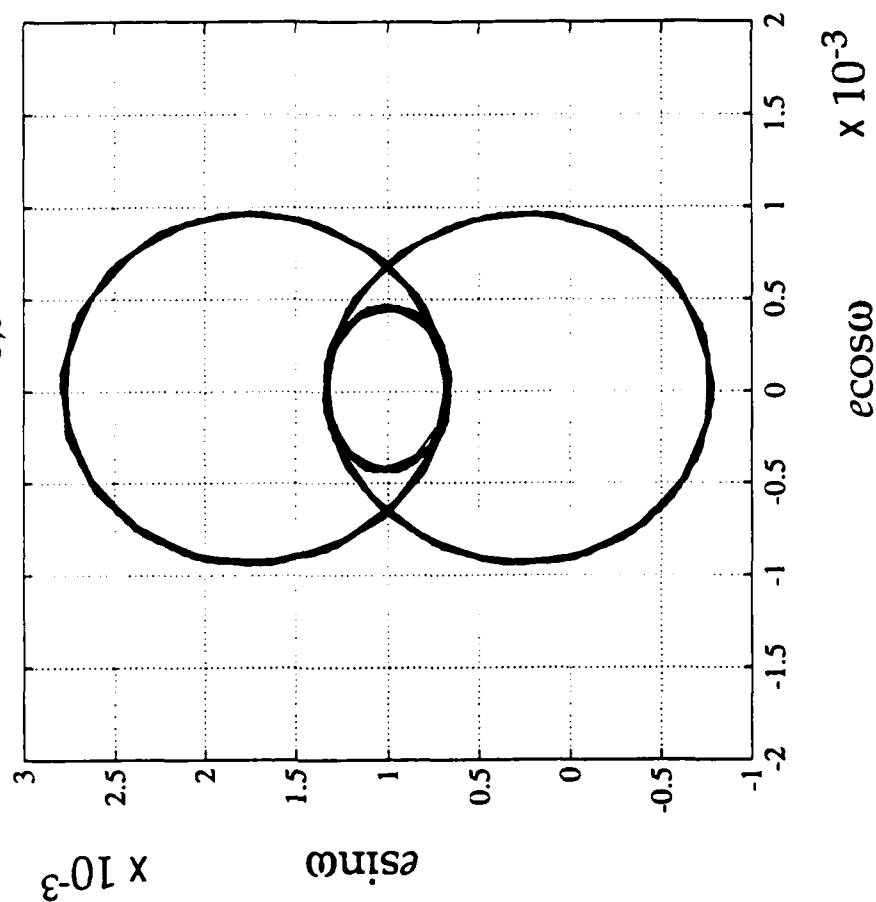
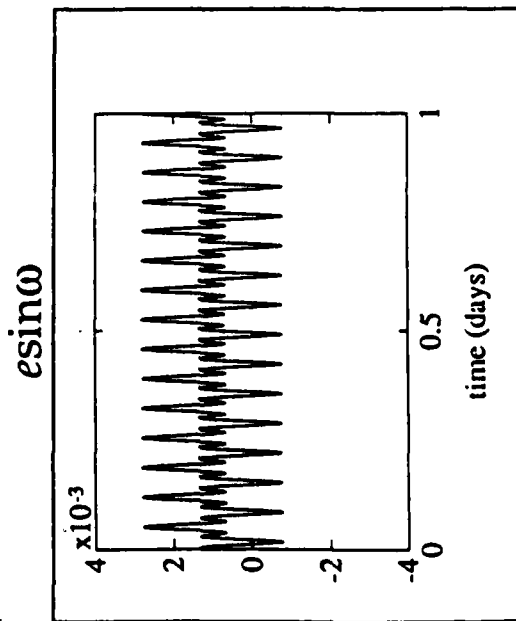
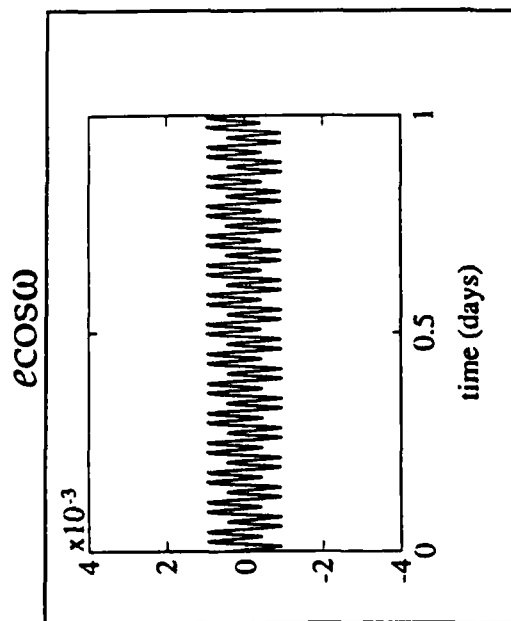


# TARGET ORBIT ELEMENTS ( IN-PLANE)

Short Term Variation caused by  $U_{2,0}$

Long Term Stable Point:

$esin\omega = 0.001$  caused by  $U_{3,0}$





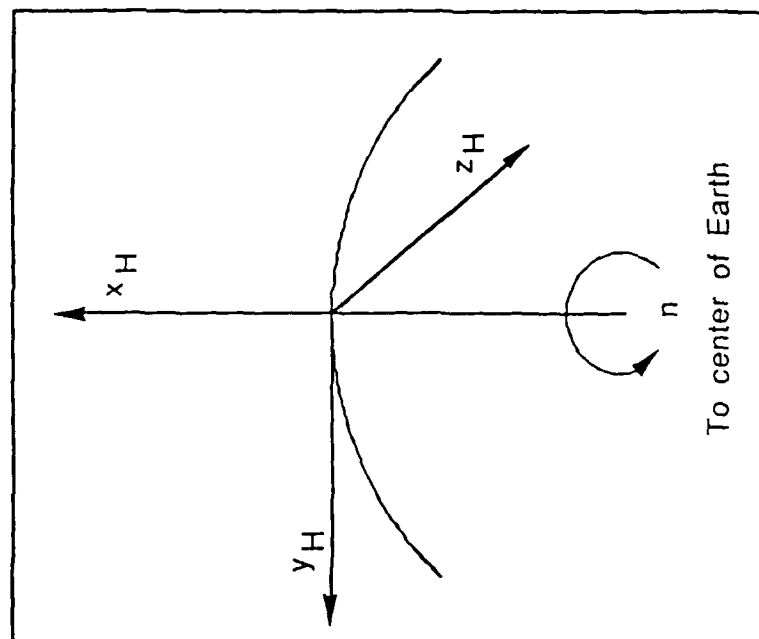
## NAVIGATION SYSTEM

- Propagates the target orbit using closed form solution.
- Estimates deviations from the target using a Kalman Filter, and linearized equations of motion in Hill's coordinates.

$$\ddot{x}_H - 2n\dot{y}_H - 3n^2x_H = a_{c_x} + a_{d_x}$$

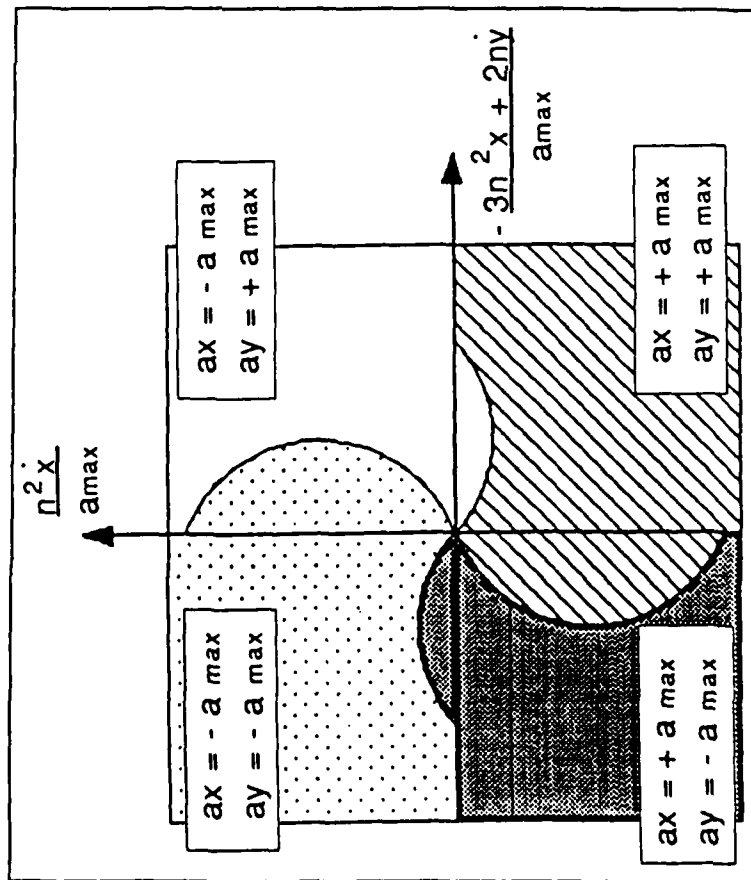
$$\ddot{y}_H + 2n\dot{x}_H = a_{c_y} + a_{d_y}$$

$$\ddot{z}_H + n^2z_H = a_{c_z} + a_{d_z}$$

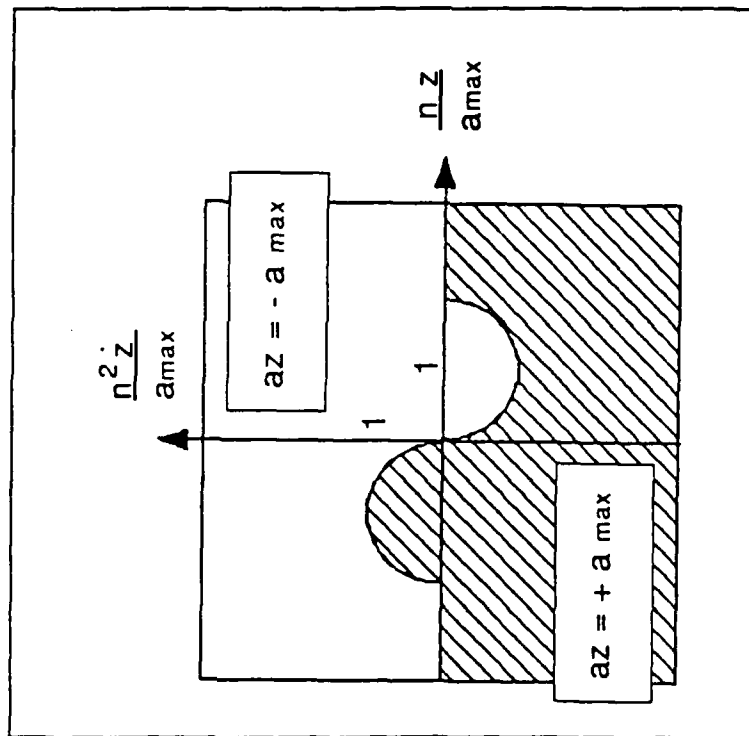


## CONTROL SYSTEM

Computes suboptimal control to eliminate in-plane and out-of-plane deviations from the target in minimum time.



IN-PLANE CONTROL



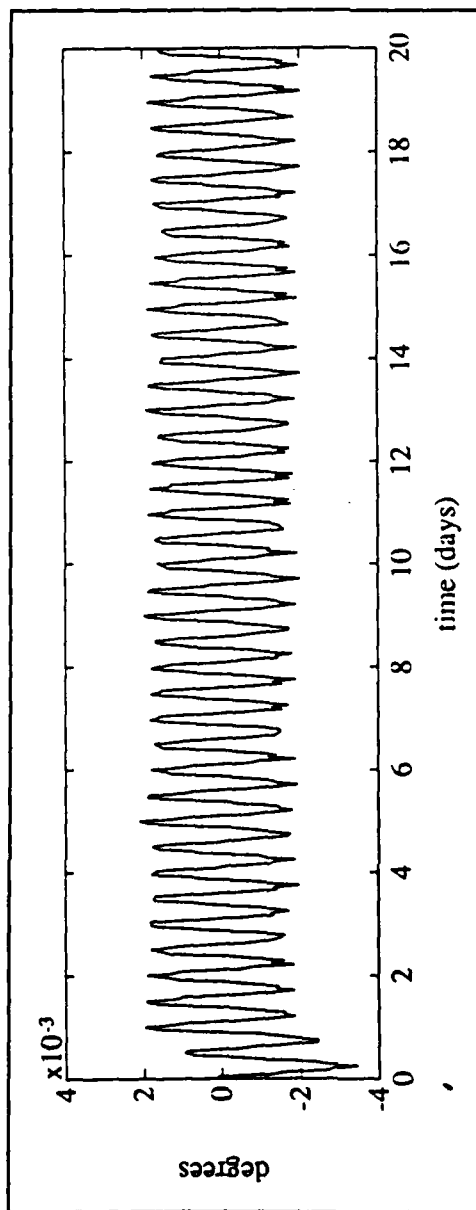
OUT-OF-PLANE CONTROL

## CLOSED LOOP CONTROL (OUT-OF-PLANE)

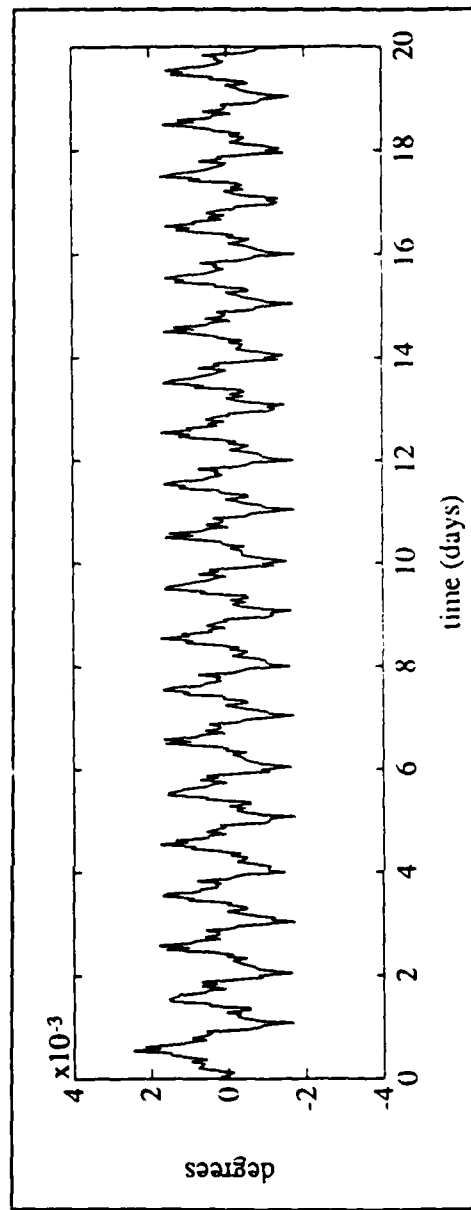
Initial Conditions:  $i' = 0$  deg,  $\Omega = 0$  deg,  $e = 0$ .

Helium Thrusters ( $a_{\max} = 5 \times 10^{-6}$  m/s<sup>2</sup>), Time = 20 days

COINCLINATION ( $i'$ )



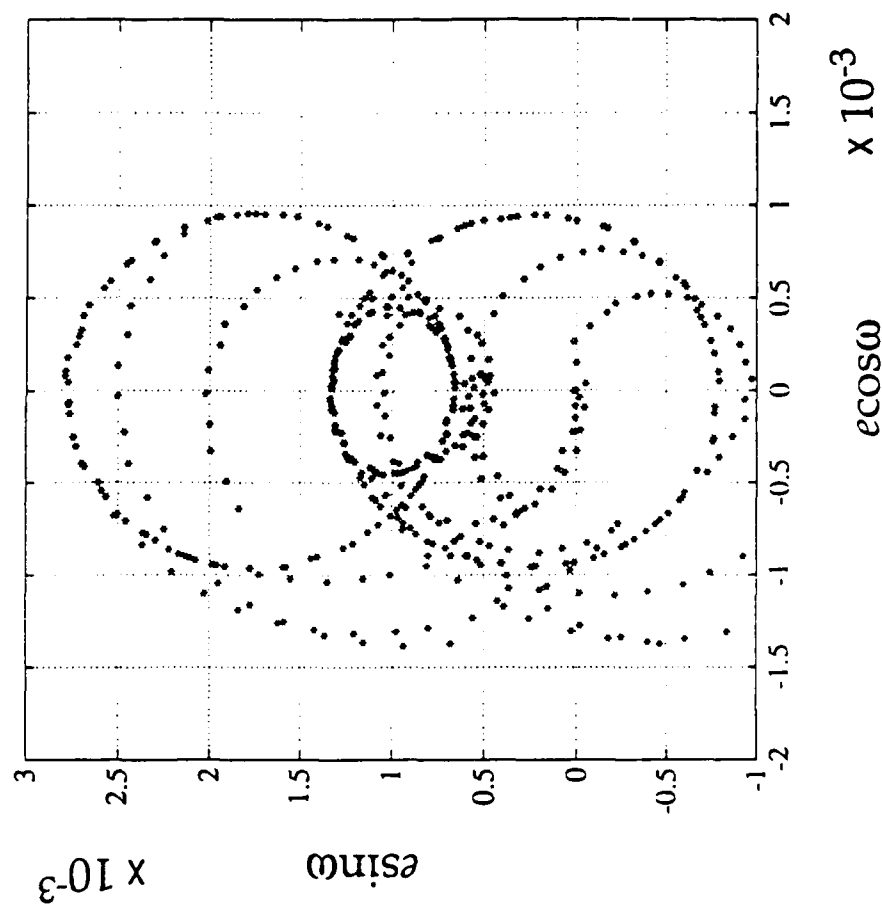
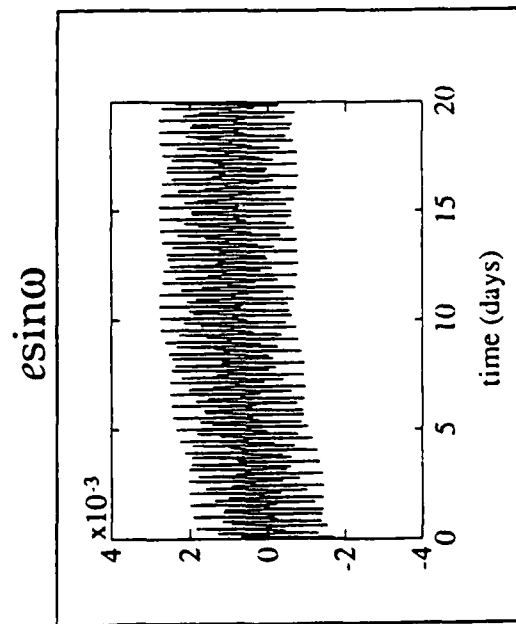
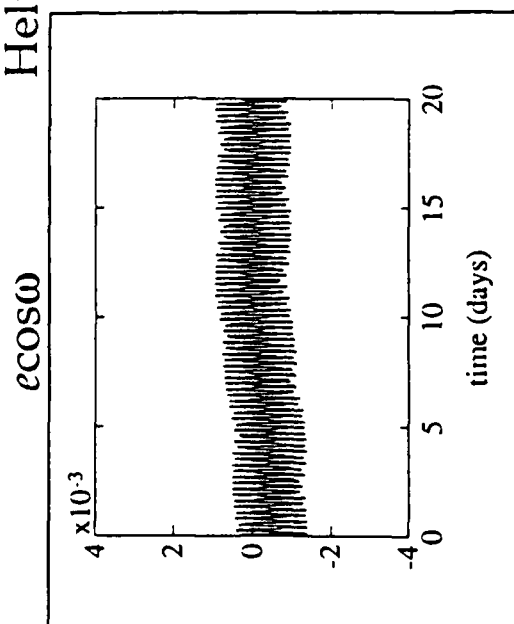
NODE ( $\Omega$ )



## CLOSED LOOP CONTROL (IN-PLANE)

Initial Conditions:  $i' = 0$  deg,  $\Omega = 0$  deg,  $e = 0$ .

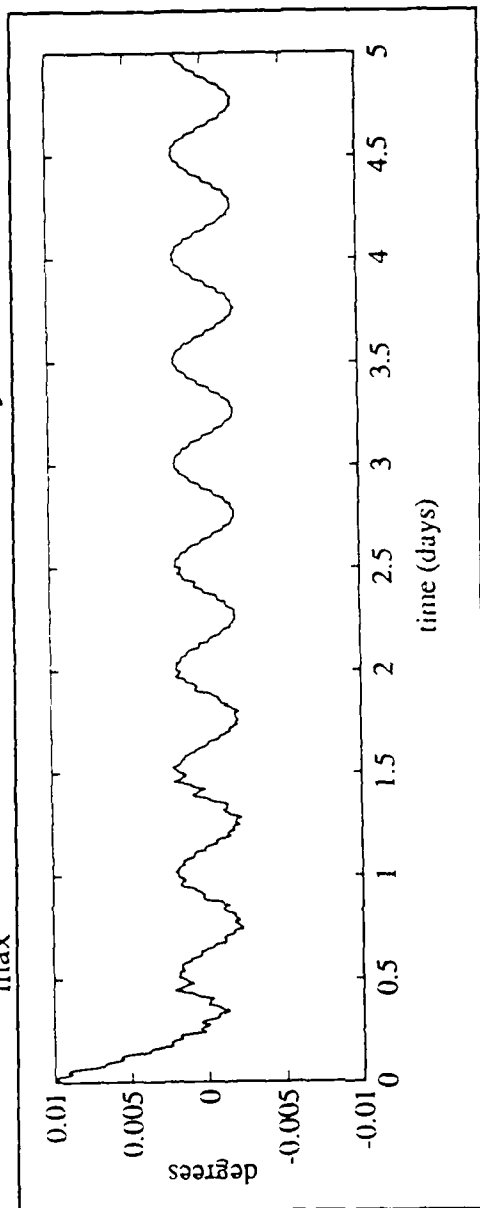
Helium Thrusters ( $a_{\max} = 5 \times 10^{-6}$  m/s<sup>2</sup>), Time = 20 days



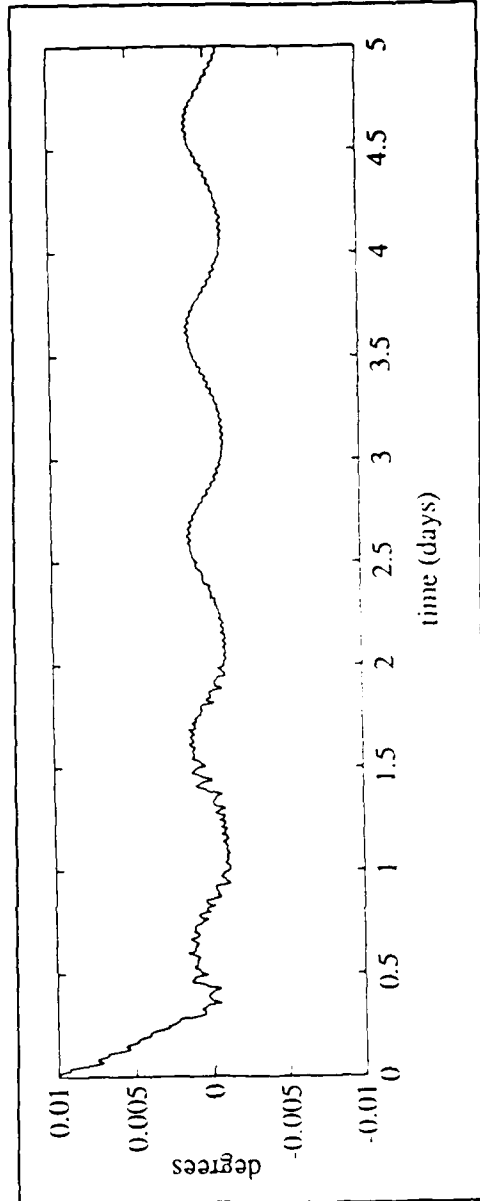
## CLOSED LOOP CONTROL (OUT-OF-PLANE)

Initial Conditions:  $i' = 0.01$  deg,  $\Omega = 0.01$  deg,  $e \cos \omega = 0.005$ ,  $e \sin \omega = 0.005$   
 0.2 N Thrusters ( $a_{\max} = 10^{-4} \text{ m/s}^2$ ), Time = 5 days

COINCLINATION ( $i'$ )

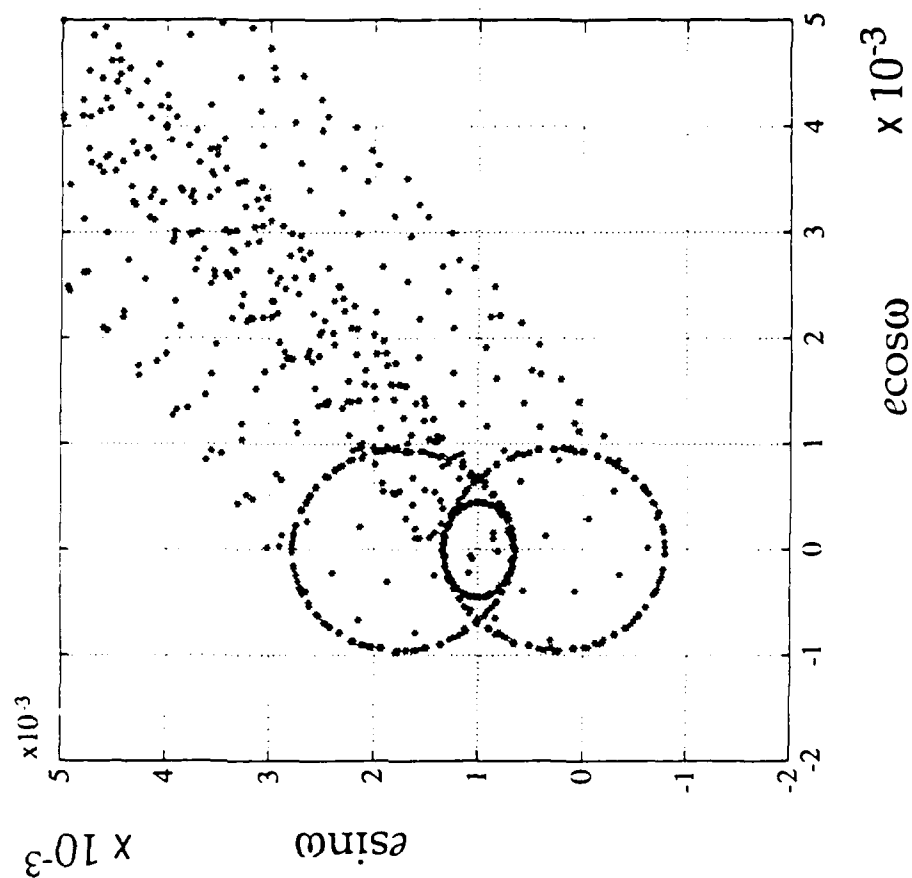
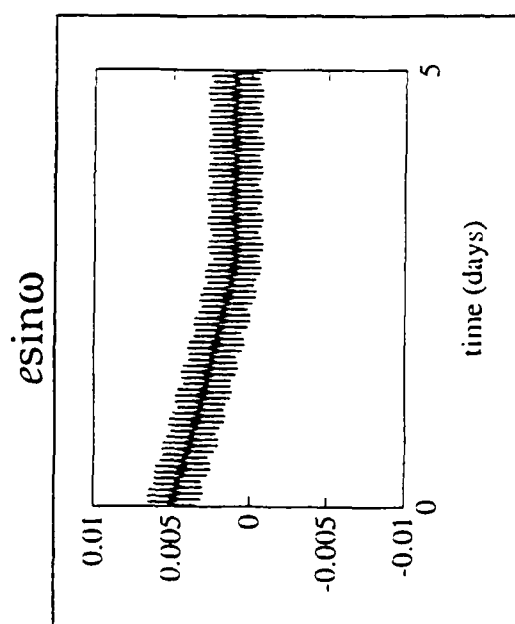
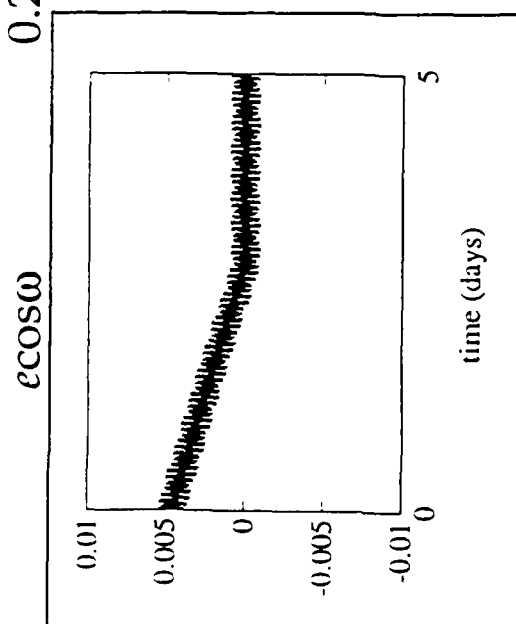


NODE ( $\Omega$ )



## CLOSED LOOP CONTROL (IN-PLANE)

Initial Conditions:  $i' = 0.01$  deg,  $\Omega = 0.01$  deg,  $e \cos \omega = 0.005$ ,  $e \sin \omega = 0.005$   
 0.2 N Thrusters ( $a_{\max} = 10^{-4}$  m/s<sup>2</sup>), Time = 5 days



10/10/89

## SUMMARY

- Demonstrated the use of a closed loop orbit trim system for initial orbit adjust of GP-B.
- Dynamic modeling is needed to precisely define the target orbit as compared to the nominal orbit. This is particularly important when thruster capability is small compared to gravitational and atmospheric disturbances.
- The GPS based navigation system consisting of a closed form target orbit propagation and an extended Kalman filter estimate of the deviations from the target provided sufficient accuracy for the closed loop controller.

## FUTURE WORK

1. Determine maximum errors which can be corrected using low level Helium thrusters on GP-B .
2. Model effects of attitude motions, realistic thruster response characteristics, GPS satellite outages, and loss of carrier lock.
3. Apply the technique to other spacecraft missions such as Earth observation satellites and orbital transfer vehicles.
4. Extend the technique to other phases of flight such as aircraft flight and launch vehicle guidance.





## GLOBAL GRAVITY FIELD MAPPING WITH GPS TRACKING OF THE SPACE SHUTTLE

George J. Priovolos, Triveni N. Upadhyay  
MAYFLOWER COMMUNICATIONS COMPANY, INC.

and

Christopher Jekeli  
GEOPHYSICS LABORATORY (AFSC)

This paper concerns the concept of tracking the Shuttle using GPS for gravity field mapping, an error analysis and processing techniques to mitigate some of the errors, and some simulation results on estimating the gravity field.

The tracking experiment is one of high-low mode where the GPS space vehicles are the high satellites. This provides very good visibility - other high-low configurations (only one high satellite) generally give only 20% of the data volume of a low-low configuration for an equal period of time. Another advantage is the ability using the entire constellation of the GPS to estimate the entire gravity vector rather than just one line-of-sight component. The measurement concept is as follows: the GPS receiver tracks three or more satellites giving the total acceleration of the Shuttle; an IMU on board the Shuttle provides the non-gravitational components; and the difference between these two yields the gravitational effect.

A major error source in the error budget for this experiment is the GPS satellite clock error and the second most important error is the misalignment of the accelerometer axis from inertial space. The GPS clock error estimate is based on a 100-fold reduction in the Allan variance of the clocks assumed achievable by modeling the short term behavior of the clocks at ground stations. Using double differencing of the data this error can almost entirely be eliminated. The alignment of the experiment IMU must be known to better than 1 mrad. It can be aligned to the IMU of the Shuttle, which is updated by a star tracker, using a recursive Kalman filter to estimate the misalignment from attitude data gathered by both IMU's during Shuttle rotations. Simulations indicate that this misalignment can be estimated to 0.4 mrad. The calibration of accelerometer bias and scale factor to an accuracy of 0.1 mgal has already been demonstrated by an Air Force experiment using a controlled motor table system. We are investigating an alternative technique to calibrate the bias using a fixed mount system whereby the shuttle is rotated.

The gravity parameter estimation is based on a one-week mission set of line-of-sight acceleration data (sampling interval = 30 sec.). Simulated 2°-mean gravity anomalies were estimated in the southern U.S. using the least-squares collocation technique. The true field was taken to be the 180-degree harmonic expansion (OSU86F) which gives, e.g., LOS accelerations at altitude in this case of about plus or minus 9 mgal. This is reassuring in that the noise of our system is about an order of magnitude lower. The GPS satellites selected for observation were the ones with minimum PDOP. Also, all data and estimates were referenced to the GEM-T1 gravity model which contains harmonics to degree 36. The residual LOS accelerations are attenuated to only a few mgal and we should not expect a dramatic improvement with the experiment to what the GEM-T1 model has already provided.

The covariance function used in the estimation of the surface gravity anomalies was the Tscherning/Rapp model with harmonics up to degree 36 deleted. Covariances of mean anomalies were obtained by numerically integrating the covariances of point anomalies over the  $2^\circ$  squares.

The plots of the differences between control and predicted  $2^\circ$  mean anomalies show that going from a data cap of  $2^\circ$  radius to  $3^\circ$  radius improved the stability of the solution as a function of data accuracy. That is, with the larger data sets, there was a wider range of data accuracies for which the signal to prediction accuracy ratio was greater than one.

In summary, we have identified techniques to mitigate the effects of the main errors associated with the Shuttle tracking experiment and they are being evaluated and developed. A shuttle mission would benefit primarily the long wavelength gravity models and models in areas where gravity data coverage is currently poor. The best predictions from our simulations were obtained for a data noise of 0.3 - 1 mgal. Some questions to be answered include what is the optimal integration time - data noise combination, and how is the optimal regularization factor determined for the estimation of gravity on the ground. It should be noted that the Shuttle experiment is just a demonstration of the concept. A more desirable mission would put the hardware into a lower altitude and polar orbit.

#### Discussion:

Question: To what level does the drag compensation mechanism affect the accuracy of gravity estimation on the Earth's surface?

Answer: We did not break the prediction errors down into contributing components, so we have no specific numbers for that.

Question: Did you use line-of-sight accelerations directly as input to the estimation or did you first convert them to vertical components of gravity at altitude?

Answer: We used LOS accelerations directly.

## **GLOBAL GRAVITY FIELD MAPPING**

- **Shuttle-GPS tracking experiment concept**
- **Error analysis and processing techniques**
- **Preliminary simulation results on mean gravity anomaly estimation**

## GLOBAL GRAVITY FIELD MAPPING

- Satellite-to-Satellite Tracking Experiment in the High-Low Mode
  - Space shuttle is the low vehicle
  - GPS satellites are the high vehicles
- Two Advantages
  - Good visibility ( $HL = 20\%$  of LL)
  - Recovery of gravity vector (as opposed to one component) by tracking three satellites
- Measurement system
  - GPS receiver measurements provide estimate of total vehicle acceleration
  - IMU measurements provide estimate of non-gravitational acceleration
  - Their difference is the gravitational effect

# GLOBAL GRAVITY FIELD MAPPING

## Error Budget of the Experiment

<u>Error Source</u>	<u>Effect on Acceleration (mgals)</u>
Shuttle Position Error	<0.13
GPS Receiver Bias	<0.1
GPS Receiver Noise	0.06
→ Satellite Clock Error	0.43
Accelerometer Bias	0.1
Accelerometer Scale Factor	0.1
Gyro Bias	0.17
Gyro Scale Factor	0.05
→ Misalignment	0.2
Other (multipath, shuttle flexure, etc.)	0.1
TOTAL (Root Sum Square)	0.56

## GLOBAL GRAVITY FIELD MAPPING

- GPS Satellite Clock Error

- Comparison of in-plant test data and ground tracking data for several GPS satellite clocks showed that short-term behavior of the clock is observable

Reduction of Allan variance by a factor of 100 was assumed which resulted in 0.43 mgal error in acceleration

- Double differencing of carrier phase measurements of the Shuttle and ground tracking stations will cancel most of the satellite clock-induced errors

Clock error effect reduces to about 0.1 mgal due to lack of simultaneous measurements and due to residual tropospheric errors

## GLOBAL GRAVITY FIELD MAPPING

### Transfer of Alignment of the Shuttle IMU to the Experiment IMU

- Experiment accelerometers axes' orientation must be known to better than 1 mrad
- Met by the Shuttle IMU (via Star-Tracker updates)
- Transfer the alignment to the experiment IMU
  - Post processing by a recursive estimator of the Kalman type
  - Attitude data (quaternions) from both IMUs
  - Simulation Study
    - Two one-minute rotations
    - Misalignment in all three axes was estimated to 0.4 mrad (60% improvement over the 1 mrad requirement)
- Current investigation with real data from the Space Shuttle Inertial Upper Stage experiment to validate the technique is in progress



## GLOBAL GRAVITY FIELD MAPPING

### Experiment IMU Acceleration Bias and Scale Factor Calibration

- Rotating table calibration (LOGACS technique)
  - Accelerometers mounted on a control motor table system
  - Estimate bias and scale factor to 0.1 mgal
  - Technique has been demonstrated by the Air Force and is currently being used by NASA on OARE experiment
- Fixed-mount calibration
  - Rotate the shuttle
  - Estimate bias to 0.1 mgal
  - Does not estimate scale factor (limited by the uncertainty in the knowledge of the CG of the Shuttle)
  - Reduces size, power, weight and cost
  - Technique currently under investigation

# GLOBAL GRAVITY FIELD MAPPING

## Gravitation Parameter Estimation

- GPS and IMU data will be processed to yield line-of-sight accelerations (LOSA) to GPS satellites
- Simulation Study
  - Least-Squares Collocation
  - Use LOSA observations to compute mean gravity anomalies
  - Generate simulated orbits of the shuttle and the GPS satellitesOne week mission - orbit density: one point every 30 seconds
- Southern United States

$$\phi_N = 26^\circ\text{N} \quad , \quad \phi_S = 20^\circ\text{N}$$

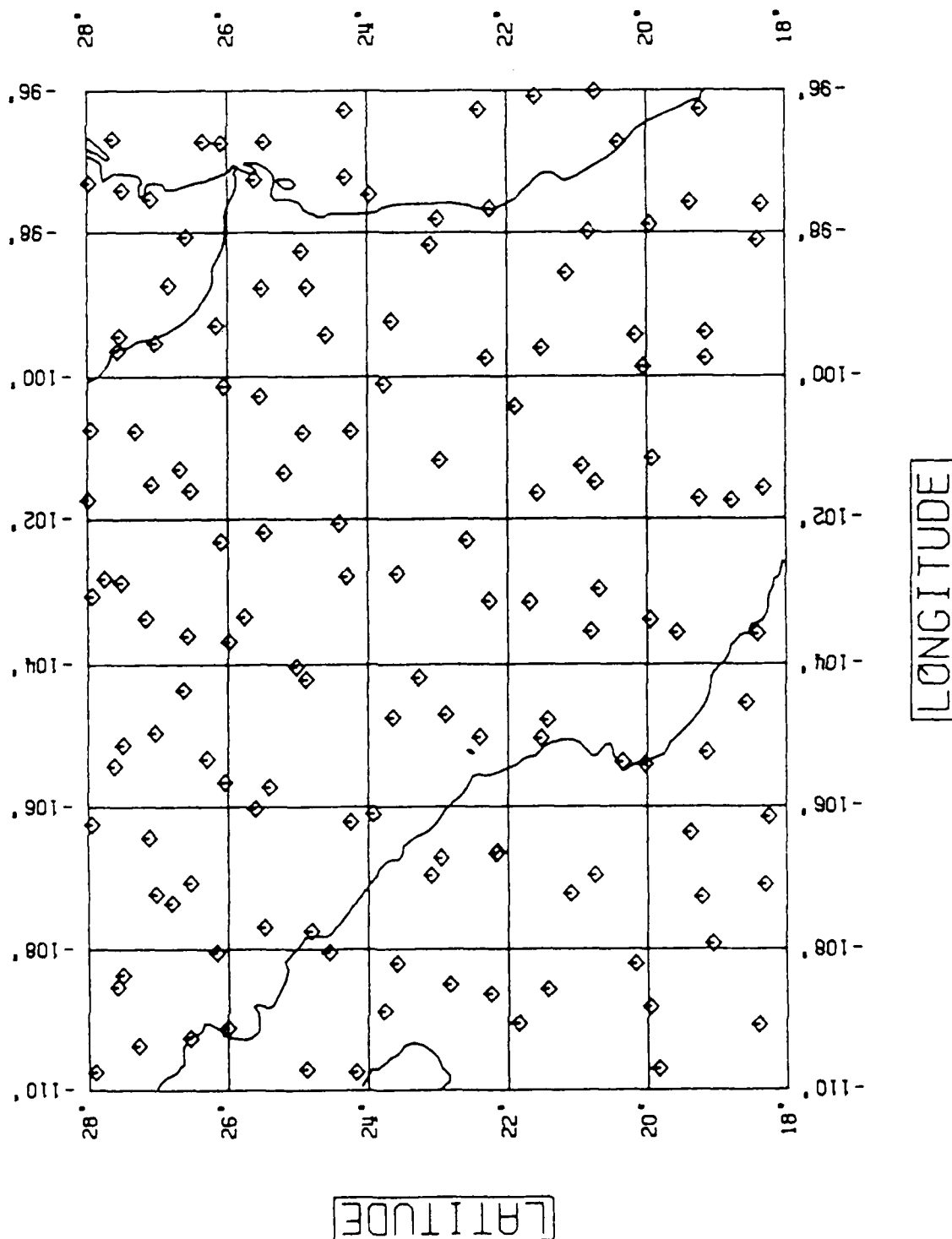
$$\lambda_E = 262^\circ\text{E} \quad , \quad \lambda_W = 252^\circ\text{E}$$

# GLOBAL GRAVITY FIELD MAPPING

SUB-SATELLITE POINTS / SOUTHERN U.S.

SCALE = 1:10000000

# OF POINTS : 143

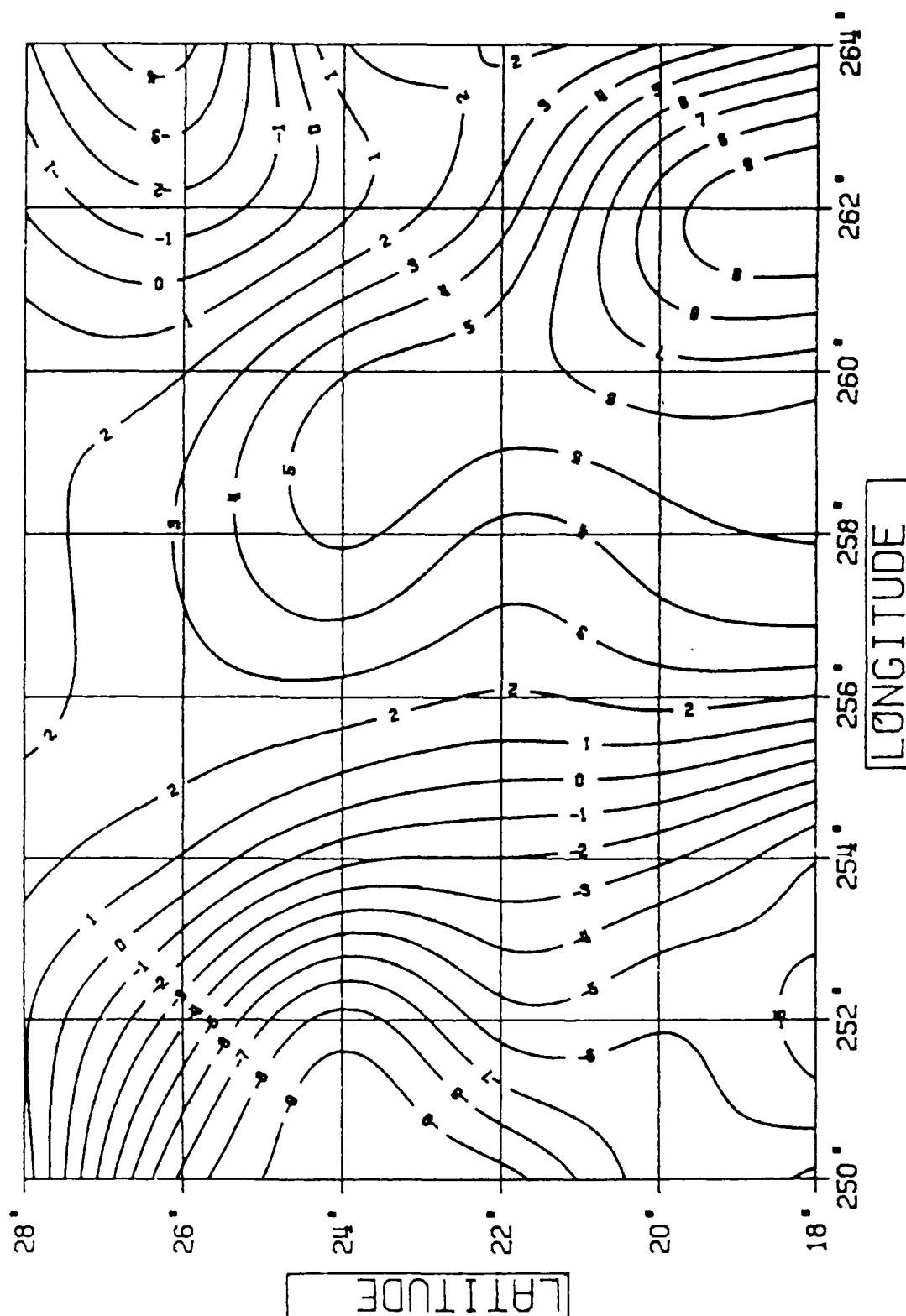


# GLOBAL GRAVITY FIELD MAPPING

LINE OF SIGHT ACCELERATION TO THE SECOND GPS SAT.

OBSERVED VALUES

CI = 1 MGAL



## GLOBAL GRAVITY FIELD MAPPING

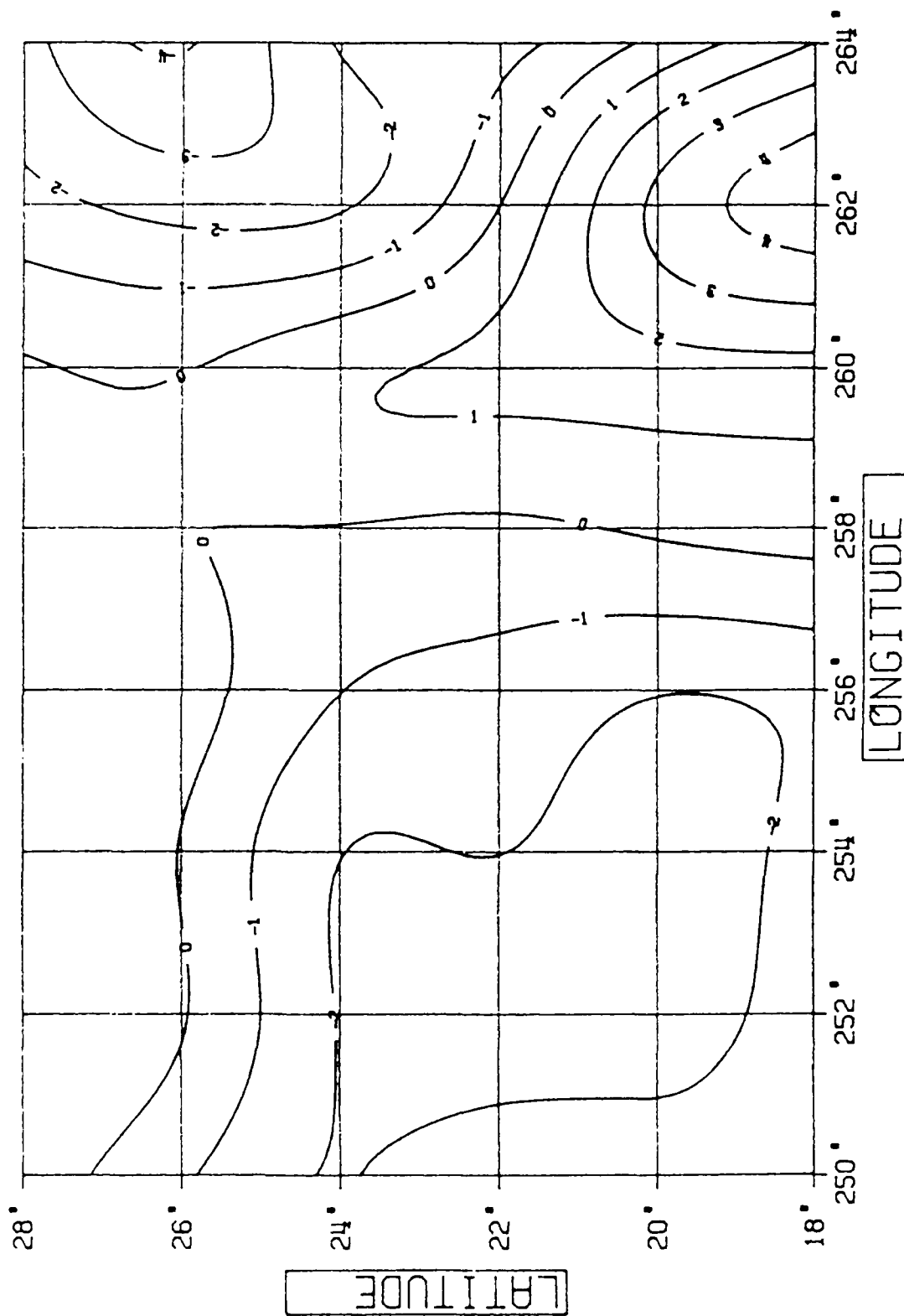
- True field: CSU86F to degree and order 180
- Select three GPS satellites with minimum PDOP and compute LOSA, residual to GEM-T1 to degree and order 36
- Compute  $2^\circ$  mean gravity anomalies, residual to GEM-T1

# GLOBAL GRAVITY FIELD MAPPING

LINE OF SIGHT ACCELERATION TO THE SECOND GPS SAT.

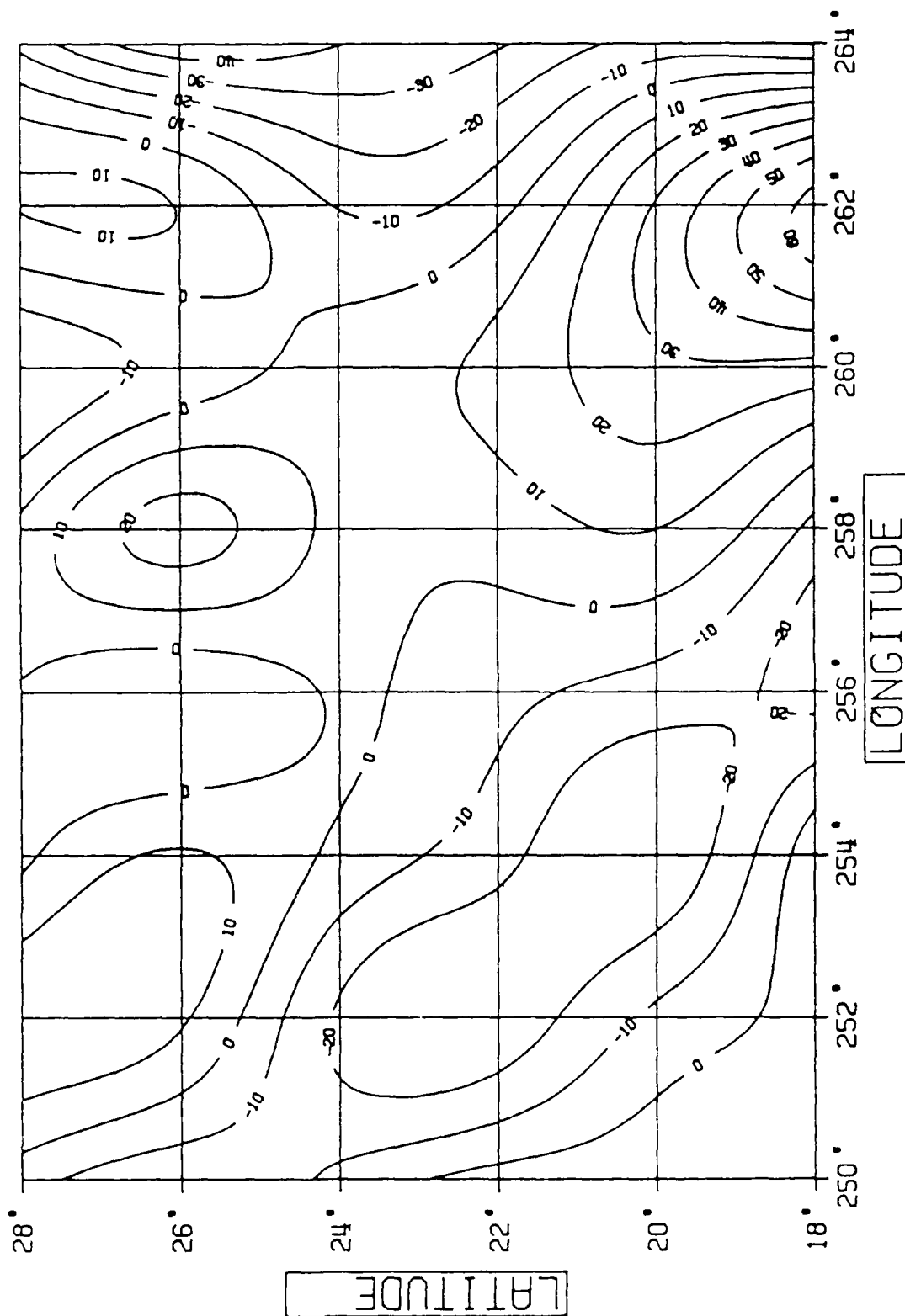
RESIDUAL VALUES

CI = 1 MGAL



# GLOBAL GRAVITY FIELD MAPPING

MEAN ANOMALIES (2 DEG X 2 DEG) / SOUTHERN U. S.	
RESIDUAL (0-G) FIELD	CI = 10 MGALS

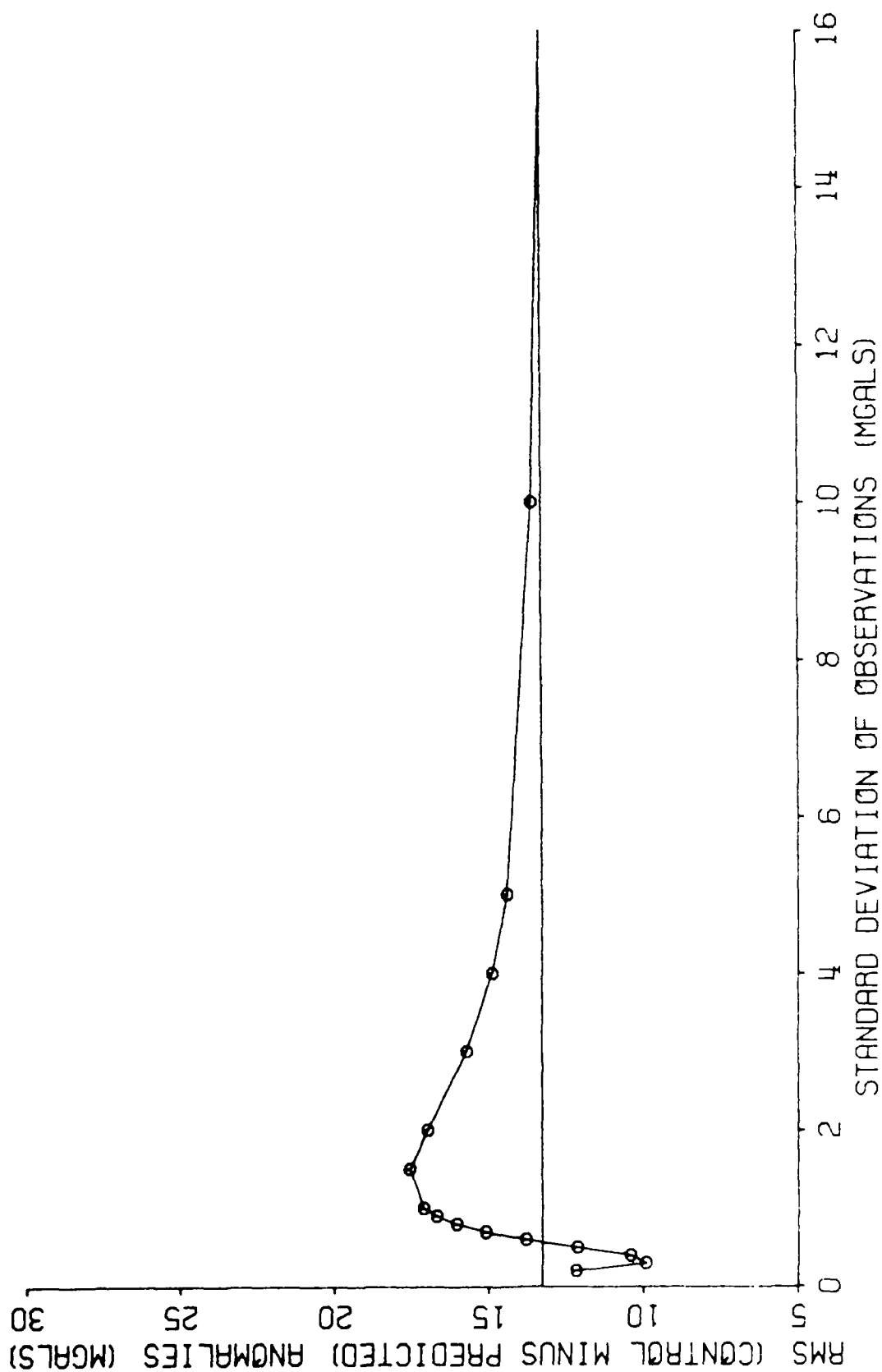


## GLOBAL GRAVITY FIELD MAPPING

- Use Least-Squares Collocation to estimate residual  $2^\circ$  mean gravity anomalies from residual line-of-sight accelerations
- Tscherning/Rapp covariance model beyond degree 36
- Cross-covariances involving mean anomalies were computed by numerical integration of point covariances



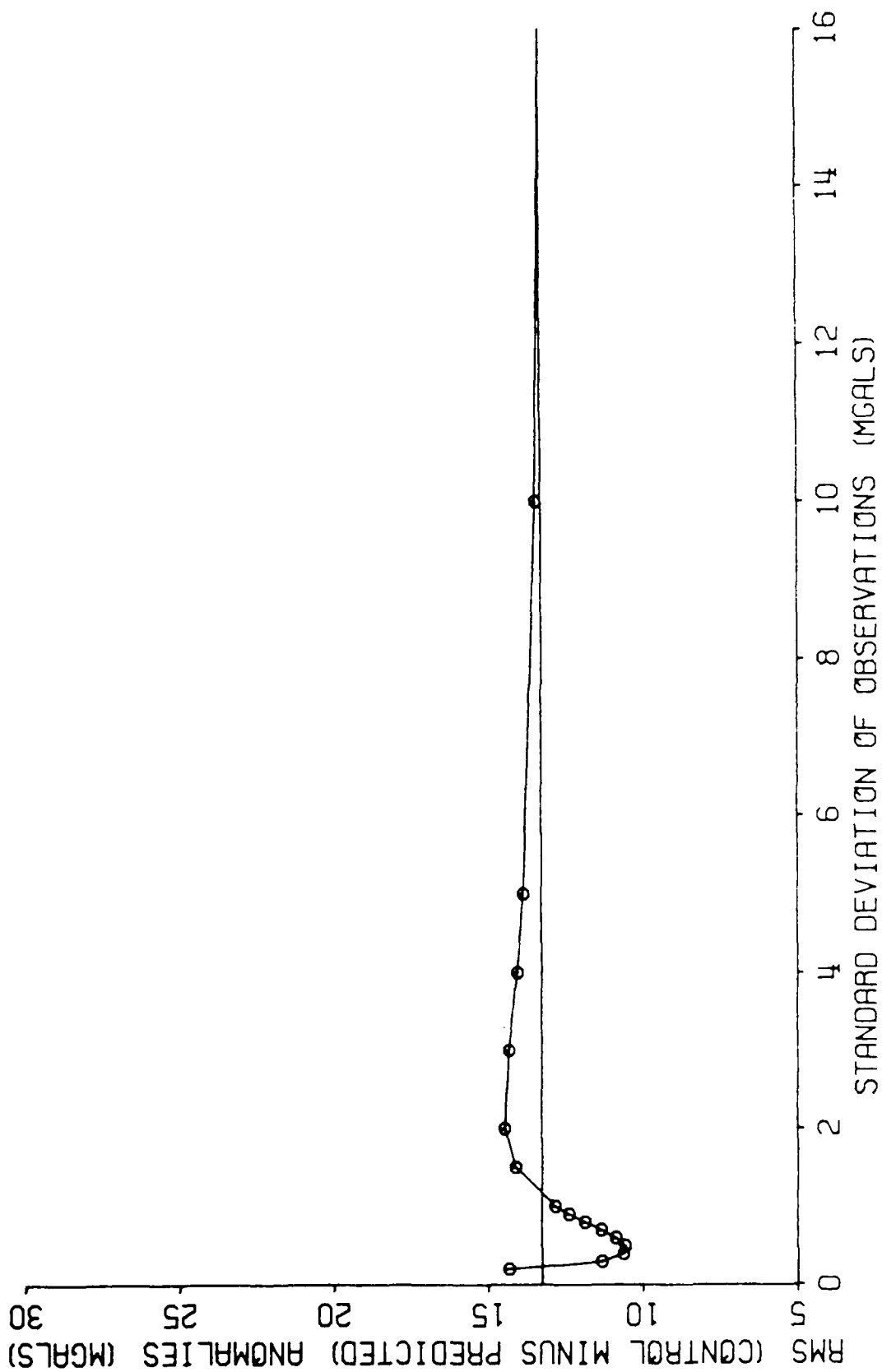
# GLOBAL GRAVITY FIELD MAPPING



RECOVERY OF 2 DEGREE MEAN ANOMALIES / SOUTHERN U.S.

DATA CAP RADIUS = 2 DEGREES

# GLOBAL GRAVITY FIELD MAPPING



RECOVERY OF 2 DEGREE MEAN ANOMALIES / SOUTHERN U.S.

DATA CAP RADIUS = 3 DEGREES

# GLOBAL GRAVITY FIELD MAPPING

## Conclusions

- GPS and INS Processing techniques to mitigate the effect of primary errors have been identified and are being developed
- Features beyond degree 36 are attenuated at the Shuttle altitude of 300 km thus such a mission will benefit
  - Low degree fields
  - Fields computed from data in poorly accessible areas or areas with poor coverage
- Need to evaluate the experiment at areas where the GEM-T1 field is poor
- Best predictions for this experiment at  $\sigma = 0.3 - 1$  mgal
  - Use smaller integration time and get higher data density
  - Use 75 sec integration time and get more accurate (0.5 mgal) data
  - Need an optimal method for the estimation of the regularization factor
- Shuttle-based experiment validates the concept and is a precursor to a dedicated free-flyer at a lower altitude and in a polar orbit

# TECHNIQUES OF GPS-BASED PRECISION ORBIT DETERMINATION FOR LOW EARTH SATELLITES

Sien C. Wu  
JET PROPULSION LABORATORY

This paper describes some technical detail regarding precise orbit determination of low Earth orbiters using GPS. It is well known that the effects of GPS and user clock errors can be eliminated and those of the GPS ephemeris errors can be reduced by using doubly differenced data from two or more GPS satellites and one or more ground stations. The accuracy is then limited by measurement noise and geometrical weakness which can be improved by global smoothing, that is, by solving for the user state parameters at only one epoch but using data over a period of time. The three methods of smoothing discussed here are the dynamic, non-dynamic (or kinematic), and reduced-dynamic techniques.

In dynamic smoothing we use a dynamic model to perform the state transition, and therefore, the solution is sensitive to dynamic mismodeling but relatively insensitive to geometrical weakness (i.e., the PDOP). In general, this is applicable to altitudes higher than 2000 km where gravity and atmospheric drag errors are small. With non-dynamic (kinematic) smoothing the position solutions inferred from pseudorange measurements are smoothed by the positional change inferred from GPS carrier phase measurements. Since no dynamic model is used, this technique is insensitive to dynamic mismodeling but highly sensitive to geometrical weakness. The non-dynamic smoothing technique is applicable to altitudes less than 400 km where gravity and drag effects are quite large. The third technique, reduced-dynamic smoothing, is a hybrid of the other two and is moderately sensitive to dynamic mismodeling and geometrical weakness. It applies to orbits with altitudes between 400 to 2000 km.

In reduced-dynamic smoothing, the estimated position at time  $j+1$  is related to the position at time  $j$  through the dynamic state-transition matrix and to an introduced 3-D fictitious force, treated as a process-noise parameter. The process-noise parameter at time  $j+1$  is, in turn, related to its predecessor at time  $j$  by the "batch-to-batch correlation" and a white noise component which is characterized by a "batch-to-batch sigma." A larger process-noise sigma is equivalent to having lower weight on the dynamic model. A zero sigma yields the dynamic smoothing while an infinite sigma yields the non-dynamic smoothing; any non-zero finite sigma will result in reduced-dynamic smoothing.

Two applications of these smoothing techniques have been investigated. These are the TOPEX/POSEIDON and the EOS/SPACE STATION missions; the former at 1334 km altitude is amenable to the reduced-dynamic smoothing, while non-dynamic smoothing will be considered for the latter (300 - 700 km). An analysis of the TOPEX application shows that the 10-cm altitude accuracy goal can be achieved if the proposed 6-station ground tracking network is utilized which performs a factor of two better than the minimum 3-station network. For EOS, which is scheduled for launch in the late 1990's, a number of favorable factors (full 24-GPS constellation, more tracking sites with better known positions, more channels on GPS receiver, etc.) contribute to an improved performance in orbital position accuracy. The expected accuracy is about 3 cm with a 2-hour tracking and monotonically improves to 1.5 cm with an 8-hour tracking.

In summary, even with a suboptimal tracking system, such as for TOPEX, orbital uncertainty can be less than 10 cm; and with an optimal tracking system, such as for EOS, the uncertainty is on the order of 1 to 3 cm.

Discussion:

Question: Is the 18-channel receiver for EOS in existence or in development?

Answer: It's concept has been developed, but it is not being built yet.

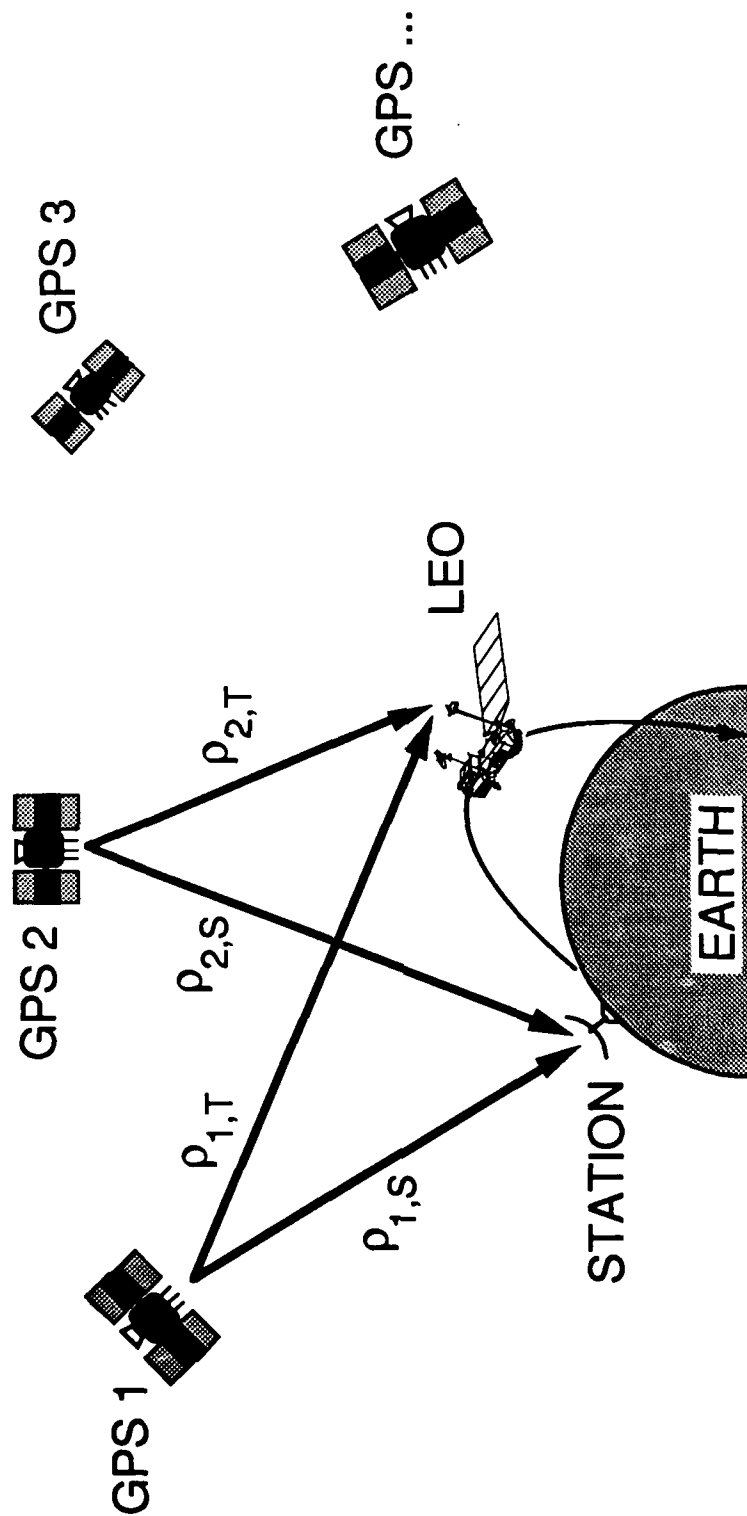
Question: What was the assumed data rate?

Answer: The data rate for these results was assumed to be once per 5 minutes.

Question: Was this analysis done assuming encrypted GPS signals?

Answer: The results are not affected by selective availability. It is just assumed that some kind of pseudorange is available.

### DOUBLY DIFFERENCED GPS MEASUREMENTS



$$\Delta^2 \rho = (\rho_{1,T} - \rho_{1,S}) - (\rho_{2,T} - \rho_{2,S})$$

- Instantaneous OD is limited by geometrical weakness and measurement uncertainty
- Smoothing over a long arc improves OD solution
- Three smoothing techniques:
  - Dynamic (conventional)
  - Non-dynamic (kinematic)
  - Reduced-dynamic



## THREE SMOOTHING TECHNIQUES

	Dynamic	Non-Dynamic	Reduced-Dynamic
Smoothing	Model	$\Phi$	Model + $\Phi$
Sensitivity to Dynamic Error	High	None	Moderate
Sensitivity to PDOP	Low	High	Moderate
Altitude Range	> 2000 km	< 400 km	400 – 2000 km



# JPL IMPLEMENTATION OF NON-DYNAMIC AND REDUCED-DYNAMIC SMOOTHING

- Use GPS carrier phase as well as pseudorange data
- Successively degrade state transition model by introducing process-noise parameters representing a 3-D force

User State:  $\tilde{\mathbf{x}}_{j+1} = \Phi_{\mathbf{x}}(j+1, j)\hat{\mathbf{x}}_j + \Phi_{\mathbf{x}p}(j+1, j)\hat{\mathbf{p}}_j$

Process-noise force:  $\tilde{\mathbf{p}}_{j+1} = m_j \hat{\mathbf{p}}_j + \omega_j$

$m_j = \exp[-(t_{j+1} - t_j) / \tau]$  (batch-to-batch correlation)

'  $\omega_j = N \{ 0, q_j \}$

$q_j = (1 - m_j^2)\sigma^2$  (batch-to-batch  $\sigma$ )

- Larger  $\sigma$  reduces weight on dynamic model:

$\sigma \rightarrow 0 \Rightarrow$  dynamic smoothing

$\sigma \rightarrow \infty \Rightarrow$  non-dynamic smoothing



## TREATMENT OF OTHER PARAMETERS

- **Adjusted as constant parameters:**
  - User and GPS epoch states
  - Geocenter position
  - Non-fiducial baselines
  - Carrier phase biases
- **Adjusted as white-noise processes:**
  - GPS and receiver clocks
- **Adjusted as random-walk processes:**
  - Zenith tropospheric delays

*TOPEX/Poseidon*

- 1992–1995
- 1,334 km Circular Orbit
- Reduced-dynamic tracking

*EOS/SpaceStation*

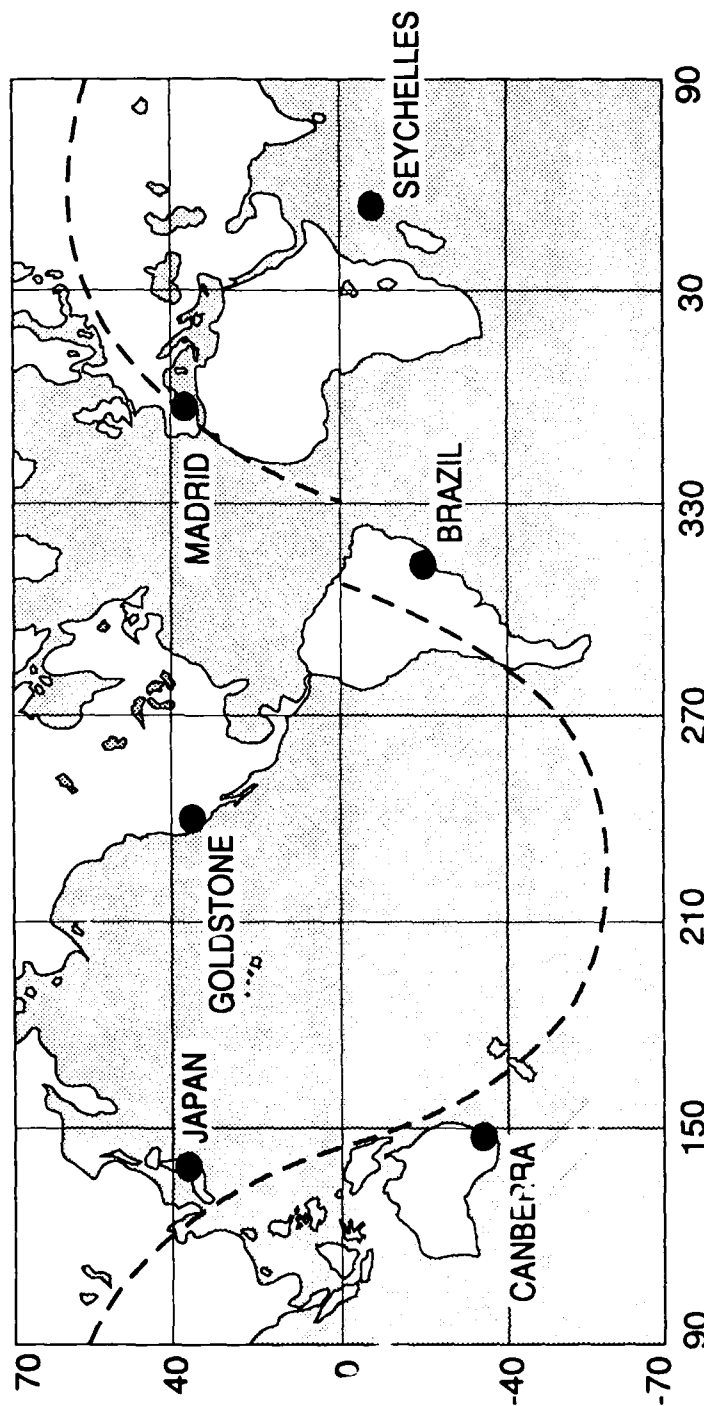
- Late 1990s
- 300 – 700 km Circular Orbits
- Non-dynamic tracking

# **JPL**      **GPS-BASED POD FOR TOPEX/Poseidon**

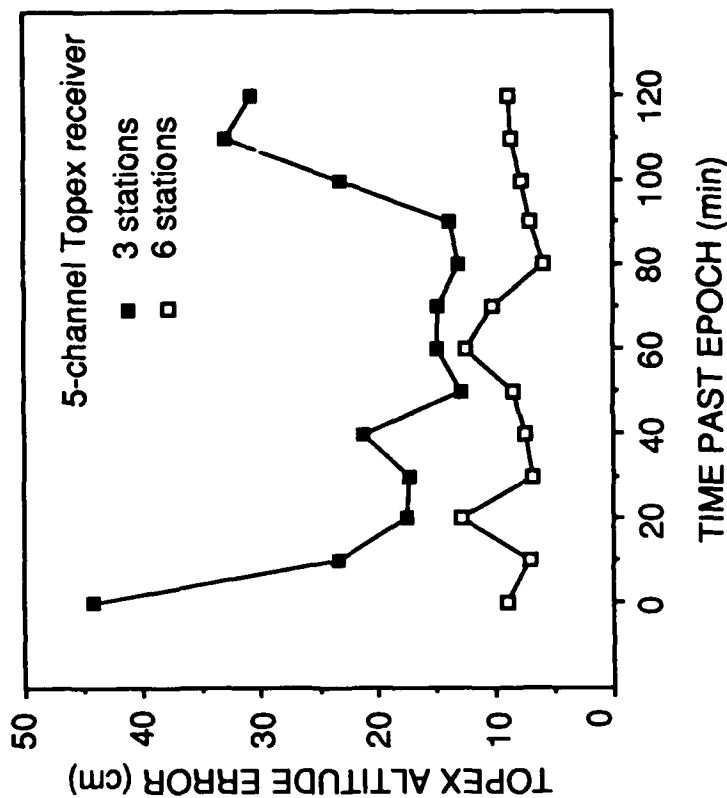
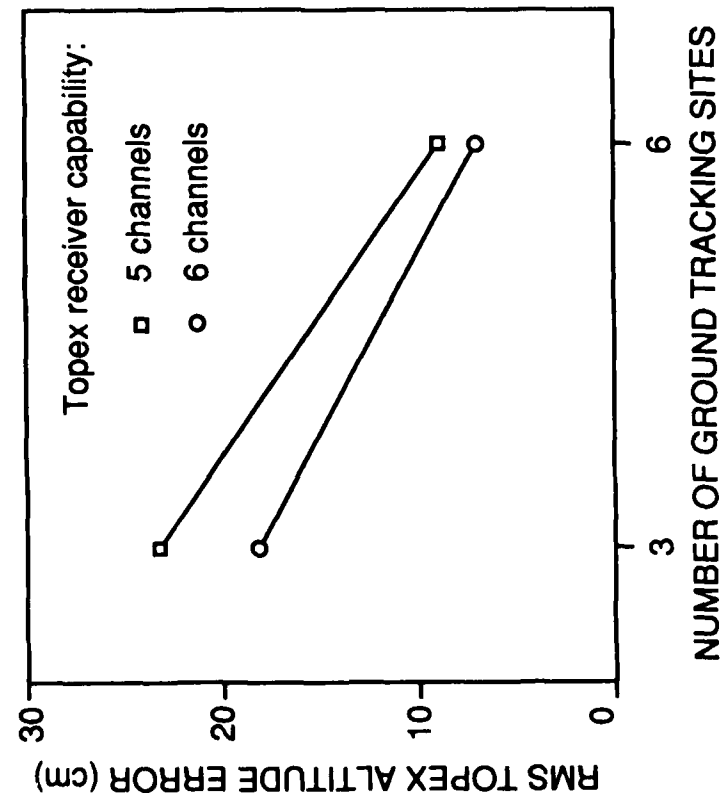
- **Accuracy goal:**
  - < 10 cm in altitude
- **Physical constraints:**
  - Onboard receiver with only 6 independent channels
  - Limited number of ground tracking sites
  - Multipath on pseudorange

### GROUND TRACKING NETWORK

- Minimum network: 3 NASA DSN sites
- Adding 3 complementary sites improves global coverage

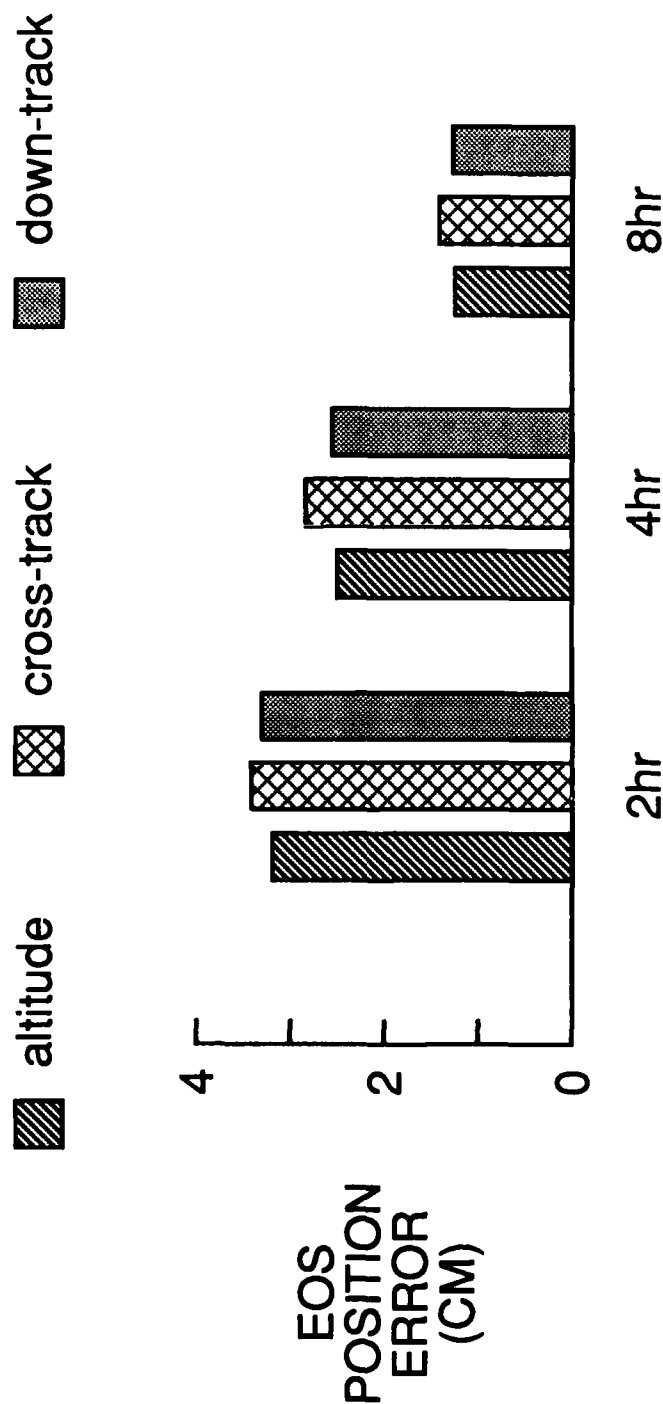


**PERFORMANCE OF TOPEX ALTITUDE DETERMINATION**



# **JPL**      **GPS-BASED POD FOR *EOS/SpaceStation***

- **Potential accuracy:**
  - 1–3 cm in all three components
- **Favorable factors:**
  - Full 24-satellite GPS constellation
  - State-of-the-art receiver with 18 independent channels
  - Multiple shaped-beam antennas providing full view window with low multipath
  - Ground tracking network of more than 10 sites
  - Fiducial sites predetermined to 2-cm accuracy



- Space Station OD error similar





## GPS-BASED LEO TRACKING

### SUMMARY

- GPS-based tracking is capable of high-accuracy OD for LEO
  - $< 10$  cm for *TOPEX/Poseidon* (1992–95)
  - 1–3 cm for *EOS/SpaceStation* (late 1990s)

## Ambiguity Bootstrapping to Determine GPS Orbits and Baselines

CHARLES C. COUNSELMAN III

*Department of Earth, Atmospheric, and Planetary Sciences  
and Center for Space Research  
Massachusetts Institute of Technology, Cambridge*

**Abstract:** For GPS satellite-orbit and interstation-baseline determination, the most accurate observable available is carrier phase, differenced between observing stations and between satellites to cancel both transmitter- and receiver-related errors. For maximum accuracy, the integer cycle ambiguities of the doubly differenced observations must be resolved. To perform this ambiguity resolution, Counselman (*Eos*, 68, 1238, 1987) proposed a bootstrapping strategy. This strategy requires the tracking stations to have a wide ranging progression of spacings. By conventional "integrated Doppler" processing of the observations from the most widely spaced stations, the orbits are determined well enough to permit resolution of the ambiguities for the most closely spaced stations. The resolution of these ambiguities reduces the uncertainty of the orbit determination enough to enable ambiguity resolution for more widely spaced stations, which further reduces the orbital uncertainty.

Abbot and Counselman (*ibid.*, 1987) and Counselman and Abbot (*JGR*, 94, 7058-7064, 1989) applied this strategy to a network of six tracking stations spaced by 71 km, 245 km, ..., up to 4000 km. Resolving ambiguities for the shortest, 71-km baseline made it possible to resolve them for the next-longer, 245-km baseline, and reduced both the formal and the true errors of determining the GPS satellite orbits by a factor of 2. The precision of baseline determination was also significantly improved.

Ionospheric refraction interferes with ambiguity resolution, by systematically biasing the doubly-differenced phase observations. However, the signature of ionospheric refraction resembles that of orbital position error; either effect, although time-variable, is spatially coherent, characterized by a nearly uniform gradient across a few-hundred-kilometer-size tracking network. Thus, the same bootstrapping principle which facilitates ambiguity resolution in the presence of orbital uncertainty, can be effective in the presence of significant ionospheric refraction.

To test this prediction, Abbot, Counselman, and Gourevitch (*Eos*, in press, Fall 1989) analyzed GPS observations from a recent period of high solar activity, with daily observation periods spanning the morning hours during which the ionosphere varies most rapidly. The ionospheric refraction effects in these observations (5 am - noon, November 1988, in Texas) were some 20 times stronger than in the night-time, April 1985, observations originally studied by Abbot and Counselman.

Using a very simple, five-parameter, ionospheric model, Abbot *et al.* processed observations from 12 dual-band receivers which were arranged in a logarithmic "Nautilus" spiral with spacings from 10 to 320 km. The use of this model increased the interstation baseline length for which ambiguities could be resolved by a factor of two (to the maximum length available). Observations on successive days were processed independently; *i.e.*, the ionospheric parameters, the position coordinates of nine receiving stations (three stations served as "fiducials"), and all the orbital elements of each satellite were determined from "single-day" arcs. The standard deviations of the horizontal station-position coordinate estimates were 2.5-4 mm, or 2-3 parts in  $10^8$  of the distance to the nearest fiducial.

Discussion:

Question: How were the stations of the Nautilus network selected and is there a latitude dependence?

Answer: The stations were selected on the basis of wanting round number (10, 20, 40, 80, km, etc.) baseline lengths with the baselines at right angles to each other. Latitude dependence has not been investigated.

The doubly differenced carrier phase observable:

$$\Delta\Delta\phi_{kq}^{ij} = -(1/\lambda) \Delta\Delta r_{kq}^{ij} + N_{kq}^{ij}$$

$\Delta\Delta r_{kq}^{ij}$  is the doubly differenced range between satellites  $i, j$  and stations  $k, q$ ;

$\lambda$  is the carrier wavelength; and

$N_{kq}^{ij}$ , known as the “ambiguity parameter” or the “bias,” is an **integer number of cycles**.

## AMBIGUITY BOOTSTRAPPING:

1. The tracking stations should have a **wide-ranging progression of spacings**.
2. Conventional processing of observations from the most widely spaced stations (without any ambiguity resolution) determines the orbits well enough to permit resolution of ambiguities for the most closely spaced stations.
3. The resolution of these ambiguities reduces the uncertainty of the orbit determination enough to enable ambiguity resolution for more widely spaced stations, which **further** reduces the orbital uncertainty,....

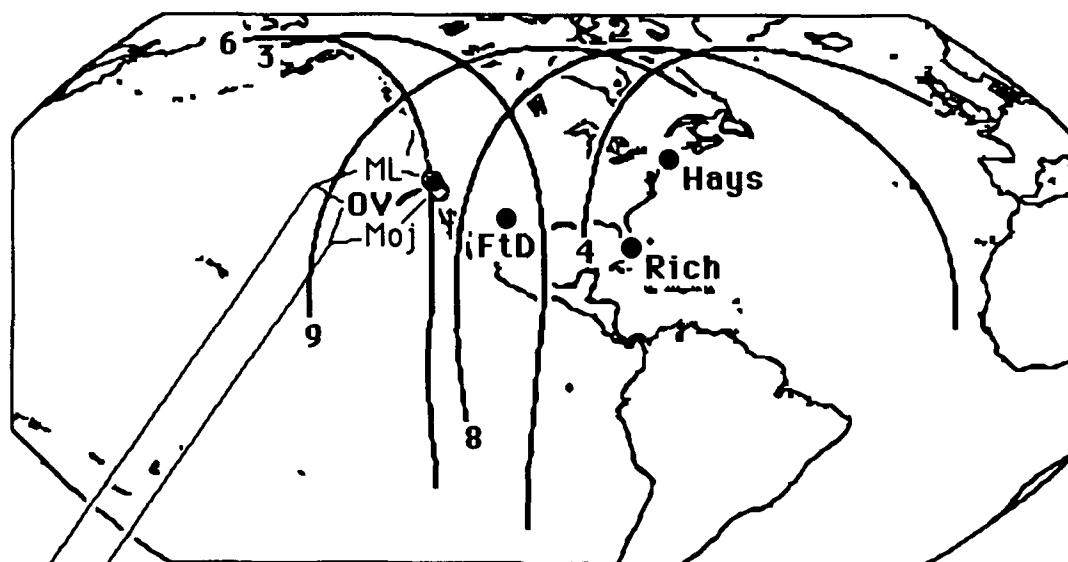
(from *J. Geophys. Res.* 94, 7058-7064, June 10, 1989)

Four widely spaced tracking stations:

OV, FtD, Rich, Hays

Two additional stations, very close to OV:

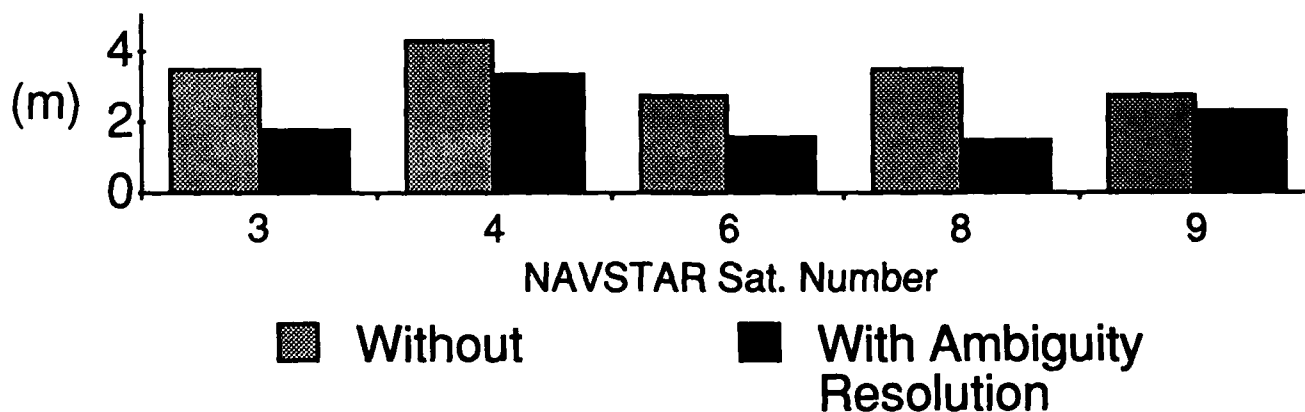
ML, Moj



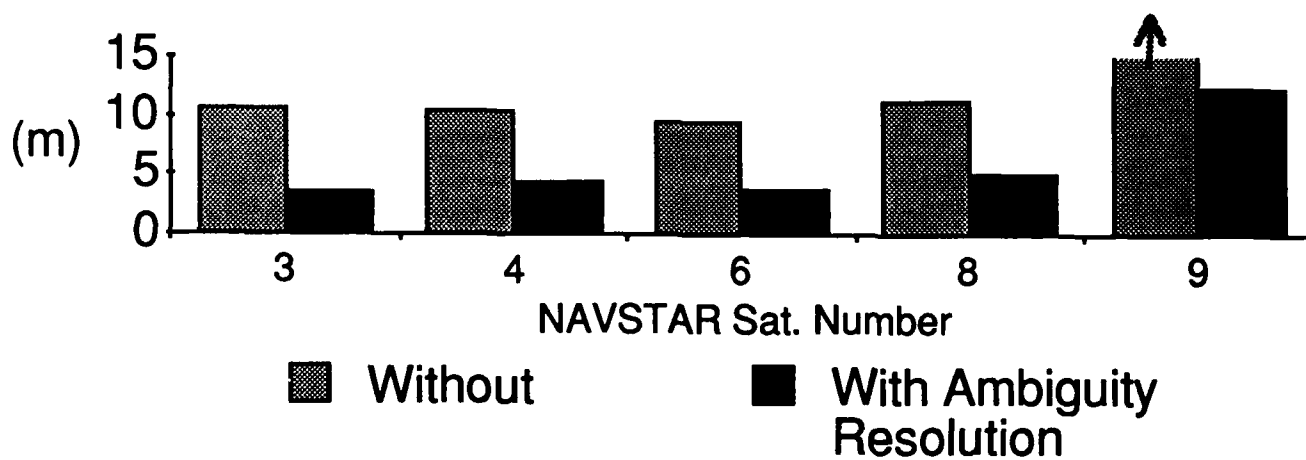
ML-OV distance  $< 2\%$  of OV-Hays distance.

OV-Moj distance =  $6\%$  " " " "

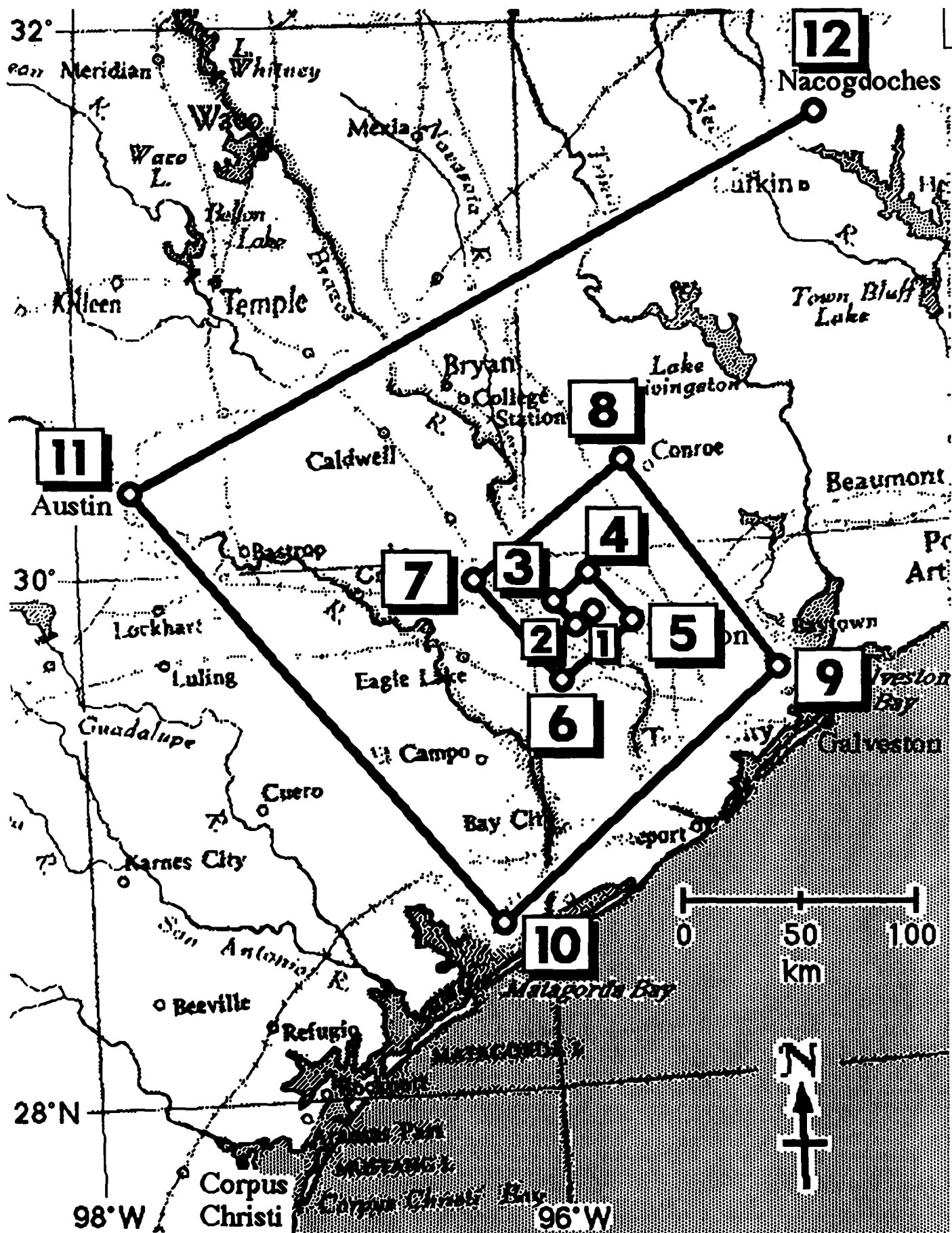
Formal Standard Errors of Orbit Determination  
With and Without Ambiguity Resolution  
for ONLY THE CLOSEST (<6%) Station-Pairs  
(all stations' phase obs'ns equally precise)



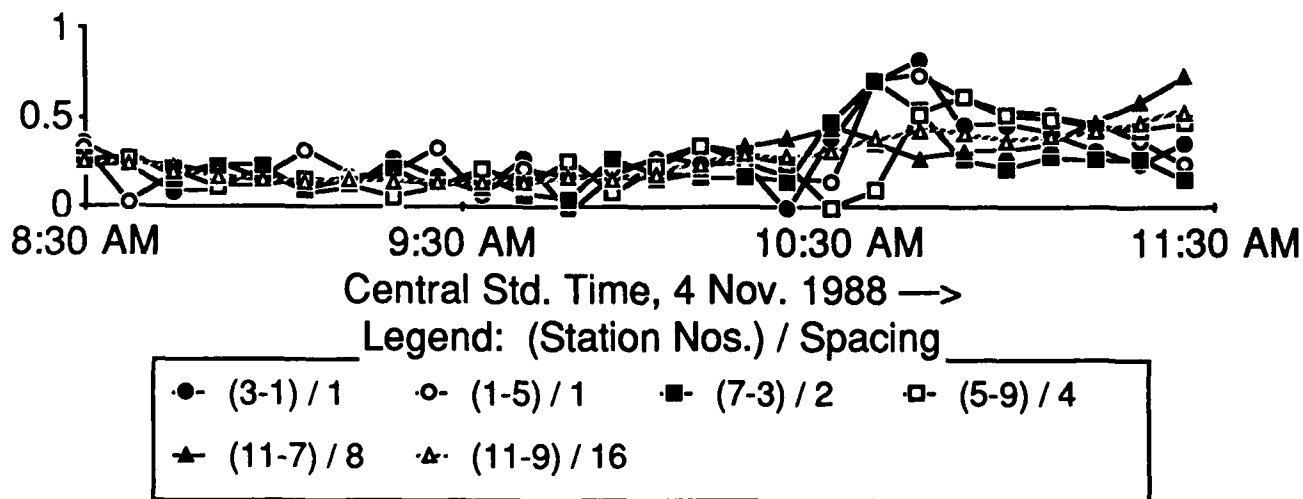
ACTUAL Peak Errors of Orbit Determination  
With and Without Ambiguity Resolution  
for ONLY THE CLOSEST (<6%) Station-Pairs  
(all stations used in either case)



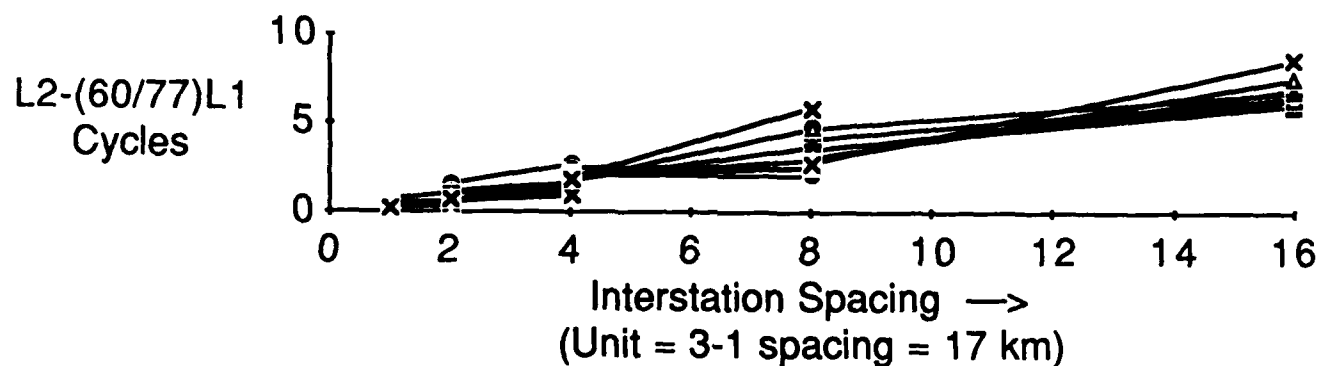




GRADIENT OF IONOSPHERIC PHASE-SHIFT  
Along E-W Axis of "Nautilus" Network  
[L2-(60/77)L1 Cycles Per Unit Station-Spacing;  
NAVSTAR 8 - 10 Difference]



# IONOSPHERIC PHASE SHIFT Along E-W Axis of "Nautilus" Network



Legend: Local Time on 4 Nov. 1988

●- 10:43	○- 10:50	■- 10:57	□- 11:04
▲- 11:11	△- 11:18	×- 11:25	

## STATION-POSITION (& ORBIT) DETERMINATIONS

Using observations from one day at a time, constraining just three fiducial-station positions, we estimated **independently for each day**

- all three position coordinates of each other station
- all six orbital elements of each satellite ("single day arcs")
- one tropospheric (zenith delay) parameter for each station except no. 1
- five ionospheric parameters [1 const. +  $2 \times 2 \sin/\cos(\text{lat./lon.})$  coeff's]
- and a few receiver clock synchronization parameters,

and used bootstrapping to **resolve all ambiguities from scratch each day.**

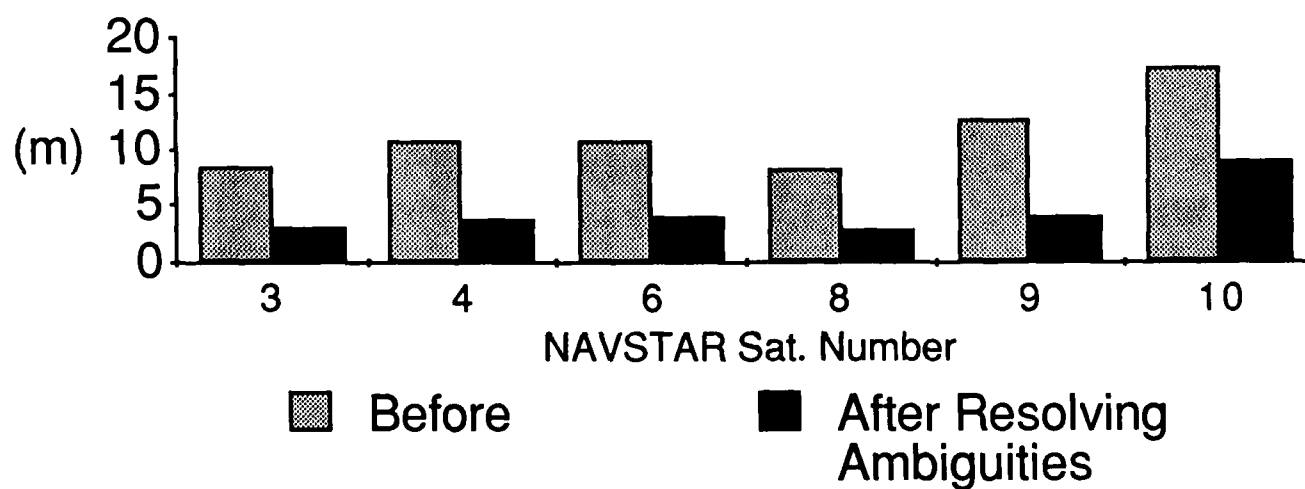
Note: Antennas and receivers were replaced daily at all stations except nos. 5, 11, and 12.

## STANDARD DEVIATIONS OF INDEPENDENT SINGLE-DAY DETERMINATIONS

from scatters of 17-d.o.f. samples (9 stns. on each of 3 days except for one receiver failure on one day):

LATITUDE	LONGITUDE
2.5 mm	4.0 mm
or, expressed as fractions of the distance to the nearest fiducial station (no. 10):	
$1.8 \times 10^{-8}$	$2.9 \times 10^{-8}$

Formal Standard Errors of Orbit Determination  
With the 240 x 320 km 'Nautilus' Network  
(Single-Day Arc, 8 Nov. 1988)



MINIATURE GPS-BASED GUIDANCE PACKAGE

by  
L. Stotts (DARPA)  
Program Manager  
Defense Advanced Research Projects Agency  
1400 Wilson Boulevard  
Arlington, Virginia 22209 USA

J. Aein (RAND)  
Senior Staff Scientist  
The RAND Corporation  
2100 M Street, N.W.  
Washington, D.C. 20037 USA

N. Doherty (MITRE)  
D-81 Department Head  
The MITRE Corporation  
Burlington Road  
Bedford, Massachusetts 01730 USA

SUMMARY

The technical goals, issues, and status of the GPS-based Guidance Package or GGP effort within the Aerospace and Strategic Technology Office of DARPA are presented. The GGP exploits the synergisms achieved by combining inertially sensed (IMU) movement with externally sensed GPS reference signals. The goal is to produce a combined GPS/IMU navigation grade system which will be miniaturized for easy insertion to any host vehicle and inexpensive for use by expendable vehicles (weapons and platforms). Efforts already under way within the DoD community based on integrating conventional navigation technologies result in systems on the order of 65 lbs, 160 watts, 1800 cu.in., and \$65 K per unit. The GGP effort aims to match the navigation performance of the conventional technologies but fit within an envelope of 10 lbs, 20 watts, 120 cu.in., and \$15 K per unit. The GGP builds upon the integrated circuit technology from the preexisting DARPA mini GPS receiver (MGR) program combined with the following: (a) solid state linear accelerometers and fiber optic rotation rate sensors (gyros) for three axes inertial sensing, and (b) a data processor and associated software to implement a Kalman filter to integrate the sensor outputs and provide the navigation solution as well as any filtered velocity, acceleration, and orientation data needed by the host vehicle. Major cost reduction breakthroughs are offered by FOG sensors which employ integrated optic chips for light wave processing along with the polarization preserving fiber optic rotation sensing coil and laser diode optical source. GGP host vehicle insertion is also facilitated by its packing/customizing achieved through modularity of MGR, IMU, and navigation microprocessor subsystems. Modularity is achieved with standardization of (1) the Kalman filter architecture in the navigation processor and (2) data transfer points (ports) interfacing the MGR and IMU sensors to the navigation processor. Technical detail is provided on the following topics: functional architecture, technology, and status of the MGR chip set; desired performance, approach, status, and technology issues for a FOG sensor, and system level integration and performance issues.

INTRODUCTION

This paper reviews the technical goals, issues, and status of the navigation technology efforts within the Aerospace and Strategic Technology Office of DARPA. The primary objective of the DARPA/ASTO navigation effort, known as the GPS Guidance Package, or GGP, is to exploit the synergisms<sup>1</sup> achieved by combining inertially sensed (IMU) body movement with externally sensed radio reference signals from

<sup>1</sup>The IMU drift coefficients can be calibrated through an extended "initialization" provided by GPS sensing while GPS receiver tracking during high dynamic maneuvers can be aided by the IMU. Additionally, the IMU provides

multiple satellites comprising the Global Positioning System (GPS). The DARPA goal is to produce a combined GPS/IMU system, the GGP, which will be miniaturized for easy (if not trivial) insertion to almost any host vehicle and inexpensive for use even by expendable vehicles (weapons and platforms).

Several efforts are already under way within the DoD community based on integrating conventional navigation technologies employing tuned rotor gyros and analog GPS receivers. To date, these configurations result in somewhat bulky systems on the order of 65 lbs, 160 watts, 1800 cu.in., and \$65 K per unit. These require sizable host vehicles and at best are only infrequently expendable.

The DARPA GGP effort aims to match the navigation performance of the conventional technologies but fit within an envelope of 10 lbs, 20 watts, 120 cu.in., and \$15 K per unit. To succeed, the GGP must maximally utilize solid state (like) devices, fabrication, and assembly methods, i.e., minimize labor input. Consequently, the GGP builds upon the integrated circuit technology base developed from the preexisting DARPA mini GPS receiver (MGR) program sometimes referred to as "Virginia Slims" for its packaging resemblance to a product of the same name [1].

To an MGR-type GPS sensor (hereinafter referred to as an MGR) must be added the following: (a) solid state linear accelerometers and rotation rate sensors (gyros) for three axes to provide inertial sensing, and (b) a data processor and associated software to implement a Kalman filter to integrate the sensor outputs and provide the navigation solution as well as any filtered velocity, acceleration, and orientation data needed by the host vehicle. The MGR and "solid state" IMU may each have its own embedded processor chip dedicated to running the necessary real time, lower level, sensor signal processing. The subsystem structure is shown in Fig. 1.

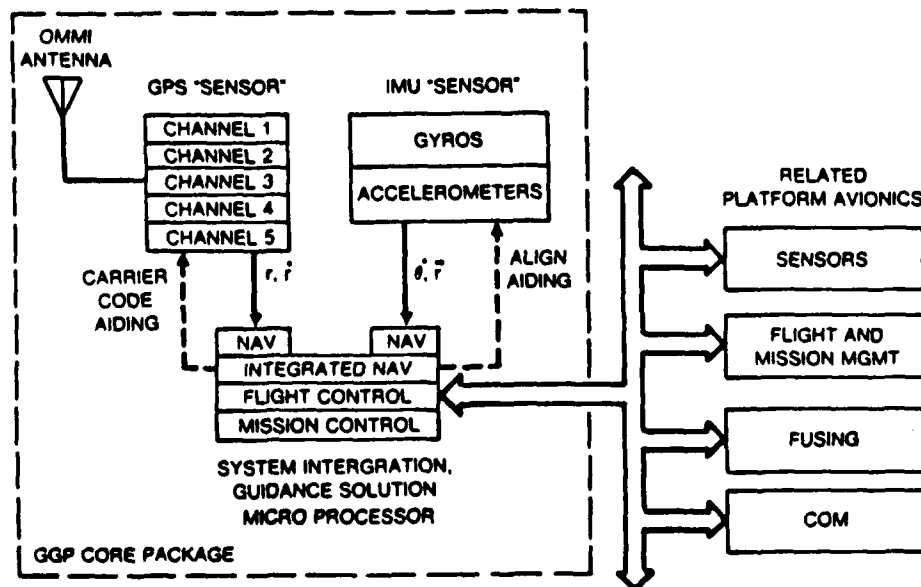


Fig. 1— Low-Cost GPS Guidance Package

As there are several silicon accelerometer (SiAccel) efforts already under way upon which the GGP can draw, the primary GGP technology push is on developing a solid state like rotation sensor (gyro) for the IMU. A review of the gyro technology base indicates use selections of a rotation sensor based on the Sagnac effect; either the Ring Laser Gyro (RLG) or the Fiber Optic Gyro (FOG). Of the two technologies, the RLG is by far the more mature, e.g., RLGs which have very high performance are now going into production. However, the prospects for meeting the low cost goals for the GGP using high performance RLGs do not look promising.

navigation during periods of GPS signal loss; remember four separate satellite signals are required to navigate with GPS alone. Moreover, mutually combining GPS with inertial sensing allows slower GPS receiver sequencing amongst the satellites even in high dynamics. This then provides fault tolerance amongst receiver channels.

There are major cost reduction breakthroughs offered by FOG sensors which employ integrated optic chips for light wave processing along with the fiber optic rotation sensing coil and laser diode source. The objective is to provide FOG performance levels comparable to RLGs. Consistent with DARPA's acceptance of technology risk in order to induce jump advances in technology, the FOG rotation sensor was selected for GGP development. The integration of a GPS receiver with an RLG-based IMU is a lower risk approach which is likely to be pursued elsewhere in the DoD community.

Insertion of the GGP to host vehicles is facilitated through its very small size (to minimize host burden) and flexible packaging/customizing achieved through modularity of MGR, IMU, and navigation microprocessor subsystems. The modularity with interface control between the data processor and sensor subsystems will allow swapouts of either MGR or IMU sensors without redesigning the whole system. The modularity is facilitated through standardization of (1) the Kalman filter architecture in the navigation processor and (2) data transfer points (ports) interfacing the MGR and IMU sensors to the navigation processor. This will allow flexible choices in the selected number of MGR processing channels (e.g., two-channel sequencing MGR for low dynamics vice six-channel parallel MGR for high dynamics) and easy IMU upgrades with improving FOG sensors.

This paper is organized as follows: Section II outlines functional architecture, technology, and status of the MGR chip set; Section III discusses the desired performance, approach, status, and technology issues for a FOG sensor, and Section IV discusses system level integration and performance issues.

#### MINI GPS RECEIVER MGR

The following section reviews the specific Rockwell Collins MGR technology of reference 1 as an example only of the MGR needs, capabilities, and issues for a GGP. A DARPA GGP will employ a similar MGR technology but need not be identical with that described here.

The physical MGR chip partitioning developed in reference 1 is shown in Fig. 2. A summary of the technical parameters for each chip with their respective power consumption is shown in Table 1. The performance requirements for the MGR are exactly the same for conventional GPS receivers as specified in SS-US-200 [2]. [Summary shown in Table 2] Referring to Fig. 2, the three key new chips developed (out of five) in order of their technical difficulty are as follows:

- o GaAs RF/IF/AD Receiver Front End
- o CMOS Hi-Speed Digital Signal Processor (VHISC Technology)
- o Silicon Bipolar Synthesizer

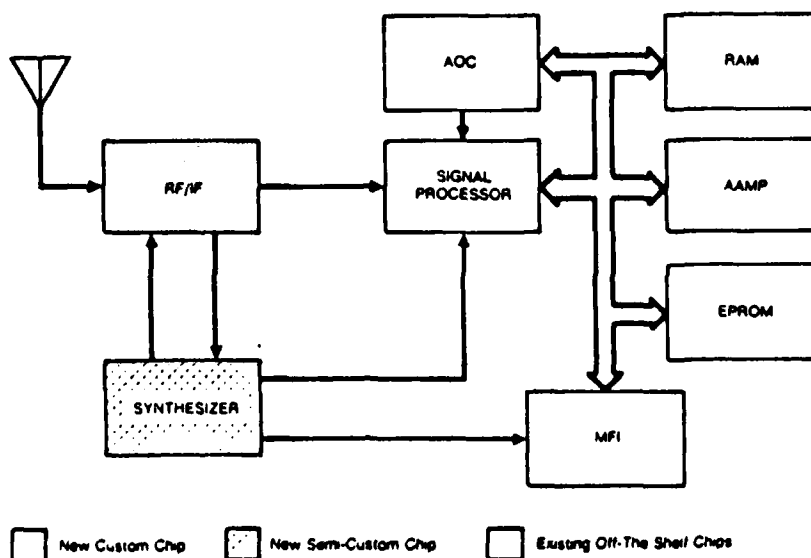


Fig. 2—Generic MGR Architecture



Table 1  
CHIP SET SUMMARY

Chip Type	Device Count	Dimensions (Inches)	Implementation Technology	Power (mW)
RF/IF Translator	300-400	0.200 x 0.240	GaAs	1700
Signal processor	20,000	0.185 x 0.220	1.25 micron bulk CMOS	90
Multifunction Interface	29,000	0.370 x 0.370	1.6 micron bulk CMOS	20
Micro processor	60,000	0.214 x 0.261	2 micron bulk CMOS	80
Frequency synthesizer	600-700	0.250 x 0.250	bipolar silicon	500

Table 2  
USER EQUIPMENT REAC AND TTFF TIME REQUIREMENTS

	REAC 1 (MIN)	TTFF 1 (MIN)	UNCERTAINTY			MAX ACCEL (M/SEC <sup>2</sup> )	MAX JERK (M/SEC <sup>3</sup> )
	REAC 2 (MIN)	TTFF 2 (MIN)	POSITION (KM)	VELOCITY (M/SEC)	TIME (SEC)		
LOW DYNAMIC SET	10.5	5.5	100 (3 $\sigma$ )	25 (3 $\sigma$ )	20 (1 $\sigma$ )	8	20
	NOT REQUIRED	NOT REQUIRED					
MEDIUM DYNAMIC SET	9.0	4.0	100 (3 $\sigma$ )	75 (3 $\sigma$ )	20 (1 $\sigma$ )	10	20
	NOT REQUIRED	NOT REQUIRED					
HIGH DYNAMIC SET	7.0	2.0	100 (3 $\sigma$ )	150 (3 $\sigma$ )	20 (1 $\sigma$ )	10	100
	6.5	1.5*			10 (1 $\sigma$ ) (u SEC)		

NOTE: The probability of success in achieving the stated REAC and TTFF times shall exceed 0.9. These REAC and TTFF requirements are valid over the -40°C to +55°C temperature range.

\*TTFF 2 can be reduced to 0.5 minutes if position and time uncertainties are also negligible.

The advanced data processor, control chip--AAMP--was developed by Rockwell Collins to reduce power consumption in the conventional technology manpack GPS receiver while the multifunction interface or glue chip was produced with a straightforward (silicon) foundry. The AAMP is an embedded MGR data processor and will not be used for MGR/IMU sensor integration and control. A summary description of these chips is given in tables 3 and 4.

Modularity needs for multiple GPS signal tracking (2 to 6 channels) are determined by the host vehicle dynamics and fault tolerance requirements. Multiple channel modularity is obtained through the MGR chip partitioning chosen with a matching software structure provided. Each GaAs MMIC chip processes either one of the two possible L-band frequencies (L1/L2) identically radiated by all GPS satellites. Each digital signal processing chip fully processes one C/A and P-coded transmission. Using mix and match the minimal configuration for low dynamics uses a one MMIC two-signal processor configuration with L1 and L2 and 4 P-codes sequentially processed. The maximal configuration for a high dynamics set, which simultaneously processes two frequencies and six channels, will use two GaAs MMIC and six signal processor chips. The rest of the high dynamics set remains the same as the two-channel set (synthesizer, MFI, AAMP) although the data processing throughput requirements on the AAMP increase to where two AAMP chips may be required.

The most unique chip technology challenge for the MGR has been the GaAs MMIC chip whose layout is shown in Figs. 3 and 4. On this common die two unique suites of circuits must be processed in the GaAs foundry. Specifically, a low noise (3 db NF) high quality analog RF amplifier path with over 90 db of gain must be accomplished along with gigabit digital FET gates to implement the necessary on-chip frequency dividers and the analog-to-digital converter. Moreover, the digital FETs employ balanced enhancement and depletion modes for ultra low power drain.

The GaAs foundry must find a compromise process to fabricate in common both the analog and digital devices with adequate yield. An optimized "conventional" GaAs foundry process for exclusively digital or analog transistors cannot be employed. Moreover, more than 90 db of gain must be accomplished across only 0.2 in. without any parasitic oscillations.

The GaAs MMIC RF chip outputs fully digitized (2 bits/sample) both in-phase and quadrature samples of the full 10 MHz IF bandwidth to the digital signal processor CMOS chip shown in Fig. 5. On this custom CMOS chip, carrier frequency and PN-code tracking along with C/A and P-code correlation is achieved in hardware. The signal

processor chip outputs every 1 m-sec both in-phase and quadrature code cross-correlates (received signal with receiver stored reference) for the prompt, early, and late correlation channels used by the AAMP for data symbol detection and code tracking.

Table 3

## MGR SUMMARY MMIC AND SIGNAL PROCESSOR CHIPS

CHIP	FUNCTION
<ul style="list-style-type: none"> <li>A GaAs MMIC that contains all RF, IF, mixing and signal quantizer functions along with some high speed digital dividers for the synthesizer. This chip provides nearly 100dB of gain and has a noise figure under 3 dB.</li> </ul>	<p>Analog</p> <ul style="list-style-type: none"> <li>Antenna/filter input</li> <li>On-chip RF overload limiter</li> <li>Low noise amplifier</li> <li>SPDT switch to off-chip image-rejection filter</li> <li>SPDT switch from off-chip image-rejection filter</li> <li>1st downconversion mixer (dual-gate FET)</li> <li>1st IF stage and lowpass filter</li> <li>1st IF amplifier</li> <li>In-phase and quadrature 2nd downconversion mixers</li> <li>2nd IF stage with active band limiting filter</li> <li>2nd IF amplifier and AGC</li> <li>Signal digitizer</li> <li>Buffers to drive off-chip signal processor.</li> </ul> <p>Digital</p> <ul style="list-style-type: none"> <li>L-band voltage-controlled oscillator</li> <li>Buffer amplifiers—1st mixer</li> <li>On-chip digital dividers to synthesize second IF I and Q injections</li> <li>On-chip SPDT switch logic.</li> </ul>
<ul style="list-style-type: none"> <li>A single digital signal processor chip that demodulates the GPS signal and provides 1 ms signal integrations to the data processor. The chip contains all code VCO and code generation functions.</li> </ul>	<ul style="list-style-type: none"> <li>Carrier phase rotation</li> <li>Carrier VCO</li> <li>Code generation</li> <li>Code removal</li> <li>Code VCO</li> <li>Signal integration</li> <li>Built-in test</li> <li>Timing and bus interface.</li> </ul>

Table 4

## MGR SUMMARY: SYNTHESIZER, MICROPROCESSOR, AND BLUE CHIPS

CHIP	FUNCTION
<ul style="list-style-type: none"> <li>A frequency synthesizer chip that includes the intermediate speed dividers and locks the VCO to a frequency standard. An on-chip dual-mode oscillator or an external oscillator can be used as the frequency standard</li> </ul>	<ul style="list-style-type: none"> <li>Frequency standard</li> <li>Phase detector</li> <li>Loop filter</li> </ul>
<ul style="list-style-type: none"> <li>A single-chip advanced architecture microprocessor (AAMP) that contains on-chip floating point operations and has sufficient throughput to handle all the processing for a two-channel GPS set</li> </ul>	<ul style="list-style-type: none"> <li>Real time executive</li> <li>Application software initialization</li> <li>Control/display drivers</li> <li>Navigation</li> <li>Receiver manager</li> <li>Receiver processing</li> <li>Signal preprocessing</li> <li>Satellite database manager</li> <li>Satellite position/velocity processing</li> <li>Built-in test</li> <li>Utilities.</li> </ul>
<ul style="list-style-type: none"> <li>A single multifunction interface chip that incorporates all the functions required for controlling one-, two- and five-channel GPS sets. It also contains the memory and interrupt controllers, as well as low frequency set timing functions.</li> </ul>	<ul style="list-style-type: none"> <li>memory control</li> <li>Interrupt control</li> <li>Frequency/time generation</li> <li>Serial interface</li> <li>Built-in test.</li> </ul>

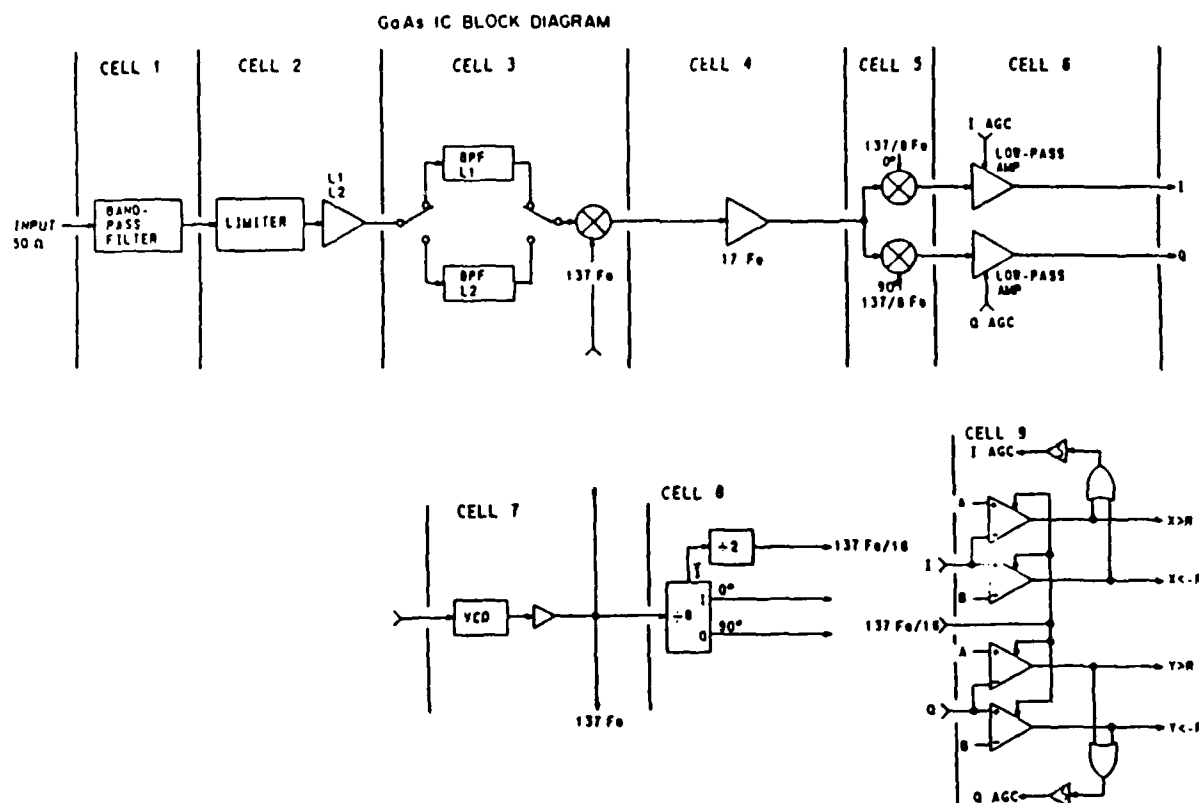


Fig. 3—GaAs MMIC Block Diagram

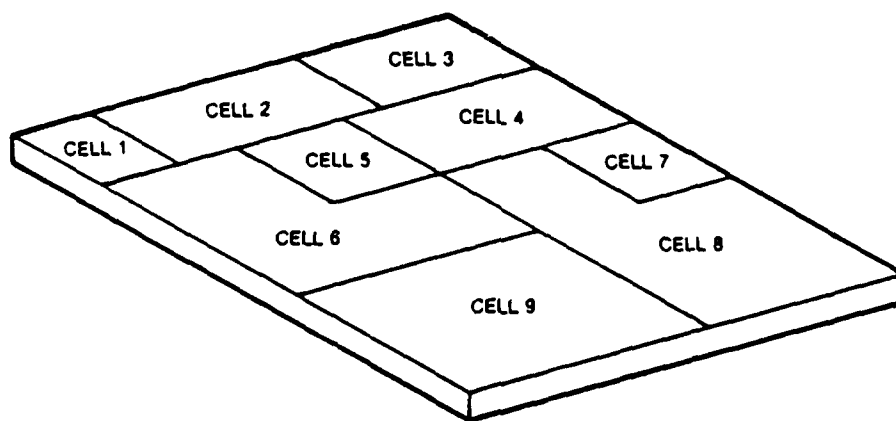
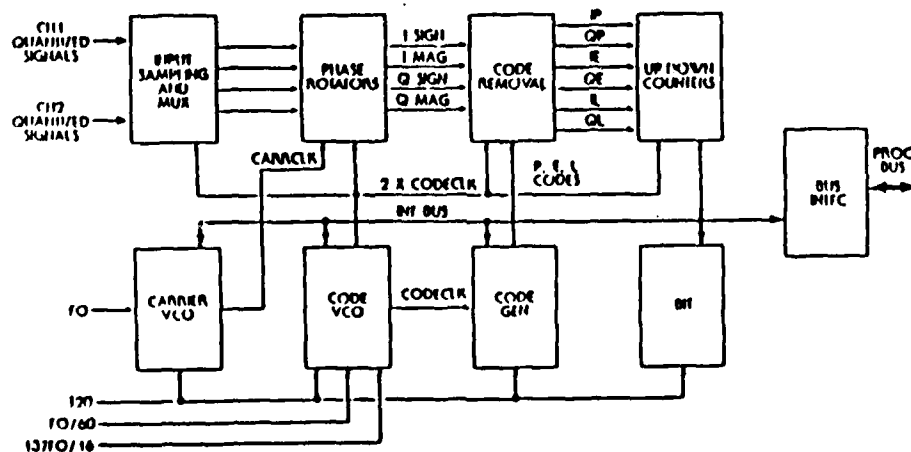


Fig. 4—GaAs MMIC Floor Plan



The signal processor output data are supplied every millisecond to the AAMP microprocessor where real time signal processing software further processes this 1 KHz data down to 50 Hz bandwidth (20 msec correlates) or less for GPS system data detection as well as signal carrier and code tracking. The error null steering commands determined by AAMP tracking loop software modules are returned by the carrier and code VCO steering control lines on the signal processor chip.

Examples of all the Rockwell Collins 2-channel MGR chips set are now functioning in a navigating breadboard, including the GaAs MMIC chip. The challenge of realizing low noise high RF gain (without oscillation) concurrent with gigabit digital logic gate speed on a common MMIC has now been successfully demonstrated.

#### FIBER OPTIC GYRO

Two sets of performance goals for the IMU components of the GGP are shown in Table 5. These values are based on improving the current generation of Fiber Optic Gyros (FOG) and the availability of Silicon Accelerometers. The early time frame performance in FOG is almost achievable now but with discrete fiber parts instead of the desired integrated optics. The early DARPA goal is to incorporate integrated optics and a modest improvement in current performance. The later goal is to match navigation grade Ring Laser Gyro (RLG) performance.

Table 5  
IMU PERFORMANCE GOALS

	EARLY DEMONSTRATION	MIDTERM DEMONSTRATION
GYRO DRIFT BIAS	0.01 DEG/HR	0.003 DEG/HR
GYRO SCALE FACTOR	50 PPM	10 PPM
GYRO RW COEFFICIENT	0.005 DEG/ $\sqrt{\text{HR}}$	0.0015 DEG/ $\sqrt{\text{HR}}$
ACCELEROMETER SCALE	50 $\mu\text{G}^a$	10 $\mu\text{G}^a$
ACCELEROMETER SCALE FACTOR	100 PPM	50 PPM
ACCELEROMETER RW COEFFICIENT	0.03 (M/S)/ $\sqrt{\text{HR}}^b$	0.03 (M/S)/ $\sqrt{\text{HR}}^b$

<sup>a</sup>Micro G's of gravity.

<sup>b</sup>Meters per second per root hour.

Sagnac effect [3,4,5] based rotation rate sensors establish a pair of contra-propagating beams of light in a planar light guide circuit having exquisite optical symmetry (reciprocity) between the clockwise and counterclockwise propagation paths around the light circuit. Mechanical rotation rate measurably upsets this symmetry which can be photoelectronically detected and processed to provide a rotation rate output. A broad characterization of Sagnac effect rotation rate sensors (RLG, IFOG, RFOG) is shown in Fig. 6. The ring laser gyro (RLG) is now becoming commercially available with a very high grade of inertial measurement quality. Although a major improvement over mechanical gyro technology, it was judged to suffer the following drawbacks with respect to the DARPA GGP goals:

- (a) Not amenable to employing integrated optics
- (b) Requires complex glass machining with very high quality corner mirrors
- (c) High voltage discharge needed to excite laser
- (d) Mechanical motion dither needed to break up measurement deadband caused by common mode locking between contrapropagating beams

Of these drawbacks, the second item, (b), may through extensive development and production experience reduce present costs by creating a large industrial robotic glass machining base. Mechanical path dither, currently used, may be replaced by an electro-optic dither technique. However, these evolutionary RLG tech base improvements are deemed not commensurate with an early time frame, nor are they expected to reduce the rotation sensor costs to the level expected of a successful (albeit risky) fiber optic gyro, FOG, effort.

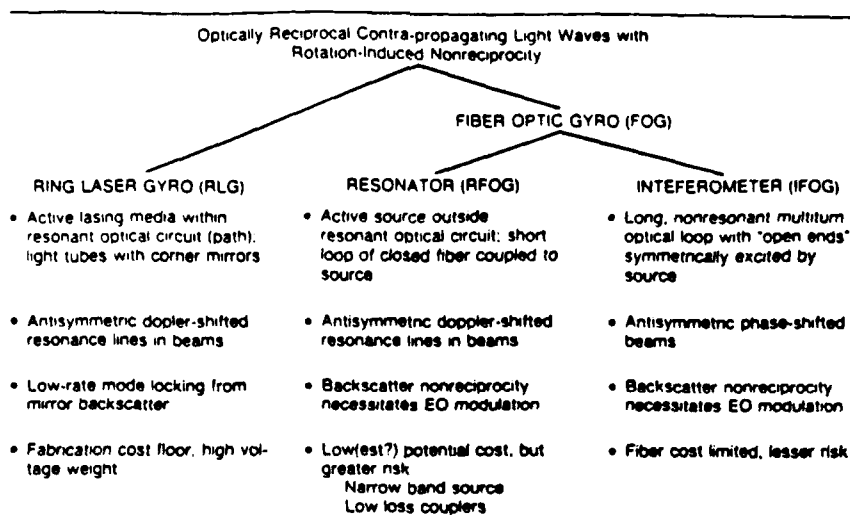
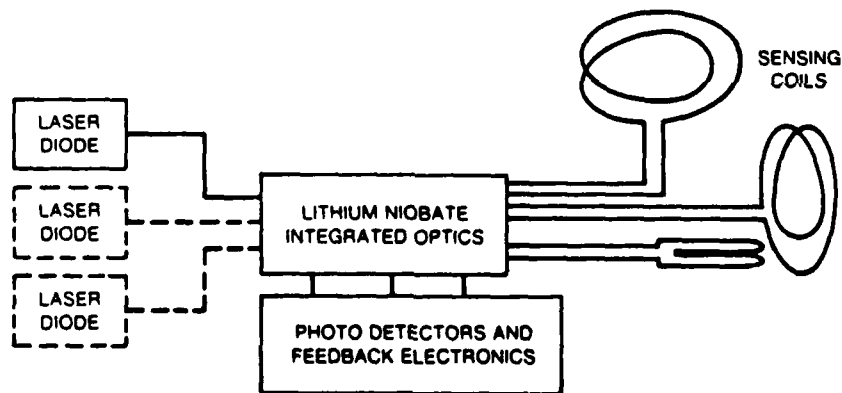


Fig. 6—SAGNAC effect

From these considerations DARPA selected the FOG sensor approach to be assembled with an integrated optics chip, using crystalline lithium niobate and conceptually shown in Fig. 7. Initially, each rotation sensing axis will be composed of its own sensing coil, IO chip, diode light source, and photodetector. With IO chip fabrication improvements, one chip can be shared by all axes. With increased optical source intensity, one source (with one IO chip) can be power-divided amongst all axes.



- SAGNAC NULLING FEEDBACK ARCHITECTURE — LARGE MEASUREMENT RANGE
- POLARIZATION PRESERVING FIBER (PPF) — INCREASED OPTICAL RECIPROCALITY
- LONGER WAVELENGTH — ELIMINATE PHOTODARKENING & REDUCE BACKSCATTER
- INTEGRATED OPTICS — LOW COST

Fig. 7—Three-Axis Fiber Optic Rotation Sensor

There are two fundamentally different implementations of a FOG sensor; a resonant structure or RFOG, and an interferometric structure or IFOG. An oversimplified comparison of the properties of the RFOG and IFOG are summarized in Fig. 8.

The RFOG [6] utilizes a short loop of fiber as an extremely high Q resonant light circuit. Ideally, when there is no rotation input, each of the two contra-propagating light beams remain trapped in the fiber sensing coil at the resonant light frequency and no light escapes<sup>2</sup> the coil coupler structure. Mechanical rotation doppler offsets the beams from the coil resonance frequency and light begins to escape from the coil. The special optical coupler (Fig. 8, "dashed box"), together with the lithium niobate IO chip, route the escaping coil output light

<sup>2</sup>Ideally, the optical source power is fully absorbed with carefully matched

(under mechanical rotation) for each circulating beam to photodetectors; one for each beam direction. Since the beams are doppler shifted off resonance in opposite (light) frequency directions, the corresponding photodetectors provide skew symmetric outputs.

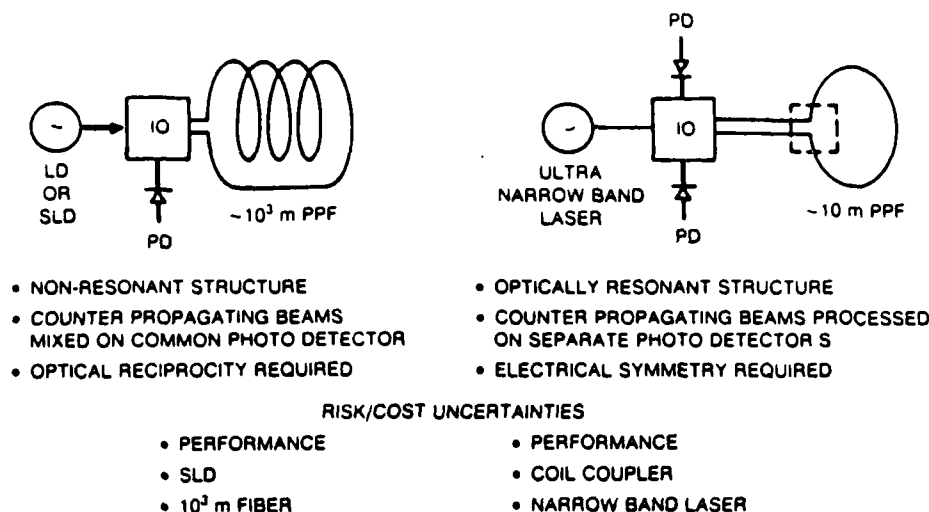


Fig. 8—IFOG or RFOG

Inasmuch as the short fiber loop is a delay line, the input-output optical system transfer function,  $H(j\omega)$ , of the resonant optical structure has a periodic null pattern in frequency spaced about 40 MHz apart. Referring to Fig. 9, a single, laser diode optical source is physically divided in two to launch each of the contrapropagating beams. Each beam is then individually heterodyned by optical frequency modulators in order to place beams in separate (usually adjacent) resonant nulls of the sensing coil. In this manner, the RFOG effectively operates as two separate gyros multiplex sharing, in optical frequency and propagation direction, a common coupler fiber coil sensing structure. The two balanced and symmetric gyros operate in a push-pull mode so that even order channel impairments cancel.

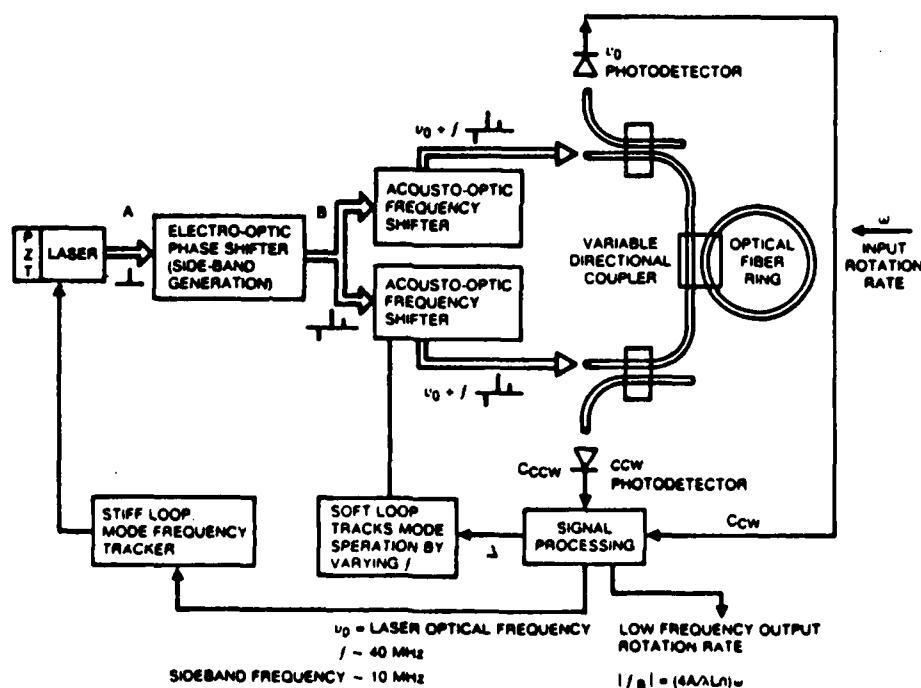


Fig. 9—Resonant Ring Gyro Control and Measurement Approach

In contrast to the RFOG, the IFOG structure [5,9] is a single gyro with one photodetector to which both contrapropagating beams additively output. The long (many turns) fiber coil is a nonresonant, very broadband structure. Consequently, a broadband diode light source can be used, which the present IFOG technology requires, as will be explained below.

The IFOG photodetector physically performs a mathematical crosscorrelation between the two contrapropagating output beams which were launched from a common light source. Ideally, with no path imperfections or asymmetries (optical reciprocity), the photodetector then produces the autocorrelation function of the light source after passage through the fiber coil. With no rotation, this outputs the peak of the diode source autocorrelation function. With mechanical rotation the path propagation times change producing an optical phase shift (as opposed to doppler frequency shift) between the two beams and an off-peak value of the autocorrelation function is read at the photodetector.

This simple, interferometric, configuration produces electronic difficulties with the output signal. First, since the autocorrelation functions are even, rotation direction cannot be directly read. Second, the output measurement is centered around d.c., requiring more complex d.c. electronic amplification circuits. This situation can be corrected by introducing a subcarrier frequency modulation [7] at a multi-kilohertz frequency (100 KHz) on each propagating beam prior to photodetection as shown in Fig. 10. This is accomplished with an optical phase modulator on one arm of the coil. The phase modulator device periodically (at the FM subcarrier frequency) changes the optical path delay<sup>3</sup> through itself. Note that one beam is frequency modulated prior to entering the fiber sensing coil while the other beam is modulated after exiting the coil. This produces optical frequency modulations time shifted with respect to each other by the beam propagation time through the coil.

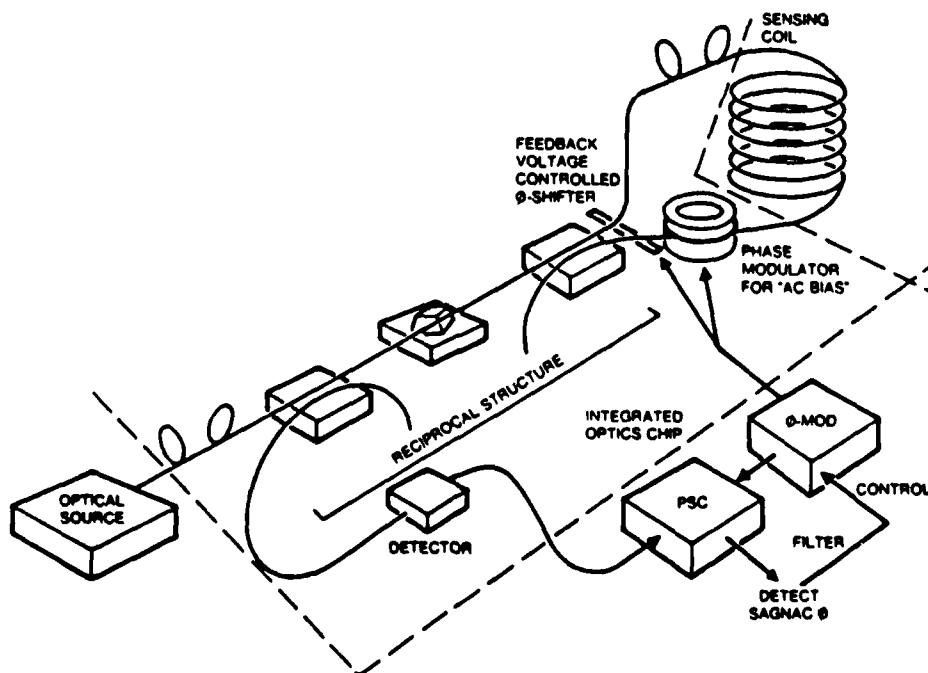


Fig. 10—Interferometer FOG with Feedback

The photodetector correlation output can be narrowband processed around the first harmonic of the FM modulation frequency and then synchronously detected by multiplying and smoothing the product of the first harmonic output signal with the same periodic signal driving the optical phase modulator. The consequences of this modulation/signal processing arrangement are to allow use of inexpensive a.c. photodetector output amplifiers while producing a skew symmetric detector output signal which is zero for zero rotation input rate. Rotation direction is then immediately given by the sign of this output.

<sup>3</sup>Time base variation is mathematically equivalent to imposing a frequency modulation.

A brief discussion on optical sources is now in order. Recall that for the RFOG, employing the very high Q light circuit sensing coil, an extremely narrow laser diode optical source bandwidth is required to fit within the resonance linewidth of the resonant optical structure. Now, in general, the autocorrelation function of any narrowband waveform is an attenuated cosine function with a period equal to that of source (optical) wavelength and a rate of envelope decay equal to the reciprocal of the source bandwidth (i.e., "spectral linewidth"). The effective time duration of this correlation envelope time decay when multiplied by the speed of light produces a "length" referred to as the coherence length of the source. The coherence length of an RFOG source must be in excess of a mile!

Next consider the long optical path length (on the order of 1 km) used by a high sensitivity IFOG. Discrete imperfections in the optical path (for example, due to splices or connectors, nicks in the fiber cladding, impurities in the fiber core, etc.) will cause small-scale (1) optical reflections (backscatter), and (2) crosspolarization mode coupling (forward scatter). These unwanted optical interference signals are analogous to the multipath interference in a radio link. In direct analogy with radio multipath, spread spectrum sources [8] can be used to combat the multipath.

All such "optical multipath" interference sources separated from the desired optical signal or from each other by less than the coherence length of the source (i.e., autocorrelation envelope decay time) will upset the measurement accuracy. This results from the photodetector crosscorrelating the exiting light beams (desired plus interfering) of the fiber coil. This crosscorrelation produces not only the desired autocorrelation function of the optical source but is also corrupted by crosscorrelations between the "multipath" generated beams and the desired beams. However, those crosscorrelations separated by more than a source coherence length are zero. Consequently, short coherence length sources (large instantaneous bandwidths) considerably reduce the number of small interference signals corrupting the measurement accuracy.

The IFOG detector processing depends on the wavelength periodicity of the optical source autocorrelation function and not its envelope. Consequently, an optical diode source having large symmetrical instantaneous spectral bandwidth (e.g., Super Luminescent Diode, SLD) with a very stable center frequency produces an autocorrelation function still useful for IFOG operation but having a fast decay time (submillimeter coherence length).<sup>4</sup> Now only multipath source pairs within a coherence length (submillimeter) of each other can beat together to produce a degraded output and most of the multipath is rejected. Consequently, current IFOG technology is facilitated by use of broadband diode sources while the RFOG must use extremely narrowband laser sources to excite their resonant structures.

In contrast to the IFOG, recall that the RFOG operates with a much shorter fiber and off-resonance frequency detection for each separately propagating beam and does not crosscorrelate the beams. Consequently, the RFOG is affected by optical multipath sources in a very different way than the IFOG. Here the resonance optical bandpass shape becomes distorted by multipath. The RFOG system phase transfer function must be kept skew symmetric about a small frequency region centered on the resonance point of the fiber coil.

Since the IFOG sensor has been in active development in industry for a longer time, it is much closer to being implementable in a nearer term, flight-testable GGP prototype. For example, the broadband optical sources, although expensive, currently exist while available narrowband solid state sources are still too wide (~1 MHz vice the 100 KHz or less needed). Consequently, the IFOG rotation sensor is the initial choice for the GGP based on early availability, but interest remains high at DARPA in the RFOG sensor technology.<sup>5</sup>

So far in the discussion, both FOG architectures suffer from a very limited measurement dynamic range. That is to say, the ratio of the maximum rotation rate usefully measurable to the random noise output is not as large as desired. The RFOG resonant structure is so narrowband that the higher rotation rate doppler shifts the

<sup>4</sup>In theory the source also could be broadbanded by electronically induced modulation. Alternatively, other signal processing techniques for multipath rejection might be employed.

<sup>5</sup>The reader is put on notice that DARPA views the RFOG and IFOG, although both rotation sensors, as distinctly different transducers with unique and different advantages, uses, risks, and cost. They are not viewed as a priori competitive technologies for the same universal application.



source out of the resonance while the IFOG cosine autocorrelation function<sup>6</sup> becomes ambiguous for large Sagnac phase shifts resulting from higher rotation rates. These effects produce measurement (not device) failure.

Actual measurement dynamic range is set by even lower maximum permissible rotation rates. Namely, as the rotation rates increase the measured output becomes nonlinear with input mechanical rate; i.e., nonlinear scale factor. Consequently, for increasing overall measurement precision, there is a further decrease in useful dynamic range.

The means to increase the dynamic range is to employ measurement feedback (Figs. 9 and 10) creating a closed loop FOG sensor. As the Sagnac effect develops and is sensed at the photodetector(s), feedback electronics filter the signal and then input to a voltage-controlled optical phase or frequency shifter(s) on the integrated optics chip. In this way the Sagnac optical signal can be nulled out. The rotation rate measurement is taken from the drive voltage to the voltage-controlled optical shifter. The Sagnac optical signal is processed as the error signal input to a tracking feedback loop. This technique is the optical analogue to the Phase Lock Loop (PLL) for the IFOG, and Automatic Frequency Control (AFC) for the RFOG.

To date, laboratory IFOGs have been assembled using discrete fiber optical parts (e.g., couplers, polarizers, splitters, modulators) operating with light sources at 0.83  $\mu$  wavelength. The net drift rate bias has been at the 0.1°/hr or less regime. Some efforts have already installed the feedback architecture and employ polarization preserving fiber (PPF) in the sensing coil. The PPF coil considerably improves optical reciprocity of the light path by drastically reducing the level of unwanted crosspolarized (nonreciprocal path) light being crosscorrelated on the photodetector. All DARPA efforts for future high performance IFOGs will incorporate these features.

Further efforts [8] at implementing individual or a few optical parts ( $\gamma$ -splitter, coupler, polarizer, phase modulator) on lithium niobate chips have succeeded. The DARPA effort will emphasize accomplishing a high level of optical integration on one Integrated Optic (IO) chip. The long-term goal is to place all optical parts on the IO chip excepting the light source.

The IO fabrication method deposits etched strip lines of titanium on a lithium niobate crystal substrate. These titanium lines are then heat diffused into the crystal forming light guides whose interguide propagation coupling properties are carefully controlled. These optical couplers and splitters are passive linear "circuits." Optical modulators and switches are obtained by using the electro-optic effect in lithium niobate where the light propagation velocity (refractive index) is a function of the strength of an imposed external E field. Capacitive "plates" are deposited over desired portions of the chip with electric control lines to which off-chip drive electronics attach. The process is quite similar to that used by solid state integrated circuit foundries (except fewer foundry steps are needed). It should be noted that lithium niobate chips produce intrinsically polarization preserving light guides, which enhances the use of PPF sensing coils.

It has been well known that lithium niobate crystals are susceptible to optical damage. It is believed that this damage is caused by energetic photon collisions with atomic iron impurities embedded in the lithium niobate lattice structure. At appropriate photon energies (i.e., optical wavelength) the outer electron shells of the iron become excited with very long relaxation time. Unfortunately, the present 0.83  $\mu$  wavelength is such an appropriate photon energy level.

When the incident rate of the energetic photons (i.e., light intensity) reaches a threshold value, enough excited iron nuclei impurities are produced to distort the lithium niobate lattice structure and produce visible photo-darkening effects. Above onset threshold, the photo-darkening is proportional to time accumulated light energy usually taking tens of minutes. When the light is removed, the crystal structure can relax back to its normal condition, but may take a week or more to do so.

There appears to be no reasonable prospect to significantly reduce iron impurities in today's lithium niobate foundry processes. Current telecommunications

<sup>6</sup>It is made into a sine rotation detector characteristic by the phase

experience at the 0.83  $\mu$  wavelength has detected photo-darkening onset at milliwatt light intensity levels, a light intensity level which most IFOGs would be well under. Unfortunately, this measurement for darkening onset was made based on intensity loss from input to output of the chip with primarily unidirectional propagation through the chip (in comparison with bidirectional for the IFOG). With the IFOG's critical dependence on optical reciprocity, the light intensity onset threshold could be considerably reduced, especially for high levels of functional chip integration (i.e., optical devices on the chip).

For the GGP, this risk to successful IO chip employment has been judged too high! Fortunately, longer wavelength fiber technology (1.3 to 1.55  $\mu$ ) does not suffer from the effect as the individual photon energy is too low to excite the iron impurities. Even more fortuitously, there is considerably greater optical quality in the fiber parts at the longer wavelength (e.g., lower loss 1/2 db/km vice 3 db/km, reduced scatter, increased polarization extinction in PPF, etc.) while the lithium niobate chip fabrication is more tolerant in its critical dimension requirements. It is to these longer wavelengths that the telecommunications industry migrated successfully several years ago.

The 0.83  $\mu$  wavelength was originally employed in IFOG research because of the availability of quality diode optical sources with adequate power level and photodetectors. Currently, quiet photodetectors are readily available at the longer wavelengths while broadband superluminescent diodes, SLD (remember a quality spread spectrum source is needed for multipath scatter reduction) are just now becoming available at these wavelengths. It is on this longer wavelength optical technology that the GGP will evolve for lower cost (using nonphoto-damaging IO chip) and obtain better performance (higher quality fiber).

Listed below are current research areas to the longer wavelength closed loop IFOG effort by DARPA for its GGP.

- o Component Level

- Light source--SLD, LD, LED
- IO chip & optronic devices--voltage controlled optical phase modulator, high-level integration
- Physical characterization--reciprocity, scattering mechanisms, optical loss, g load & thermal gradient effects
- Connectors/splicers--alignment, reflections

- o System Level

- Closed loop signal processing and sensor modeling
- Error analysis and performance prediction
- Parameter optimization

The current GGP IMU effort is completing several preliminary designs of a closed loop IFOG along with selection and integration of miniature accelerometers with performance at the 0.01°/hr level given in Table 3. In the next phase of the GGP program, two designs will be selected and parallel efforts to build IMU brassboards of the selected designs will be pursued. These brassboards are to commence flying-laboratory tests within three years of contract award. For this GGP flight testing, an MGR will also have been integrated, as discussed in the following section.

#### GGP SYSTEM INTEGRATION

System integration effort for the GGP is being conducted at the functional levels, listed below:

- o Mechanical Packaging
  - Form/Fit, Temperature, Shock
- o System Data Processor/Bus Hardware
  - Thruput, Memory, Sensor Interface Control
- o System Software Modules
  - Filter Design, Resource Manager
- o System Simulation/Trade-off Optimization
  - Covariance and Monte Carlo Simulation

o User Mission Analysis  
Trajectories/Profiles, Performance Measures

With the exception of the mechanical integration, there is strong interaction amongst the other system integration functions, listed above.

Since the modular GGP is planned for a wide variety of host/mission applications on the one hand, and the system scope is both broad and interconnected on the other hand, the system's effort must be partitioned by an appropriate development philosophy in order to avoid needlessly locking out useful GGP applications while partitioning the system's effort into manageable assignments. The key requirements for DARPA to achieve this goal is (1) to host guidance/navigation functions as well as top-level resource control with all attendant software strictly in the Navigation Systems Microprocessor(s) (Fig. 1), and (2) to maintain tight control over electrical/data exchange interfaces/standards between the two GGP sensor suites (MGR and IMU) and the system microprocessor.

A consequence of this approach may produce a fairly significant throughput, memory space, and coding burden on the system's microprocessor. This will be strongly driven by the size (i.e., number of states modeled) of the Kalman Filter employed [10]. However, the latest high-speed commercial microprocessors (possibly RISC machines) should be able to accommodate the expected throughput of several MIPS. The standard, multimegabit high-speed backbone data bus will be used with either 16 or 32 bit width.

Software development will initially focus on the following: (1) implementing the Kalman Filter, (2) separating out of the existing software modules in the MGR and IMU sensors their low-level real-time signal processing modules from their resource management modules, (3) determining software data access and command methods from top-level resource management in the system's microprocessor to the low-level real-time software in the sensor microprocessor, and (4) reconcile data formats and timing actions. Resource management decision tree/execution action tables will be developed for various host applications. Finally, the software will be thoroughly tested and validated.

System simulations will be performed at two distinctly different, but highly interactive, levels. At the aggregate system modeling level, mathematical input/output models for the MGR, IMU, and physical environment (e.g., gravity anomaly) are combined together with a Kalman Filter in "Covariance" simulations for specified mission dynamic profiles. Selective "Monte Carlo" simulations will then be run. Such analysis relates instrument performance requirements, generates expected system behavior, and predicts mission performance. It provides a "specification dialogue" between the user application and the GGP modular design as well as eliciting what are critical system drivers and the measures of merit/performance appropriate to each class of application. An example of this will be provided in what follows.

The aggregate system modeling simulations will not test the adequacy of the real-time operational system-level software nor the specific behavior of the MGR and IMU components and their dedicated low-level real-time software. Moreover, the dynamical detailed interactions between the three subsystems needs to be verified. To do this a sequence of hybrid-brassboard simulations will be used wherein a mixture of real-time computer simulation with hardware simulation will be set up for a selected class of mission. As GGP sensor instruments become available they will be inserted in the brassboard. The end state of the sequence will be an all-GGP brassboard customized for the selected mission class.

Returning to the aggregate system-level modeling, a series of preliminary results were obtained for two classes of mission: (a) an Unmanned Vehicle or UMV and (b) a long-range strike weapon. Representative mission trajectories were "flown" postulating a high quality IMU in the 0.003°/hr gyro drift rate and 50  $\mu$ g accelerometer bias category.

GPS received signal was then denied (e.g. jammer) at selected parts of the mission and IMU only guidance error buildup was calculated. In addition to the IMU error sources, earth gravity anomalies and vertical deflection were modeled as a first order Markov process.

The modeled MGR, IMU, vehicle motion, and gravity inputs were optimally combined in a 48-state system Kalman filter. Additionally, a 78-state model is executed as the "truth" model. The covariance simulation then flies the mission

trajectory (in non-real-time) accumulating as a function of time the  $1\sigma$  state errors for both the truth model (78-state) and the system filter (48-state). The 48-state system filter is deliberately overstated in order to identify the most significant 17 to 23 states to retain in an operational filter formulation that can execute in real time.

Finally, a perfect IMU was postulated in order to benchmark the error floor introduced by the (unmapped) gravity anomalies and vertical deflections. The primary intent of this exercise was to build the capability to make these calculations and develop preliminary insight to relate IMU quality to mission needs. The mission trajectories are purely hypothetical and were used only to develop this system level skill. They have no validity as to any specific real missions.

Shown in Figs. 11, 12, and 13 are three sample mission trajectories used with GPS signal loss introduced. Figs. 11 and 12 are two unmanned vehicle trajectories in which the first passes by a single jammer and the second passes by a series of jammers. Fig. 13 shows in plan view a long-range strike weapon-type trajectory with a jammer in the immediate neighborhood of the target.

The model results plotting one sigma horizontal displacement errors versus time are shown in Figs. 14, 15, and 16. The solid lines are the modeled "true"  $1\sigma$  errors and the dotted lines are what the modeled system Kalman filter "says" are the  $1\sigma$  errors. The corresponding results for the gravity errors only case with zero instrument error showed only a few meter increase in  $\sigma_H$ . This establishes that additional improvements in IMU performance beyond the .003°/hr level (Table 5) will require maps of gravity anomaly and vertical deflection, thus increasing somewhat system memory and requiring increased microcomputer capacity. In all probability these considerations will be less demanding than the added mission planning burden, i.e., obtaining gravity surveys.

#### CONCLUSIONS

The DARPA GGP program objective to exploit GPS/IMU synergisms in an extremely small package with little burden to an extremely wide variety of host vehicles and applications is being actively pursued. The goal to achieve current navigation grade of performance (~ 1 nm/hr.) but with major per unit cost reductions in large-scale production should be achievable. Except for the IMU, solid state technology is now either off the shelf (system integration microprocessor) or becoming available (mini-GPS receivers). The silicon accelerometers are currently under active development by DoD. Consequently, the Fiber Optic Gyro (FOG) is the primary technology needed to produce a successful GGP.

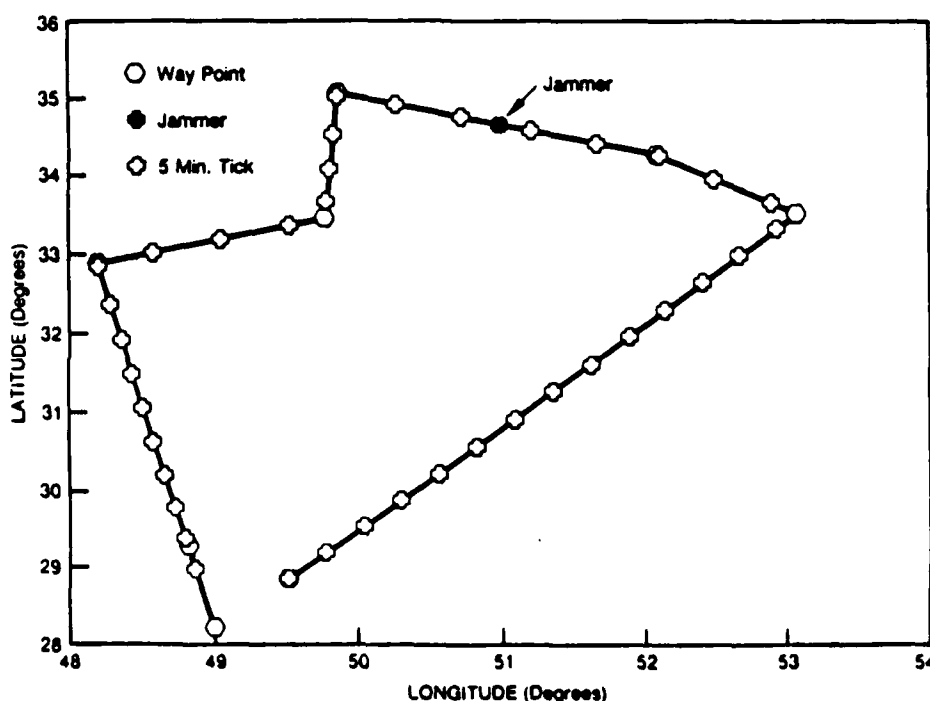


Fig 11 - Ground Track (IMV-1)

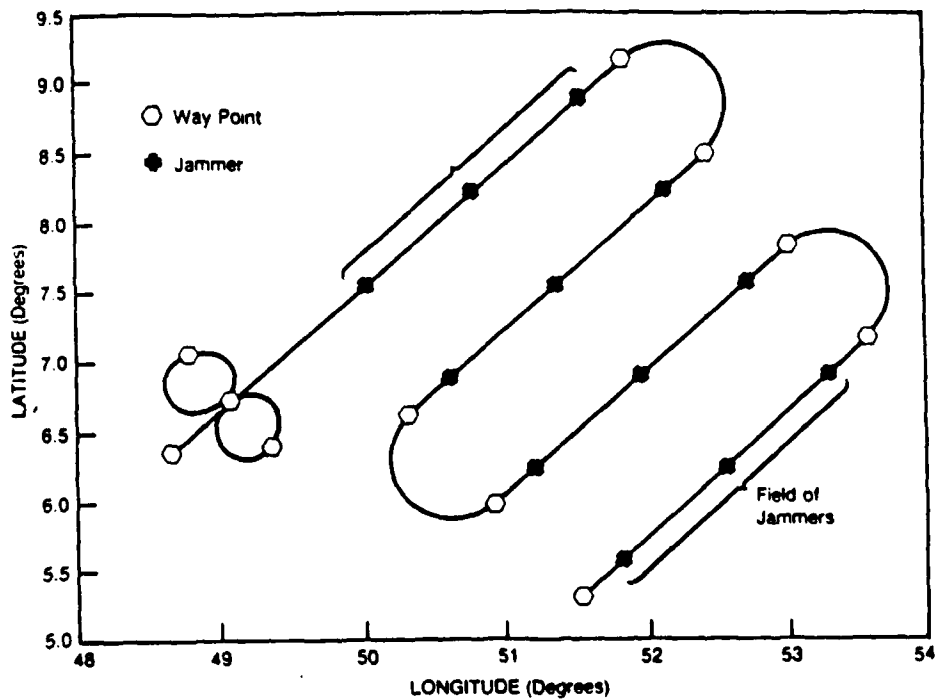


Fig. 12—Ground Track (UMV-2)

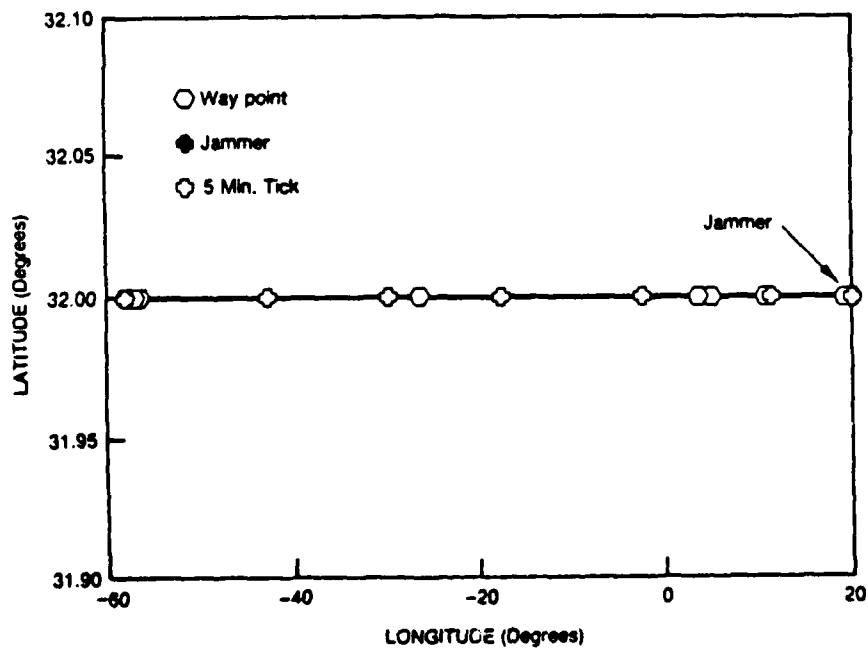


Fig. 13—Ground Track (SW-22)

In this paper the principal technical approaches being pursued in the DARPA GGP program have been reviewed along with discussion of the issues associated with these approaches. The performance and size goals of the GGP (i.e., FOG) can be met with low to moderate risk. The higher risk resides in making the cost reduction breakthroughs for the FOG instruments. This risk principally falls on the following FOG components: (1) integrating high-level optical signal processing parts on the integrated optics chip, (2) producing higher power, long wavelength optical sources, and (3) automated parts assembly machinery and infrastructure, e.g., sensing coil winders and automated polarization aligning connections/splices between the optical subassemblies of source, chip, and coil. These challenges are commensurate with the broad DARPA charter to significantly advance the DoD technology base.

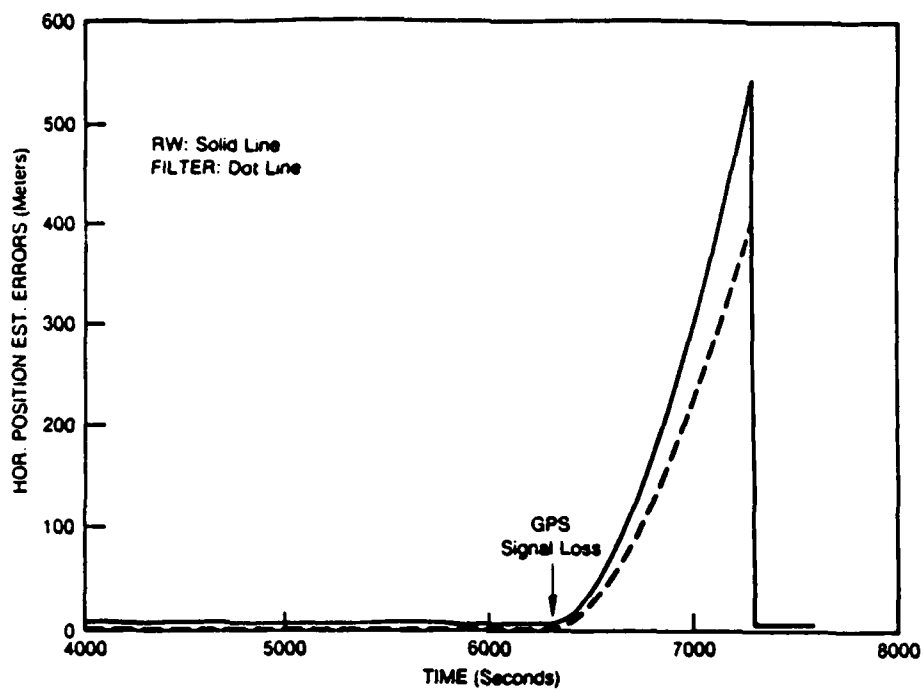


Fig. 14—Estimation Errors of Navigation States (UMV-1)

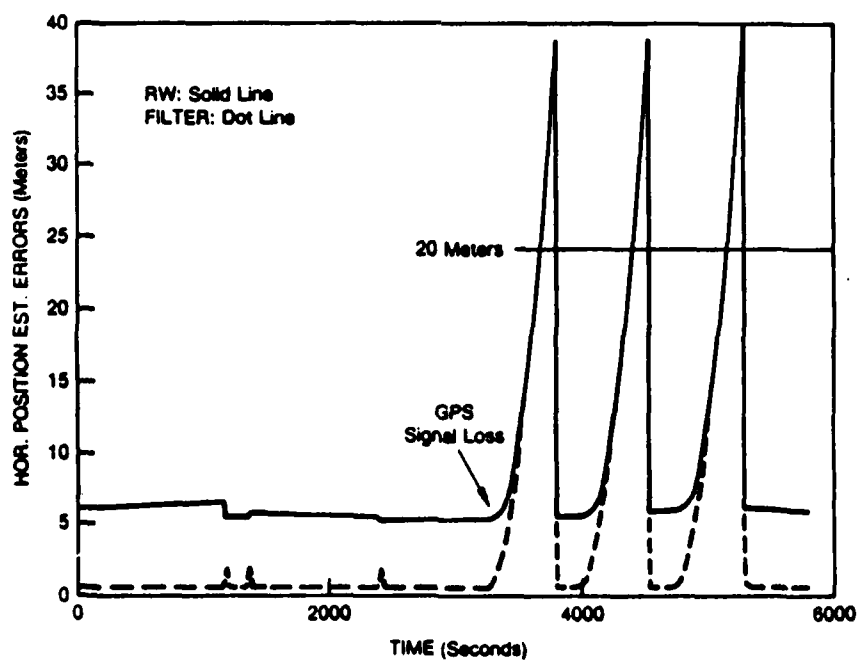


Fig. 15—Estimation Errors of Navigation States (UMV-2)

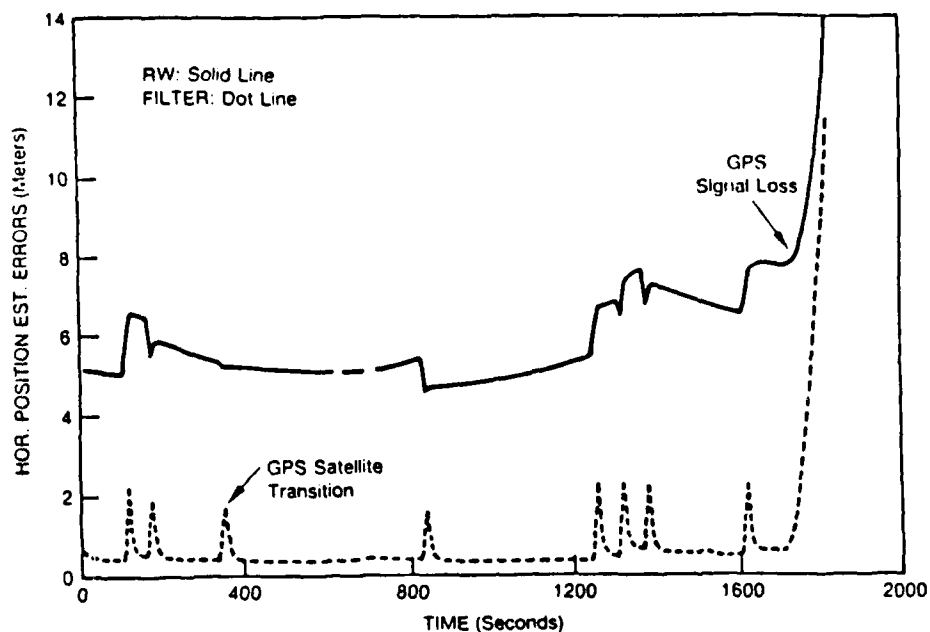


Fig. 16—Estimation Errors of Navigation States

#### REFERENCES

1. Hemesath, N. B., J.M.H. Bruckner, R. J. Weber, and J. P. Young, "A Miniature GPS Receiver," Microwave Journal, September 1987, pp. 1-104
2. U.S. Air Force, "System Segment Specification for the User System Segment, Navstar Global Positioning System, Phase II," 31 January 1979
3. Chow, W. W., J. Gea-Banacloche, and L. M. Pedrotti, "The Ring Laser Gyro," Reviews of Modern Physics, Vol. 57, No. 1, January 1985
4. Ezekiel and Arditty, "Fiber-Optic Rotation Sensors Tutorial Review," Springer-Verlag Optical Science Series, Vol. 32, pp. 2-26, November 1981
5. Bergh, Ralph A., H. C. Lefevre, and H. J. Shaw, "An Overview of Fiber-Optic Gyroscopes," J. Lightwave Tech., Vol. LT-2, No. 2, April 1984, pp. 91-107, F-1a 16
6. Carroll, R., C. D. Coccoli, D. Cardarelli, and G. T. Coate, "The Passive Resonator Fiber Optic Gyro and Comparison to the Interferometer Fiber Gyro," Fiber Optic gyros: 9th Anniversary Conference, SPIE, Cambridge, Mass., Vol. 719
7. Page, J. L., "Fiber Gyro with Electro-Optic Phase Modulation," SPIE, Cambridge, Mass., September 1986
8. Fredricks, R. J., "Scattering Matrix Analysis on the Use of Wideband Laser Source in a Passive Fiber Rate Sensor," Springer-Verlag Optical Science Series, Vol. 32, November 1981, pp. 82-92
9. Bartman, R. K., B. R. Youmans, and N. M. Nerheim, "Integrated Optics Implementation of a Fiber Optic Rotation Sensor: Analysis and Development," Fiber Optic Gyros: 10th Anniversary Conference, SPIE, Vol. 719, pp. 122-134
10. Sorenson, Harold W. (ed.), Kalman Filtering: Theory and Application, IEEE Press, New York, 1985



**ASTO**

# **STATUS OF DARPA GUIDANCE AND CONTROL PROGRAM**

223

**DR. LARRY STOTTS  
27 APRIL 1989**

VC 89 U 0119  
14 APR 89



**I. A COMMON BASIC SENSOR DESIGN WITH A MODULAR ARCHITECTURE PRODUCING A WIDE RANGE OF ACHIEVABLE "GYRO" PERFORMANCE INCLUDING, AT THE HIGH END, PERFORMANCE COMPARABLE TO CURRENT CONVENTIONAL, IMU QUALITY, GYROS.**

**II. SOLID STATE-LIKE PROPERTIES, EG., LIGHT WEIGHT, SMALL, WITH NO MOVING PARTS (FOR QUIETNESS AS WELL AS RELIABILITY), LOW POWER DRAIN, AND LOW OPERATING VOLTAGES.**

**III. VERY HIGH VOLUME, NON-LABOR INTENSIVE, MANUFACTURABILITY TO PRODUCE VERY LOW PER UNIT COSTS.**

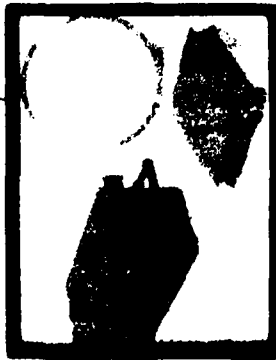
**IV. FIT IN 6" BALL OR SMALLER USING LESS THAN 20 W.**



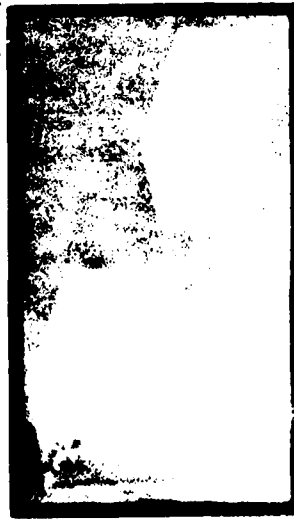
ASTO

	VOLUME IN <sup>3</sup>	WEIGHT LBS	POWER WATTS	ROM \$K
F-16 5 CHANNEL GPS	970	37	100	75
IMU-201 WITH IMU PROCESSOR (10°/HR)	675	19	60	30
GGP (0.01°/HR)	1645	56	160	105
SUM	120	19	20	15

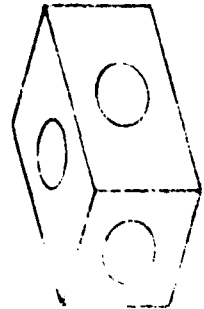
F-16 5 CHANNEL GPS



IMU-201 WITH IMU PROCESSOR (10°/HR)



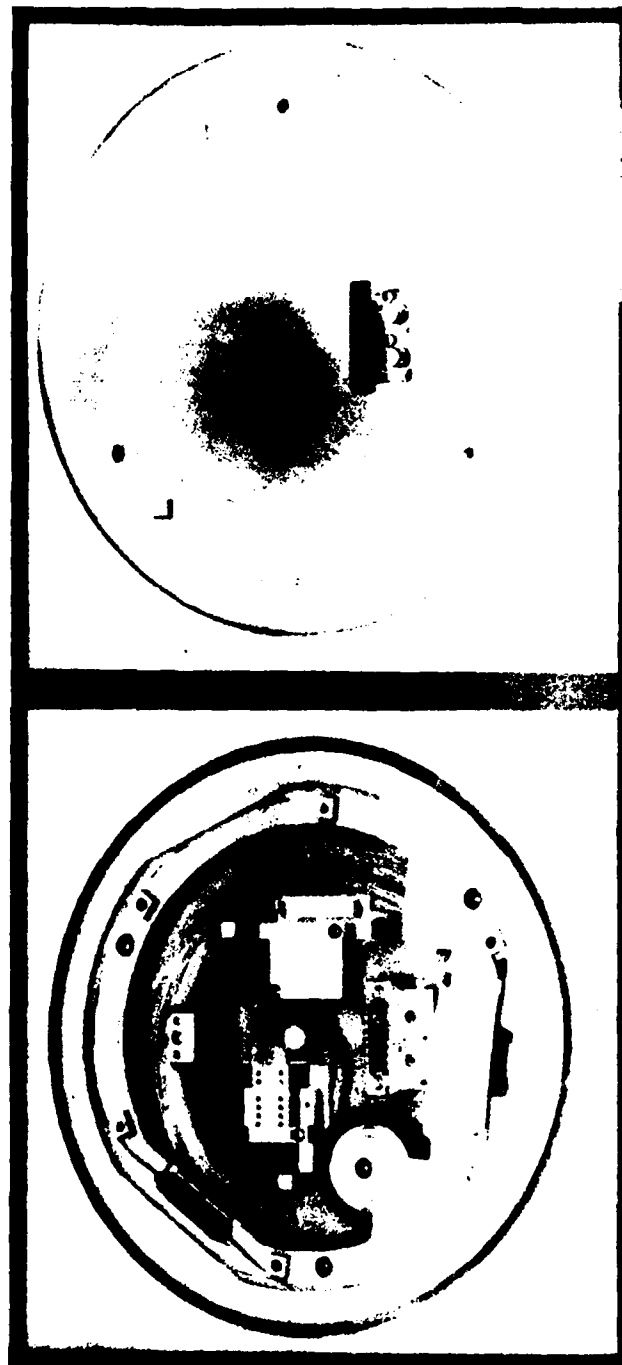
GGP (0.01°/HR)





## 16 CM HIGH PERFORMANCE IFOG

ASTO





# HIGH PERFORMANCE IFOG PERFORMANCE SUMMARY



ASTO

RANDOM NOISE

0.0016  $\text{°}/\sqrt{\text{HR}}$

BIAS STABILITY

0.02  $\text{°}/\text{HR}$

SCALE FACTOR

LINEARITY

30 PPM

REPEATABILITY

10 PPM



## "THE MULTIPATH SIMULATOR", A TOOL TOWARD CONTROLLING MULTIPATH

George A. Hajj  
JET PROPULSION LABORATORY

One of the major error contributors to GPS orbit determination and baseline measurements is multipath. Its source can be the GPS satellite itself, the ground antenna environment, and the user spacecraft body. Multipath error is scaled according to wavelength and is therefore larger for P-code than carrier phase. Averaging over time does reduce the error.

The multipath simulator basically uses a ray-tracing technique to determine the different paths that a GPS-transmitted signal can take. Its capabilities include modeling a multitude of differing geometric environments for the transmitter and receiver antenna, simulating both L1 and L2 frequencies and the polarization of the direct and reflected signals, and performing sensitivity studies related to antenna gain and receiver tracking strategy.

Using TOPEX as an example, multipath effects were analyzed with respect to antenna position, antenna gain, and data analysis technique. The model included signals from up to 6 GPS satellites reflecting off of a variety of surfaces descriptive of the TOPEX satellite; its attitude and the orientation of the solar panel and TDRSS antenna were also modeled. As a function of boom height of the antenna above the satellite, it is shown that at a height of 4.3 m the multipath effect is about 20 db lower than the direct signal; whereas at zero height, there is considerable interference. The instantaneous multipath error in P-code is approximately 100 times greater than in the carrier phase, and each of these can be reduced by an order of magnitude by time averaging; 5 minute averages are shown here. Analyzing real data at the Ovro site, we see an error on the order of 10 cm for 2-min. averages of the P-code using L1 (P1) showing that our simulations are reasonable. A simulation of a precise orbit determination for TOPEX shows that proper weighting of the data (i.e., 100 to 1 ratio for the carrier phase versus the P-code measurements) effects reduced orbit altitude residuals due to multipath.

In conclusion, the multipath simulator can be used in the design phase of an experiment to determine antenna location and gain, to quantify multipath for precise orbit determination, and, ultimately, to calibrate multipath errors. It is shown that multipath can be reduced also by properly weighting the carrier phase and P-code data.

### Discussion:

Question: How can one analyze the multipath for another satellite, such as Lightsat, instead of TOPEX?

Answer: Simply define the configuration and geometry of the main objects that are expected to cause multipath.

Question: Are the multipath effects due to irregularities in the ionosphere and troposphere negligible compared to the reflection effects.

Answer: These are higher-order ionospheric effects which require different analysis altogether.

Question: How are the range errors due to multipath obtained for a given reflection of the signal?

Answer: We looked at the correlation function of the direct signal and the correlation function of the reflected signal and determined how far the correlation peak shifted to obtain the range error.

Question: How much multipath is due to the GPS satellites?

Answer: This has not yet been analyzed; it is expected to be much less than for the TOPEX satellite.



## THE PROBLEM OF MULTI-PATH WITH GPS MEASUREMENTS

- Sub-centimeter accuracy level in baseline measurements was demonstrated
- Future goal for orbit determination is 10 cm for Topex, 1-3 cm for EOS
- A major contributor to the error is multi-path from
  - GPS satellites
  - Ground antenna environment
  - Spacecraft body
- Instantaneous multi-path error can reach several meters for P-code and few cm's for carrier phase
- 5 min. averaging can reach 1 m for P-code and .5 cm for carrier

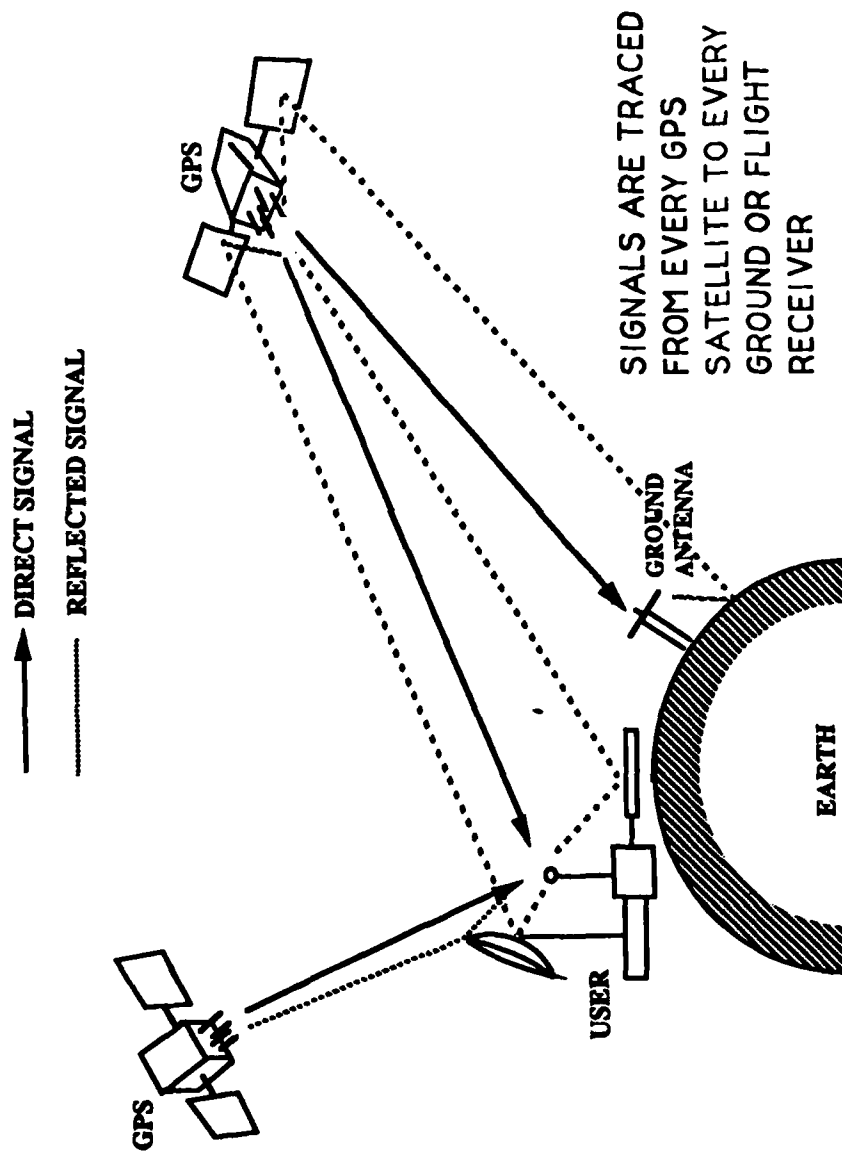
### THE NEED FOR A MULTI-PATH SIMULATOR

- Gives a realistic estimate of the error introduced by multi-path
- Helps finding means of minimizing multi-path





## PICTORIAL REPRESENTATION OF THE MULTI-PATH SIMULATOR



**CAPABILITIES OF THE MULTI-PATH SIMULATOR****TRANSMITTER OR RECEIVER ENVIRONMENT**

- Flat surfaces of arbitrary shape
- Spheres or sections of spheres (Antenna dishes, inside and outside)
- Cylinders or sections of cylinders
- Conducting or dielectric surfaces
- Reflection from many surfaces simultaneously
- Geometrical optics (main effect) or Geometrical Theory of Diffraction (includes diffraction from edges)

**GPS SIGNAL**

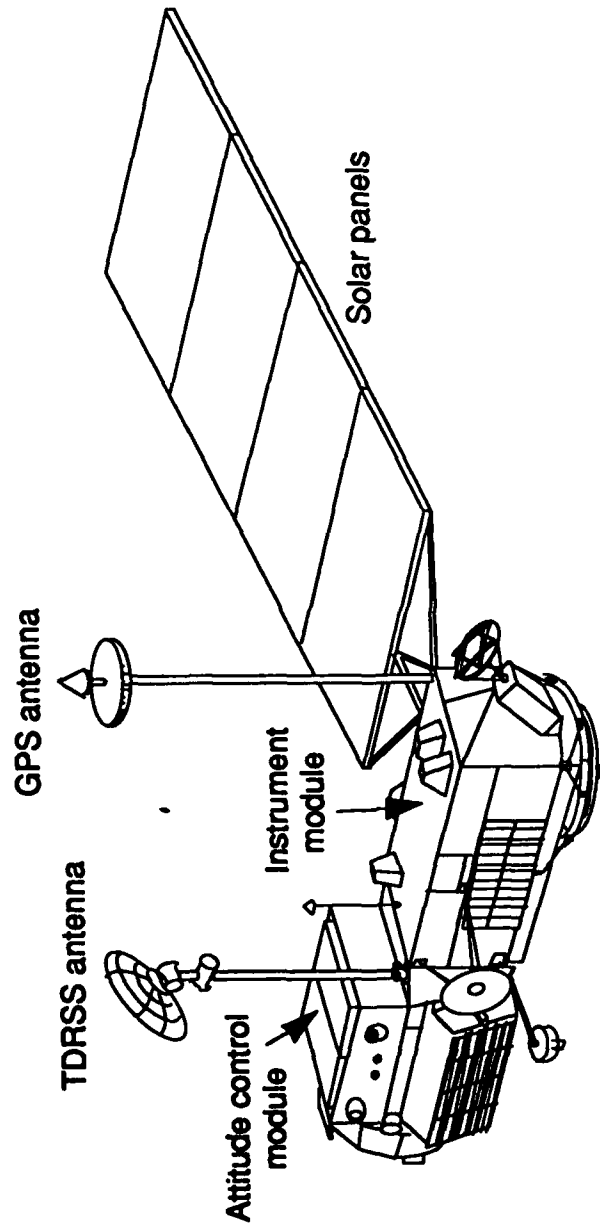
- Simulates L1 (1575.42 MHz) and L2 (1227.6) frequencies
- Both RCP and LCP direct or reflected signals are simulated
- Finds P-code and carrier phase multi-path delay

**ANTENNA AND RECEIVER**

- Simulates the antenna gain pattern for L1, L2, RCP and LCP
- Simulates the receiver's tracking strategy

## USABILITY OF THE MULTI-PATH SIMULATOR TOPEX AS AN EXAMPLE

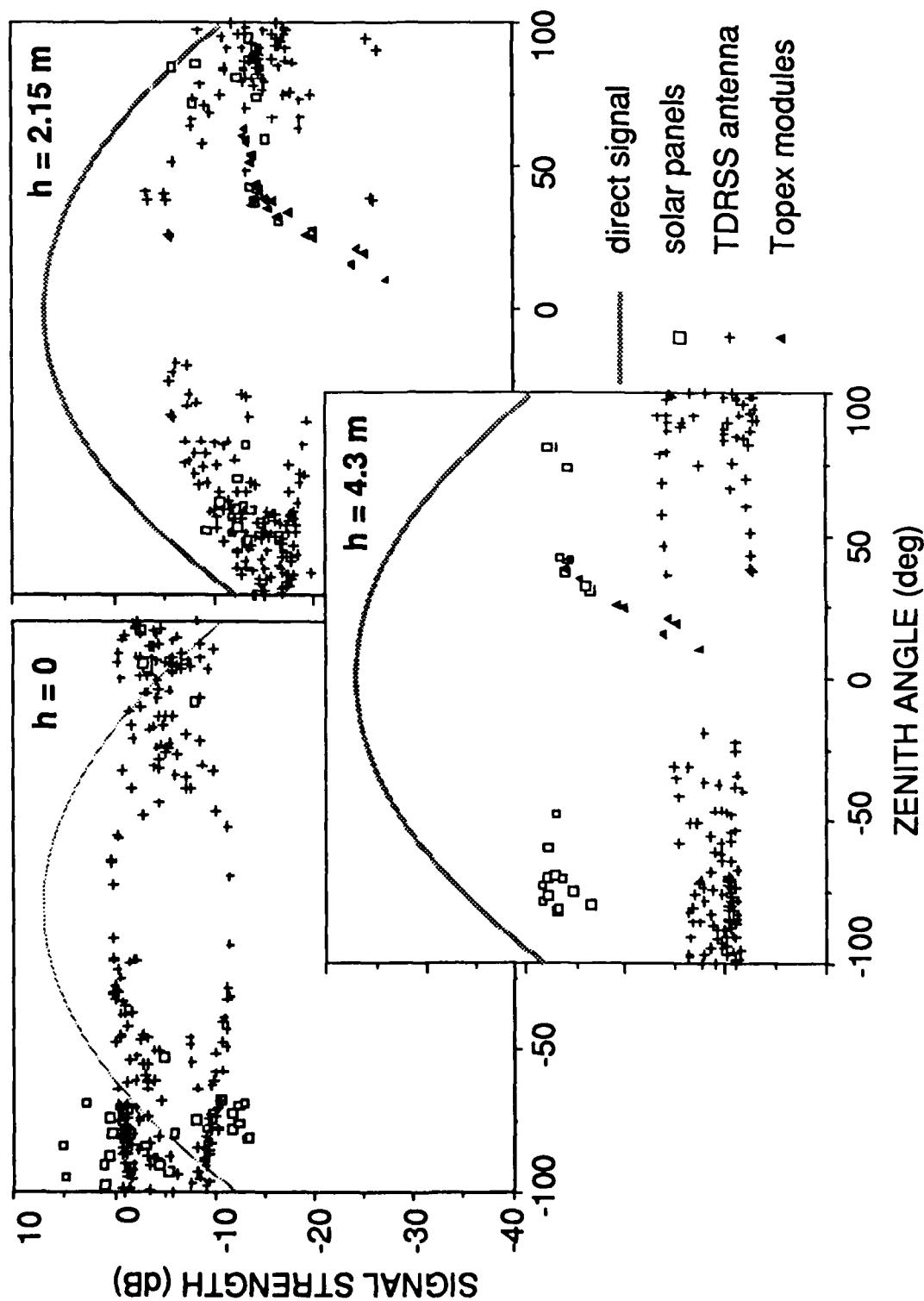
- Topex multi-path can be very serious
- Do various tests to reduce multi-path effects
  - elevate GPS antenna to above reflecting surfaces
  - use proper antenna to improve gain pattern
  - try different data analysis schemes to improve altitude solution



**ANALYSIS OF TOPEX MULTI-PATH EFFECTS**

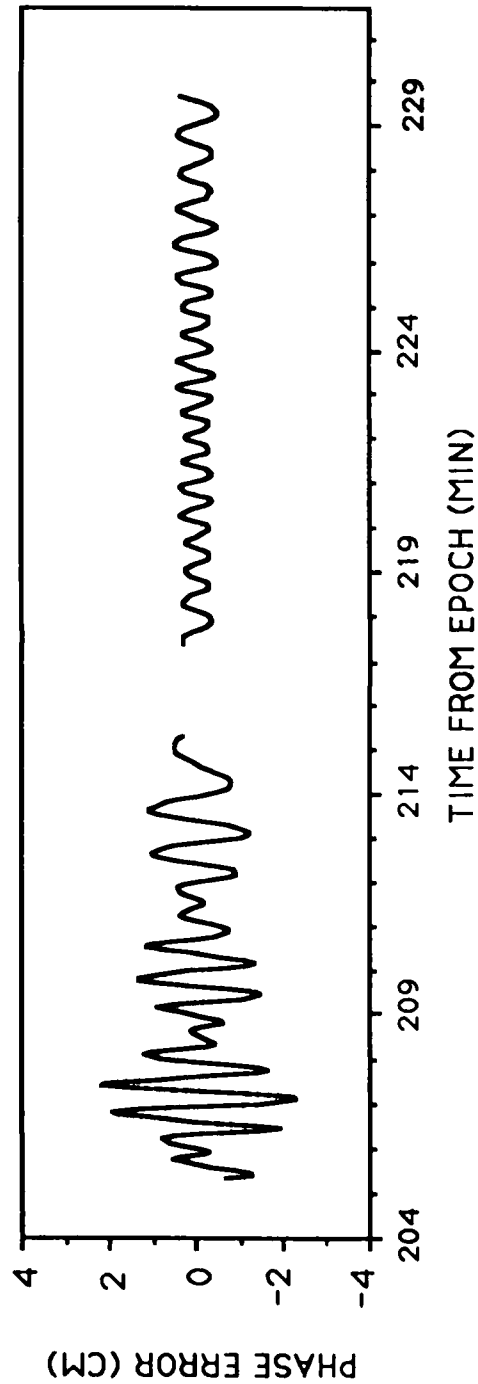
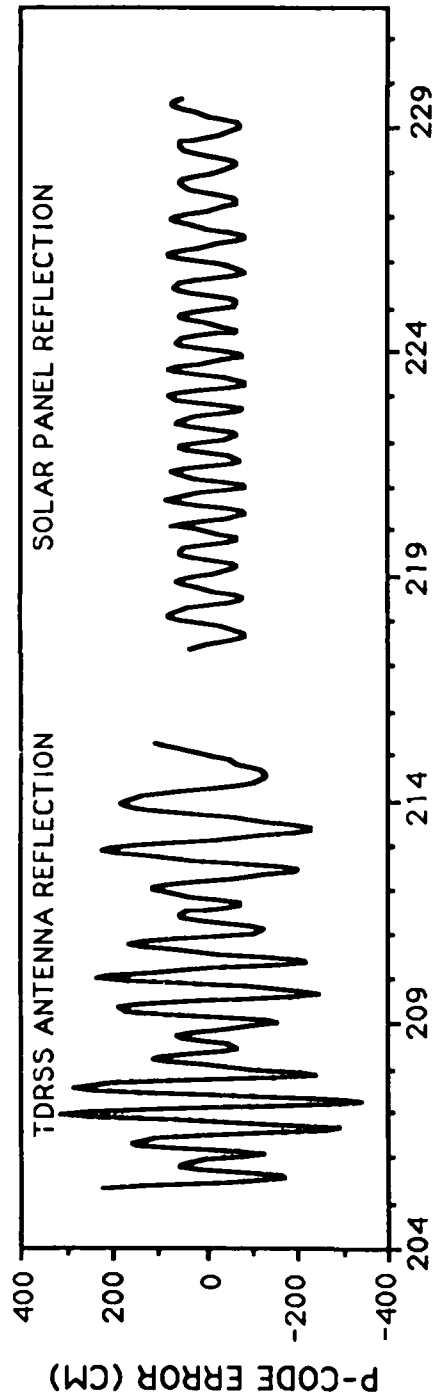
- Topex tracking 18 GPS, up to 6 GPS at one time
- Total received signal is sum of direct and reflected on topex from each GPS satellite
- Reflecting surfaces are
  - Solar panels
  - TDRSS antenna
  - Instrument module
  - Attitude control module
  - Reflection from more than one object at one time is possible (all surfaces are modeled as perfect conductors)
- Only specular reflection is considered
- Topex attitude, solar array and TDRSS antenna orientation are modeled

# TOPEX MULTI-PATH EFFECTS





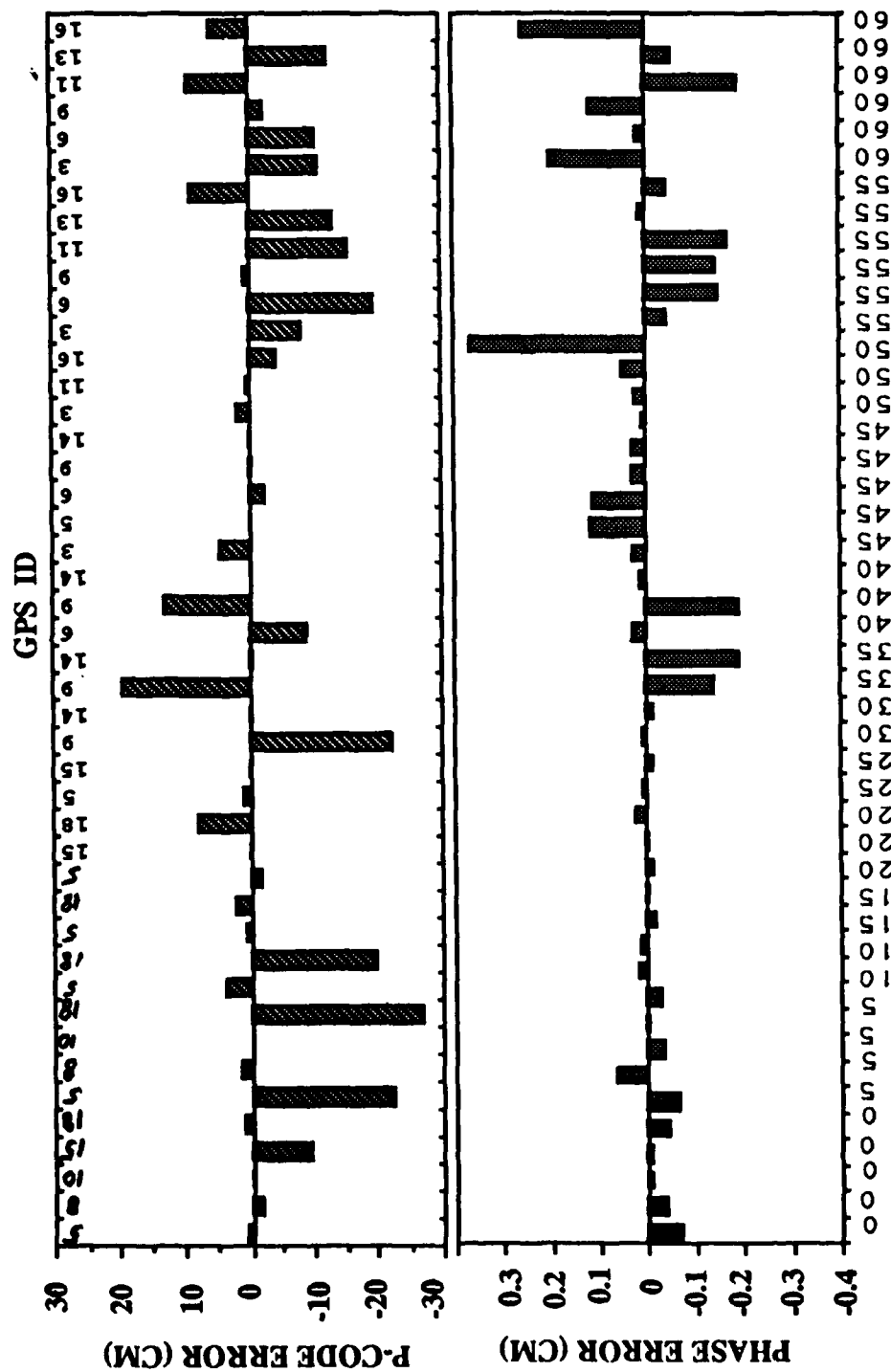
# INSTANTANEOUS MULTI-PATH ERROR ON TOPEX SIMULATED MULTI-PATH ERRORS FOR 2.5 L1-1.5 L2 FROM GPS#7



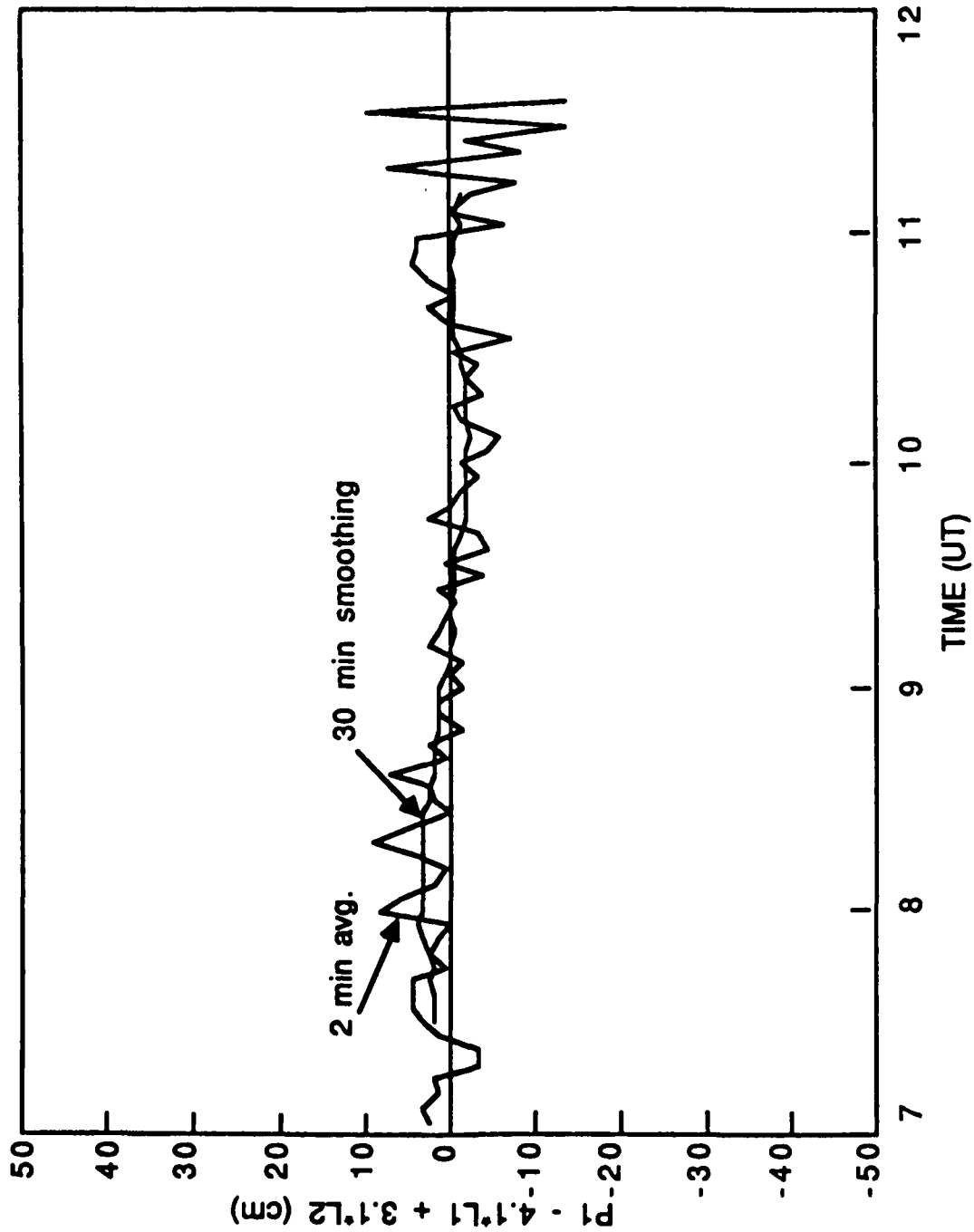
237

# MULTI-PATH FROM TOPEX 5 MINUTES AVERAGING OF 2.5 L1 - 1.5 L2

2



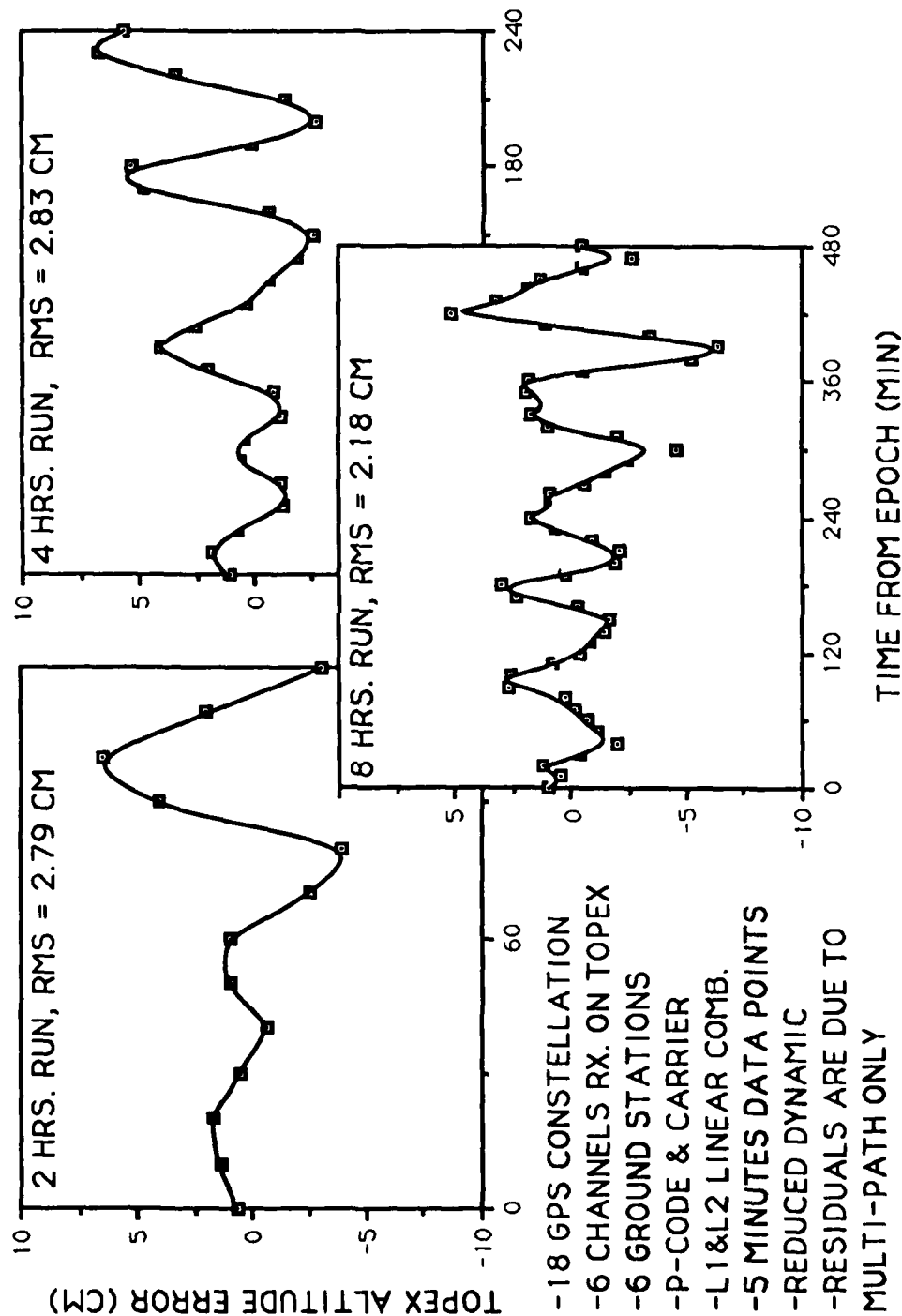
**P1 DELAY NOISE @ OVRO (PRN 9))**





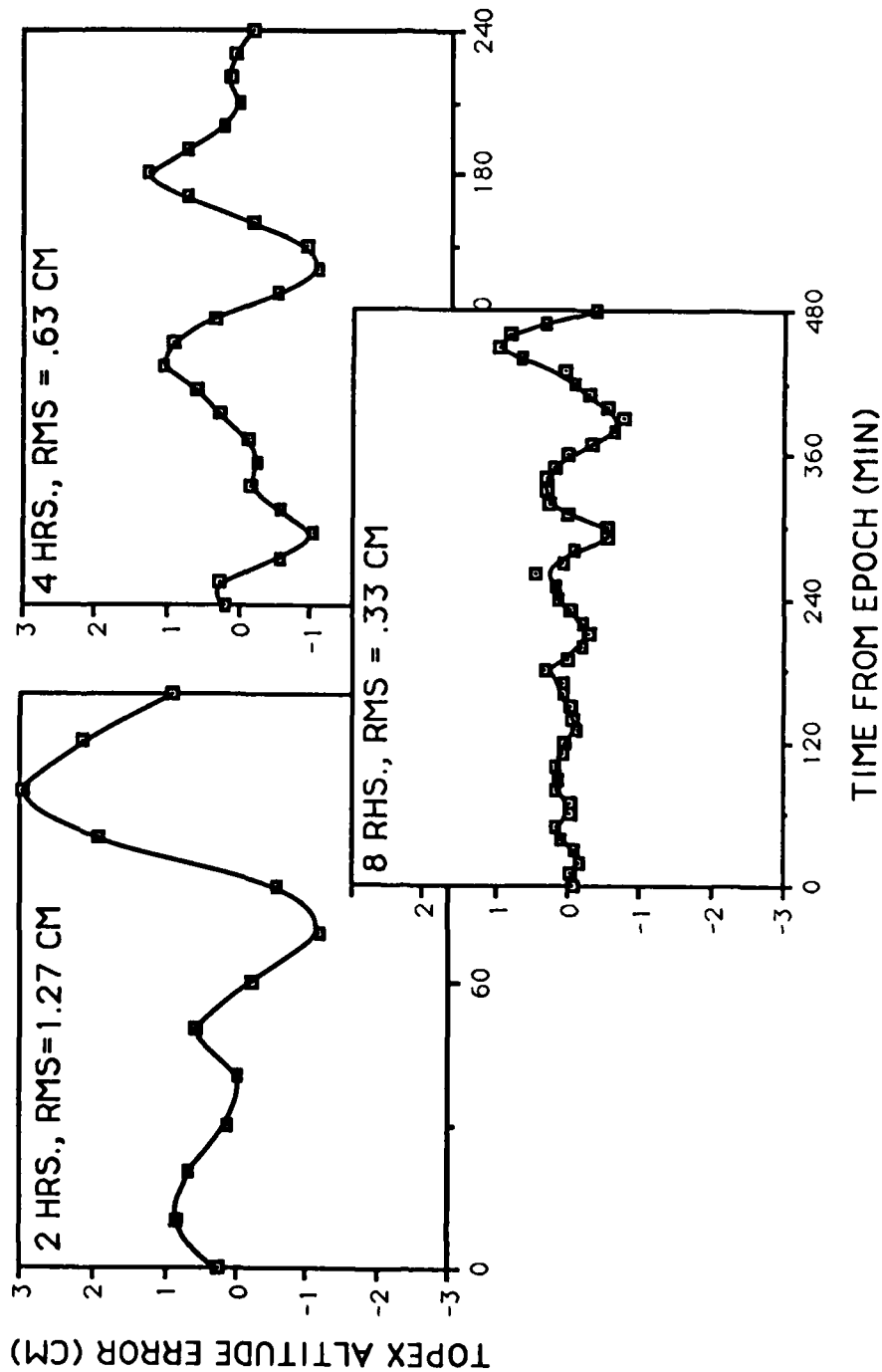
## SIMULATING MULTI-PATH EFFECT ON TOPEX POD COMPLETE POD RUN

DATA WEIGHTS: 5 CM FOR P-CODE, .5 CM FOR CARRIER



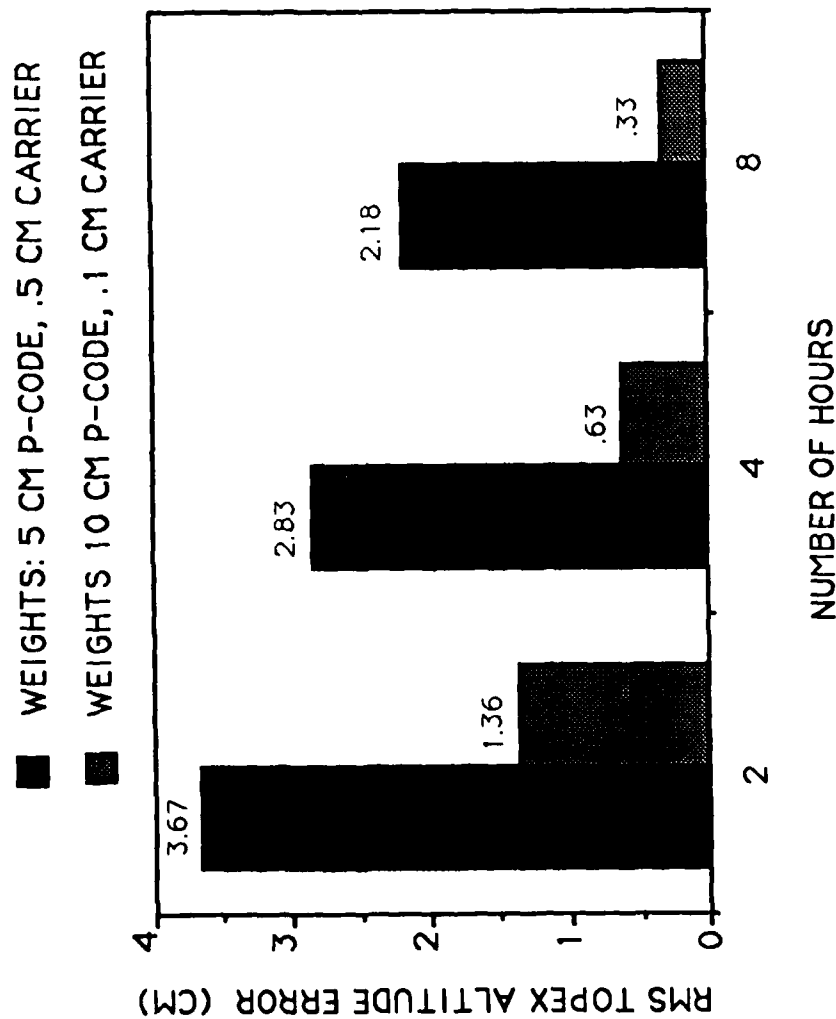
# **TOPEX ALTITUDE ERROR MORE REALISTIC DATA WEIGHT**

DATA WEIGHT: 10 CM FOR P-CODE, .1 CM FOR CARRIER



## TOPEX POD ERRORS DUE TO MULTI-PATH

### RMS OF TOPEX ALTITUDE ERROR FOR DIFFERENT RUNS TWO DIFFERENT WEIGHTING SCHEMES



## **CONCLUSION**

### **THE USABILITY OF THE MULTI-PATH SIMULATOR**

- Can be used in the design phase of an experiment to determine
  - best antenna location and orientation
  - upper limits on the antenna backlobes gains
  - foretell hazardous environmental configurations that can cause severe multi-path
- Provides a quantitative estimate of multi-path errors on Precise Orbit Determination
- Provides a mean of testing different ways of analyzing the data to reduce POD errors
- Ultimately, might be used to calibrate multi-path

243

### **POD ERROR DUE TO MULTI-PATH**

- With current receivers, POD errors due to multi-path can be reduced to sub-centimeter level by
  - choosing a suitable position for the antenna
  - minimizing backlobe gain of antenna
  - long time averaging
  - Properly weighting carrier phase and P-code data

U.S. GOVERNMENT PRINTING OFFICE: 1990-700-000/00048